Forschungszentrum Jülich

Institut für Kernphysik

Workshop on a_0 Physics with ANKE

Proceedings

Held at the Institute for Theoretical and Experimental Physics (ITEP), Moscow, July 13/14, 2000

edited by Markus Büscher and Vera Kleber

JÜL-3801

Workshop on a_0 Physics with ANKE

Proceedings

Held at the Institute for Theoretical and Experimental Physics (ITEP), Moscow, July 13/14, 2000

edited by Markus Büscher and Vera Kleber

Berichte des Forschungszentrums Jülich ; 3801
ISSN 0944-2952
Institut für Kernphysik Jül-3801

Zu beziehen durch: Forschungszentrum Jülich GmbH · Zentralbibliothek
D-52425 Jülich · Bundesrepublik Deutschland
☎¶ 02461/61-6102 · Telefax: 02461/61-6103 · e-mail: zb-publikation@fz-juelich.de

Preface

The workshop on "a_0 Physics with ANKE" was held at the *Institute for Theoretical and Experimental Physics (ITEP)* in Moscow on July 13/14, 2000. During the workshop the possibilities to study the nature of the scalar $a_0(980)$-mesons with the ANKE spectrometer at the proton synchrotron COSY of the *Forschungszentrum Jülich (FZJ)* were intensively discussed. The nature of the lightest scalar mesons is a problem of fundamental interest in the physics of hadrons and one of the most important topics of present-day medium-energy physics.

The workshop was triggered by a decision of the COSY Program-Advisory-Committee (PAC) in May 2000. A proposal to measure the production of charged a_0-mesons in the reaction $pp \rightarrow da_0^+$ at ANKE received strong support and the corresponding beam time for a first experiment of two weeks was granted. It is scheduled for February 2001. One goal of the meeting at *ITEP* was a thorough preparation of those measurements. Another major point of interest was to develop ideas for future experiments with ANKE and to hear about recent theoretical achievements in the field of scalar mesons. About 35 scientists mostly from Russia and Germany joined the workshop and 16 talks were presented.

This booklet starts with the approved proposals for a_0^+ measurements with ANKE. It contains a short summary of each talk as well as copies of the transparencies shown during the workshop. Finally, a list of responsibilities - as it was agreed on at the end of the meeting - is attached.

The workshop benefitted greatly from financial support by the Deutsche Forschungsgemeinschaft (DFG)[1], the German Ministry for Education and Research (BMBF)[2], the Russian Foundation for Fundamental Research (RFFI)[3] and the European Community[4] which is gratefully acknowledged. It allowed to organize for the first time a meeting of this size in the framework of the ANKE collaboration within Russia.

Last but not least we would like to thank the local organizers, Dr. V. Chernyshev and colleagues, for the technical organization of the meeting. We enjoyed very much the hospitality at *ITEP* which led to a stimulating atmosphere with extremely lively and fruitful discussions.

Jülich, July 2000

Markus Büscher Vera Kleber

[1] 436 RUS 113/337, 436 RUS 113/444, 436 RUS 113/561
[2] WTZ-RUS-684-99
[3] 99-02-04034, 99-02-18179a
[4] INTAS-98-500

Contents

Workshop on "a_0 Physics with ANKE"
July 13/14, 2000
ITEP, Moscow

Thursday, July 13

Chairperson: V. Chernyshev

10:00		Welcome
10:10	*M. Büscher (FZJ)*	Status of ANKE and planned measurements on pp → da_0^+
10:40	*Yu. Kalashnikova (ITEP)*	Scalar mesons: Why they are interesting
11:10	*L. Kondratyuk (ITEP)*	Properties of the $a_0/f_0(980)$ mesons
11:40	*V. Grishina (INR)*	a_0 production at COSY energies

L. Kondratyuk

13:30	*J. Haidenbauer (FZJ)*	Description of the $a_0/f_0(980)$ mesons with the Jülich model
14:00	*A. Kudryavtsev (ITEP)*	Perspectives of a_0^- studies
14:30	*V. Tarasov (ITEP)*	A possibility for direct measurements of a_0/f_0 mixing
14:50	*B. Kerbikov (ITEP)*	Superallowed a_0/f_0 mixing

H. Ströher

16:00	Round-table discussion:	Perspectives of the a_0^+ studies with ANKE
17:00	Dinner	

Friday, July 14

M. Büscher

10:00	*V. Kleber (FZJ)*	Simulations for the a_0^+ studies with ANKE
10:30	*N. Lang (Münster)*	Status of the cluster-jet target
11:00	*V. Komarov (JINR)*	The ANKE forward detectors and luminosity monitoring
11:50	*Chr. Leim (FZJ)/ G. Macharashvili(JINR)*	Preparation of the forward Cerenkov counters
12:10	*H. Junghans (FZJ)*	Data-analysis software
12:30	*I. Lehmann (FZJ)*	Luminosity monitoring with the spectator counters
14:00	Excursion to experimental facilities of ITEP	

K. Sistemich

15:00	*V. Chernyshev (ITEP)*	Future activities at ITEP/Status of the pellet target
15:30	*H. Ströher (FZJ)*	Future activities at ANKE

M. Büscher

16:30	Concluding discussion:	Future activities, responsibilities, ...

List of participants

	Name	Institution	e-mail
1	V. Baru	ITEP, Moscow / FZ Jülich	
2	A. Boukharov	MEI, Moscow	bav@monsy.mpei.ac.ru
3	M. Büscher	FZ Jülich	m.buescher@fz-juelich.de
4	V. Chernetsky	ITEP, Moscow	chernetsky@vitep5.itep.ru
5	V. Chernyshev	ITEP, Moscow	yurikis@vxitep.itep.ru
6	P. Fedorets	ITEP, Moscow / FZ Jülich	fedorets@vitep5.itep.ru
7	V. Gani	ITEP, Moscow	
8	Ye. Golubeva	INR, Moscow	golubeva@al20.inr.troitsk.ru
9	V. Grishina	INR, Moscow	grishina@cpc.inr.ac.ru
10	J. Haidenbauer	FZ Jülich	j.haidenbauer@fz-juelich.de
11	M. Hartmann	FZ Jülich	m.hartmann@fz-juelich.de
12	H. Junghans	FZ Jülich	h.junghans@fz-juelich.de
13	A. Kacharava	JINR, Dubna	andro@nusun.jinr.ru
14	V. Kanavets	ITEP, Moscow	kanavets@vitep5.itep.ru
15	Yu. Kalashnikova	ITEP, Moscow	yulia@vxitep.itep.ru
16	B. Kerbikov	ITEP, Moscow	
17	Yu. Kiselev	ITEP, Moscow	yurikis@vxitep.itep.ru
18	V. Kleber	FZ Jülich	v.kleber@fz-juelich.de
19	V. Komarov	JINR, Dubna	komarov@nusun.jinr.ru
20	L. Kondratyuk	ITEP, Moscow	kondrat@heron.itep.ru
21	V. Koptev	PNPI, Gatchina	koptev@hep486.pnpi.spb.ru
22	A. Kudryavtsev	ITEP, Moscow	kudryavt@heron.itep.ru
23	V. Kurbatov	JINR, Dubna	kurbatov@jinr.dubna.ru
24	N. Lang	Univ. Münster	langn@ikp.uni-muenster.de
25	I. Lehmann	FZ Jülich	i.lehmann@fz-juelich.de
26	C. Leim	FZ Jülich	c.leim@fz-juelich.de
27	G. Macharashvili	JINR, Dubna	gogi@nu.jinr.ru
28	A. Petrus	JINR, Dubna	petrus@nusun.jinr.ru
29	K. Sistemich	FZ Jülich	k.sistemich@fz-juelich.de
30	H. Ströher	FZ Jülich	h.stroeher@fz-juelich.de
31	V. Tarasov	ITEP, Moscow	tarasov@itep.ru
32	V. Ushakov	ITEP, Moscow	ushakov@vxitep.itep.ru
33	Yu. Uzikov	JINR, Dubna	uzikov@nusun.jinr.ru
34	S. Yashenko	JINR, Dubna	yashenk@nu.jinr.ru

COSY Proposal # 55, March 1997

Spokesperson: V. Chernyshev

Institute for Experimental and Theoretical Physics
B. Cheremushkinskaya 25
117259 Moscow
Russia

Study of a_0 mesons in the reaction $pp \to d\,a_0^+ \to d\,K^+\overline{K}^0$ at ANKE

L. A. Kondratyuk, V. P. Chernyshev
Institute of Theoretical and Experimental Physics,
117259 Moscow, Russia

Ye. S. Golubeva
Institute of Nuclear Research,
117312 Moscow, Russia

M. Büscher, O. W. B. Schult, H. Seyfarth, K. Sistemich
Institut für Kernphysik, Forschungszentrum Jülich,
D-52425 Jülich, Germany

H. Müller
Institut für Kern- und Hadronenphysik, Forschungszentrum Rossendorf
D-01314 Dresden, Germany

A. Kacharava
Laboratory of Nuclear Problems, Joint Institute of Nuclear Research
141980 Dubna, Russia

and the ANKE collaboration

Spokesperson: V. Chernyshev (chernyshov@vitep3.itep.ru)
Local contact: M. Büscher (m.buescher@kfa-juelich.de)

March 10, 1997

Abstract

We propose to measure the cross section of the reaction $pp \to d\,a_0^+ \to d\,K^+\overline{K}^0$ and the mass spectra of the $K^+\overline{K}^0$ system at energies $T_p = 2.52 \ldots 2.60$ GeV at COSY using the ANKE spectrometer and a frozen-pellet target. Within approx. one week of beam time we intend to collect a few thousand events of a_0^+ decays into $K^+\overline{K}^0$ at different energies between 2.52 and 2.60 GeV. The results will help to clarify whether the a_0^+ is a real resonance or a $K^+\overline{K}^0$ threshold cusp.

Contents

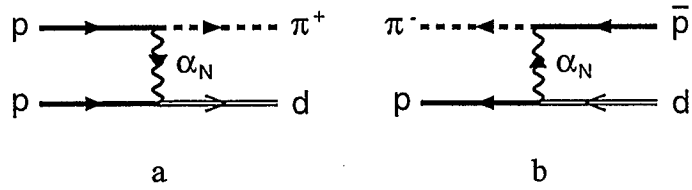

Figure 1: Exchange of a neutron-like Reggeon (three valence quarks udd) in the direct $pp \to d\pi^+$ **a** and line-reversed $\bar{p}d \to p\pi^-$ **b** reactions

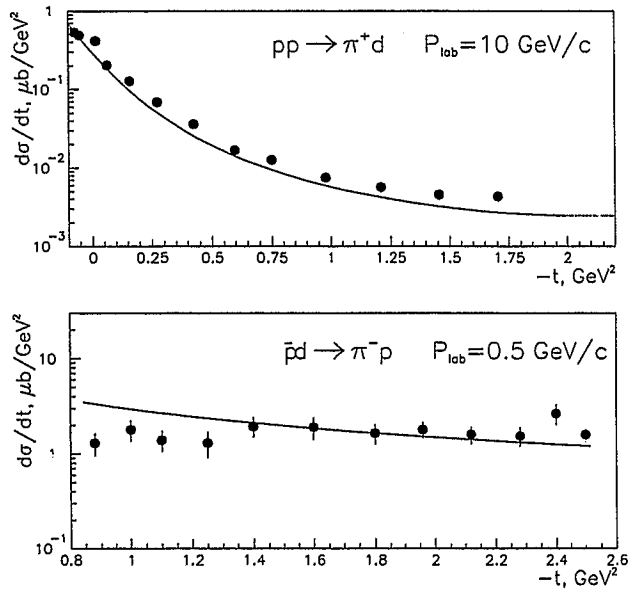

Figure 2: Differential cross sections of the reactions $pp \to d\pi^+$ **a** and $\bar{p}d \to p\pi^-$ **b**. The solid curves are calculated within the QGSM

of the amplitudes $\bar{p}d \to pa_0^-$ and $\bar{p}d \to p\pi^-$. The latter can be found using the calculations of the branching ratios for the Pontecorvo reaction $\bar{p}d \to pa_0^-$, performed by Bussa et al. [11]. In Table 1 we show that the predictions of the branching ratios for different Pontecorvo reactions $\bar{p}d \to NM$ within the framework of the relativistic two step model developed in [12] agree very well with the available experimental data of the Crystal Barrel and OBELIX collaborations [13, 14]. The calculated branching ratio of the reaction $\bar{p}d \to pa_0^-$ presented in Table 1 is in agreement with preliminary data from OBELIX [15] which show comparable yields for $a_0^0 n$ and ϕn production in $\bar{p}d$ annihilation at rest into K^+K^-n.

Table 1: Branching ratios for different reactions $\bar{p}d \to NM$ found in [11] in comparison with the experimental data of the Crystal Barrel and OBELIX collaborations [13, 14]

$\bar{p}d \to MN$	Exp. BR in 10^{-6}	Theor. BR in 10^{-6}
$\pi^- p$	12.9 ± 0.8	12.9 ± 0.7
ηn	3.19 ± 0.48	6.22 ± 0.6
$\eta' n$	8.2 ± 3.4	5.95 ± 0.75
$\rho^- p$	29.0 ± 7.0	31.1 ± 3.4
ωn	22.8 ± 4.1	17.0 ± 0.3
ϕn	2.7 ± 0.5	1.7 ± 0.3
$a_0^- p$	?	$6 \ldots 12$

In Fig.3 we present the cross sections of the reactions $pn \to d\phi$ and $pp \to da_0^+$ calculated within this approach. We used branching ratios $BR(\bar{p}d \to N\phi) = 2 \cdot 10^{-6}$ and $BR(\bar{p}d \to pa_0^-) = (9 \pm 3) \cdot 10^{-6}$. The cross section of the reaction $pn \to da_0^0$ is expressed through the cross section of reaction (1) using isotopic invariance. If there is strong mixing of a_0 and f_0 ([6]) then the isotopic invariance will be violated in this case. From Fig.3 it can be seen that at the maximum energy for COSY $T_p = 2.60$ GeV ($p_p \approx 3.4$ GeV/c) the cross section of reaction (1) is about (0.33 ± 0.11) μb. This value is in agreement with the cross section found within the framework of the Rossendorf-Collision Model [16, 17] which predicts $\sigma(p(2.6\ \text{GeV})p \to da_0^+) \approx 0.3$ μb.

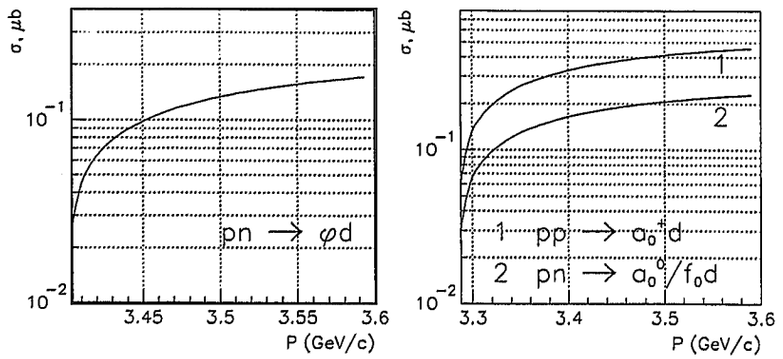

Figure 3: Total cross sections of the reactions $pn \to d\phi$, $pp \to da_0^+$ and $pn \to da_0^0$ calculated within the QGSM

In Fig.4 we present the missing-mass spectrum of a_0^+ mesons $M(a_0^+) = MM(pp,d)$ at $T_p = 2.52$ GeV and $T_p = 2.60$ GeV. We compare two different approaches for the description of the a_0 peak, seen by the Crystal Barrel collaboration [13] in $\eta\pi^0$ invariant mass from $\bar{p}p$ annihilation at rest: i) Breit-Wigner distribution with $M_R = 982$ MeV and $\Gamma_R = 54$ MeV [13]; ii) Flatte distribution [5]. Both approaches give an equally good description of the Crystal Barrel data on $M(\eta\pi^0)$, because the sharp peak in the Flatte distribution is smoothed by the experimental mass resolution. In our case the shapes of the mass distributions are essentially different for cases i) and ii) at $T_p \leq 2.60$ GeV because of the strong influence of the threshold cut at higher masses, compare Fig. 4a and b.

The $K^+\overline{K}^0$ invariant mass distributions for case i) are shown in Fig.5 a at different T_p. They are cut by the threshold effect at higher masses and by the $K\overline{K}$ phase space at lower masses. Those cuts cause a rather strong energy dependence of the cross section of reaction (1) which is equal to $8.35 \cdot 10^{-4}$, $7 \cdot 10^{-3}$ and $1.7 \cdot 10^{-2}$ μb at 2.52, 2.56 and 2.60 GeV, respectively.

The shape of the $K^+\overline{K}^0$ mass distribution is model dependent. In Fig.5 b we present $d\sigma/dM$ for case i) at two different values of $\Gamma_R = 54$ and 100 MeV and for the Flatte distribution (case ii)) normalised to the BW case with $\Gamma_R = 54$ MeV. The positions of the maxima of the solid and dotted curves are shifted by 15 MeV. The dashed curve is rather smooth. As the mass resolution in our case is expected to be about 7 MeV (see chapter 4.5), all three presented shapes of $d\sigma/dM$ can be distinguished.

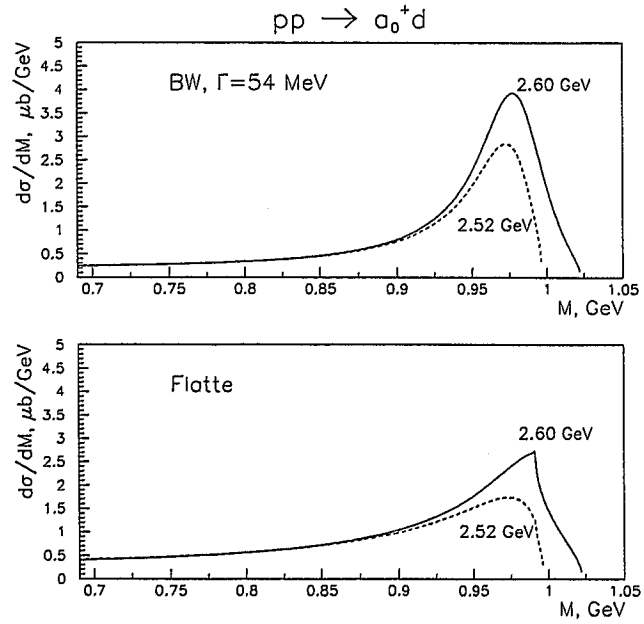

Figure 4: Missing-mass spectrum $MM(pp,d)$ for the reaction $pp \to da_0^+$ at different beam energies for the Breit-Wigner approach **a** and a Flatte distribution **b**

Reaction (1) can be identified detecting the deuteron and the K^+ meson. The main goal will be to measure the cross section of reaction (1) and the mass spectra of the $K^+\overline{K}^0$ system at different energies. If the a_0 is a molecule or a threshold cusp some narrow structure in $d\sigma/dM$ should appear at small masses and it will not change much with increasing beam energy from 2.52 to 2.60 GeV. However, if it is a genuine resonance the shape of the peak

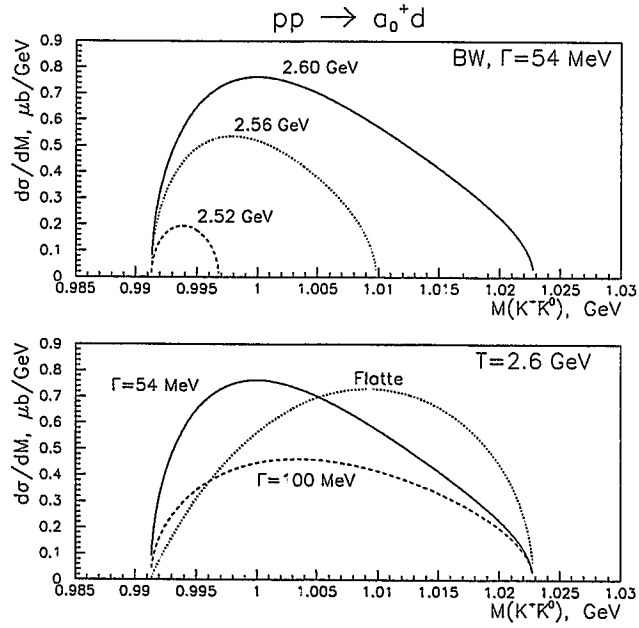

Figure 5: Invariant mass spectrum $M(\mathrm{K}^+\overline{\mathrm{K}}^0)$ for the reaction $\mathrm{pp} \to \mathrm{da}_0^+$ at different energies for the Breit-Wigner approach **a** and for various shapes of the a_0 peak at $T_\mathrm{p} = 2.6$ GeV **b**

will change as it is shown in Fig.5 **b** for the BW case or Flatte distribution.

In Fig.6 we present the momentum and angular distributions of deuterons and kaons at $T_\mathrm{p} = 2.52$ and 2.60 GeV. The maximum of the momentum distribution is near 2.2 GeV/c for deuterons and near 0.6 GeV/c for kaons. The angular distribution for deuterons and kaons (only for $T_\mathrm{p} = 2.52$ GeV) is forward peaked at $\vartheta \leq 8°$. At $T_\mathrm{p} = 2.6$ GeV the kaons have a broader angular distribution with a maximum at $\vartheta = 6 \ldots 10°$.

3 Experimental program

We intend to study the a_0^+ production in the reaction $\mathrm{pp} \to \mathrm{d}\,\mathrm{a}_0^+ \to \mathrm{d}\,\mathrm{K}^+\overline{\mathrm{K}}^0$ at different beam energies between $T_\mathrm{p} = 2.52$ and 2.60 GeV. We propose to start with the measurement of the cross section of reaction (1) and the shape of the $\mathrm{K}^+\overline{\mathrm{K}}^0$-mass distribution. This is possible by simultaneously measuring the deuteron and K^+ momenta and angles. The 4-momenta of the $\overline{\mathrm{K}}^0$ mesons can be reconstructed by a missing mass analysis. The structure of the a_0^+ meson can then be investigated by analyzing the invariant mass of the $\mathrm{K}^+\overline{\mathrm{K}}^0$ system. In principle, the inclusive measurement of deuterons would also allow the reconstruction of the a_0^+ mass. However, according to our estimates in the inclusive case the background of deuterons from channels not related to a_0^+ production is more than two orders of magnitude stronger and makes such an inclusive study impossible.

As the first measurement it seems useful to measure inclusive deuteron spectra from the reaction $\mathrm{pp} \to \mathrm{dX}$ since here the counting rates are larger and valuable information about the background conditions can be obtained in relatively short beam times. These kind of measurements have already been described in [18] and will be a part of the commissioning of the detection systems at ANKE.

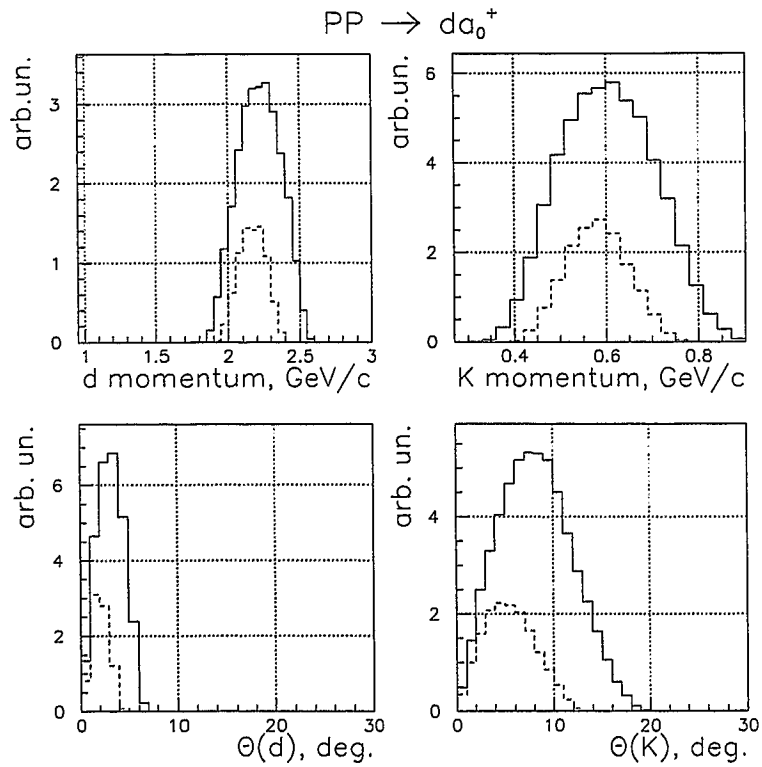

Figure 6: Mometum and angular distributions of deuterons and kaons from the reaction $pp \to da_0^+ \to dK^+\overline{K}^0$ at $T_p = 2.52$ GeV (dashed line) and $T_p = 2.60$ GeV (solid line)

After the study of the a_0^+ meson described here it is also foreseen to measure the production of the neutral mesons f_0 and a_0^0 in proton-neutron reactions ($pn \rightarrow da_0/f_0$) using deuterons as target material.

4 Experimental set-up

4.1 Description of the apparatus

The ANKE spectrometer [19] (see Fig.7) will allow to measure simutaneously positively and negatively charged particles emitted under forward angles $\leq 10°$. For the detection of K^+ mesons and deuterons and for the reduction of the background the following concept is suggested.

The K^+ mesons will be detected in the side detection system [20, 21] which will offer a K^+-detection efficiency of $\sim 10\%$ (including decay-in-flight between detectors and target) and a background supression (pions, protons and ejectiles scattered at the magnet iron) of more than 5 orders of magnitude [21, 22, 23, 24, 25] in the momentum range between 150 and 600 MeV/c. It allows to select events where a K^+ meson is produced with almost no background from other reaction channels. Kaons from a_0^+ decay have momenta in the range 400...800 MeV/c (Fig.6). Thus, the momentum acceptance of ANKE is about 50%. The angular distributions of kaons are also shown in Fig.6. If the primary proton-beam energy will be about 2.52 GeV practically all K^+ mesons are emitted into the forward angle cone $\vartheta \leq 10°$ and can be detected at ANKE.

The forward detector which is located between D2 and D3 will detect positively charged particles with momenta between 1.0 and 3.2 GeV/c [26]. At beam energies below 2.6 GeV deuterons from reaction (1) are emitted into a narrow forward cone with typical momenta around 2.2 GeV/c (Fig.6). Thus, they can be detected in the ANKE forward detector. According to simulation calculations the deuteron detection efficiency is $\sim 40\%$ and the background (mainly fast protons) suppression is about three orders of magnitude.

We conclude that the kinematical features of the process to be studied match the abilities of the ANKE set-up and that the detection systems will allow to identify reaction (1) with only very little background from other reaction channels by measuring K^+ mesons and deuterons.

4.2 The ITEP frozen-pellet target

Since we should be able to measure rather small cross sections $\sigma \approx 0.01...0.1\mu$b it is necessary to work at maximum luminosity. According to the time resolution of the ANKE detectors luminosities up to $L_{max} \approx 10^{33}$ sec^{-1} cm^{-2} can be used.

In order to achieve such high luminosities an effective target thickness of $d \approx 10^{16}$ atoms cm^{-2} at a proton beam intensity $n \approx 10^{11}$ is desirable. Since we plan to study meson production in pp and pn collisions, the target material should be hydrogen or deuterium. The only device which fulfills these requirements is a frozen-pellet target. Such a target is currently being built at ITEP and could be ready for operation at ANKE in 1999; its properties are listed in Table 2.

The pellet-target systems in ITEP were developed during 1992–1993. Since 1994 part of the equipment has been fabricated and an infrastructure for target tests has been prepared. A scheme of the target is shown in Fig.8. There are the following operational conditions for the pellet target developed at ITEP.

- The target can make available different kinds of target nuclei. For the measurements proposed here H_2 and D_2 will be used.
- The diameter of the spherical pellets can be varied between 20 and 100 μm.

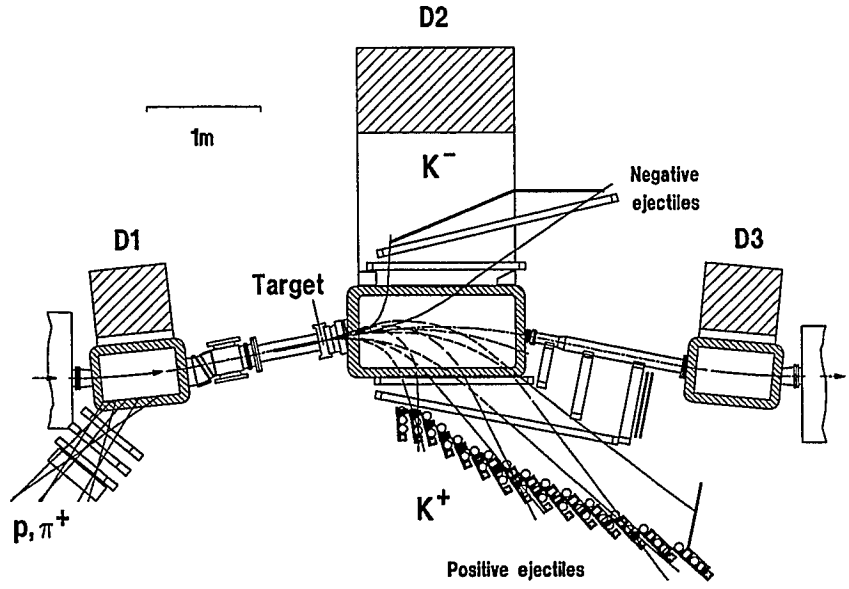

Figure 7: Layout of the setup at the ANKE spectrometer

Table 2: Densities of the ITEP frozen-pellet target with hydrogen as target material, a COSY-beam diameter of 2 mm, a beam intensity of $n = 3 \cdot 10^{10}$ and under the assumption that one pellet is in the beam

Diameter of pellet (μm)	Mass (g)	Total number of atoms per pellet	Luminosity · ($cm^{-2}s^{-1}$)
20	$3 \cdot 10^{-10}$	$1.8 \cdot 10^{14}$	$2.8 \cdot 10^{32}$
40	$2.3 \cdot 10^{-9}$	$1.4 \cdot 10^{15}$	$2.2 \cdot 10^{33}$
60	$8 \cdot 10^{-9}$	$4.8 \cdot 10^{15}$	$7.4 \cdot 10^{33}$

- The deviations of the pellet sizes is expected to be not more than 10%.
- The deviation of the pellet tracks in the horizontal plane is smaller than 100 μm.
- The flow rate of liquid Helium during the measurements is not higher than 1.5 liters per hour. The flow rate of liquid Nitrogen does not exceed two liters per hour.

It is foreseen to build the target such that as much existing equipment as possible (e.g. pumps and vacuum chambers of the Münster cluster-jet target for ANKE) can be used. A close collaboration with the target group from the University of Münster has been agreed upon.

4.3 Angular and momentum acceptance

With the ANKE detection systems positively charged particles in the momentum range $p_+ = 150 \ldots 3200$ MeV/c can be measured. Ejectiles with vertical emission angles between $\pm 8°$ ($p \approx 150$ MeV/c) and $\pm 3.5°$ ($p > 550$ MeV/c) can be detected. The K^+ mesons will be identified with the side-detector system which will offer a horizontal acceptance of $-10° < \vartheta < 10°$. Fast deuterons with momenta up to $p_{\rm max} \approx 3.2$ GeV/c will be detected in the forward detection system. Horizontal emission angles in the range $\vartheta \approx -1 \ldots 10°$ can be detected.

In Fig.9 the effect of the angular and momentum acceptance of ANKE on the measured K^+ and deuteron spectra is illustrated. In the lower part of the figure the calculated distributions are folded with the acceptance for the detection of K^+/d pairs in coincidence. From a comparison of the two momentum spectra in Fig.9 it can be concluded that the geometrical acceptance of ANKE for the detection of K^+/d pairs is $\epsilon \approx 9\%$. If one takes into account that $\sim 70\%$ of the kaons decay in flight between the target and the telescopes and that the detection efficiency in the detectors is $\sim 35\%$ for kaons and $\sim 90\%$ for deuterons, the total probability to detect a K^+/d pair is

$$\epsilon(K^+, d) \approx 0.8\% \, .$$

We also calculated the detection efficiency for the inclusive measurement of deuterons from the reaction $pp \to d a_0^+$ at $T_p = 2.60$ GeV. In this case we expect:

$$\epsilon(d) \approx 40\% \, .$$

4.4 Counting rates

For a detailed study of particle spectra we plan to observe about 10^3 a_0^+ decays into $K^+\overline{K}^0$ according to reaction (1) at different beam energies between 2.52 and 2.60 GeV. The predicted total cross section for $K^+\overline{K}^0$ production via the a_0^+ meson is about $\sigma_{\rm tot} \approx 0.017$ μb at $T_p = 2.60$ GeV (see Sect. 2). In order to minimize background we shall detect coincident deuterons and K^+ mesons from a_0^+ decay. Thus, for a luminosity of 10^{32} cm^{-2}s^{-1} (pellet target) the expected rate to observe an a_0^+ meson via its decay into $K^+\overline{K}^0$ is about:

$$\dot{n}(K^+, d) = \sigma \cdot \epsilon(K^+, d) \cdot L \approx 0.017 \cdot 10^{-30} \cdot 0.8 \cdot 10^{-2} \cdot 10^{32} = 0.014 \ {\rm s}^{-1}$$

or ~ 50 events per hour. Since about 10^3 a_0^+ shall be detected ~ 20 hours of production beam time will be needed at $T_p = 2.60$ GeV. At lower energies longer beam times will be needed in order to collect sufficient statistics.

In order to confirm the counting rate extimates described in this chapter we have also performed detailed GEANT simulations (for illustration see also e.g. [16] and Fig. 10) including a realistic 3 dimensional description of the magnetic field in D2. Within statistical uncertainties the results agree with the estimates given above.

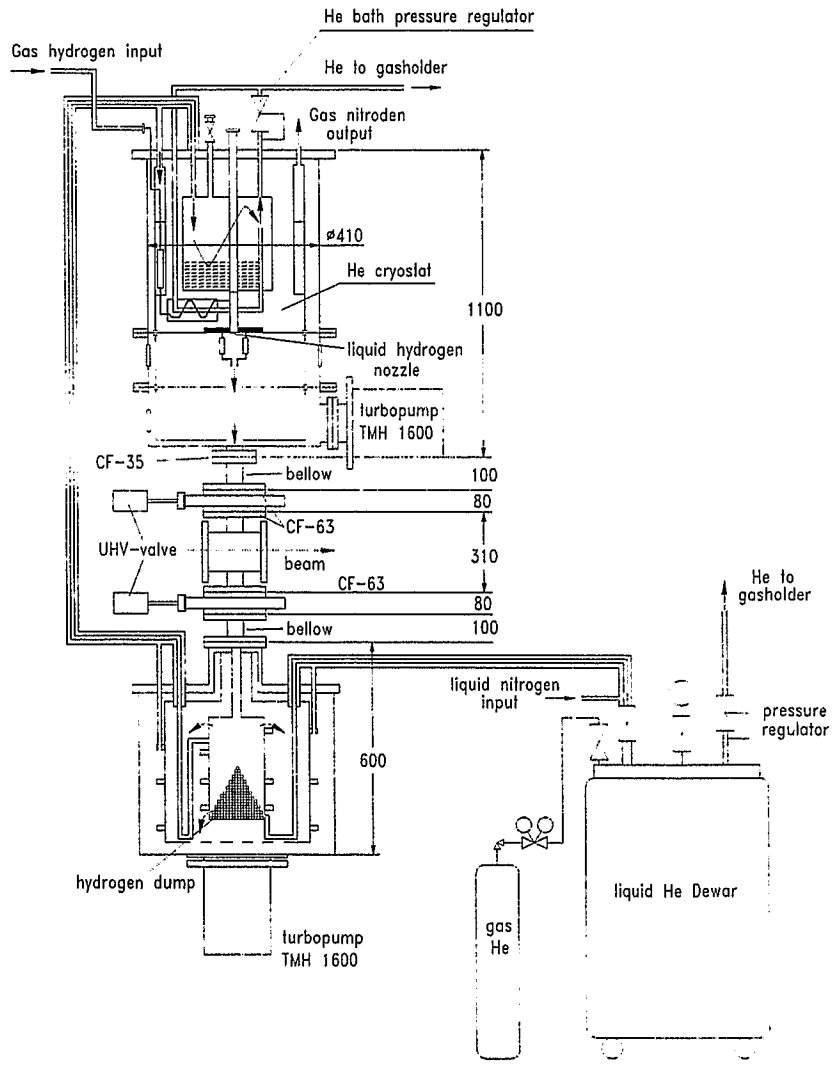

Figure 8: Layout of the ITEP frozen-pellet target

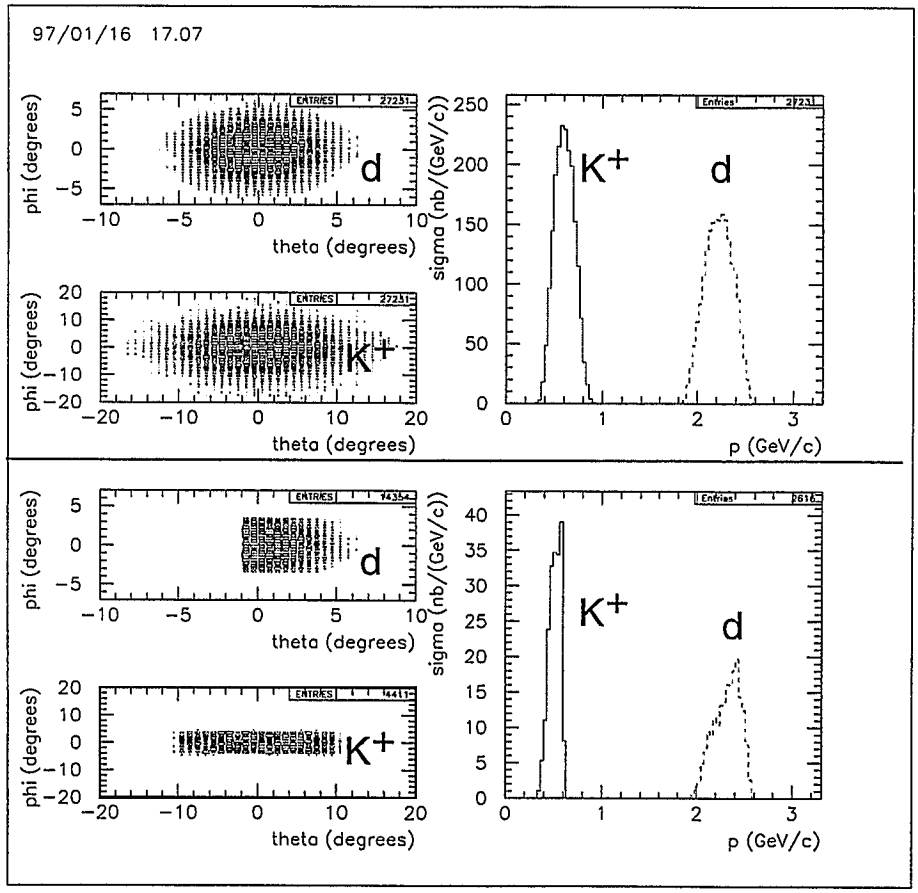

Figure 9: Angular (left) and momentum (right) distributions of K^+ mesons and deuterons from the reaction $pp \to da_0^+ \to dK^+\overline{K}^0$ at $T_p = 2.52$ GeV. The upper part of the figure shows the distributions calculated with the QGSM, in the lower part the angular and momentum acceptance of ANKE is taken into account

4.5 Missing mass resolution

The extraction of information on the structure of the a_0^+ meson requires a good resolution of the reconstructed a_0^+ mass. The accuracy should be in the range of a few MeV/c^2 (see also Fig. 5). We have performed GEANT simulations taking into account the particle propagation through D2, multiple scattering and energy losses in vacuum foils and detector components as well as the uncertainties of the track reconstruction procedure. Figure 10 shows the simulated tracks of K^+/d pairs which can be detected at ANKE. The simulation yields 'measured' track coordinates from the wire chamber information which allows to reconstruct the ejectile momenta at the target and, thus, the calculation of missing mass spectra.

Figure 11 shows the result of the calculations. The a_0^+ mass has been reconstructed from the measured tracks of the emitted deuterons according to the formula:

$$M(a_0^+) = MM(\mathrm{pp,d}) = (\mathcal{P}_{\mathrm{P_P}} + \mathcal{P}_{\mathrm{P_T}} - \mathcal{P}_{\mathrm{d}})^2 \ ,$$

where $\mathcal{P}_{\mathrm{P_P}}$, $\mathcal{P}_{\mathrm{P_T}}$ are the known 4-momenta of the projectile and target protons and $\mathcal{P}_{\mathrm{d}}$ the measured 4-momentum of the deuteron. It is known from earlier simulations that the momentum resolution for the measurements of deuterons with the forward detector is $\Delta p/p \approx$ 1.5% (FWHM).

From the right plot in Fig. 11 we conclude that the accuracy of the reconstructed a_0^+ mass ($\Delta m/m \approx 7$ MeV/c^2 (FWHM)) will be good enough to draw conclusions about the structure of this meson.

4.6 Background

For the study of reaction (1) the K^+ mesons will be detected in coincidence with deuterons and the a_0^+ will be reconstructed from the missing mass distribution MM(pp,d). We can expect the following background reactions during this experiment:

$$\mathrm{pp} \to \mathrm{d}\,\mathrm{K^+}\overline{\mathrm{K}}^0, \tag{2}$$

non-resonant production, and

$$\mathrm{pp} \to \mathrm{p}\,\mathrm{K^+}\mathrm{X} \ , \tag{3}$$

with misidentification of the proton as a deuteron.

Non-resonant $K^+\overline{K}^0$ production: The non-resonant $K^+\overline{K}^0$ production is expected to be rather small. We estimate it as follows: First we take the parametrization of the cross section of the reaction

$$\mathrm{pp} \to \mathrm{pp}\,\mathrm{K^+K^-} \tag{4}$$

from [27] $\sigma_{\mathrm{K^+K^-}} = A(1 - s_0/s)^3(s_0/s)^{0.8}$ where $\sqrt{s_0}$ is the threshold c.m. energy, $A = 0.8$ mb. This value of A can be found using the data $\sigma_{\mathrm{exp}} = (12 \pm 3)$ μb at $p_{\mathrm{lab}} = 4.95$ GeV/c. At 6 MeV above threshold this model predicts $\sigma_{\mathrm{K^+K^-}} \approx 60$ pb which is in reasonable agreement with preliminary data from COSY 11 [28]. At 32 MeV above threshold ($T_{\mathrm{p}} \approx 2.6$ GeV) we have $\sigma \approx 10^{-3}\mu$b which is essentially lower than the cross section of reaction (1) at the same energy. The main reason is the very sharp threshold behaviour of $\sigma_{\mathrm{K^+K^-}} \propto A(1 - s_0/s)^3$. On the other hand the threshold behaviour of σ for the quasi two-body reaction (1) is $\sigma_{\mathrm{da_0^+}} \propto (1 - s_0/s)^{0.5}$.

We have assumed that the cross section of the reaction

$$\mathrm{pp} \to \mathrm{pn}\,\mathrm{K^+}\overline{\mathrm{K}}^0 \tag{5}$$

is two times larger which is valid in the one-pion exchange model. Then we have calculated $\mathrm{d}\sigma/\mathrm{d}M$ in the OPE model for a relative energy of the pn pair of less than 5 MeV and found

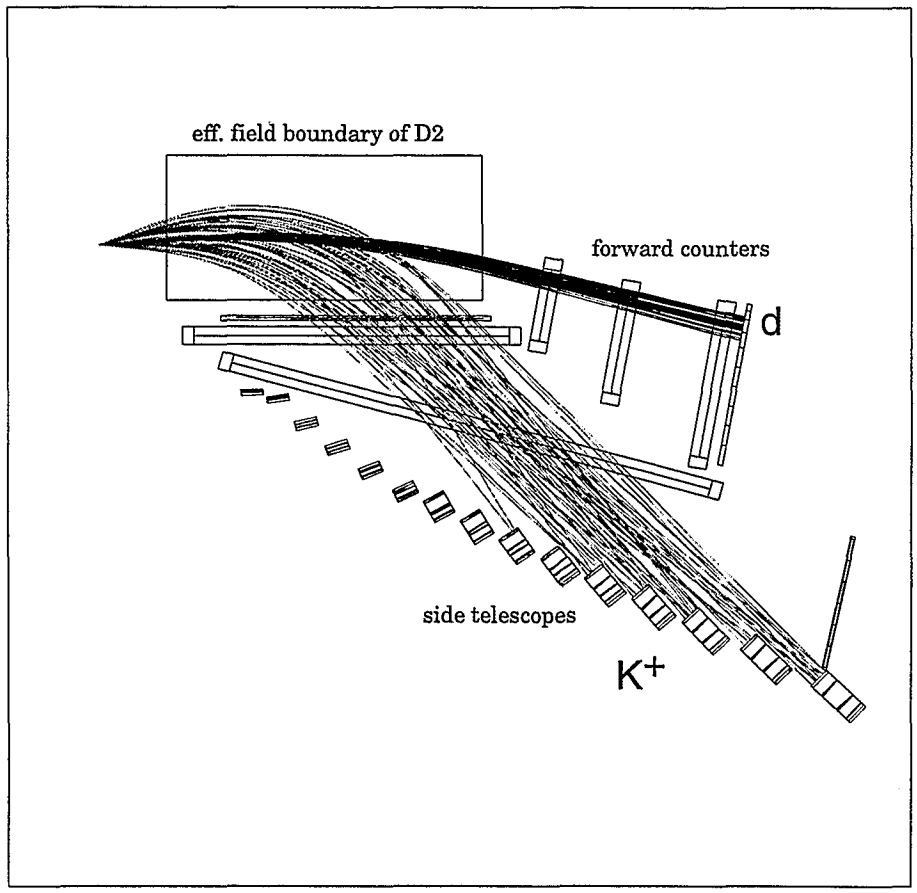

Figure 10: Tracks of 50 correlated K^+ mesons and deuterons from the reaction $pp \to da_0^+ \to dK^+\overline{K}^0$ at $T_p = 2.52$ GeV which are detected in the side and forward detectors

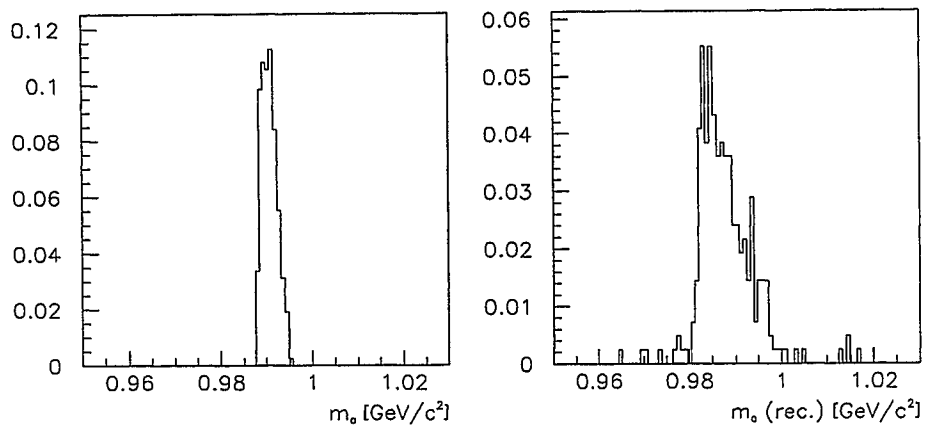

Figure 11: Missing mass $MM(\mathrm{pp,d})$ of deuterons from the reaction $\mathrm{pp} \to \mathrm{da}_0^+ \to \mathrm{dK}^+\overline{\mathrm{K}}^0$ at $T_\mathrm{p} = 2.52$ GeV. The left side of the figure shows the mass distribution from Fig. 5 folded with the acceptance of ANKE and measured with perfect resolution. In the right plot multiple scattering, energy losses and the uncertainties of the track reconstruction have been taken into account

$\mathrm{d}\sigma/\mathrm{d}M \leq 0.5 \cdot 10^{-3}$ μb/GeV at $M = 1$ GeV. This cross section is approximately three orders of magnitude smaller than for reaction (1), see Fig. 5. Therefore, the nonresonant background can be neglected.

Proton misidentification: The proton momentum spectrum for the reaction $\mathrm{pp} \to \mathrm{p}\Lambda\mathrm{K}^+$ and emission angles $\vartheta < 10^\circ$ is rather flat for momenta 1.5...2.5 GeV/c, see Fig. 12. We obtained

$$\left(\frac{\mathrm{d}\sigma}{\mathrm{d}\Omega \mathrm{d}p}\right)_\mathrm{p} \approx 40 \ \mu\mathrm{b}/(\mathrm{sr\,GeV/c}) \ . \tag{6}$$

According to our calculations with the Rossendorf-Collision Model all other channels of K^+ production can increase the proton yield not more than by a factor of two.

From the deuteron momentum spectrum shown in Fig. 12 we found for deuterons with momenta 2.0...2.5 GeV/c:

$$\left(\frac{\mathrm{d}\sigma}{\mathrm{d}\Omega \mathrm{d}p}\right)_\mathrm{d} \approx 1 \ \mu\mathrm{b}/(\mathrm{sr\,GeV/c}) \ . \tag{7}$$

Therefore, the expected d/p ratio at $p \approx 2.2$ GeV/c is about $n(\mathrm{d})/n(\mathrm{p}) \approx 10^{-2}$.

According to our GEANT simulation calculations of the p/d discrimination in the forward detector, these counters will suppress protons by at least three orders of magnitude whereas the deuteron detection efficiency is higher than 80%. This high proton suppression can be achieved with tilted Čerenkov counters based on the principle of total internal reflection [29]. These counters offer an on-line proton suppression by more than two orders of magnitude. Additionally, in an off-line analysis of the TOF between the target and forward counter (start time at the target obtained from the reconstruction of the K^+ tracks) an additional suppression by more than one order of magnitude will be possible [21].

5 Requested time for measurements

We propose to start the study of the scalar mesons structure with the measurement of the background conditions. At the first stage of experiment we plan to measure the missing mass

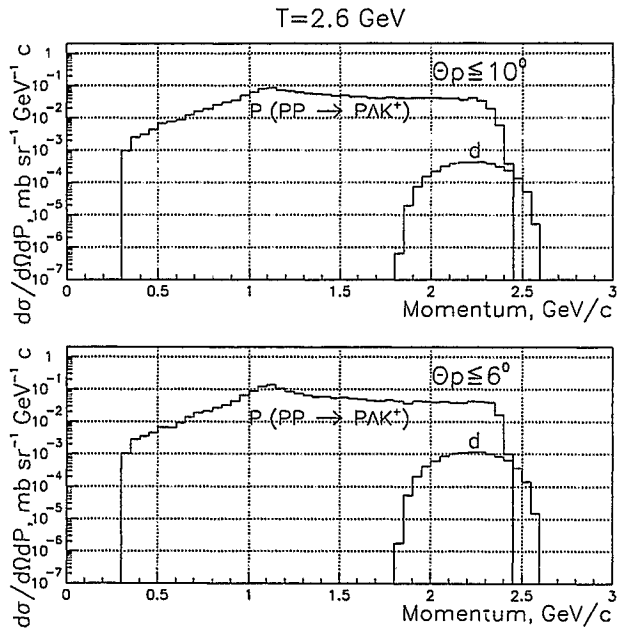

Figure 12: Calculated momentum spectrum of protons from the reaction p(2.6 GeV)p $\rightarrow$ pΛK$^+$ and deuterons from reaction (1) with emission angles $\vartheta < 10°$ **a** and $\vartheta < 6°$ **b**

distribution for the inclusive reaction pp $\rightarrow$ dX$^+$ at $T_p \approx 2.6$ GeV. Then we want to measure deuterons and K$^+$ mesons from the reaction pp $\rightarrow$ d $a_0^+ \rightarrow$ d K$^+\overline{\text{K}}^0$.

Summarizing, we apply for the following amount of beam time:

- One week for calibration measurements and background studies using a target with relatively low luminosity e.g. a cluster-jet target as soon as the detectors for K$^+$ mesons and fast deuterons are available at ANKE (Middle of 1998). These measurements will allow to calibrate the p/d suppression in the Čerenkov counters.
- One week for the invariant mass measurements when the frozen-pellet target will be ready (End of 1999).

In a later stage of the proposed studies it is also planned to apply for beam time to measure the reactions pn $\rightarrow$ dX using the frozen-pellet target.

Acknowledgements

We are very grateful to W. Cassing, C. Guaraldo, U. Mosel and J. Speth for useful discussions and to W. Oelert for providing us the cross section for the reaction pp $\rightarrow$ pp K$^+$K$^-$.

References

[1] J. Weinstein, Proc. Int. Conf. on Particle Production near Threshold, Nashville, U.S.A., 1990, Particles and Fields Series 41, H. Nann and E. J. Stephenson, Edts., AIP, New York (1991) p.256.

[2] F.E.Close et al., Phys.Lett.**B 319** (1993) 291.

[3] M.Genovese et al., Nuovo Cim.**107A** (1994) 1249.

[4] G.Janssen, B.Pierce, K.Holinde and J.Speth, Phys.Rev.**D 52** (1995) 2690.

[5] V.V.Anisovich et al., Phys.Lett.**B 355** (1995) 363.

[6] J. Speth, *private communication.*

[7] R.M.Barnett et al. (Particle Data Group), Phys.Rev.**D 54** (1996) 1.

[8] L.de Billy et al., Nucl.Phys.**B 176** (1980) 1.

[9] A.B.Kaidalov, Sov.J.Nucl.Phys.**53** (1991) 872.

[10] C.Guaraldo, A.B.Kaidalov, L.A. Kondratyuk and Ye.S. Golubeva, Proc. of the 3rd Int. Conf. on Nucleon-Antinucleon Physics (NAN'95), Phys. of Atomic Nuclei **59** (1996) 1832.

[11] M.P.Bussa, Ye.S.Golubeva,C.Guaraldo,L.A.Kondratyuk and L.Valacca, *in preparation.*

[12] L.A.Kondratyuk and C.Guaraldo, Phys.Lett.**B 256** (1990).

[13] C.Amsler et al., Yad.Fiz.**59** (1996) 1473.

[14] V.G.Ableev et al., Nucl.Phys.**A 562** (1993) 617.

[15] M.Bussa and P.Cerello, *private communication.*

[16] H.Müller et al., COSY Proposal #21: Study of K^- production (1996).

[17] H.Müller, Z.Phys.**A 339** (1991) 409.

[18] V.Koptev et al., COSY Proposal #38: NN Final-State Interactions in Single Pion Production (1996).

[19] O.W.B.Schult et al., IKP-KFA Annual Report 1992, p.11 (1993).

[20] A.Franzen, M.Büscher, IKP-KFA Annual Report 1994, p.57 (1995).

[21] M.Büscher et al., Communication of the JINR, Dubna 1996.

[22] M.Büscher et al., Z.Phys.**A 355** (1996) 93.

[23] M.Büscher and H.Müller, IKP-KFA Annual Report 1994, p.72 (1995).

[24] N.Amaglobeli et al., IKP-KFA Annual Report 1993, p.55 (1994).

[25] M.Büscher et al., IKP-KFA Annual Report 1994, p.63 (1995).

[26] V.I.Komarov et al., IKP-KFA Annual Report 1993, p.57 (1994).

[27] A.Sibirtsev et al., Preprint of Giessen University, December 16, 1996

[28] W.Oelert, *private communication.*

[29] A.K.Kacharava et al., NIM **A 376** p.356 (1996)

Beam-time Request for COSY Proposal # 55, March 2000

Spokesperson: M. Büscher

Institut für Kernphysik
Forschungzentrum Jülich
52425 Jülich
Germany

Beam-time request for COSY experiment #55 "Study of $a_0^+(980)$ mesons at ANKE"

M. Büscher, H. Junghans, V. Kleber, R. Koch, R. Schleichert, K. Sistemich, H. Ströher
Institut für Kernphysik, Forschungszentrum Jülich, D-52425 Jülich, Germany

V. P. Chernyshev, P. Fedorets, L. A. Kondratyuk
Institute of Theoretical and Experimental Physics, 117259 Moscow, Russia

Ye. S. Golubeva, V. Grishina
Institute of Nuclear Research, 117312 Moscow, Russia

V. Koptev, S. Mikirtychiants
High Energy Physics Dept., Petersburg Nuclear Physics Institute 188350 Gatchina, Russia

A. Khoukaz
Institut für Kernphysik, Universität Münster Wilhelm-Klemm-Str. 9, D-48149 Münster, Germany

A. Kacharava, G. Macharashvili
Lab. of Nuclear Problems, Joint Institute of Nuclear Research 141980 Dubna, Russia

B. Chiladze, M. Nioradze
High Energy Physics Institute, Tbilisi State University University Str. 9, 380086 Tbilisi, Georgia

I. Zychor
The Andrzej Soltan Institute for Nuclear Studies PL-05400 Swierk, Poland

and the ANKE collaboration

Spokesperson: M. Büscher (m.buescher@fz-juelich.de)

March 28, 2000

Abstract

We request two weeks of beam time for a simultaneous measurement of the reactions $pp \to d a_0^+ \to d K^+ \bar{K}^0$ and $pp \to d a_0^+ \to d \pi^+ \eta$ with ANKE at maximum COSY-beam energy of $T \approx 2.6$ GeV. The data will be used to determine the branching ratio $a_0^+ \to K^+ \bar{K}^0 / \pi^+ \eta$ which is not well known so far.

1 Introduction

This beam-time request is based on COSY proposal #55 [1] which was approved during the 14th meeting of the COSY-PAC. The proposal foresees the measurement of the reaction $pp \to d\,a_0^+ \to d\,K^+\overline{K}^0$ at various beam energies between threshold ($T = 2.48$ GeV, $p = 3.29$ GeV/c) and the maximum achievable COSY energy ($T \approx 2.6$ GeV). The goal of the measurements is to determine the mass distribution of the $a_0^+(980)$ with high statistical accuracy as a function of T which should allow to draw conclusions about the nature of this resonance.

The measurements proposed here are a natural extension of the original proposal. The simultaneous measurement of the two decay channels $a_0^+ \to K^+\bar{K}^0/\pi^+\eta$ seems to be suitable to shed light on the nature of the a_0^+ resonance. It is shown that the measurements can be performed within two weeks of beam time with the cluster-jet target which has been installed and successfully put into operation at ANKE in summer of 1999. Furthermore, the data on the a_0^+-production cross section obtained during this first beam time at maximum COSY energy will allow to determine the total beam time needed to perform the full measurements closer to threshold described in the original proposal.

This beam-time request updates the theoretical and simulation calculations of the original proposal and gives rate estimates on the $a_0^+ \to \pi^+\eta$ channel which has not been considered before. It is shown that also for this reaction channel the background can be sufficiently suppressed.

2 Physics case

The scalar meson sector plays a very important role in the physics of hadrons. Nevertheless, the structure of the lightest scalar mesons $a_0(980)$ and $f_0(980)$ is not understood yet and is one of the most important topics of hadronic physics (see e.g. [2, 3, 4, 5, 6, 7] and references therein). It has been discussed that they could be either "Unitarized $q\bar{q}$ states", "Four-quark cryptoexotic states", $K\overline{K}$ molecules or vacuum scalars (Gribov's minions) (see e.g. [6]). Nowadays theory gives some preference to the Unitarized Quark Model (UQM), proposed by Tornqvist [8] (see e.g. [6, 7]). However, other options cannot be ruled out completely. Moreover, there is a strong mixing between the uncharged $a_0(980)$ and the $f_0(980)$ due to coupling to $K\overline{K}$ intermediate states [9]. Therefore, it is of particular interest to study the charged components of the $a_0(980)$ which are not mixed with the $f_0(980)$ and preserve their original quark content.

Until now the charged components of the $a_0(980)$ were studied mainly in the $\eta\pi^+$ or $\eta\pi^-$ channels [10]. Recent experimental data from the E852 Collaboration at BNL yield for the charged a_0^+ meson a mass of (998.3 ± 4.0) MeV/c^2 and a width of (72 ± 10) MeV/c^2[11]. Note that the mass of the a_0 reported by the E852 Collaboration is significantly larger than the average value of 983.4 ± 0.9 MeV/c^2 quoted by the particle data group (PDG) [10].

The Branching Ratios (BR's) into the two main a_0 decay channels $\eta\pi$ and $K\overline{K}$ are still unclear: the $\eta\pi$ mode is quoted by the PDG [10] as "dominant" and the $K\bar{K}$ mode as "seen". The data from only two experiments [12, 13], where decay of the $a_0(980)$ into $K\overline{K}$ was observed, are used for the PDG analysis. The authors of [13] report a ratio of branching ratios

$$B(\bar{p}p \to a_0\pi; a_0 \to K\bar{K})/B(\bar{p}p \to a_0\pi; a_0 \to \pi\eta) = 0.23 \pm 0.05\ . \qquad (1)$$

However, the second branching ratio which they took from [14] may have a large systematic uncertainty stemming from a strong interference of the a_0 signal with a broad resonance $a_0(1450)$, which has a width of about 265 MeV. As a result the $a_0(980)$ distribution in the reaction $p\overline{p} \to \eta\pi^0\pi^0$ appeared to be distorted. Moreover, the invariant-mass resolution in [13, 14] is only ~ 27 MeV/c^2. Therefore, it is necessary to measure the relative fraction of the two main a_0 decay channels $\eta\pi$ and $K\overline{K}$ with high mass resolution $\Delta m < 10$ MeV/c^2 and lower background in an independent experiment (see also discussion in Sect.3.1). An important dynamical feature of this experiment at COSY is that the $a_0(980)$ will be produced not far from its threshold, thus the $a_0(980)$ signal will not be contaminated by the tails from higher resonances.

The comparison of the yields from both decay channels will be used for the determination of the relative BR's into $\eta\pi$ and $K\overline{K}$. This value as well as the width of the $a_0(980)$ in both decay channels will be important for further tests of the existing a_0 models, see Sect.3.1.

It should be noted that the a_0^+-production cross section in pp collisions at near-threshold energies is basically unknown. The model calculations presented in Sect.3.2 therefore may have substantial uncertainties. Thus, the determination of the production cross section alone already is an interesting task. This quantity is also sensitive to the nature of the $a_0(980)$ and will be a "by-product" of the measurements proposed here.

3 Theoretical considerations

3.1 Models and existing data on the strengths of the $K\overline{K}$ and $\pi\eta$ decay channels

Within the framework of a coupled channel formalism the $a_0(980)$ can be considered as a normal $q\overline{q}$ resonance with a large admixture of $K\overline{K}$ and $\eta\pi$ continuum

$$|a_0\rangle = C_{q\overline{q}}|q\overline{q}\rangle + C_{K\overline{K}}|K\overline{K}\rangle + C_{\eta\pi}|\eta\pi\rangle \ . \tag{2}$$

Then an appropriate parametrization of the shape of the $a_0(980)$ in each ($\eta\pi$ or $K\overline{K}$) channel can be made in the form proposed by Flatté [15]:

$$|A_i|^2 = const. \cdot \frac{|\Gamma_i(M)|\ M_r^2}{(M^2 - M_r^2)^2 + M_r^2|\Gamma_{tot}^2(M)|} \tag{3}$$

where $\Gamma_{tot}(M) = \Gamma_1(M) + \Gamma_2(M) = g_1\rho_1 + g_2\rho_2$; g_1 and g_2 are the coupling constants to the two final states and ρ_i can be expressed through the momenta of the final particles $\rho_i = 2q_i/M$; M_r is the K-matrix pole. Molecular or "threshold cusp" cases would imply a dominance of the $|K\overline{K}\rangle$ component and, therefore, would correspond to a relatively large ratio $R = (g_2/g_1) \gg 1$. In the following table we present the most recent results for the $a_0(980)$ parameters.

Reaction	R	M_r [GeV]	g_1 [GeV]
$p\overline{p} \to \eta\pi^0\pi^0$, $\eta\eta\pi^0$ [16] $^{i)}$	$1.05 \div 2.05$	$1.013 \div 1.058$	$0.241 \div 0.287$
$p\overline{p} \to \eta\pi^0\pi^0$, $\eta\eta\pi^0$ [16] $^{ii)}$	$1.05 \div 1.45$	$1.004 \div 1.024$	$0.229 \div 0.312$
$p\overline{p} \to \eta\pi^0\pi^0$, $\eta\eta\pi^0$ [16] $^{iii)}$	$1.12 \div 1.37$	$0.999 \div 1.006$	$0.211 \div 0.275$
$p\overline{p} \to \eta\pi^0\pi^0$ [14] $^{iv)}$	1.15 ± 0.10	0.999 ± 0.006	0.218 ± 0.020
$p\overline{p} \to K_L K^{\pm}\pi^{\mp}$ [13] $^{v)}$	1.03 ± 0.4	0.999 ± 0.002	0.324 ± 0.015
$\pi^- p \to n\eta\pi^-\pi^+$, $n\eta\pi^0$ [11] $^{vi)}$	0.91 ± 0.10	$1.001 \div 0.0019$	0.122 ± 0.008

$^{i)}$ without any external constraint
$^{ii)}$ with constraint on $|A_i|^2$ at half-height from the reaction $p\overline{p} \to \eta\omega\pi^0$
$^{iii)}$ with constraint on $|A_i|^2$ at half-height from the reaction $p\overline{p} \to \eta\omega\pi^0$ and contribution from a hypothetical $a_2'(1620)$
$^{iv)}$ solution B with constraint on the a_0 mass from the reaction $p\overline{p} \to \eta\omega\pi^0$
$^{v)}$ with constraint that the ratio of integrated intensities in $K\overline{K}$ and $\eta\pi$ channels is given by Eq.(1)
$^{vi)}$ the authors of [11] present the value $g_{\pi\eta} = 0.243 \pm 0.015$ which is related to g_1 by $g_{\pi\eta} = (2/M)\, g_1$

In [16] it was shown that if the fit of the $\eta\pi$-mass distribution is made without any additional constraint, the parameters M_r, R and g_1 cannot be determined very well. They are strongly correlated and if one of them is varied in steps, χ^2 changes rather slowly but M_r, R and g_1 move together. That is why additional constraints are used in most fits.

In [11] also a Breit-Wigner (BW) fit of the $a_0(980)$ shape in the $\eta\pi$ channel was done. The mass and width of a_0^+ were determined to be (996.4 ± 1.6) and (62 ± 6) MeV/c^2, respectively. The two determinations of the a_0 mass and width (BW and Flatté) were found to be statistically consistent. As in a Breit-Wigner parametrization only two parameters enter, it is not sensitive at all to the value

of R. Thus for a reliable determination of R the measurement of both channels is necessary.

Two zero's of the function $D(M) = M^2 - M_r^2 + iM_r(g_1\rho_1(M) + g_2\rho_2(M))$ define two T-matrix poles on sheet II and III. The position of the T-matrix pole in sheet II defines the mass m_0 and width Γ_0 of $a_0(980)$; m_0 is usually different from M_r. According to PDG [10] the average value of the measured $a_0(980)$ masses is equal to 983.4 ± 0.9 MeV/c^2 for the $\eta\pi$ final state (calculated without the new result of E852 [11]) and 980.8 ± 2.7 MeV/c^2 for the $K\overline{K}$ final state. The width of $a_0(980)$ is equal to 92 ± 8 MeV in the $K\overline{K}$ final state [13] and to 72 ± 10 MeV in the $\eta\pi$ final state [11]. In view of those differences it looks also important to perform new measurements of the $a_0(980)$ mass distribution in both decay channels at ANKE, where, as we already mentioned above, we expect better resolution and lower background.

The values of R presented in the table above are not favourable to a pure molecular or pure "threshold cusp" interpretation. Nevertheless, there still is a comparatively large uncertainty in g_1 and g_2: the values of g_1 can vary from 0.12 to 0.32 GeV and R can be between 0.9 and 2.05. A more precise knowledge of g_1 and g_2 would help us to better understand the $a_0(980)$ internal structure. For example, this information can be used to determine the relative weights of the different components in the state vector of $a_0(980)$ defined by Eq.(2).

3.2 Calculation of the a_0^+-production cross section

The missing mass spectrum of deuterons from the reaction $pp \to dX^+$ produced at 0° and incident momenta of 3.8, 4.5 and 6.3 GeV/c has been measured at Lawrence Radiation Laboratory (Berkeley) [17]. Apart from peaks corresponding to π^+ and ρ^+ production, there is a distinctive structure in the missing mass spectrum at 0.95 GeV^2 which was identified with a_0^+ production. The corresponding differential cross section for the forward a_0^+ production is shown by the open circles in Fig.1.

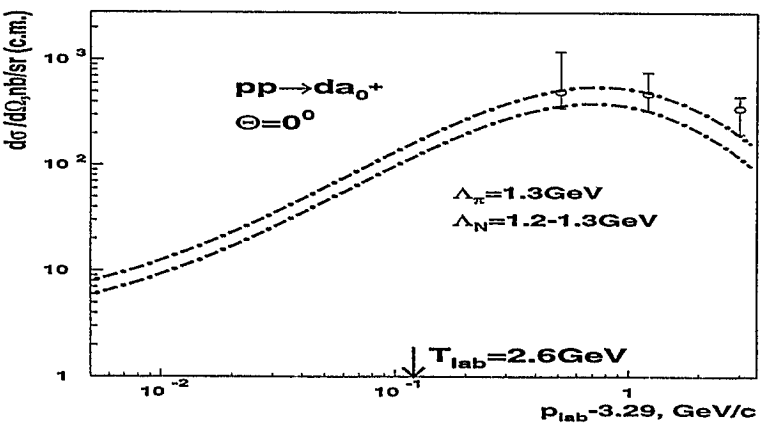

Figure 1: Forward differential cross section of the reaction $pp \to da_0^+$ as a function of $(p_{lab} - 3.29)$ GeV/c. The empty circles are the experimental data from [17]. The two dashed-dotted curves describe the results of the TSM calculations at $\Lambda_N = 1.2$ and 1.3 GeV/c.

In order to estimate the cross section of the reaction $pp \to da_0^+$ at lower momenta which are available at COSY we use the two-step model (TSM) described by a triangle diagram [18]. We took into account three different contributions: i) a_0 coupling to two nucleons through $f_1(1285)$ and π-meson exchanges; ii) similar a_0 coupling through η- and π-meson exchanges; iii) production of a_0 through π exchange with an s- and u-channel nucleon current. The coupling constants and cut-off parameters Λ_i for π- and η-meson exchanges were taken from the Bonn-potential model. In the case of the a_0 and $f_1(1285)$ mesons we used the results from [19, 20]. The cut-off for nucleon exchange was considered as a free parameter within the interval 1.2–1.3 GeV. It appeared that mechanisms i) and ii) can be neglected and that the dominant contribution stems from the nucleon u-channel exchange. The results of our calculations for the forward differential cross section at various beam energies are presented in Fig.1. The two dashed-dotted curves describe the results of the TSM calculations at different values of the nucleon cut-off parameter: $\Lambda_N = 1.2$ and 1.3 GeV/c. Rather good description of the existing data has been reached for $\Lambda_N = 1.3$ GeV/c.

The angular dependence of the differential cross section of the reaction $pp \to da_0^+$ as a function of the c.m. angle $\Theta_{c.m.}$ can be parametrized as

$$\frac{d\sigma}{d\Omega_{c.m.}} = A + B \cdot \cos^2\Theta_{c.m.} + C \cdot \cos^4\Theta_{c.m.} \; . \qquad (4)$$

The results of our calculations on the total a_0^+-production cross section for the reaction $pp \to da_0^+$ are presented in the following table:

T [GeV]	A [nb/sr]	B [nb/sr]	C [nb/sr]	σ_{tot} [nb]
2.52	21.3	15.3	−2.1	330
2.60	68	76	−22	1120
2.62	78	97	−31	1310

Note that an understanding of the $a_0^+(980)$-production mechanism may also yield information on its internal structure. For example, the WA57 collaboration measured inclusive photoproduction of $a_0^\pm(980)$ at photon energies 25–55 GeV [21]. It was found that the cross section of this process is relatively large with a value of $\sim 1/6$ of the cross sections for corresponding non-diffractive production of leading ρ^0, ω, ρ^+ and ρ^-. The authors interpreted this relatively strong production of the $a_0^\pm(980)$ as evidence that it is a $q\bar{q}$ state rather than $qq\bar{q}\bar{q}$. This argument can also be used in our case. In fact, in the LBL experiment [17] the measured values of $d\sigma/d\Omega$ for the reaction $pp \to da_0^+(980)$ are $\sim (1/4 \div 1/6)$ of the cross section for ρ^+ production:

	$d\sigma/d\Omega$ [μb/sr]	
p [GeV/c]	$pp \to d\rho^+$	$pp \to da_0^+$
3.8	3.2±0.5	$0.5^{+0.7}_{-0.15}$
4.5	2.0±0.4	$0.48^{+0.28}_{-0.15}$
6.3	0.5±0.5	$0.35^{+0.10}_{-0.15}$

If measurements made at ANKE will confirm a comparatively large value of the $a_0^+(980)$-production cross section presented in this section then this will be a good evidence that the $a_0^+(980)$ has an essential $q\bar{q}$ admixture.

4 Results of simulation calculations

4.1 Detection scheme

Figure 2 shows the trajectories of deuterons detected in coincidence with K^+ or π^+ mesons from the reaction $pp \to da_0^+$. It can be seen that the fast ($p \approx 2$ GeV/c) deuterons in both cases are detected in the forward detection system. Deuteron identification — mainly against fast protons, $p_p > 1.5$ GeV/c — is based on the measurement of time-of-flight (TOF) and energy losses. In addition the use of special inclined Čerenkov counters based on the principle of total reflection is foreseen [1, 22]. The kaons are detected and identified in the side telescopes whereas pions (which have slightly higher momenta) mainly hit the side-wall counters between the telescopes and the forward system. It has already been shown in the proposal [1] that for the case of the $a_0^+ \to K^+\overline{K}^0$ channel a sufficient background suppression can be achieved (see also [23] for the measured performance of the K^+ detectors). Therefore, in Sect.4.3 we focus on the $a_0^+ \to \pi^+\eta$ case.

The mass distribution of the a_0^+ mesons can be deduced as the missing mass of the deuterons detected with the forward counters, $m(a_0^+) = m.m.(pp, d)$. The momentum resolution for the deuterons is $\Delta p/p \approx 1.5\%$ leading to a mass resolution of $\Delta m \approx 7$ MeV/c^2 [1, 22] which is small in comparison with the natural width of the a_0^+ of 72 MeV/c^2 [11].

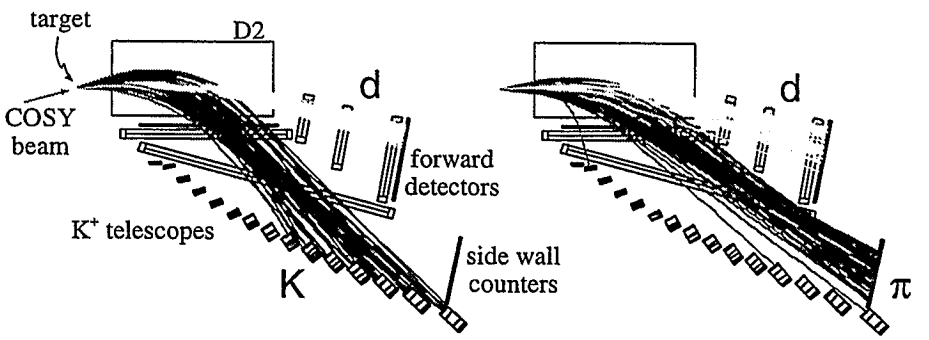

Figure 2: Ejectile trajectories in ANKE for the two decay branches $a_0^+ \to K^+\bar{K}^0/\pi^+\eta$. For the simulations a beam energy of $T = 2.62$ GeV and a field strength in D2 of $B = 1.57$ T was assumed. In the figure the field region of D2 is indicated as a rectangular box.

It is of great advantage that both decay channels can be measured simultaneously at ANKE. This allows to deduce from the measured d-K^+ and d-π^+ rates the ratio of the BR's avoiding systematical uncertainties e.g. from luminosity monitoring. The different detection efficiencies can be deduced from simulation calculations as presented here and from calibration measurements on the K^+-detection efficiencies in the telescopes [23].

4.2 Count-rate estimate

For the count-rate estimates of the two decay channels we *assume* a branching ratio of $BR(a_0^+ \to K^+\bar{K}^0) = 12\%$ and $BR(a_0^+ \to \pi^+\eta) = 88\%$. This value has been obtained by using the branching ratio from [13] and applying the phace-space corrections for $T = 2.6$ GeV where only a_0's with masses below 1022 MeV/c^2 can be produced[1]. With the cluster-jet target luminosities up to $L \approx 3 \cdot 10^{30}$ cm^{-2}s^{-1} are achievable. From the simulation calculations geometrical detection efficiencies of $\varepsilon_{geo} = 12\%$ (0.15%) for the detection of d-K^+ (d-π^+) pairs are deduced. About 70% of the kaons decay in flight between the target and the detectors whereas more than 90% of the pions reach the corresponding counters. For the detection efficiencies for kaons (pions, deuterons) in the telescopes (side-wall counters, forward detectors) we assume $\varepsilon_{det} = 30\%$ (90%, 90%) which is in line with recent measurements. Thus the following count rates can be expected for d-K^+ coincidences:

$$\begin{aligned} \dot{n}_{dK+} &= L \cdot \varepsilon_{geo} \cdot \varepsilon_{decay} \cdot \varepsilon_{det} \cdot \sigma \cdot BR \\ &\approx 3 \cdot 10^{30}\ \text{cm}^{-2}\text{s}^{-1} \cdot 0.12 \cdot 0.3 \cdot (0.3 \cdot 0.9) \cdot 1.12\ \mu\text{b} \cdot 0.12 \\ &\approx 14\ \text{h}^{-1}\ , \end{aligned} \tag{5}$$

and for d-π^+ coincidences:

$$\begin{aligned} \dot{n}_{d\pi+} &= L \cdot \varepsilon_{geo} \cdot \varepsilon_{decay} \cdot \varepsilon_{det} \cdot \sigma \cdot BR \\ &\approx 3 \cdot 10^{30}\ \text{cm}^{-2}\text{s}^{-1} \cdot 0.0015 \cdot 0.9 \cdot (0.9 \cdot 0.9) \cdot 1.12\ \mu\text{b} \cdot 0.88 \\ &\approx 12\ \text{h}^{-1}\ . \end{aligned} \tag{6}$$

Thus, it is concluded that within one week of beam time more than 1000 events can be collected for each decay channel allowing to determine the branching ratio with high statistical accuracy and to distinguish between the predictions from different models given in Sect.3.1.

4.3 Background suppression

Three major sources of background have to be considered here:

pp $\to$ dX In this case, a fast deuteron is detected and correctly identified in the forward counters. In coincidence a K^+ or a π^+ meson not stemming from resonant production via the a_0^+ is detected in the telescopes or side-wall detectors, respectively. For the case of pp $\to$ dK^+X (and also pp $\to$ pK^+X) it has already been shown in [1] that the background can be sufficiently reduced. In case of pion production our calculations show that the most dangerous background contribution stems from ρ^+ production, pp $\to$ dρ^+ $\to$ d$\pi^+\pi^0$. Figure 3 shows a missing mass analysis for this reaction channel in comparison with a_0^+ production. It can be seen that due to the high mass resolution achievable at ANKE there is a clear separation between signal and background even if one takes into account the much larger cross section for ρ^+ production. For comparison, in the figure we also show the events where the a_0^+ decays into kaons. It

[1] In [11] a mass of 998.3 MeV/c^2 was found for the charged a_0 mesons which is significantly larger than the value of 983.4 MeV/c^2 quoted by PDG [10]. If this value is correct a larger fraction of the a_0^+ mesons can decay into $K^+\bar{K}^0$

can nicely be seen that only events above the $K\overline{K}$ threshold are detected. Thus the measurements will also give the oportunity to — for the first time — simultaneously observe the a_0^+-mass distribution in both decay channels.

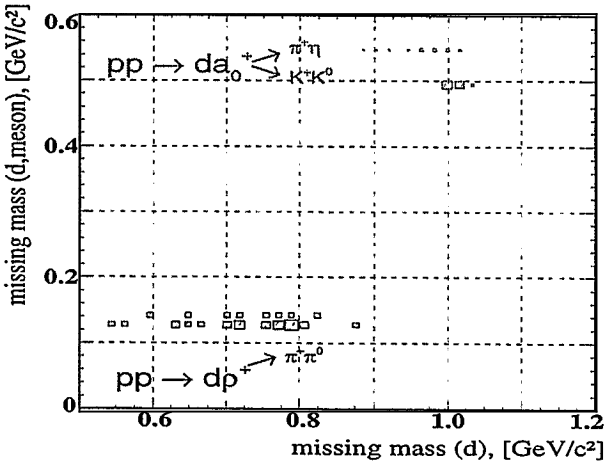

Figure 3: Missing mass distributions for a_0^+'s and for the background reaction $pp \to d\rho^+ \to d\pi^+\pi^0$. In the simulation the different production cross sections were taken into account, the box sizes represent the counting rates in a linear scale.

$pp \to p\pi^+X$ The background which demands the most thorough treatment during data analysis will be due to misidentification of fast protons as deuterons in the forward detectors. Figure 4 a) shows the detection time in the forward counters (deduced in an off-line analysis from the detection time for the coincident π^+ and the forward ejectile) vs. the deuteron or proton momentum (measured with the forward MWPC's). It is seen that for low momenta there is a good separation of the background, however, for $p > 2$ GeV/c the time differences get rather small. Taking into account the time resolutions of the scintillation counters and the much larger cross section for background production it can be deduced from the simulation calculations that in the high momentum region an additional background-reduction factor of ~ 10 is needed. One possibility for further background reduction is a missing mass analysis analogous to Fig.3 which is shown in Fig.4 b). It is seen that the a_0^+ events are concentrated around $m.m.(\mathrm{d,meson}) = m(\eta) = 547$ MeV/c^2 whereas the background from misidentified protons is spread out to different masses. It is expected that such a missing mass analysis will further suppress the background by roughly one order of magnitude. Further suppression by another order of magnitude will be supplied by the measurement of energy losses and with the use of inclined Čerenkov counters in the forward detection system. The latter are expected to yield a fast proton-to-deuteron suppression by at least one order of magnitude, see also [1, 22]. We conclude that background from proton misidentification can sufficiently be suppressed. Note

that in our simulation calculations one- and multi-pion production were taken into account.

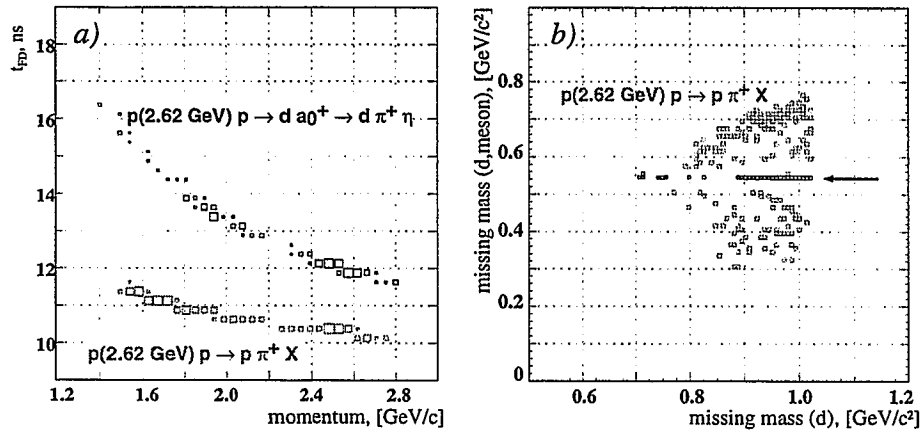

Figure 4: Detection time in the forward scintillators vs. ejectile momenta (left figure). The box sizes do *not* represent the realistic counting rates. Missing-mass distributions for the background reaction pp $\rightarrow$ pπ^+X where the proton is misidentified as a deuteron in the forward detection system. The position of 'real' a_0^+ events is indicated by the arrow (right figure).

Scattered background from the pole shoes of D2 and the vacuum chambers. According to our experience this background can very efficiently be suppressed using the wire-chamber information, even in cases of nuclear targets and subthreshold meson production where the background-to-signal ratio is much worse than in our case [23].

4.4 Data on the production of mesons other than a_0^+

It should be noted here that the data obtained from pp collisions at $T \approx 2.6$ GeV during two weeks of beam time will not only yield information on the a_0^+ meson but also on other reaction channels. Corresponding data analyses are foreseen. As example we quote following channels:

- **pp $\rightarrow$ dρ^+** In Fig.3 of Sect.4.3 this reaction channel is shown as possible background for a_0^+ production. According to our simulation calculations, the counting rate for this channel will be $\dot{n} \approx 30\ \mathrm{h}^{-1}$.
- **pp $\rightarrow$ ppϕ $\rightarrow$ ppK$^+$K$^-$** At ANKE all 4 outgoing particles can be detected and identified if appropriate detectors for negatively charged particles are placed in the return yoke of D2. Such a detection system is currently under construction. At the time of the proposed measurements prototype counters will be installed for testing purposes. Thus the data will allow tests of these detectors and development of the corresponding data-analysis software. A proposal for K$^+$K$^-$ production in pA collisions [24] for which the detectors will be used later has already been approved during an earlier meeting of the COSY-PAC.

5 Requested time for measurements

Summarizing, we apply for the following amount of beam time:

- **Two weeks** for the measurement of the branching ratio $a_0^+ \to K^+\bar{K}^0/\pi^+\eta$ using the cluster-jet target. Prefered time is November/December 2000 since then the tuning and test measurements of the ANKE forward-detection system will be finished. In order to minimize time losses due to setting up the spectrometer and the detection systems, the beam time should be a common 4 weeks block together with the measurements on deuteron breakup, see beam-time request to proposal #20 [22] presented during this PAC meeting. The two weeks of beam time include four days for the following preparatory tasks: two days of beam development including stochastic cooling at maximum COSY energy ($T \approx 2.6$ GeV) and beam intensity; one day of test measurements to optimize background conditions at ANKE (in particular in the forward counters), to adjust the degraders in the K^+ telescopes to the field strength in D2 of $B = 1.57$ T [2] and to optimize the DAQ electronics for K^+-d and π^+-d coincidence measurements; one day for the installation of the target-near semiconductor counters and for pumping of the target region.

- In a later stage of the proposed studies (see approved COSY proposal #55 [1]) it is planned to systematically study the a_0^+ production at various beam energies between threshold and the maximum COSY energy. Note that due to the lower cross sections closer to threshold these measurements will require the use of the frozen-pellet target which will offer 1–2 orders of magnitude higher luminosities. This target will be available not earlier than middle of 2001. The **estimated** beam time for these measurements is **2–3 weeks**. The actual time needed can only be estimated after the analysis of the data obtained during the beam time requested here. In this sense these measurements can be regarded as test measurements for a systematic study of the mass distribution of the a_0^+ meson.

[2] The procedure of degrader optimization is already well established since it has been developed and used for the subthreshold K^+ studies at $B = 1.30$ T. In order to keep the time needed for the optimization as short as possible a Cu-foil target will be used which provides much higher counting rates. Only after this optimization semiconductor counters for luminosity monitoring can be mounted close to the target region.

References

[1] V. Chernyshev et al., COSY proposal #55 "Study of a_0^+ mesons at ANKE" (1997) *available via www:* `http://ikpd15.ikp.kfa-juelich.de:8085/doc/Anke.html`; L.A. Kondratyuk et al. *Preprint ITEP* **18-97**, Moscow (1997).

[2] F.E. Close et al., Phys.Lett.**B 319** (1993) 291.

[3] M. Genovese et al., Nuovo Cim.**107A** (1994) 1249.

[4] G. Janssen et al., Phys.Rev.**D 52** (1995) 2690.

[5] V.V. Anisovich et al., Phys. Lett.**B 355** (1995) 363.

[6] K. Maltman, "Scalar Meson Decay Constants and the Nature of the $a_0(980)$", Review talk at Hadron-99, Beijing, Aug. 24–28, 1999 (*in print*).

[7] S. Narison,"Gluonic Scalar Mesons Hybrids from QCD Spectral Sum Rules", Review talk at Hadron-99, Beijing, Aug. 24–28, 1999 (*in print*).

[8] N.A. Tornqvist, Phys.Rev.Lett. **49** (1982) 624.

[9] O. Krehl, et al., Phys.Lett.**B 390** (1997) 23.

[10] C. Caso et al. (Particle Data Group), Eur.Phys.J.**C 3** (1998) 1.

[11] S. Teige et al., Phys.Rev.**D 59** (1998) 012001.

[12] L. de Billy et al., Nucl.Phys.**B 176** (1980) 1.

[13] A. Abele et al., Phys.Rev.**D 57** (1998) 3860.

[14] C. Amsler et al., Phys.Lett.**B 333** (1994) 277.

[15] S. Flatté, Phys.Lett.**B 63** (1976) 224.

[16] D.V. Bugg, Phys.Rev.**D 50** (1994) 4412.

[17] M.A. Abolins et al. Phys.Rev.Lett. **25** (1970)469.

[18] V.Yu. Grishina et al., Annual Report of the IKP, 1999.

[19] M. Kirchbach, D.O.Riska, Nucl.Phys.**B 176** (1980) 1.

[20] G. Janssen, "Meson-Meson-Prozesse in der starken Wechselwirkung", Dissertation Universität Bonn, Berichte des FZJ Jül-3065J, Jülich (1995).

[21] M. Atkinson et al., Phys.Lett.**B 138** (1984) 459.

[22] V. Komarov et al., beam time request #20.2, submitted to the 19^{th} meeting of the COSY-PAC (1999) *available via www:* `http://ikpd15.ikp.kfa-juelich.de:8085/doc/Anke.html`.

[23] V. Koptev et al., beam time request #18.3, submitted to the 19^{th} meeting of the COSY-PAC (1999) *available via www:* `http://ikpd15.ikp.kfa-juelich.de:8085/doc/Anke.html`.

[24] H. Müller et al., COSY proposal #21, "Study of subthreshold K^- production with ANKE" (1996) *available via www:* `http://ikpd15.ikp.kfa-juelich.de:8085/doc/Anke.html`.

Status of ANKE and Planned Measurements on $pp \to da_0^+$

M. Büscher

Institut für Kernphysik
Forschungzentrum Jülich
52425 Jülich
Germany

Workshop on "a_0 Physics with ANKE"
July, 13/14, 2000
ITEP, Moscow

- Thanks to the local organizers !!
- Proceedings
  Copies of transparencies
  Written contributions (~1 page) → V.Kleber
  List of participants
- Schedule
- Goals (M.B.'s viewpoint)
  Preparation of beam time, February 2001
  Ideas for further experiments?
  .....and..... (input from YOU)?

- Status of ANKE
  K^+ identification works
  Momentum reconstruction
- Plans for a_0 physics with ANKE

Workshop on "a_0 Physics with ANKE"
July 13/14, 2000
ITEP, Moscow

Thursday, July 13

Chairperson: V. Chernyshev

10:00		Welcome
10:10	*M. Büscher (FZJ)*	Status of ANKE and planned measurements on $pp \to da_0^+$
10:40	*Yu. Kalashnikova (ITEP)*	Scalar mesons: Why they are interesting
11:10	*L. Kondratyuk (ITEP)*	Properties of the $a_0/f_0(980)$ mesons
11:40	*V. Grishina (INR)*	a_0 production at COSY energies

Theory

12:00 Lunch

L. Kondratyuk

13:30	*J. Haidenbauer (FZJ)*	Description of the $a_0/f_0(980)$ mesons with the Jülich model
14:00	*A. Kudryavtsev (ITEP)*	Perspectives of a_0^- studies
14:30	*V. Tarasov (ITEP)*	A possibility for direct measurements of a_0/f_0 mixing

14:50 Coffee break

H. Ströher

15:00 Round-table discussion: Perspectives of the a_0^+ studies with ANKE

17:00 Dinner

Friday, July 14

M. Büscher

10:00	*V. Kleber (FZJ)*	Simulations for the a_0^+ studies with ANKE
10:30	*N. Lang (Münster)*	Status of the cluster-jet target
11:00	*V. Komarov (JINR)*	The ANKE forward detectors and luminosity monitoring

11:30 Coffee break

Exp. al issues

11:50	*Chr. Leim (FZJ)/ G. Macharashvili(JINR)*	Preparation of the forward Cerenkov counters
12:10	*H. Junghans (FZJ)*	Data-analysis software
12:30	*I. Lehmann (FZJ)*	Luminosity monitoring with the spectator counters

12:50 Lunch

K. Sistemich

14:00	*V. Chernyshev (ITEP)*	Future activities at ITEP/Status of the pellet target
14:30	*H. Ströher (FZJ)*	Future activities at ANKE

15:00 Coffee break

V. Chernyshev

15:30 Concluding discussion: Future activities, responsibilities, ...

17:00 Excursion to experimental facilities of ITEP

'History' of COSY Proposal #55

1st ideas: 12/95

"Consideration on to use of a pellet target at ANKE".

e-mail: V.Chernyshev → K. Sistemich

3. A search for K+K- atom/system close to the threshold of f(0)[975] resonance/ production in reaction pd->3He

COSY proposal: 10/97

Study of a_0 mesons in the reaction
$pp \rightarrow d a_0^+ \rightarrow d K^+ \bar{K}^0$ at ANKE

Spokesman: V. P. Tchernyshev
Local contact: M. Büscher

available as

UTэф reprint

18 -97

PAC replies:

... The PAC is positive to the physics which is approved in principle and to the construction of a hydrogen pellet target at ANKE. ...

2000: ANKE ready for measurements ...

Beam-time request for COSY experiment #55
"Study of $f_0(980)$ mesons at ANKE"

M. Büscher, H. Junghans, V. Kleber, R. Koch, R. Schleichert, K. Sistemich, H. Ströher
Institut für Kernphysik, Forschungszentrum Jülich, D-52425 Jülich, Germany

V. P. Chernyshev, P. Fedorets, L. A. Kondratyuk
Institute of Theoretical and Experimental Physics, 117259 Moscow, Russia

Ye. S. Golubeva, V. Grishina
Institute of Nuclear Research, 117312 Moscow, Russia

V. Koptev, S. Mikirtychiants
High Energy Physics Dept., Petersburg Nuclear Physics Institute 188350 Gatchina, Russia

A. Khoukaz
Institut für Kernphysik, Universität Münster Wilhelm-Klemm-Str. 9, D-48149 Münster, Germany

S. Dymov, A. Kacharava, V. Komarov, A. Kulikov, G. Macharashvili, A. Petrus, B. Zalykhanov
Lab. of Nuclear Problems, Joint Institute of Nuclear Research 141980 Dubna, Russia

B. Chiladze, M. Nioradze
High Energy Physics Institute, Tbilisi State University University Str. 9, 380086 Tbilisi, Georgia

I. Zychor
The Andrzej Soltan Institute for Nuclear Studies PL-05400 Swierk, Poland

and the ANKE collaboration

Spokesperson: M. Büscher (m.buescher@fz-juelich.de)

May 4, 2000

Outcome of COSY-PAC meeting May 4/5, 2000:

Minutes of the 20th Meeting of the
COSY Program Advisory Committee (PAC)
May 5/6, 2000
IKP, Forschungszentrum Jülich

6. ANKE
Beam-time request 55.1 (M.Büscher):
The proposal to study the a_0 properties at COSY has received strong support from the PAC. The collaboration now presents a beam-time request that can serve as an example to other groups. The request outlines the basics physics questions again and discusses the theoretical predictions for decay and production of this scalar meson. A good point is made on how a COSY experiment can contribute to clarifying the properties of this meson. Also the background suppression is discussed thoroughly. In view of the overall high quality of this proposal, the PAC recommends to grant the **2 weeks** requested by the collaboration. Since further measurements closer to threshold will require the use of the frozen pellet target, the full beam-time requirement until completion of the experiment cannot yet be reliably estimated.

2 weeks of beam time in early 2001
3 more weeks later with pellet target

COSY working scheme II/2000 + I/2001

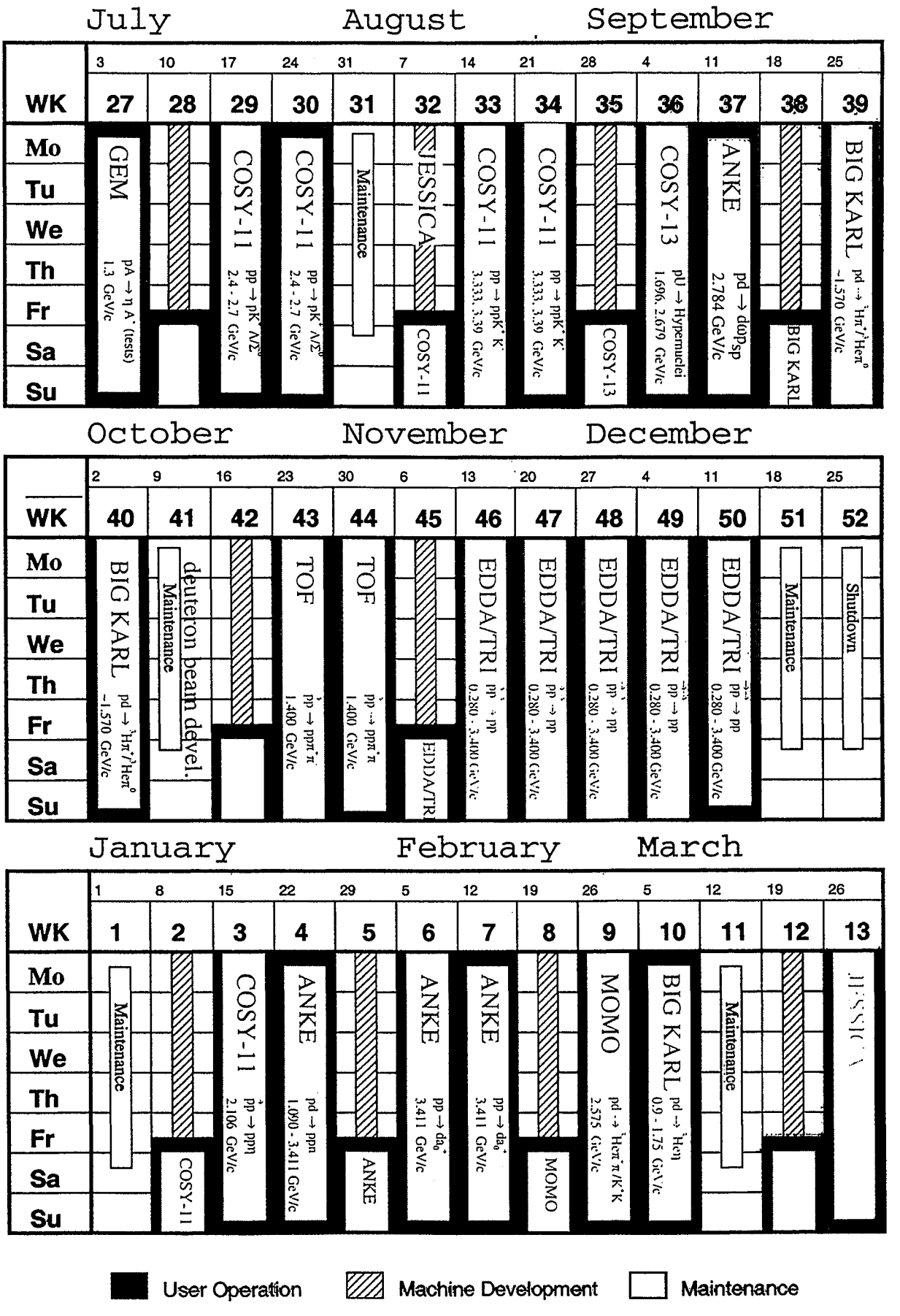

16.05.00 markus

Properties of the $a_0(980)$

Review of Particle Physics, European Physical Journal C3, 1 (1998)
(Status of April 2000)

$a_0(980)$ $I^G\ (J^{PC}) = 1^-\ (0^{++})$

... the interpretation of the scalar mesons is a long standing puzzle ...

The $f_0(980)$ and $a_0(980)$ are often interpreted as being multiquark states (JAFFE 77) or $K\bar{K}$ bound states (WEINSTEIN 90) ...

More detailed models exist, which include more theoretical input at least phenomenologically. One such unitarized quark model with coupled channels can understand ... light scalars as ... unitarized manifestations of bare quark model $\bar{q}q$ states ...

To reveal its true coupling constants a coupled channel model ... must be applied.

$a_0(980)$ MASS

VALUE (MeV)	
983.5±0.9 OUR AVERAGE	

but: most recent data from BNL →
$m(a_0^+) = 998.3 \pm 4.0$

$a_0(980)$ WIDTH

VALUE (MeV)	
50 to 100 OUR ESTIMATE	Width determination very model dependent. Peak width is about 60 MeV, but decay width can be much larger.

M.Büscher, 4/00

16.05.00 markus

Benefits from measurements with ANKE

Existing data $R = g_{KK}/g_{\pi\eta}$:

$g_{\pi\eta} =$ 0.122 ± 0.008 / 0.324 ± 0.015

- E852 (BNL): - $m(a_0^+) = 998.3 \pm 4.0$ MeV/c^2
  - $\pi\eta$ channel only
- Crystal Barrel: - $m(a_0^+) = 984.45 \pm 1.23 \pm 0.34$ MeV/c^2
  - mass resolution Δm only ~ 27 MeV/c^2
  - contaminations from heavier resonances
  - KK and $\pi\eta$ channels in different data sets

$a_0(980)$ DECAY MODES

	Mode	Fraction (Γ_i/Γ)
Γ_1	$\eta\pi$	dominant
Γ_2	KK	seen
Γ_3	$\rho\pi$	
Γ_4	$\gamma\gamma$	seen
Γ_5	e^+e^-	

$R = g_{KK}/g_{\pi\eta} = 0.9 \ldots 2.05$ (depending on fit)

ANKE:

- high mass resolution: $\Delta m \sim 10$ MeV/c^2
  (→ Forward detectors)
- simultaneous measurement of two decay channels

$p(2.6\ \text{GeV})\ p \rightarrow d\ a_0^+$ → $\pi^+\ \eta$, $K^+\ \bar{K}^0$

approved proposal #55 (PAC 14)

M.Büscher, 4/00

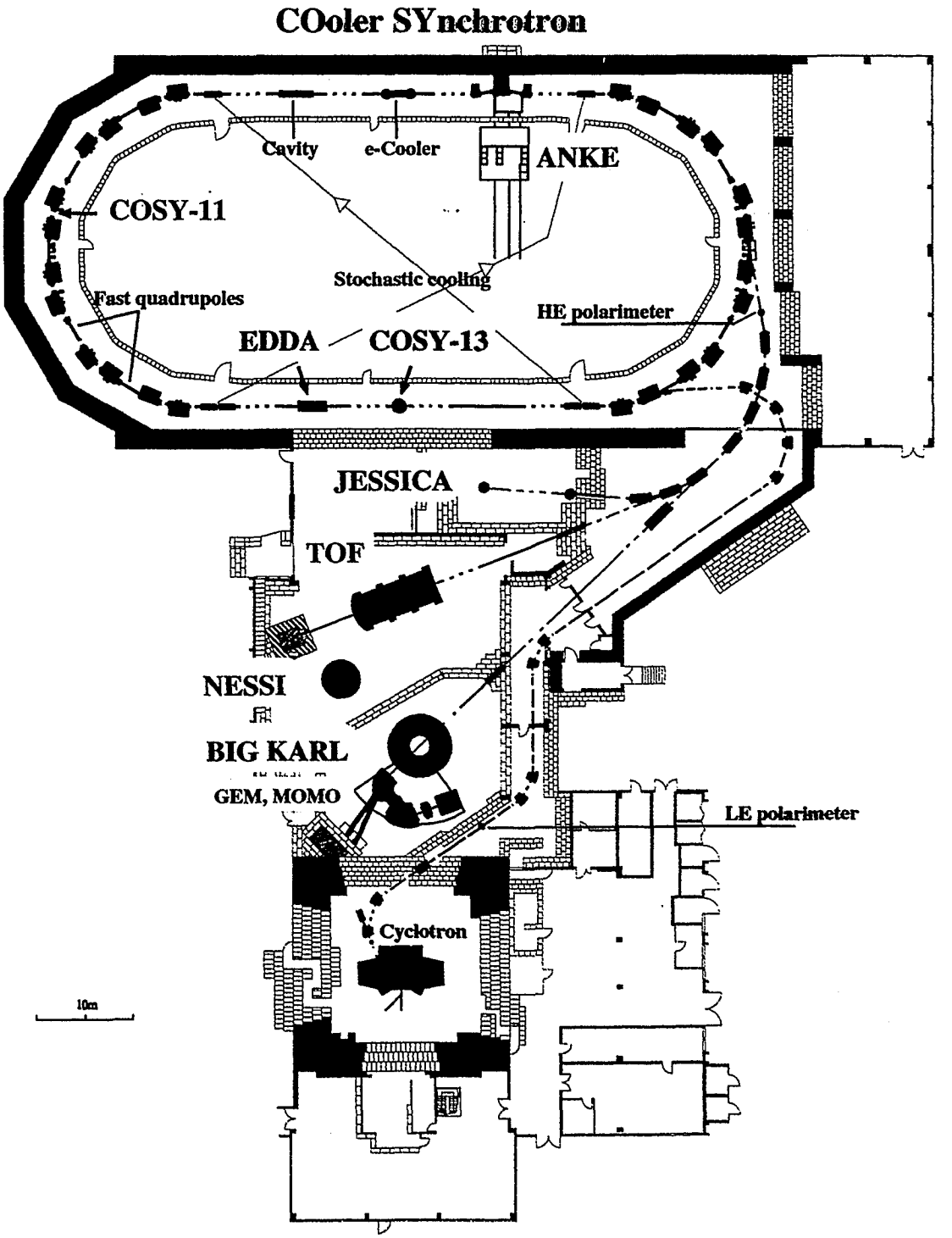
COoler SYnchrotron
Cavity
e-Cooler
ANKE
COSY-11
Stochastic cooling
Fast quadrupoles
HE polarimeter
EDDA
COSY-13
JESSICA
TOF
NESSI
BIG KARL
GEM, MOMO
LE polarimeter
Cyclotron
10m

Magnetic spectrometer ANKE

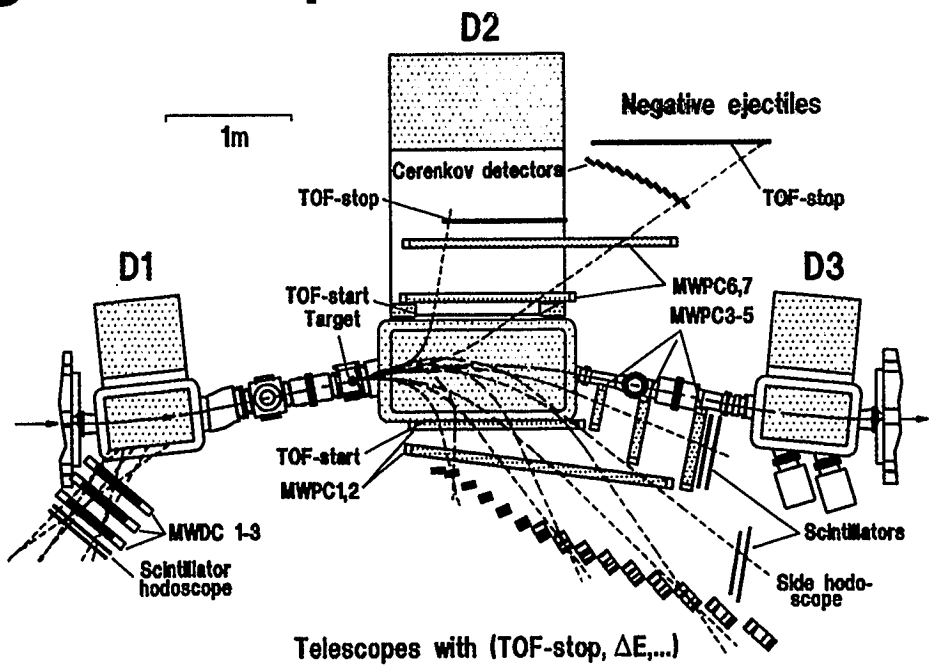

Positive ejectiles

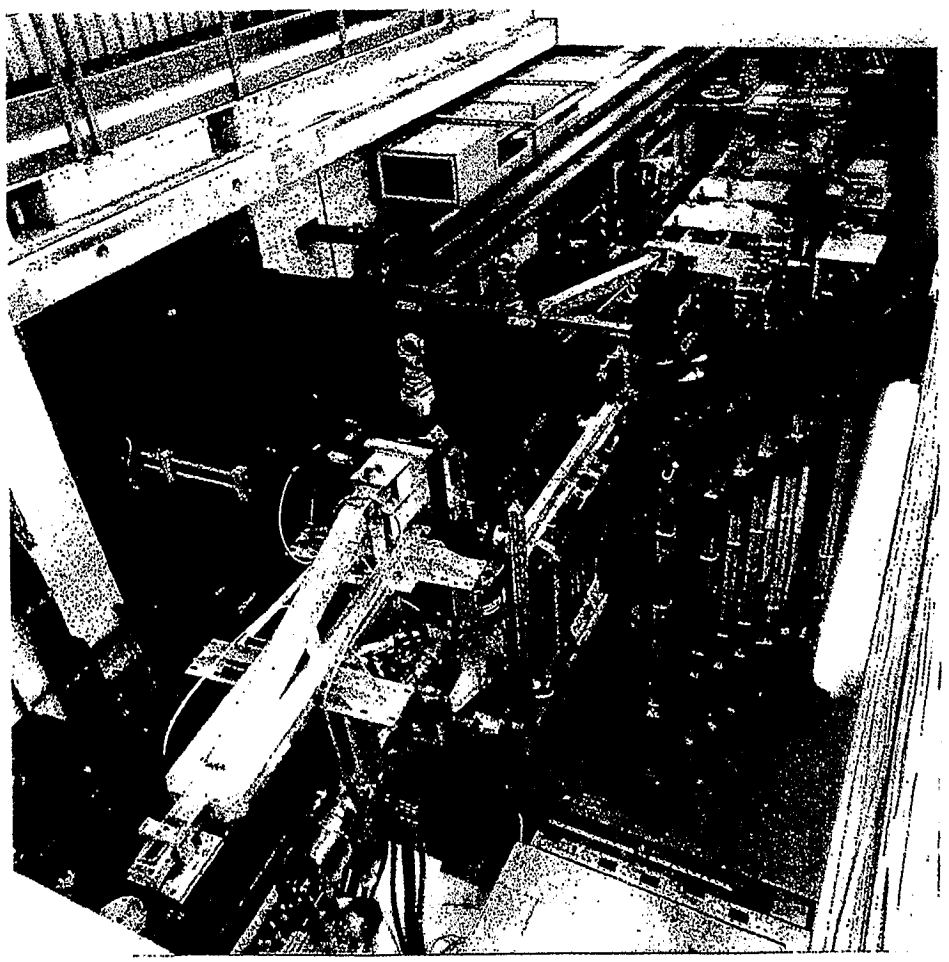

Results of GEANT simulations:

T_{beam} = 2.6 GeV

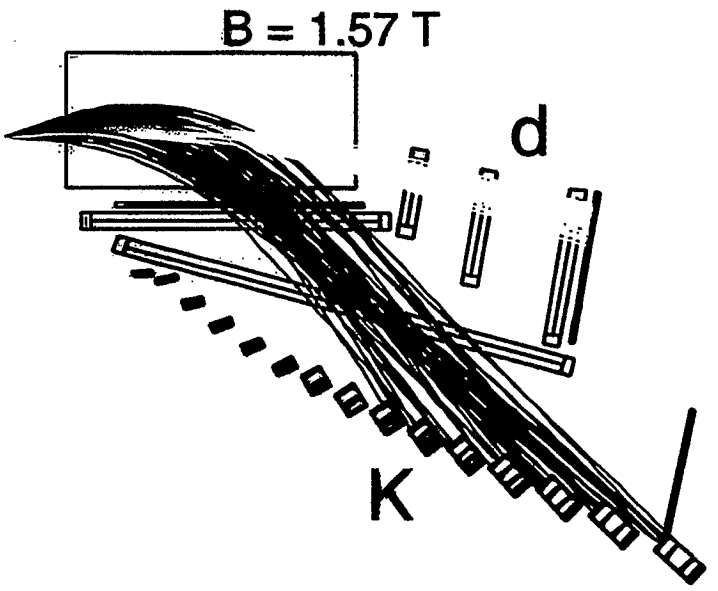

$pp \rightarrow d a_0^+$

$\hookrightarrow K^+ \bar{K}^0$

ε = 12.0 %

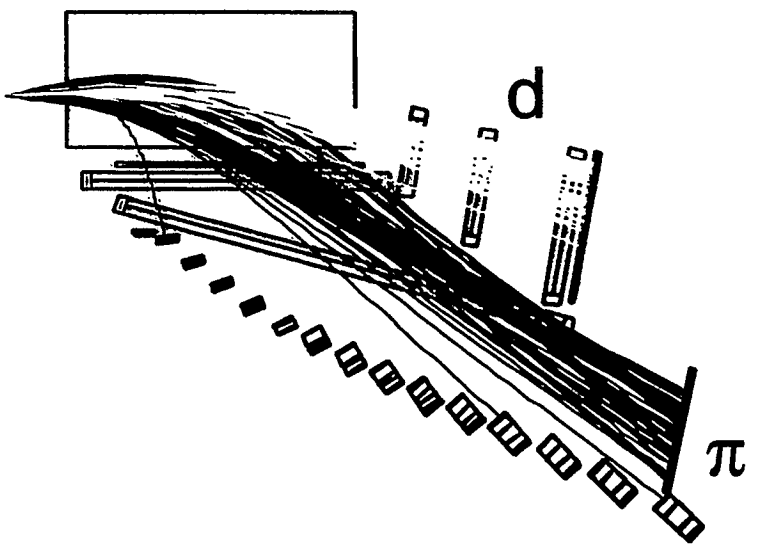

$pp \rightarrow d a_0^+$

$\hookrightarrow \pi^+ \eta$

ε = 0.30 %

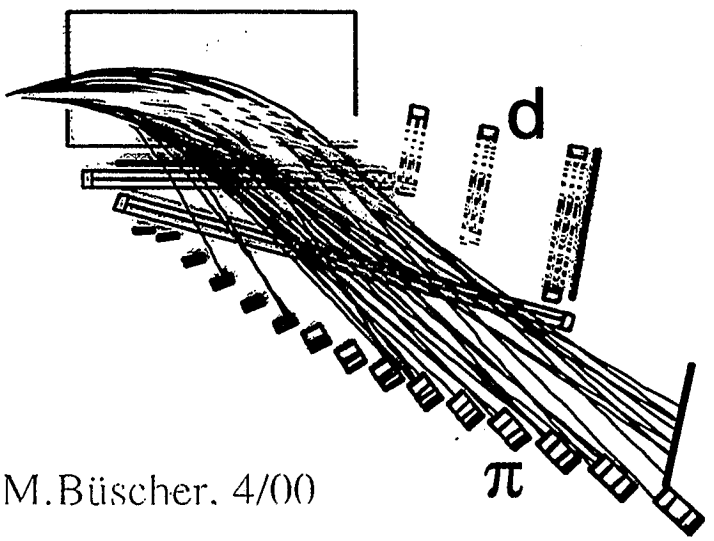

$pp \rightarrow d \rho^+$

$\hookrightarrow \pi^+ \pi^0$

ε = 0.03 %

M.Büscher, 4/00

17.05.00 markus

$pC \rightarrow K^+X$

- *understand and tune detection system (degrader thicknesses)*
- *develop tools for kaon identification*
- *measurements at T = 1.0 ... 2.3 GeV*

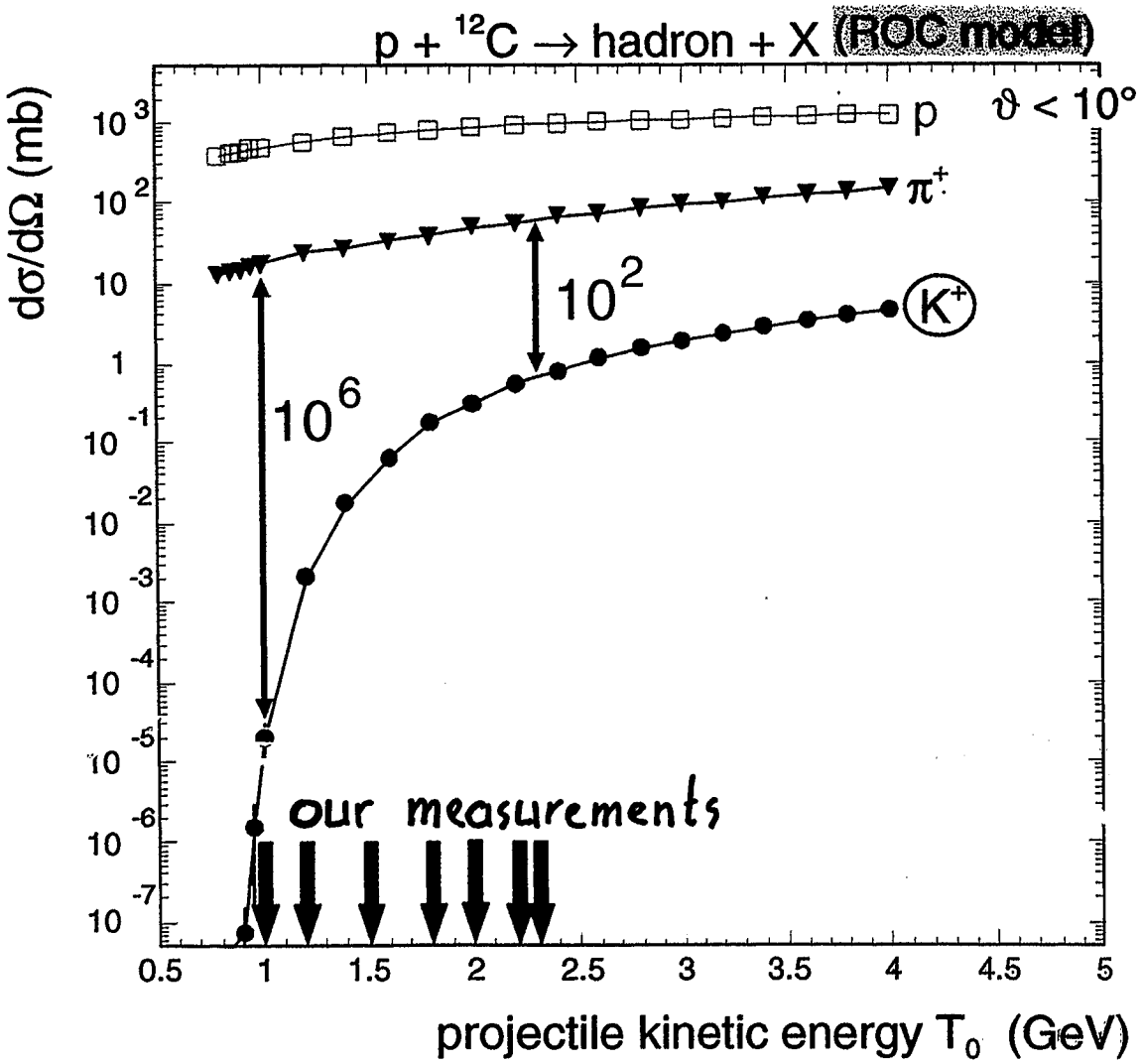

M.Büscher, MESON 2000

17.03.99 markus

D2 - momentum resolution:

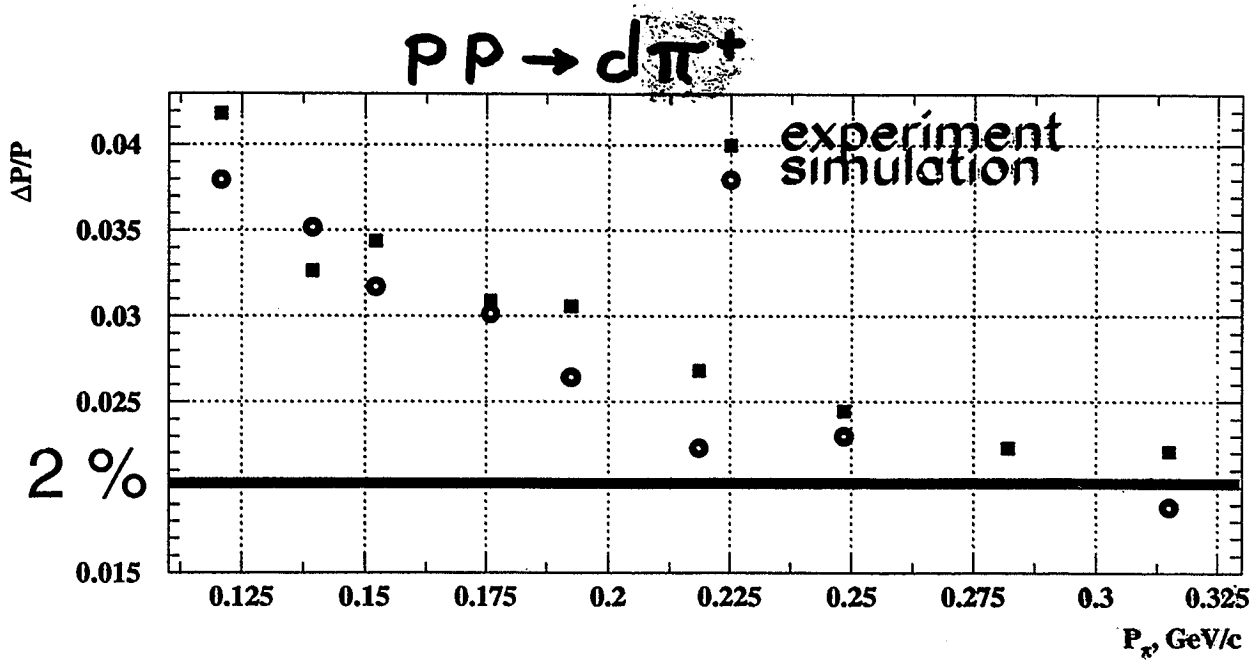

- B = 0.83 ... 1.08 T (⇒ $\Delta p/p$ = 1.2% @ 1.6 T)
- vacuum window: 500 µm Al

JINR

Momentum and missing-mass resolution of forward detectors (pp → pp)

JINR

p_0 = 1083 MeV/c
B(D2) = 0.861 T

2 (of 3) chambers installed
Cluster width = 1 wire
$\vartheta_{vert} < 1°$

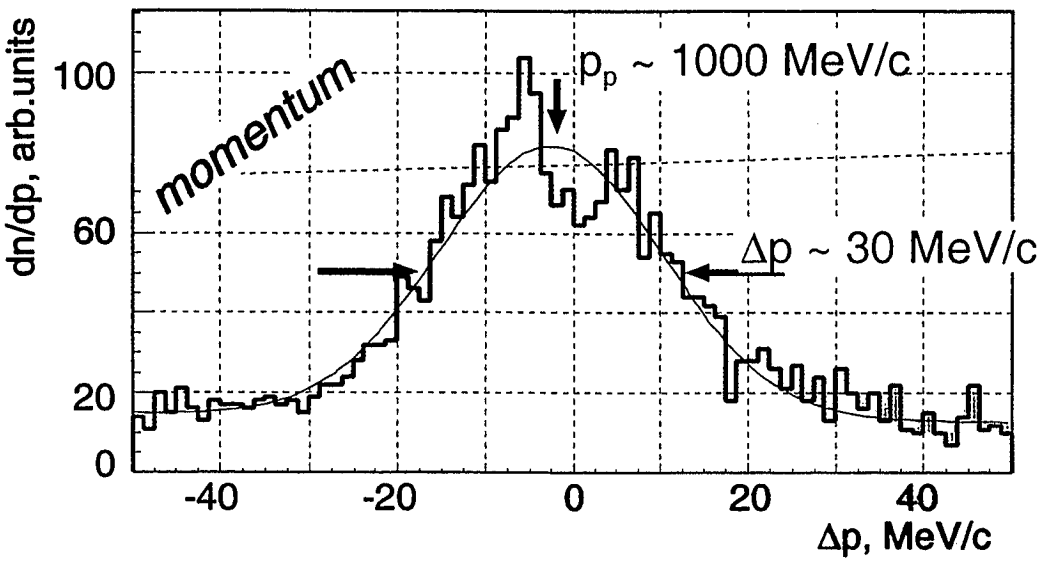

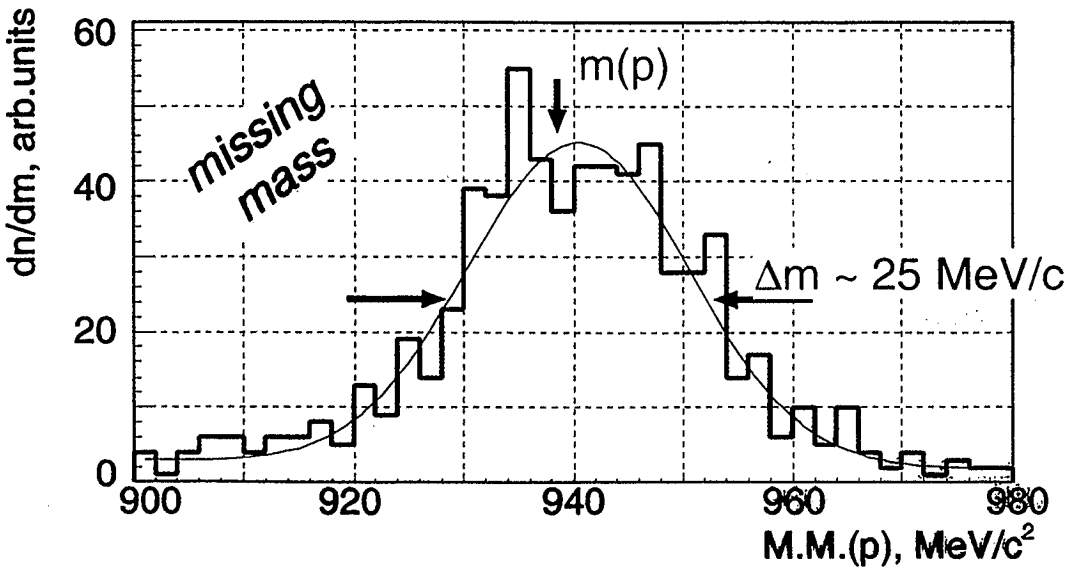

(Preliminary) analysis by S.Dymov

Expected cross section for $pp \rightarrow da_0^+$

(model calculations* compared with LBL data @ forward angles and higher T)

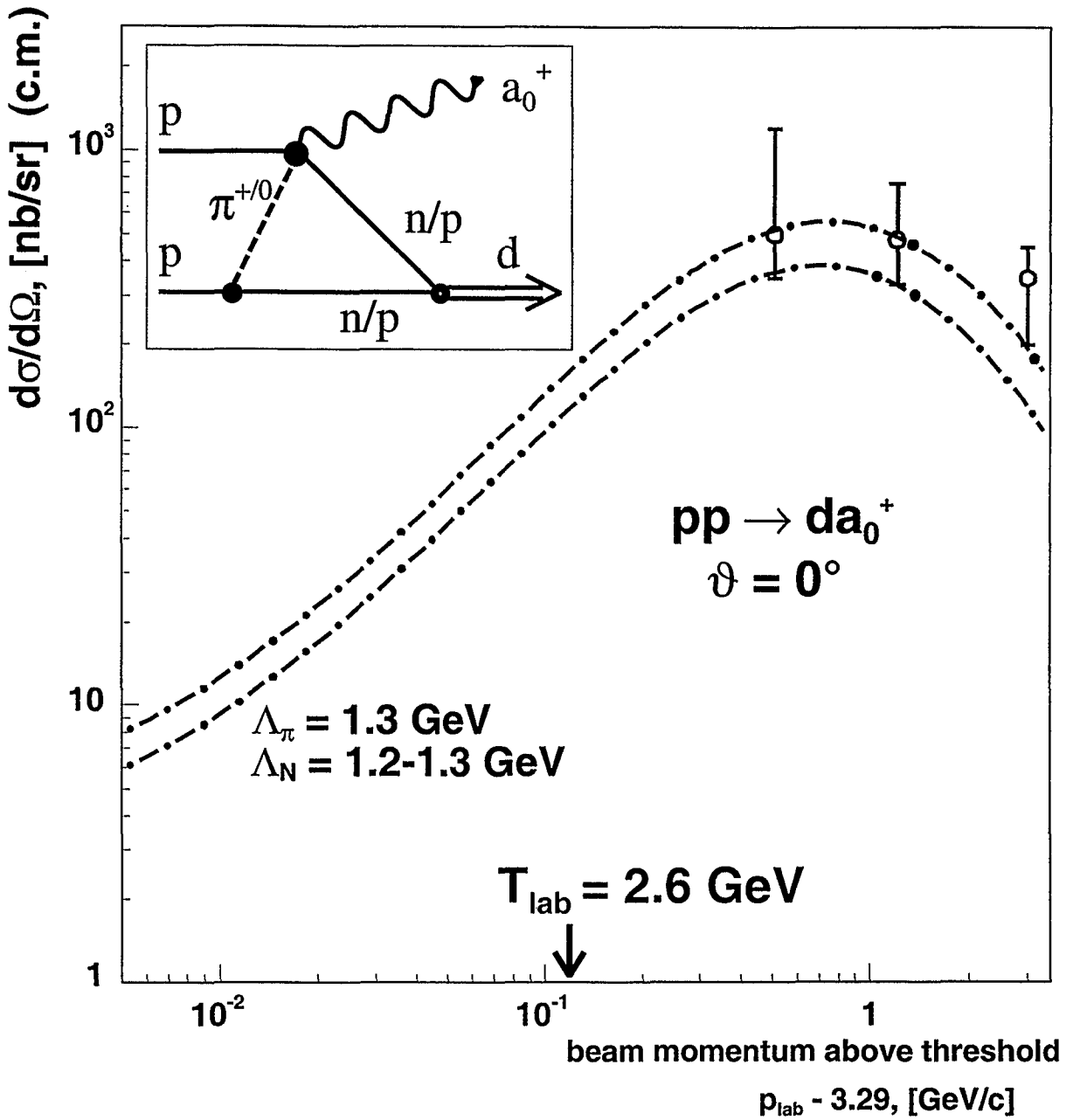

$\sigma_{total} \cong 1.1\ \mu b$

* V.Grishina, L.Kondratyuk, E.L.Bratkovskaya et al., to be published

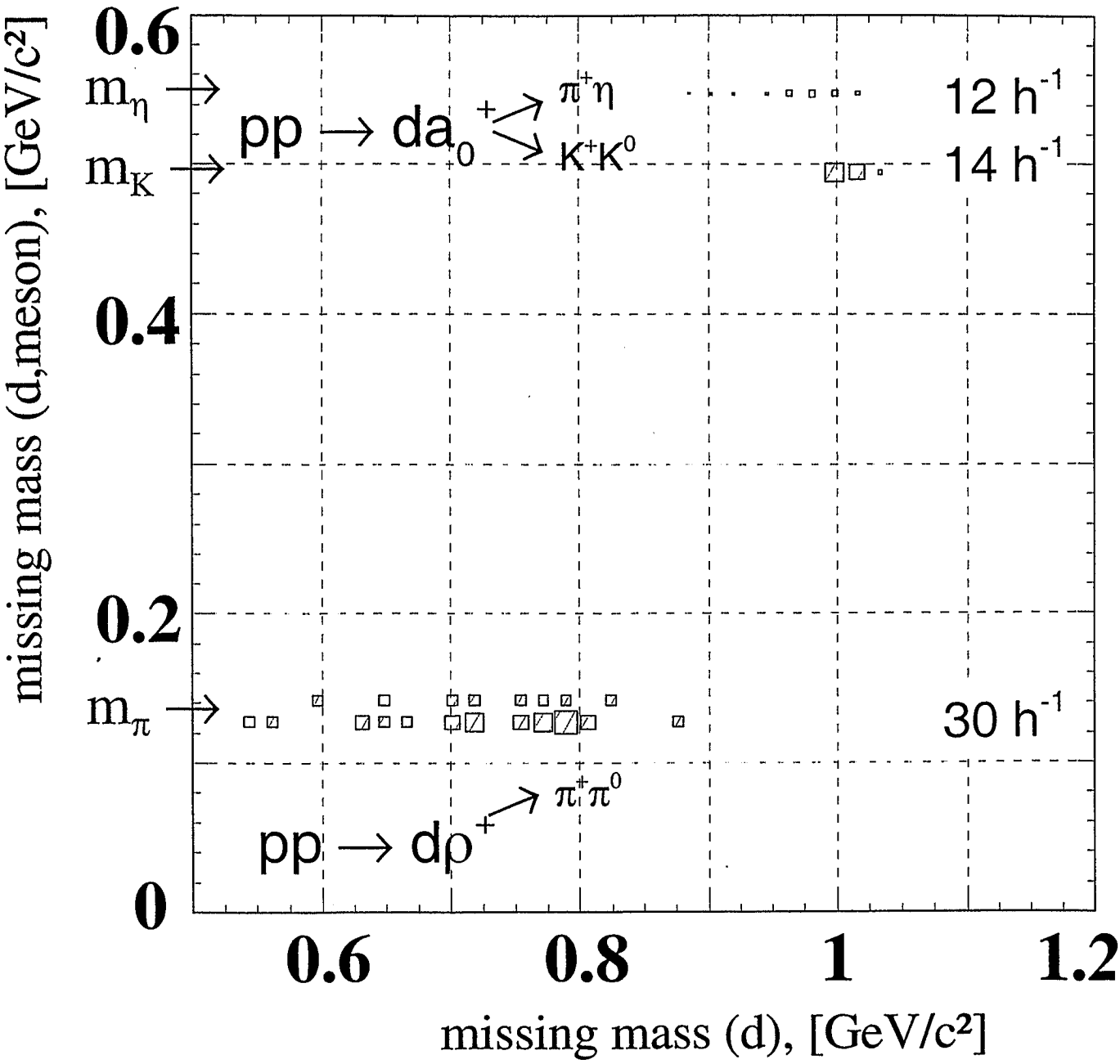

Rates @ $L = 3 \cdot 10^{30}$ cm^{-2} s^{-1}

M.Büscher, 4/00

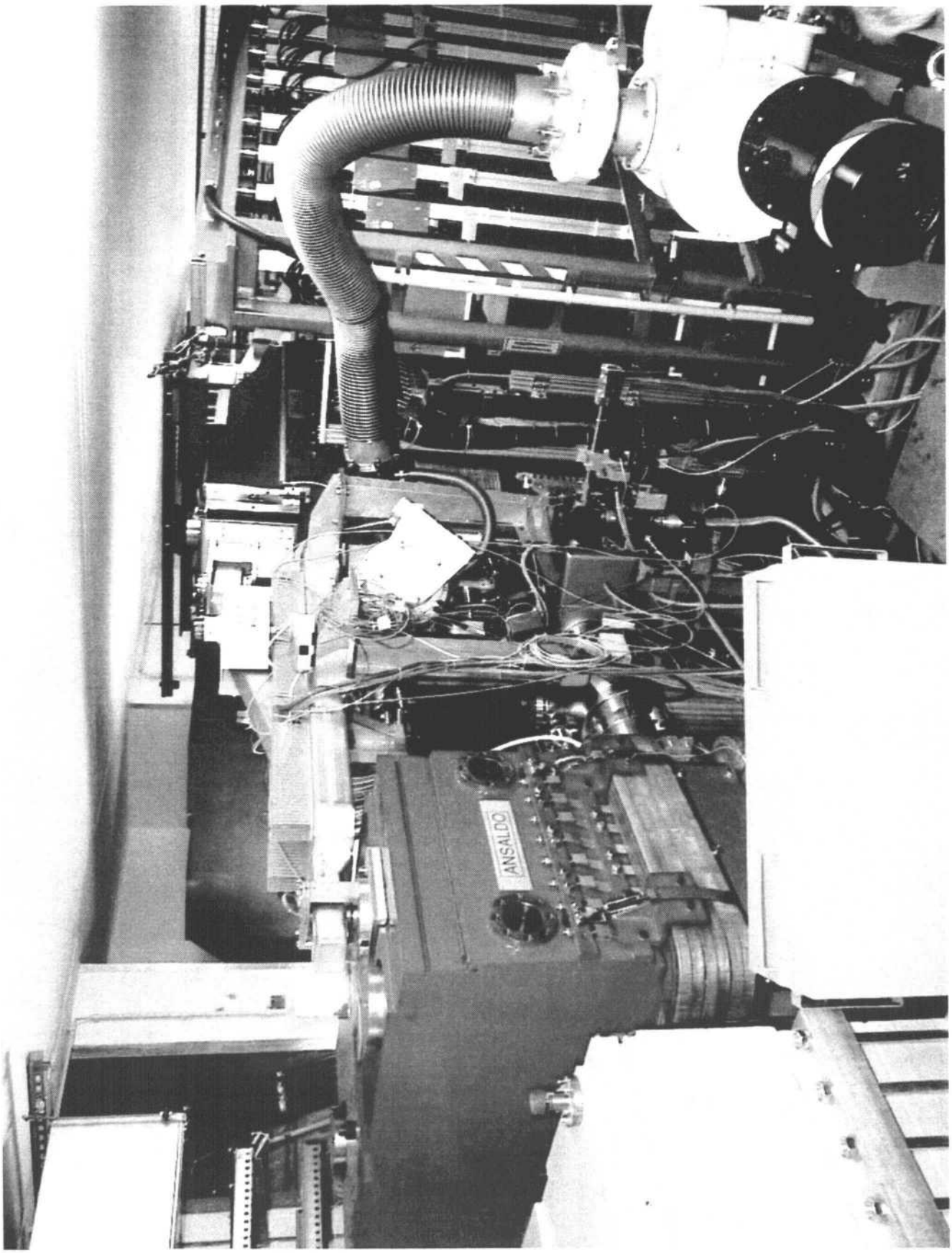
ANSALDO

BACKGROUND !

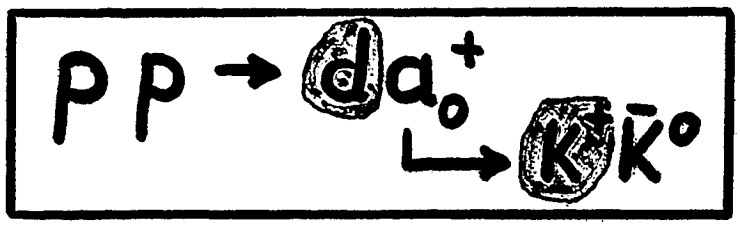

- $pp \xrightarrow{a_0^+} dK^+\bar{K}^0$ (non-resonant)

$\sigma_{NR} \approx \sigma_{a_0^+}/20$ (estimated from $pp \to ppK^+K^-$ data)

➡ not significant

- $pp \to pK^+X$
  ↳ misidentified as d

$\sigma_{pK^+X} \approx 10^{8} \cdot \sigma_{a_0^+}$

➡ suppress protons by factor $\approx 10^{8}$

Cerenkov, TOF, ΔE counters : $\sim 10^3$
$P_{K^+}(pK\Lambda) \neq P_{K^+}(a_0^+)$: ~ 20
$> 10^4$

Tilted Cerenkov counters

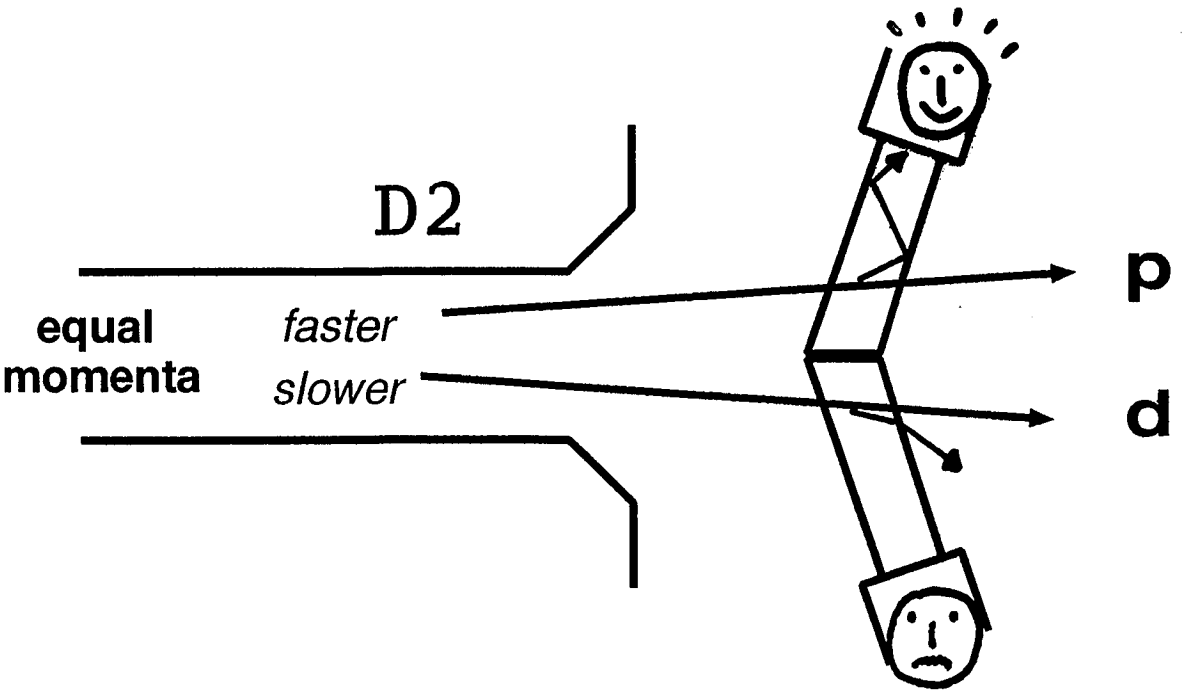

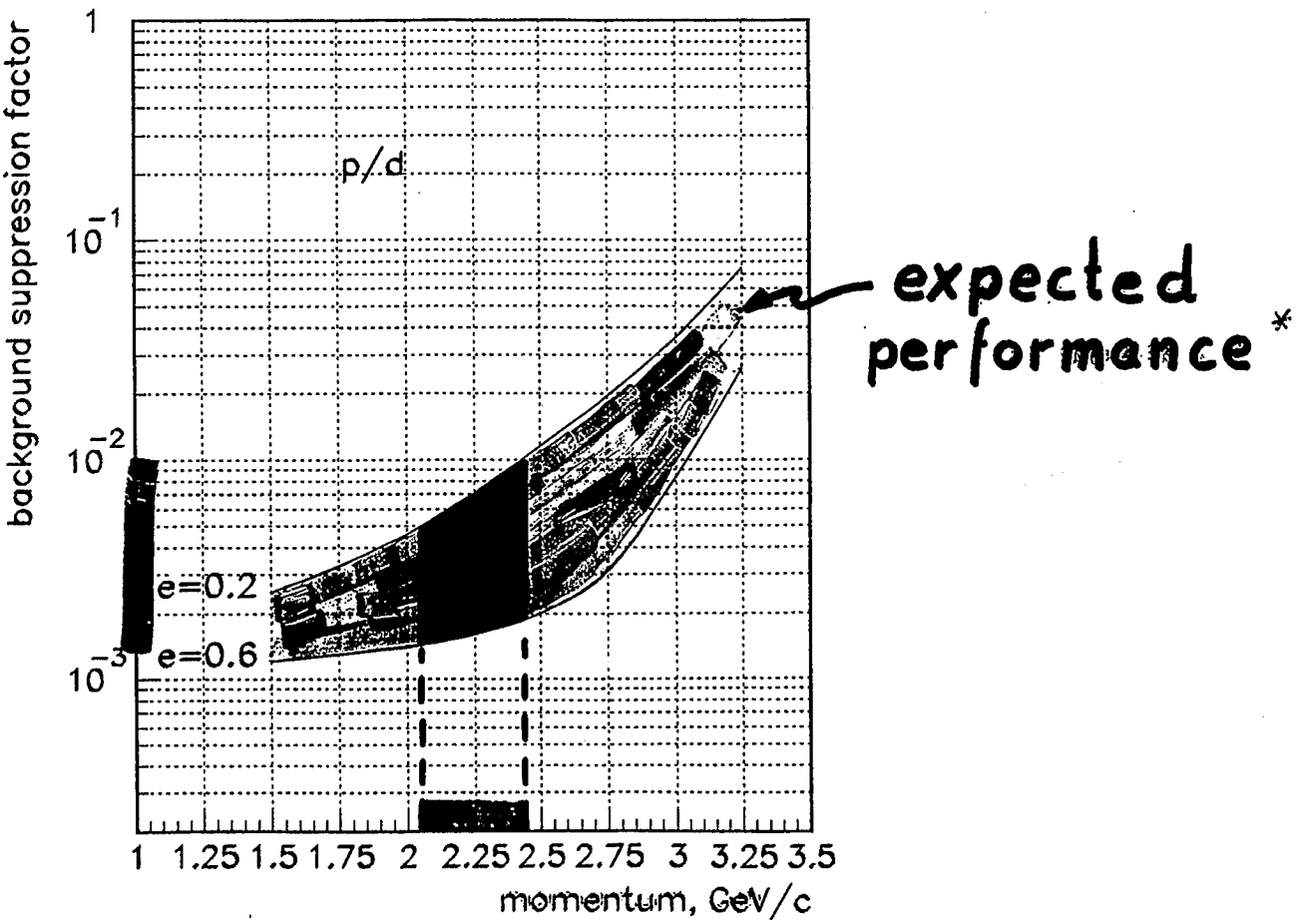

also tested with π^+, p: A.Kacharava et al., NIM A376 (1996) 356

Background suppression I

(time, momentum)

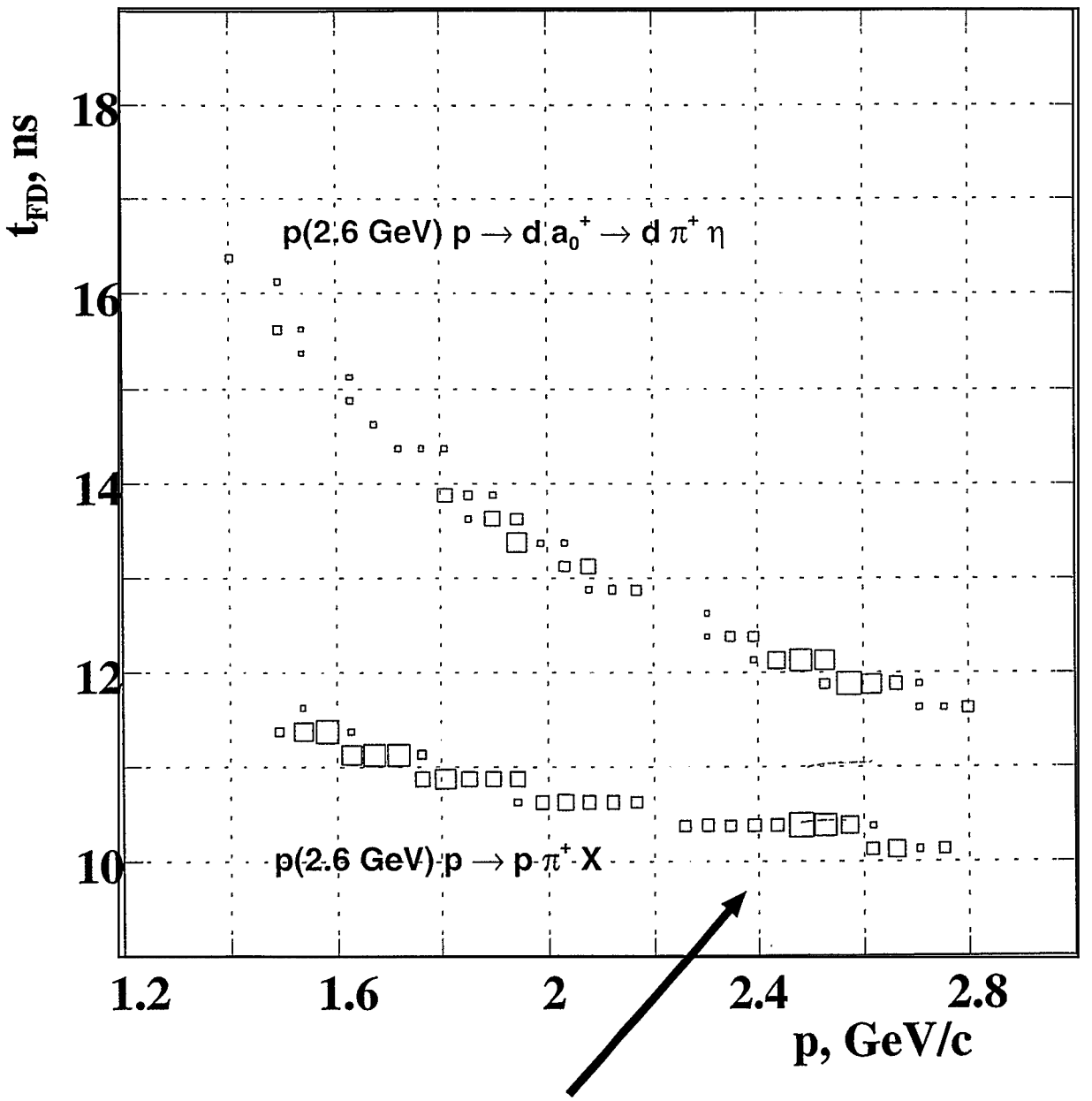

Most 'dangerous' region:

additional factor ~10

proton suppression needed

$\Rightarrow$ missing masses

M.Büscher, 4/00

FROZEN PELLET TARGET

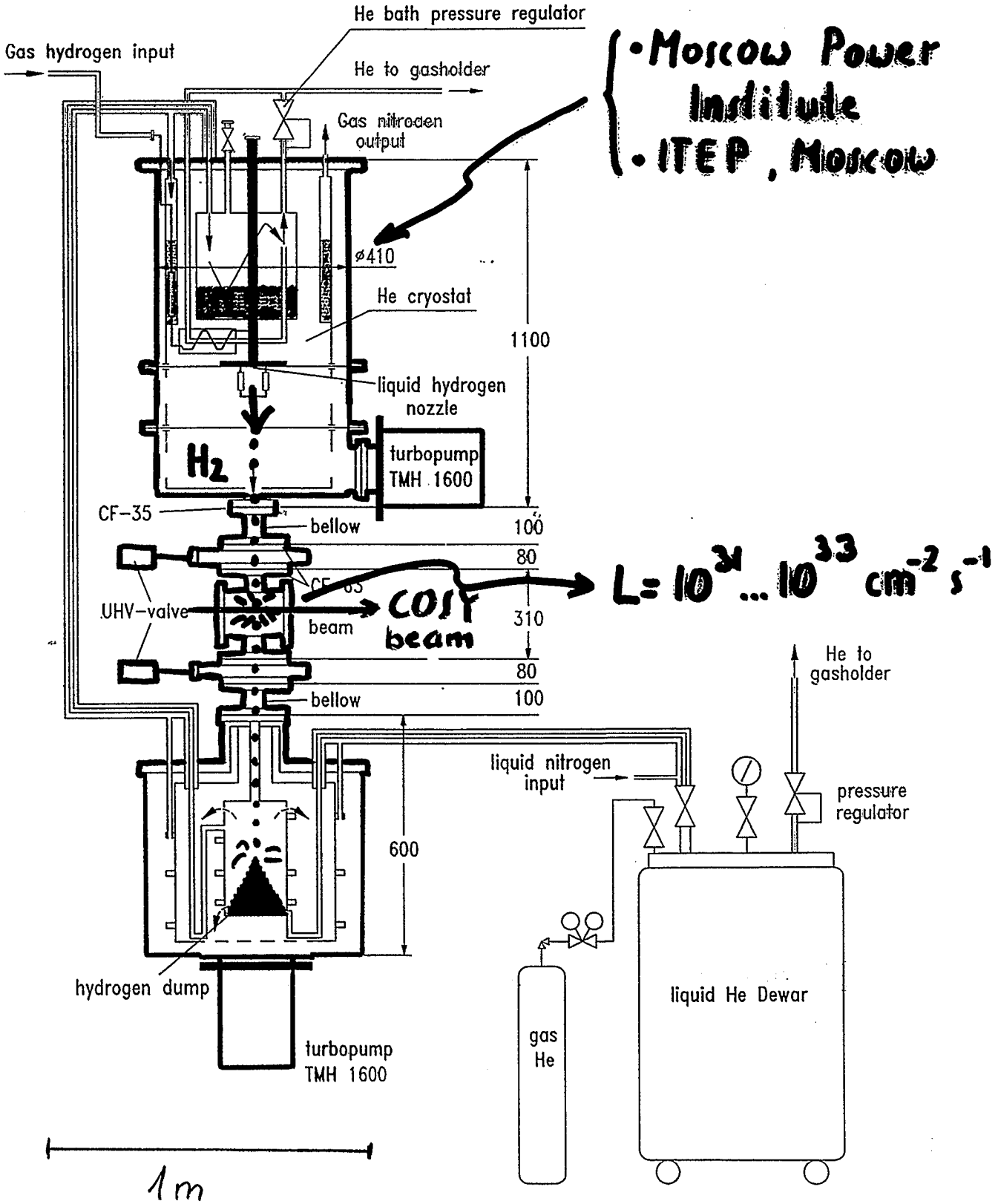

- Moscow Power Institute
- ITEP, Moscow

$L = 10^{31} \ldots 10^{33}\ cm^{-2}\ s^{-1}$

Workshop on "a_0 Physics with ANKE"
July, 13/14, 2000
ITEP, Moscow

What data can we expect from ANKE in 2/2001 ?

$p(2.6\ \text{GeV})\ p \rightarrow d\ a_0^+$

~5000 events (σ~1μb)
Production cross section

$a_0^+ \rightarrow \pi^+\eta\ /\ K^+\bar{K}^0$

Mass distributions
Branching ratio

feedback?

What can we learn from that about scalar mesons ?

Today's session !?

Ideas for future measurements at ANKE ?

Pellet target (>2001):

σ~10nb reachable
Measurements closer to threshold

Scalar Mesons: Why they are Interesting

Yu. S. Kalashnikova

Institute for Experimental and Theoretical Physics
B. Cheremushkinskaya 25
117259 Moscow
Russia

The established spectrum of scalar ($J^{PC} = 0^{++}$) mesons with isospin $I = 0, 1/2, 1$ is discussed together with the predictions of a $q\bar{q}$ model for low-lying scalars, with special attention paid to the $f_0(980)$ and $a_0(980)$ states. It is argued that the existing data on radiative ϕ decays, hadronic J/ψ decays and two-photon couplings are not compatible with the $q\bar{q}$ assignment for f_0 and a_0. The data favour an $s\bar{s}(u\bar{u} \pm d\bar{d})$ content for these states, either in the form of compact four-quarks or in the form of weakly bound $K\bar{K}$ states ($K\bar{K}$ molecules).

The unitarised coupled-channel model advocated by N. Tornqvist is reviewed, where strong couplings to hadronic channels causes the substantial shift to the lower mass of the physical state than that is naively expected from the bare $q\bar{q}$ states. The $a_0(980)$ and $f_0(980)$ mesons in this approach owe their existence to the $q\bar{q}$ component, but, due to the strong coupling to the $K\bar{K}$ threshold, the $K\bar{K}$ molecular component dominates their wave function.

The alternative explanation of the $f_0(980)/a_0(980)$ phenomenon is briefly discussed, based on the "vacuum scalars" assignment, which follows from the super-critical confinement picture suggested by V. Gribov. It is shown that the existing data seem to contradict such scenario.

(1)

Scalar mesons

(minimal list)

$I=1/2$	$I=0$	$I=1$
$K_0^*(1430)$	$\sigma/f_0(400-1200)$	$a_0(980)$
$\Gamma = 300$ MeV	$\Gamma = 1000$ MeV	$\Gamma = 50-100$ MeV
	$f_0(980)$	$a_0(1450)$
	$\Gamma = 40-100$ MeV	$\Gamma = 270$ MeV
	$f_0(1370)$	
	$\Gamma = 200-500$ MeV	
	$f_0(1500)$	
	$\Gamma = 100$ MeV	
	$f_J(1710)$?	
	$\Gamma = 150$ MeV	

The nature of f_0/a_0 should be clarified in order to

- isolate glueball signals
  admixture of glue
- isolate 1^3P_0 $q\bar{q}$ states
  string confiment vs potential model,
  $s\bar{s}$ admixture
- investigate $K\bar{K}$ couplings
  resonances and thresholds
- establish the dynamical origin of the σ meson
  confinement vs CSB

Quark model

(3)

Godfrey - Isgur $1\,^3P_0$ states

$I=1$	$I=1/2$	$I=0$
$M = 1.09$ GeV	$M = 1.24$ GeV	$M = 1.09$ GeV $(u\bar{u}+d\bar{d})$
		$M = 1.36$ GeV $s\bar{s}$

Modern wisdom

		Γ (MeV)
$b_1(1235)$	1^{+-}	140
$h_1(1170)$	1^{+-}	360
$a_1(1260)$	1^{++}	400
$f_1(1285)$	1^{++}	25
$a_2(1320)$	2^{++}	107
$f_2(1270)$	2^{++}	185

$^3P_0\,(u\bar{u}+d\bar{d}) \Rightarrow f_0(1370)$

$^3P_0\,(u\bar{d}) \Rightarrow a_0(1450)$

$^3P_0\,(u\bar{s}) \Rightarrow K_0^*(1430)$

- Large hadronic width ($^3P_0$ decay model)
- Suppression of LS splitting (Lorentz nature of confinement, string confinement)

Quark content beyond $q\bar{q}$ (Achasov) (4)

$$a_0(980) = c_1 \frac{u\bar{u}-d\bar{d}}{\sqrt{2}} + c_2 \frac{s\bar{s}(u\bar{u}-d\bar{d})}{\sqrt{2}} + \ldots$$

$$f_0(980) = \tilde{c}_0 gg + \tilde{c}_1 \frac{u\bar{u}+d\bar{d}}{\sqrt{2}} + \tilde{c}_2 s\bar{s} + \tilde{c}_3 s\bar{s}\left(\frac{u\bar{u}+d\bar{d}}{\sqrt{2}}\right) + \ldots$$

* * *

Radiative φ decays (SND)

$$Br(\varphi \to \gamma\pi^0\pi^0,\ M_{\pi^0\pi^0} > 800\ MeV) = (1.2 \pm 0.2)\cdot 10^{-4}$$

$$Br(\varphi \to \gamma\pi^0\eta,\ M_{\pi^0\eta} > 800\ MeV) = (1.3 \pm 0.5)\cdot 10^{-4}$$

- Branchings are large, and compatible with four-quark

J/ψ decays

$$\frac{Br(J/\psi \to a_0(980)\rho)}{Br(J/\psi \to a_2(1320)\rho)} < 0.04 \pm 0.008$$

$$\frac{Br(J/\psi \to f_0(980)\omega)}{Br(J/\psi \to f_2(1270)\omega)} = 0.033 \pm 0.013$$

$$\frac{Br(J/\psi \to f_0(980)\varphi)}{Br(J/\psi \to f_0(980)\omega))} \approx 2$$

- compatible with four-quark, large admixture of $s\bar{s}$

(5)

$\gamma\gamma$ couplings

Crystal Ball $\quad \Gamma(a_0 \to \gamma\gamma) = \dfrac{(0.19 \pm 0.07^{+0.1}_{-0.07})\ \text{keV}}{Br(a_0 \to \pi\eta)}$

JADE $\quad \Gamma(a_0 \to \gamma\gamma) = \dfrac{(0.28 \pm 0.04 \pm 0.1)\ \text{keV}}{Br(a_0 \to \pi\eta)}$

two-quark $\quad \Gamma(a_0 \to \gamma\gamma) = (1.5 \div 5.9)\ \text{keV}$

four-quark $\quad \Gamma(a_0 \to \gamma\gamma) = 0.27\ \text{keV}$

Crystal Ball $\quad \Gamma(f_0 \to \gamma\gamma) = (0.31 \pm 0.14 \pm 0.09)\ \text{keV}$

MARK II $\quad \Gamma(f_0 \to \gamma\gamma) = (0.24 \pm 0.06 \pm 0.15)\ \text{keV}$

two-quark $\quad \Gamma(f_0 \to \gamma\gamma) = (5 \div 15)\ \text{keV}$

"magic" $25/9$

- Compatible with four-quark

NB Data on $f_0(980)$ could be explained with

$$f_0 = \sin\alpha\, gg + \cos\alpha \frac{1}{\sqrt{2}}(u\bar{u} + d\bar{d})\sin\beta + s\bar{s}\cos\beta\,\eta,$$

$$\sin^2\alpha \leq 0.08, \quad \cos^2\beta > 0.8$$

But if $a_0 = \dfrac{s\bar{s}(u\bar{u} - d\bar{d})}{\sqrt{2}}$, and $f_0 \approx s\bar{s}$,

why are they degenerate ?

(6)

If four-quarks, then which ones ?

⇒ compact bag-like or 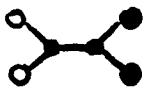 ?

(too many states, too high with strings attached, open isospin exotics, out of fashion)

⇒ loosly bound $K\bar{K}$ molecules ?

* * *

$K\bar{K}$ molecules (Weinstein, Isgur)

mass degeneracy	OK
strong coupling to $K\bar{K}$	OK
J/ψ decays	OK
$\gamma\gamma$ couplings ~ 0.6 keV	a bit too large?
$Br(\psi \to \gamma f_0) \approx Br(\psi \to \gamma a_0) \sim 10^{-5}$	too small ?

?

Molecules are loosly bound states, and are large !

$\pi^- p \to \pi^0 \eta n$ for $0 < -t < 1$ GeV^2

$\pi^- p \to \pi^0 \pi^0 n$

- Data from VES do not confirm large size

Hadronic loops (N. Törnqvist)

Feynman 72

" It is the most important problem in the theory of strong interactions"

" No calculation of such virtual strong interactions in any problem has ever been successful"

" Dead end is a result of lack of imagination of how to get further"

2000

May be too much imagination ?

* * *

Dispersion relations approach

Iterating the decay graph and preserving unitarity

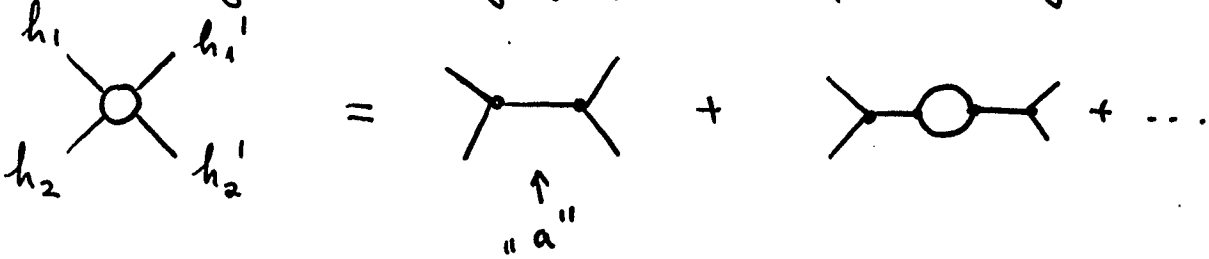

$$T_{if} = -\sum_{ab} g^{*}_{af}\, \tau_{ab}\, g_{bi} \quad , \quad g_{ai} = \;\; a \;\rightarrow\; h_1(i) \;+\; h_2(i)$$

$$\tau^{-1}_{ab} = (s - m_a^2)\,\delta_{ab} + \Delta_{ab}$$

$$\mathrm{Im}\,\Delta_{ab} = \sum_i g_a(i)\, g_b(i) \qquad \Gamma_a = \frac{1}{m_a}\,\mathrm{Im}\,\Delta_{aa}(m_a^2)$$

(8)

$$\mathrm{Re}\,\Delta_{\alpha\beta} = \sum_i \mathrm{Re}\,\Delta_{\alpha\beta}(i)$$

$$\mathrm{Re}\,\Delta_{\alpha\beta}(i) = \frac{1}{\pi} P \int_{s_i}^{\infty} ds' \, \frac{\mathrm{Im}\,\Delta_{\alpha\beta}(s', i)}{s - s'}$$

- Physical mass = Bare mass + Re Δ
- $\mathrm{Re}\,\Delta = \sum_i \mathrm{Re}\,\Delta(i)$

  ↑ sum over all channels, incl. closed ones

Approximate sum rule: (Geiger, Isgur)

$$\Delta = \sum_n \frac{\langle i|\hat{P}|n\rangle\langle n|\hat{P}|i\rangle}{E - E_n} \cong \sum_n \frac{\langle i|\hat{P}|n\rangle\langle n|\hat{P}|i\rangle}{\tilde{E}}$$

$$= \frac{1}{\tilde{E}} \langle i|\hat{P}\hat{P}|i\rangle = \text{const} \quad \text{Closure approximation}$$

- Beyond the closure approximation:

- only „reduced" shifts matter (dispersion relation with subtraction)

- strong violation of closure approximation by thresholds

- the S-wave thresholds are the strongest ones

(9)

Indeed,

$$\mathrm{Re}\,\Delta = \int_{s_0}^{\infty} ds' \, \frac{\mathrm{Im}\,\Delta(s')}{s-s'}$$

$$\mathrm{Im}\,\Delta \sim k^{2l+1}$$

$$\frac{\partial}{\partial s}\mathrm{Re}\,\Delta = -\int_{s_0}^{\infty} ds' \, \frac{\mathrm{Im}\,\Delta(s')}{(s-s')^2} \xrightarrow[s\to s_0]{} \infty \qquad \text{for } S\text{-wave}$$

- Threshold cusp

- No one-to-one correspondence between bare state and resonance

- The admixture of hadronic state (molecule) is proportional to $\frac{\partial}{\partial s}\mathrm{Re}\,\Delta$

$\Rightarrow$ Resonance at the threshold inevitably contains a large molecular component !

Just the case of a_0/f_0 coupled to $K\bar{K}$ in the S-wave !!

Model for PP S-wave (N. Törnqvist)

- Analyticity preserved

Input: $u\bar{u}$, $d\bar{d}$ bare 0^{++} state: $m_0 = 1.420$ GeV

$m_s = 100$ MeV

$q\bar{q}$ coupling + $SU_f(3)$ Clebsch coef.

Cutoff parameter

\+ Adler zeros

Channels: $I = 1/2$ $K\pi, K\eta, K\eta'$

$I = 1$ $\pi\eta, K\bar{K}, \pi\eta'$

$I = 0$ $\pi\pi, K\bar{K}, \eta\eta, \eta\eta'$

Resonance	m_{BW}	Γ_{BW}	m_{pole}	$-\frac{Im(m_{pole})}{m_{pole}}$	Sheet	
$f_0(600)$	860	880	397	590	II	$u\bar{u}+d\bar{d}$
$\rightarrow f_0(980)$	?	?	1006	34	II	$s\bar{s}$
$\rightarrow f_0(1200)$	1186	360	1202	338	III	$s\bar{s}$
$K_0^*(1430)$	1349	498	1441	320	III	
$\rightarrow a_0(980)$	987	? 100	1084	270	II	

(11)

- Two (or more) nearly degenerate resonances with large couplings to common channels result in a bump + dip structure

- $f_0(980)$ and $f_0(1200)$ are the manifestations of the same $s\bar{s}$ bare state

- $f_0(980)$ and $a_0(980)$ spend most of their time as $K\bar{K}$ molecules

- actual position of the poles depend more on the thresholds and Clebschs than on model parameters

? Why should we study the strange corners of the multi-sheeted Riemann surface ?

The $\pi\pi - K\bar{K}$ Coupled Channel Model (Locher, Markushin (12))

Input: Broad resonances which are coupled to $\pi\pi$ and $K\bar{K}$ channels

$K\bar{K}$ potential producing a weakly bound state

ς and K^* t- and u- channel exchanges

+ Adler zeros

Pole structure:

- The ς meson is generated dynamically on the II sheet

- Two possibilities for $f_0(980)$:

  a) $f_0(980)$ pole on the sheet II originates direct from $K\bar{K}$ bound state

  $q\bar{q}$ state pole on the sheet II developes large imaginary part

  b) $q\bar{q}$ state pole is attracted to the $K\bar{K}$ thresho. and corresponds to the narrow $f_0(980)$

In both cases $f_0(980)$ contains

large admixture of $K\bar{K}$ molecule

(13)

From the low-energy side σ looks like the dynamical pole due to attractive interaction:

ChPT + left hand cut (ρ-exchange)

From the high-energy side σ looks like the CDD pole

Bare $q\bar{q}$ state shifted nonperturbatively due to strong coupling to open channel and interference with $f_0(980)$ phenomenon

CSB vs confinement ?

* * *

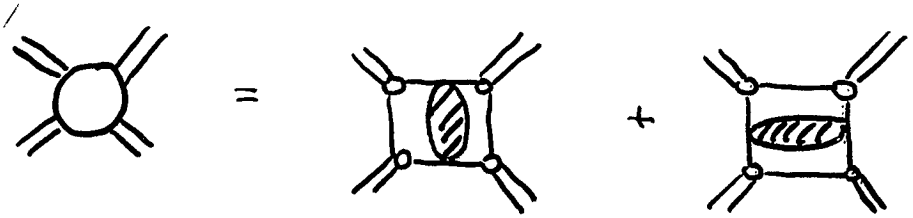

t-channel exchanges CDD

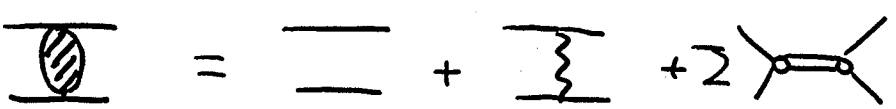

A dream: confinement and CSB are interrelated

i) π is $q\bar{q}$ and Goldstone at the same time

ii) Soft pion theorems are satisfied automatically

iii) The interaction is defined by meson exchanges

iv) Crossing, unitarity, analyticity .... automatically

(14)

f_0 / a_0 as „Vacuum Scalars"

Gribov picture of confinement (super-critical)

Complete departure from constituent model for „vacuum states"

QED with $Z > 137$ — Stationary states with negative electron energy, $\varepsilon < -m$

$Z \to (Z-1) + e^+$ instability.

QCD $m \ll \lambda \sim 1$ GeV

From nonlinear equation for quark Green function (gap equation)

For $\frac{\alpha_s}{\pi} > \frac{\alpha_c}{\pi} \sim 0.2 \Rightarrow$ two solutions

a) CSB breaking solution (as NJL) $q_{(+)}$

b) Solution with quarks with negative kinetic energy $q_{(-)}$

„Vacuum excitations" $\Rightarrow$ pair creation in the new zone below Fermi surface

New condensates consist only of u, d flavours (quarks with positive kinetic energy are clustered into „super-bound" states with negative total energy)

(15)

Size matters : „Novel" mesons contain quarks

(+) with negative kinetic energy; the interaction is repulsive to produce a meson with positive total energy ⇒ very compact states

$$r^{-1} \gtrsim \lambda \sim 1\ \text{GeV}$$

* * *

Vacuum Scalar pair : $f_0(980)$, $a_0(980)$

Vacuum Pseudoscalar pair : $\pi(1300)$, $\eta(1280)$

- Ground state π and η are „conventional" mesons
- $f_0(1370)$ and $a_0(1450)$ are „conventional" $^3P_0$

The heavier is the „vacuum" state, the smaller it is ⇒

- Couplings to „conventional" mesons are suppressed due to small overlap
- $\Gamma(a_0 \to \pi\eta) \geq \Gamma(f_0 \to \pi\pi)$,

as η is heavier, and admixture of „novel" meson in η is more and has more compact distribution than in π

$\gamma\gamma$ couplings

(16)

Very compact states:

$$\Gamma(f_0 \to \gamma\gamma) \Big/ \Gamma(a_0 \to \gamma\gamma) = \frac{25}{9}$$?

φ decays

Shoul not be large (OZI) ?

J/ψ decays

$$\frac{Br(J/\psi \to f_0(980)\varphi)}{Br(J/\psi \to f_0(980)\omega)} \times 2$$?

$$\frac{Br(J/\psi \to f_0(980)\omega)}{Br(J/\psi \to f_2(1270)\omega)} \approx 0.03$$

$$\frac{Br(J/\psi \to a_0(980)\rho)}{Br(J/\psi \to a_2(1320)\rho)} < 0.04$$

? short distances should be enchanced for VS ?

Properties of the a_0/f_0 Mesons

L.A. Kondratyuk

Institute for Theoretical and Experimental Physics
B. Cheremushkinskaya 25
117259 Moscow
Russia

In this talk I briefly review existing models of a_0/f_0 mesons and available experimental information on the main parameters of the $a_0(980)$. The necessity of new measurements on a_0 production and its decay to the $K\bar{K}$ and $\pi\eta$ channels is emphasised for clarifying the a_0 structure. The main mechanisms of the a_0 production in the reactions $\pi N \to a_0 N$ and $pp \to da_0^+$ are discussed. It is concluded that the future ANKE experiment on a_0 production in the reaction $pp \to da_0^+$ can shed new light on the a_0 nature.

Properties of a_0/f_0 mesons.

Leonid Kondratyuk

ITEP, Moscow

Workshop on "a_0 Physics with ANKE"

July 13/14, 2000
ITEP, Moscow

- models of a_0/f_0
- a_0/f_0 parameters
- a_0 production in $\pi N \to a_0 N$

the structure of lightest scalars
is not yet understood

$a_0(980)$ / $f_0(980)$???

- $q\bar{q}$ 2 quark state $L=1$
- $qq\bar{q}\bar{q}$ 4 quark state
- $K\bar{K}$ molecules
- $K\bar{K}$ threshold cusp
- vacuum scalars Gribov et al
(eye-witnesses of confinement)

strong mixing of $a_0 \rightleftarrows f_0$ (Speth et al)

$a_0^{\pm}$ are not mixed with f_0

$pp \to d\, a_0^+$ is the isospin filter
- $\to \eta \pi^+$
- $\to K^+ \bar{K}^0$

Hadron 99
"the most favourable is
Unitarized Quark Model"

$$|a_0\rangle = C_0|q\bar{q}\rangle + C_1|\pi\eta\rangle + C_2|K\bar{K}\rangle$$

$q\bar{q}$ - core + 2-meson continuum

However other options are not
completely rejected

$\bar{q}q$ model Problems

$^3P_0$ $q\bar{q}$ states $f_0(980)$, $a_0(980)$

a long standing problem Γ_{tot}

$\bar{q}q$ quark model $\Gamma_{tot} \gtrsim 500$ MeV

f_0 $\Gamma_{exp} = 40 \div 100$ MeV

a_0 $\Gamma_{exp} = 50 \div 100$ MeV

$q\bar{q}$??? $f_0(400-1200)$ $0^+(0^{++})$

σ

$M - i\frac{\Gamma}{2} = (400-1200) - i(300-500)$ MeV

$f_0(980)$ decouples from $f_0(400-1200)$

$\gamma\gamma$ width

$\Gamma(f_0 \to \gamma\gamma) = 0.56 \pm 0.11$ keV

$\Gamma(a_0 \to \gamma\gamma)\, B_2(a_0 \to \pi\eta) = 0.24 \pm 0.08$ keV

$B_2(a_0 \to \pi\eta)$?

$\Gamma^{\gamma\gamma}_{exp} \sim \frac{1}{10}\Gamma^{\gamma\gamma}_{q\bar{q}}$; $\frac{\Gamma^{\gamma\gamma}_{exp}}{\Gamma_{tot}}$ O.K.

Suppression of Γ_{tot} and $\Gamma^{\gamma\gamma}$ is needed

- $K\bar{K}$ molecule $\quad R \gg z_{q\bar{q}}$
- vacuum scalars $\quad z \sim 0.2\,fm \ll z_{q\bar{q}}$
  (mignons)

$$\Gamma_{tot}^{v.s.} \sim \frac{1}{10}\,\Gamma_{q\bar{q}}$$

$$\Gamma_{\gamma\gamma}^{v.s.} \sim \frac{1}{10}\,\Gamma_{q\bar{q}}$$

molecule fo $\Gamma_{\pi\pi}$ $\Gamma_{K\bar{K}}$

why $\Gamma_{\pi\pi} \gg \Gamma_{K\bar{K}}$?? L.B.

a_0 $\Gamma_{\pi\eta}$ $\Gamma_{K\bar{K}}$

why $\Gamma_{\pi\eta} \gg \Gamma_{K\bar{K}}$??

is there suppression mechanism of Γ_{tot} and $\Gamma_{\gamma\gamma}$ in $q\bar{q}$ model?

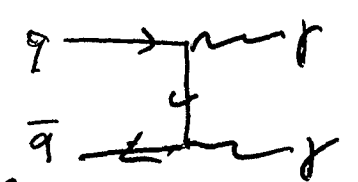

gluon corrections ??
Sudakov f-f. ??
String dynamics ??

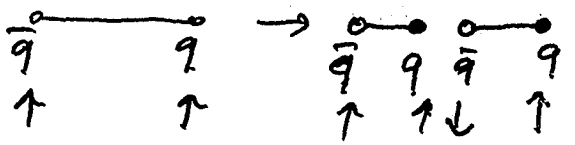

different models →

i) different production mechanisms.

ii) different fo/a_0 N scattering cross sections

$$\sigma_{molecule} \gg \sigma_{q\bar{q}} \gg \sigma_{v.s.}$$

what is known : M_2, B_2, Γ ?

PDG

Crystal Barrel

$$B(\bar{p}p \to a_0\pi;\ a_0 \to K\bar{K}) / B(\bar{p}p \to a_0\pi;\ a_0 \to \pi\eta) = 0.23 \pm 0.05$$

$\bar{p}p \to a_0\pi$?

a_0 is distorted

WA 102, CERN Omega Spectrometer

$pp \to p_f (X^0) p_s$, 450 GeV/c

$\downarrow f_2(1285) \to K_S^0 K^\pm \pi^\mp$

$\to 2\pi^+\pi^-$

$$\frac{a_0(980) \to K\bar{K}}{a_0(980) \to \eta\pi} = 0.166 \pm 0.01 \pm 0.02$$

(However assuming that

$B(f_2 \to a_0\pi) \simeq 100\%$???

hep-ex/9810003

ANKE

$pp \to d\, a_0^+$

$\hookrightarrow K^+\bar{K}^0$

$\hookrightarrow \pi^+\eta$ (no f_2)

$$\frac{B(K^+\bar{K}^0)}{\sigma(K^+\bar{K}^0) + \sigma(\bar{\pi}^+\eta)} \simeq B(K^+\bar{K}^0)$$

340

Meson Particle Listings

$f_0(980)$, $a_0(980)$

OTHER RELATED PAPERS

AU	87	PR D35 1633	+Morgan, Pennington	(DURH, RAL)
AKESSON	86	NP B264 154	+Albrow, Alexander+	(Axial Field Spec. Collab.)
MENNESSIER	83	ZPHY C16 241		(MONP)
BARBER	82	ZPHY C12 1	+Daiesse, Brodbeck, Brookes+	(DARE, LAAC, SMEP)
ETKIN	82C	PR D25 2446	+Foley, Lai+	(BNL, CUNY, TUFTS, VAND)
BIGI	62	CERN Conf. 247	+Brandt, Carrara+	(CERN)
BINGHAM	62	CERN Conf. 240	+Bloch+	(EPOL, CERN)
ERWIN	62	PRL 9 34	+Moyer, March, Walker, Wangler	(WISC, BNL)
WANG	61	JETP 13 323 Translated from ZETF 40 464.	+Veksler, Vrana+	(JINR)

$a_0(980)$ $I^G(J^{PC}) = 1^-(0^{++})$

See our minireview on scalar mesons under $f_0(1370)$ and on the non-$q\bar{q}$ candidates.

$a_0(980)$ MASS

VALUE (MeV)	DOCUMENT ID
983.5±0.9 OUR AVERAGE	Includes data from the 2 datablocks that follow this one.

$\eta\pi$ FINAL STATE ONLY

VALUE (MeV)	EVTS	DOCUMENT ID	TECN	CHG	COMMENT
The data in this block is included in the average printed for a previous datablock.					
983.7 ± 0.9 OUR AVERAGE					
984.45± 1.23±0.34		AMSLER	94C	CBAR	0.0 $\bar{p}p \to \omega\eta\pi^0$
982 ± 2		[1] AMSLER	92	CBAR	0.0 $\bar{p}p \to \eta\eta\pi^0$
984 ± 4	1040	[1] ARMSTRONG	91B	OMEG ±	300 $pp \to pp\eta\pi^+\pi^-$
976 ± 6		ATKINSON	84E	OMEG ±	25–55 $\gamma p \to \eta\pi n$
986 ± 3	500	[2] EVANGELISTA	81	OMEG ±	12 $\pi^- p \to \eta\pi^+\pi^-\pi^- p$
990 ± 7	145	[2] GURTU	79	HBC ±	4.2 $K^- p \to \Lambda\eta 2\pi$
977 ± 7		GRASSLER	77	HBC −	16 $\pi^\mp p \to p\eta 3\pi$
972 ±10	150	DEFOIX	72	HBC ±	0.7 $\bar{p}p \to 7\pi$
• • • We do not use the following data for averages, fits, limits, etc. • • •					
987		TORNQVIST	96	RVUE	$\pi\pi \to \pi\pi, K\overline{K}, K\pi, \eta\pi$
991		JANSSEN	95	RVUE	$\eta\pi \to \eta\pi, K\overline{K}, K\pi, \eta\pi$
980 ±11	47	CONFORTO	78	OSPK −	4.5 $\pi^- p \to pX^-$
978 ±16	50	CORDEN	78	OMEG ±	12–15 $\pi^- p \to n\eta 2\pi$
989 ± 4	70	WELLS	75	HBC −	3.1–6 $K^- p \to \Lambda\eta 2\pi$
970 ±15	20	BARNES	69C	HBC −	4–5 $K^- p \to \Lambda\eta 2\pi$
980 ±10		CAMPBELL	69	DBC ±	2.7 $\pi^+ d$
980 ±10	15	MILLER	69B	HBC −	4.5 $K^- N \to \eta\pi\Lambda$
980 ±10	30	AMMAR	68	HBC ±	5.5 $K^- p \to \Lambda\eta 2\pi$

[1] From a single Breit-Wigner fit.
[2] From $f_1(1285)$ decay.

$K\overline{K}$ ONLY

VALUE (MeV)	EVTS	DOCUMENT ID	TECN	CHG	COMMENT
The data in this block is included in the average printed for a previous datablock.					
976 ± 6	316	DEBELLY	80	HBC ±	1.2–2 $\bar{p}p \to f_1(1285)\omega$
• • • We do not use the following data for averages, fits, limits, etc. • • •					
1016 ±10	100	[3] ASTIER	67	HBC ±	0.0 $\bar{p}p$
1003.3± 7.0	143	[4] ROSENFELD	65	RVUE ±	

[3] ASTIER 67 includes data of BARLOW 67, CONFORTO 67, ARMENTEROS 65.
[4] Plus systematic errors.

$a_0(980)$ WIDTH

VALUE (MeV)	EVTS	DOCUMENT ID	TECN	CHG	COMMENT
50 to 100 OUR ESTIMATE		Width determination very model dependent. Peak width is about 60 MeV, but decay width can be much larger.			
• • • We do not use the following data for averages, fits, limits, etc. • • •					
~ 100		TORNQVIST	96	RVUE	$\pi\pi \to \pi\pi, K\overline{K}, K\pi, \eta\pi$
202		JANSSEN	95	RVUE	$\eta\pi \to \eta\pi, K\overline{K}, K\pi, \eta\pi$
54.12± 0.34±0.12		AMSLER	94C	CBAR	0.0 $\bar{p}p \to \omega\eta\pi^0$
54 ±10		[5] AMSLER	92	CBAR	0.0 $\bar{p}p \to \eta\eta\pi^0$
95 ±14	1040	[5] ARMSTRONG	91B	OMEG ±	300 $pp \to pp\eta\pi^+\pi^-$
62 ±15	500	[6] EVANGELISTA	81	OMEG ±	12 $\pi^- p \to \eta\pi^+\pi^-\pi^- p$
60 ±20	145	[6] GURTU	79	HBC ±	4.2 $K^- p \to \Lambda\eta 2\pi$
60 $^{+50}_{-30}$	47	CONFORTO	78	OSPK −	4.5 $\pi^- p \to pX^-$

[5] From a single Breit-Wigner fit.
[6] From $f_1(1285)$ decay.
[7] Using a two-channel resonance parametrization of GAY 76B data.

$K\overline{K}$ ONLY

VALUE (MeV)	EVTS	DOCUMENT ID	TECN	CHG
• • • We do not use the following data for averages, fits, limits, etc. • • •				
~ 25	100	[8] ASTIER	67	HBC ±
57±13	143	[9] ROSENFELD	65	RVUE ±

[8] ASTIER 67 includes data of BARLOW 67, CONFORTO 67, ARMEN
[9] Plus systematic errors.

$a_0(980)$ DECAY MODES

	Mode	Fraction (Γ_i/Γ)
Γ_1	$\eta\pi$	dominant
Γ_2	$K\overline{K}$	seen
Γ_3	$\rho\pi$	
Γ_4	$\pi\eta'(958)$	
Γ_5	$\gamma\gamma$	seen
Γ_6	e^+e^-	

$a_0(980)$ $\Gamma(i)\Gamma(\gamma\gamma)/\Gamma^2$(total)

$\Gamma(\eta\pi) \times \Gamma(\gamma\gamma)/\Gamma_{\text{total}}$

VALUE (keV)	EVTS	DOCUMENT ID	TECN	COMM
$0.24^{+0.08}_{-0.07}$ OUR AVERAGE				
0.28±0.04±0.10	44	OEST 90	JADE	e^+e^-
0.19±0.07 $^{+0.10}_{-0.07}$		ANTREASYAN 86	CBAL	e^+e^-

$\Gamma(\eta\pi) \times \Gamma(e^+e^-)/\Gamma_{\text{total}}$

VALUE (eV)	CL%	DOCUMENT ID	TECN	COMM
<1.5	90	VOROBYEV 88	ND	e^+e^-

$a_0(980)$ BRANCHING RATIOS

$\Gamma(K\overline{K})/\Gamma(\eta\pi)$

VALUE	DOCUMENT ID	TECN	CHG
• • • We do not use the following data for averages, fits, limits, etc. • • •			
1.16±0.18	[10] BUGG 94	RVUE	
0.7 ±0.3	[11] CORDEN 78	OMEG	
0.25±0.06	[11] DEFOIX 72	HBC	±

[10] BUGG 94 uses AMSLER 94C data. This is a ratio of couplings.
[11] From the decay of $f_1(1285)$.

$\Gamma(\rho\pi)/\Gamma(\eta\pi)$

VALUE	CL%	DOCUMENT ID	TECN	CHG
• • • We do not use the following data for averages, fits, limits, etc.				
<0.25	70	AMMAR 70	HBC	±

$a_0(980)$ REFERENCES

TORNQVIST	96	PRL 76 1575	+Roos
JANSSEN	95	PR D52 2690	+Pearce, Holinde, Speth
AMSLER	94C	PL B327 425	+Armstrong, Ravndal+
BUGG	94	PR D50 4412	+Antovich+
AMSLER	92	PL B291 347	+Augustin, Baker+
ARMSTRONG	91B	ZPHY C52 389	+Barnes+ (ATHU, BARI,
OEST	90	ZPHY C47 343	+Olss n+
VOROBYEV	88	SJNP 48 273 Translated from YAF 48 436.	+Golubev, Dolinsky, Druzhinin+
ANTREASYAN	86	PR D33 1847	+Aschman, Besset, Blenlein+
ATKINSON	84E	PL 138B 459	+ (BONN, CERN, GLAS, LAI
EVANGELISTA	81	NP B178 197	+ (BARI, BONN, C
DEBELLY	80	NP B176 1	+Briand, Duboc, Levy+ (CURIN,
GURTU	79	NP B151 181	+Gavillet, Blokzijl+ (CERN
CONFORTO	78	LNC 23 419	+Conforto, Key+ (RHEL, T
CORDEN	78	NP B144 253	+Corbett, Alexander+ (BIRM,
GRASSLER	77	NP B121 189	+ (AACHS, BERL, BONN, CE
FLATTE	76	PL 63B 224	
GAY	76B	PL 63B 220	+Chaloupka, Blokzijl, Heinen+
WELLS	75	NP B101 338	+Rodojicic, Roscoe, Lyons
DEFOIX	72	NP B44 125	+Nascimento, Bizzarri+
AMMAR	70	PR D2 430	+Krupac, Davis+ (KANS
BARNES	69C	PRL 23 610	+Cheng, Eisner, Bassano, Goldberg+
CAMPBELL	69	PRL 22 1204	+Lichtman, Loeffler+
MILLER	69B	PL 29B 255	+Kramer, Carmony+

BNL E852 (1998)

$m_{a_0^+} = (0.9983 \pm 0.0040)$ GeV, $\Gamma = (72 \pm 10)$ MeV

the shape of $a_0(980)$

Flatté distribution

$$|A_i|^2 = \text{Const} \frac{|\Gamma_i(M)| M_2^2}{(M^2 - M_2^2)^2 + M_2^2 |\Gamma_{tot}^2(M)|}$$

M_2 is the K-matrix pole

$$\Gamma_{tot}(M) = g_1 \rho_1 + g_2 \rho_2$$
$$\Gamma(\pi\eta) \quad \Gamma(K\bar{K})$$

$\rho_i = 2q_i/M$; molecule $g_2/g_1 \gg 1$

$R = \frac{g_2}{g_1}$, different fits

$M_2 \simeq 1.0$ GeV $R \simeq 1 \div 2$, $g_1 \simeq (0.122 \div 0.324)$ GeV

I

1 Models and data on the $K\bar{K}$ and $\pi\eta$ decay channels of the a_0

Within the framework of a coupled channel formalism an appropriate parametrization of the shape of the $a_0(980)$ in each ($\eta\pi$ or $K\bar{K}$) channel can be taken in the form proposed by Flatté [?]

$$|A_i|^2 = Const \frac{|\Gamma_i(M)|\ M_r^2}{(M^2 - M_r^2)^2 + M_r^2|\Gamma_{tot}^2(M)|} \tag{1}$$

where M_r is the K-matrix pole, $\Gamma_{tot}(M) = \Gamma_1(M) + \Gamma_2(M) = g_1\rho_1 + g_2\rho_2$, where g_1 and g_2 are coupling constants to the two final states and ρ_i can be expressed by the momenta of final particles as $\rho_i = 2q_i/M$. Molecular or "threshold cusp" cases would certainly imply a dominance of the $|K\bar{K}\rangle$ component and therefore correspond to a relatively large ratio $R = (g_2/g_1) \gg 1$. In Table 1 we present the most recent results for the $a_0(980)$ parameters.

Table 1: Parameters of the Flatté parametrization for $a_0(980)$.

Reaction	R	M_r(GeV)	g_1(GeV)	Comment	Reference
$p\bar{p} \to \eta\pi^0\pi^0, \eta\eta\pi^0$	1.05÷2.05	1.013÷1.058	0.241÷0.287	i)	[?]
$p\bar{p} \to \eta\pi^0\pi^0, \eta\eta\pi^0$	1.05÷1.45	1.004÷1.024	0.229÷0.312	ii)	[?]
$p\bar{p} \to \eta\pi^0\pi^0, \eta\eta\pi^0$	1.12÷1.37	0.999÷1.006	0.211÷0.275	iii)	[?]
$p\bar{p} \to \eta\pi^0\pi^0$	1.15±0.10	0.999±0.006	0.218±0.020	iv)	[?]
$p\bar{p} \to K_L K^+\pi^-$, $K_L K^-\pi^+$	1.03±0.4	0.999±0.002	0.324±0.015	v)	[?]
$\pi^- p \to n\eta\pi^-\pi^+, n\eta\pi^0$	0.91±0.10	1.001÷0.0019	0.122±0.008	vi)	[?]

i) without any external constraint;

ii) with constraint on $|a_0(980)|^2$ at half-width from the reaction $p\bar{p} \to \eta\omega\pi^0$;

iii) with constraint on $|a_0(980)|^2$ at half-width from the reaction $p\bar{p} \to \eta\omega\pi^0$ and contribution from a hypothetical $a_2'(1620)$ in the fit;

iv) solution B with constraint on the a_0 mass from the reaction $p\bar{p} \to \eta\omega\pi^0$;

v) with constraint that the ratio of integrated intensities in the $K\bar{K}$ and $\eta\pi$ channels is given by Eq. (??);

vi) the authors of Ref. [?] present the value $g_{\pi\eta}$ =0.243±0.015 which is related to g_1 as $g_{\pi\eta} = (2/M)g_1$.

Production of a_0-mesons in the reactions $\pi N \to a_0 N$ and $pp \to da_0^+$ at GeV energies *

V. Yu. Grishina [a], L.A. Kondratyuk [b], E.L. Bratkovskaya [c], M. Büscher [d], and W. Cassing [c]

[a] Institute for Nuclear Research, 60th October Anniversary Prospect 7A, 117312 Moscow, Russia
[b] Institute of Theoretical and Experimental Physics, B.Cheremushkinskaya 25, 117259 Moscow, Russia
[c] Institut für Theoretische Physik, Universität Giessen, D-35392 Giessen, Germany
[d] Institut für Kernphysik, Forschungszentrum Jülich, D-52425 Jülich, Germany

July 13, 2000

Abstract

We investigate the reactions $\pi N \to a_0 N$ and $pp \to da_0^+$ near threshold and at medium energies. An effective Lagragian approach and the Regge pole model are used to analyze different contributions to the cross section of the reaction $\pi N \to a_0 N$. These results are used to calculate the differential and total cross section of the reaction $pp \to da_0^+$ within the framework of the two-step model in which two nucleons produce an a_0-meson via π -meson exchange and fuse to a deuteron. The necessity of new measurements of a_0 production and its decay to the $K\bar{K}$ and $\pi\eta$ channels is emphasized for clarifying the a_0 structure.

*Supported by DFG and RFFI

Mechanisms of a_0 production

$\pi N \longrightarrow N a_0$

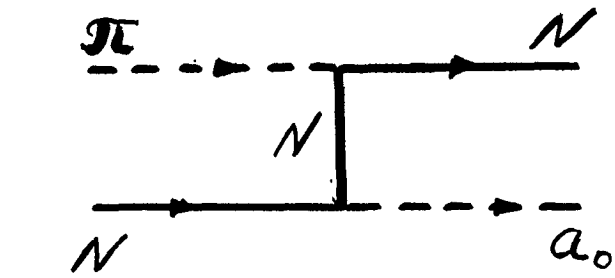

u-channel
main

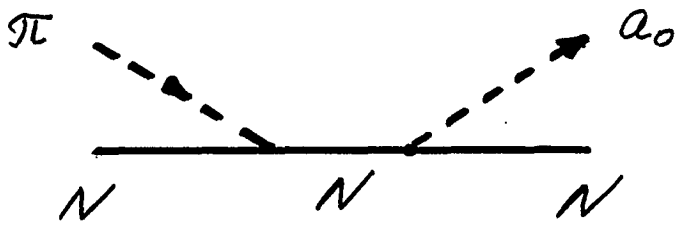

s-channel

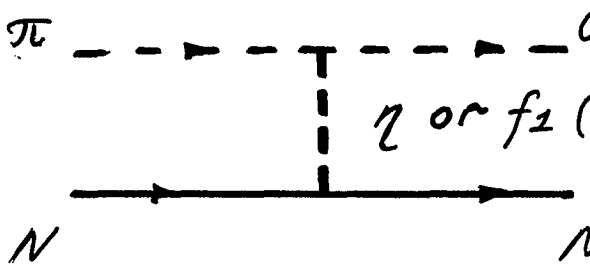

t-channel

This vertex includes different mechanisms

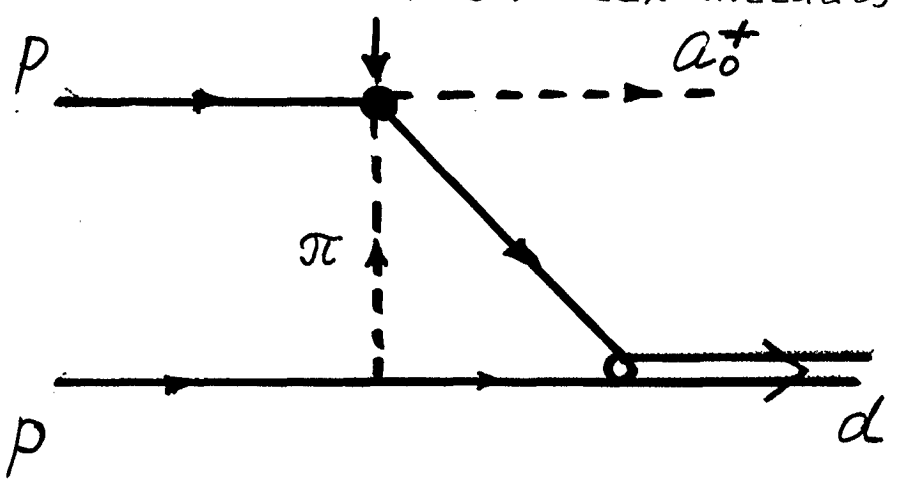

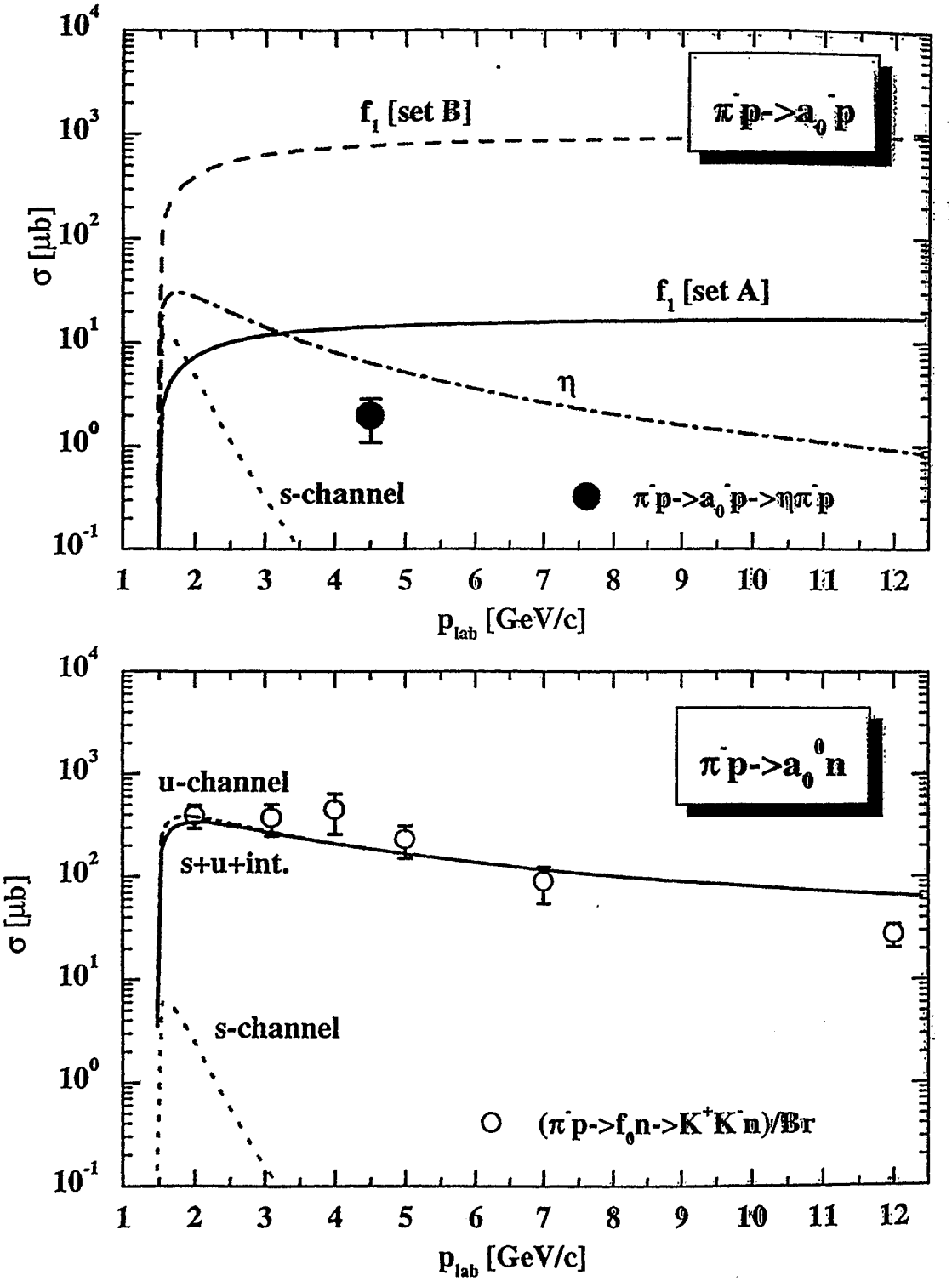
$\pi^- p \to a_0^- p$
f_1 [set B]
f_1 [set A]
η
s-channel
$\pi^- p \to a_0^- p \to \eta\pi^- p$
σ [μb]
p_{lab} [GeV/c]
$\pi^- p \to a_0^0 n$
u-channel
s+u+int.
s-channel
$(\pi^- p \to f_0 n \to K^+K^- n)/Br$
σ [μb]
p_{lab} [GeV/c]

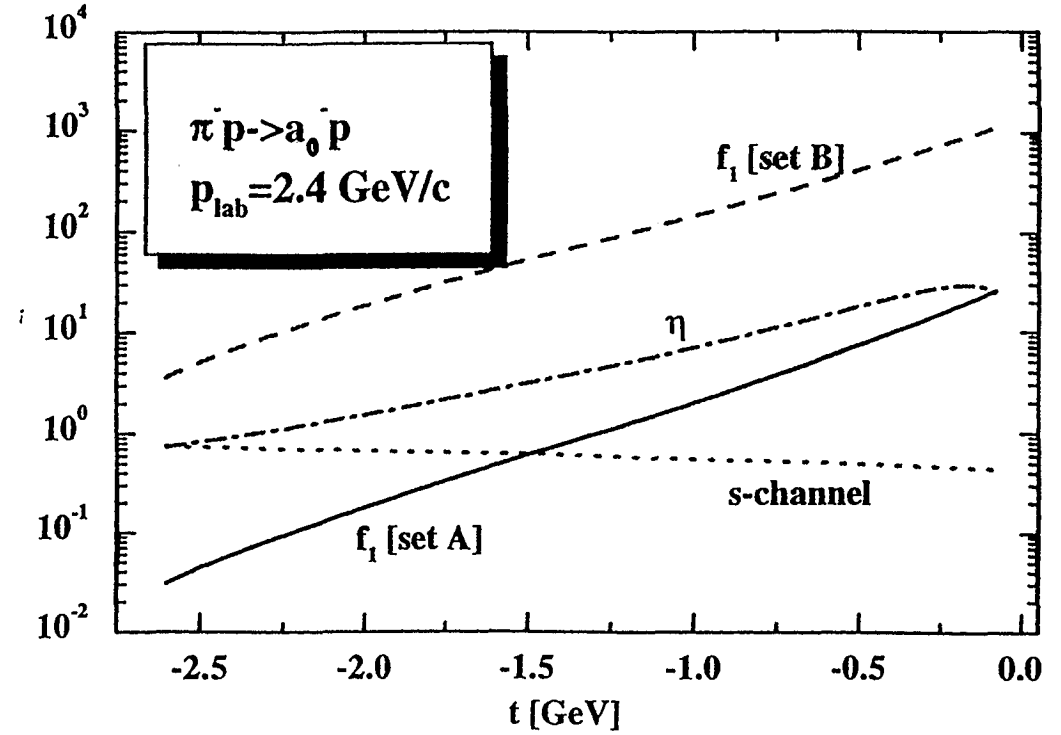
$\pi^- p \to a_0^- p$
p_{lab}=2.4 GeV/c
f_1 [set B]
η
s-channel
f_1 [set A]
10^4
10^3
10^2
10^1
10^0
10^{-1}
10^{-2}
-2.5
-2.0
-1.5
-1.0
-0.5
0.0
t [GeV]

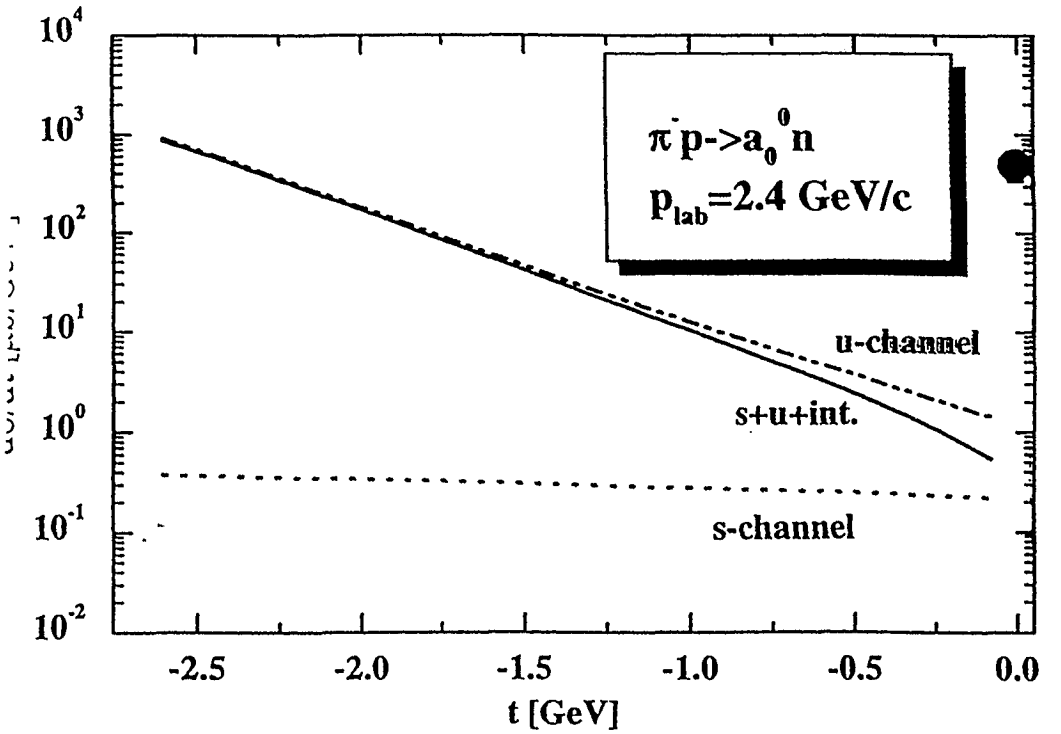
$\pi^- p \to a_0^0 n$
p_{lab}=2.4 GeV/c
u-channel
s+u+int.
s-channel
10^4
10^3
10^2
10^1
10^0
10^{-1}
10^{-2}
-2.5
-2.0
-1.5
-1.0
-0.5
0.0
t [GeV]

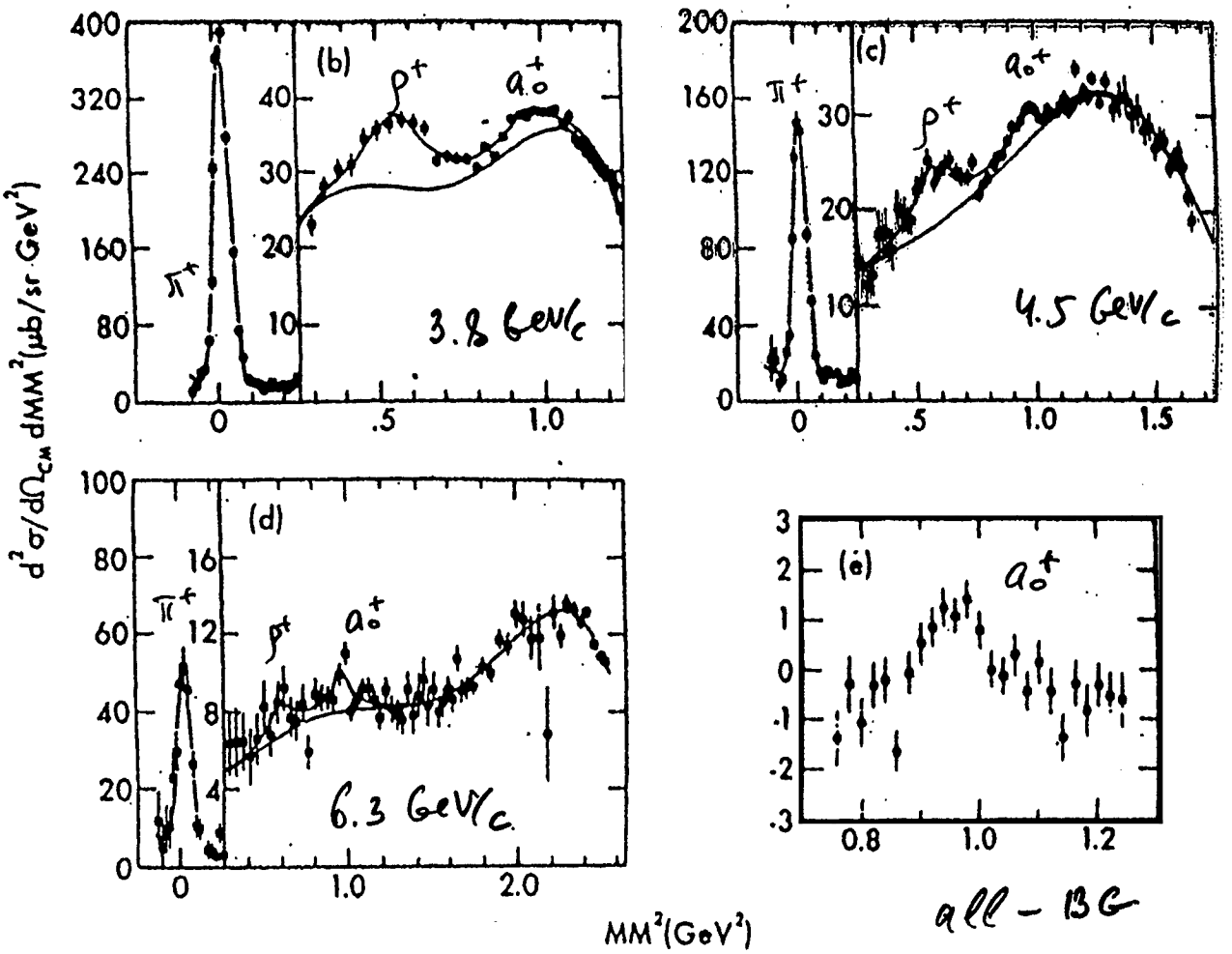

$pp \rightarrow d X^+$

$$R\left(\frac{a_0}{p}\right) \simeq \frac{1}{6} \div \frac{1}{4}$$

Table I. Parameters determined from the fitted data.

p_{inc}(GeV/c)	3.8	4.5	6.3
$pp \to d\pi$			
$d\sigma/d\Omega$, μb/sr(c.m.)	21.0±0.5	9.4±0.3	4.6±0.5
$pp \to d\rho$			
$d\sigma/d\Omega$, μb/sr(c.m.)	3.2±0.5	2.0±0.4	0.5±0.5
Γ (GeV)	0.10±0.01	0.10±0.02	0.09[a]
MM^2(GeV^2)	0.572±0.008	0.574±0.012	0.59[a]
$pp \to d\pi_N(980)$ [b]			
$d\sigma/d\Omega$, μb/sr(c.m.)	$0.5^{+0.7}_{-0.15}$	$0.48^{+0.28}_{-0.15}$	$0.35^{+0.10}_{-0.15}$
MM^2(GeV^2)	0.952[a]	0.952±.012	0.952[a]
Γ (GeV)	0.06[a]	$0.060^{+0.016}_{-0.010}$	$0.055^{+0.016}_{-0.015}$
χ^2 probability (%)[c]	16 (21)	5.3 (4.6)	3.4 (3.1)
χ^2 probability (%) with $d\sigma/d\Omega = 0$[c]	6 (14)	0.22 (0.78)	0.15 (0.11)
no. bins fitted	127	78	38
$pp \to d\delta(962)$			
$d\sigma/d\Omega$, μb/sr(c.m.)	0.043±.023	0.019±.032	0.069±.074

[a]Fixed.

[b]Background polynominal has 4 terms at 3.8 GeV/c, 3 terms at 4.5 GeV/c, and 1 term at 6.3 GeV/c.

[c]Values in parentheses refer to fits with one more background term.

$\sigma(\pi^- p \to \rho^0 n) \simeq 1.8\,mb$ at $2.4\,GeV/c$

$\sigma(\pi^- p \to a_0^0 n) \simeq \frac{1}{6}(\pi^- p \to \rho^0 n) \simeq 0.3\,mb$

u-channel contribution

$\sigma_u(\pi^- p \to a_0^0 n) \simeq 0.3\,mb$

$\left.\frac{d\sigma}{dt}(\pi^- p \to a_0^0 n)\right|_{t=0} = 0.49\,mb/GeV^2$ exp

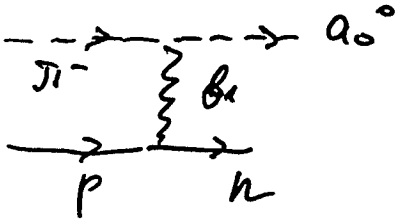

$b_1(1^{+-})$

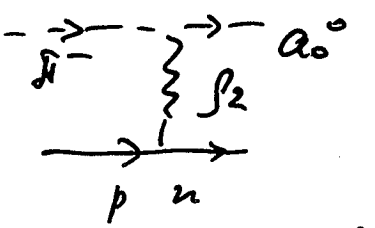

$\rho_2(2^{--})$

Comparison with Brookhaven data,

E852

Achasov - Ghestakov

conspiring ρ_2-Regge exchange

$\pi^- p \to a_0^0 n$ $18\,GeV/c$

$\left.\frac{d\sigma}{dt}\right|_{t\simeq 0} \simeq 1.2\,\mu b/GeV^2$

$\sigma \sim 0.25\,\mu b$ $B(a_0^0 \to \pi^0\eta) \simeq 0.8$

at $t=0$ only β_2 survives

$$\left.\frac{d\sigma_{Regge}}{dt}(\pi^- p \to a_0^0 n)\right|_{t=0} \approx \left.\frac{d\sigma_{\beta_2}}{dt}\right|_{t=0} \approx \frac{1}{(p^1_{c.m.})^2}\left(\frac{s}{s_0}\right)^{-2.2} \times c$$

$$\left.\frac{d\sigma}{dt}(\pi^- p \to a_0^0 n)\right|_{t=0} \simeq 0.46 \text{ mb/GeV}^2$$

at 2.4 GeV/c

$$\frac{d\sigma}{dt}(\pi^- p \to a_0^- p) = \frac{1}{2}\frac{d\sigma}{dt}(\pi^- p \to a_0^0 n)$$

quark diagram (planar)

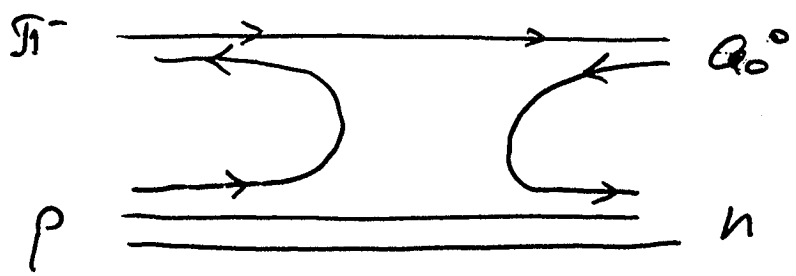

production σ for $q\bar{q}$ model

Vera Grishina

$\sigma(pp \to d a_0^+)$

Let us hope that ANKE experiment will shed new light on the a_0 problem.

a_0^+-Production at COSY Energies

V. Yu. Grishina

Institute for Nuclear Research
60th October Anniversary Prospect 7A
117312 Moscow
Russia

We investigate the reactions $\pi N \to a_0 N$ and $pp \to da_0^+$ near threshold and at medium energies. An effective Lagrangian approach is applied to analyse different contributions to the cross section of the elementary reaction $\pi N \to a_0 N$. It is known that the a_0 couples quite strongly to the channels $\pi\eta$ and $\pi f_1(1285)$. Therefore, for the t-channel contribution to the $\pi N \to a_0 N$ transition amplitude we took into account the exchanges of $\eta(550)$ and $f_1(1285)$-mesons. The $a_0\pi\eta$ and $a_0\pi f_1$ coupling constants were calculated using the following experimental values of the partial widths: $\Gamma_{a_0\to\pi\eta} = 80$ MeV and $\Gamma_{f_1\to a_0\pi} \simeq 8.2$ MeV. The parameters of the ηNN, $f_1 NN$ and $a_0 NN$ vertices are taken from literature. We consider also the s and u-channel diagrams with a nucleon in the intermediate state. These results are used to calculate the differential and total cross sections of the reaction $pp \to da_0^+$ within the framework of the two-step model in which two nucleons produce an a_0-meson via π -meson exchange and fuse to a deuteron. It is found that the main contribution comes from the u-channel diagram for the elementary amplitude $\pi N \to a_0 N$. The forward $pp \to da_0^+$ differential cross section is about 120 nb/sr at $T_{\rm lab} = 2.6$ GeV. This value of the cross section makes the corresponding experiment at COSY quite feasible.

a_0 production at COSY energies

Vera Grishina

Institute for Nuclear Research,

Moscow, Russia

Workshop on "a_0 Physics with ANKE"

July 13 / 14, 2000

ITEP, Moscow

Contents

The two-step model (TSM) for the reaction $pp \to d a_0^+$

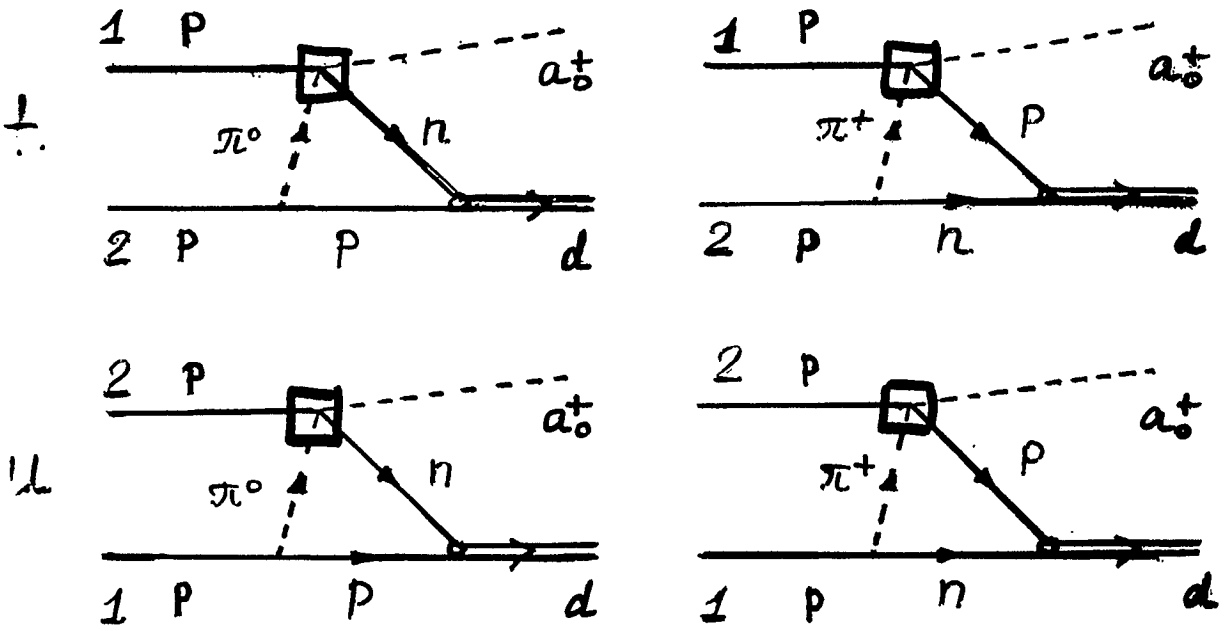

We have $pp \to d a_0^+$ amplitude as a difference of t and u amplitudes (P-wave in the final state near the threshold)

$$T_{pp \to d a_0^+}(s,t,u) = A_{pp \to d a_0^+}(s,t) - A_{pp \to d a_0^+}(s,u)$$

$s = (p_1 + p_2)^2$, $t = (p_3 - p_1)^2$,

$u = (p_3 - p_2)^2$

p_1, p_2 are the 4momenta of the protons

p_3 is the 4-momentum of the a_0^+

p_4 is the 4-momentum of the deuteron

$\Lambda_{\pi NN} = 1.3$ GeV/c

Reaction $\pi N \to N a_0$ within the Effective Lagrangian Approach

The t-channel contribution due to meson exchanges

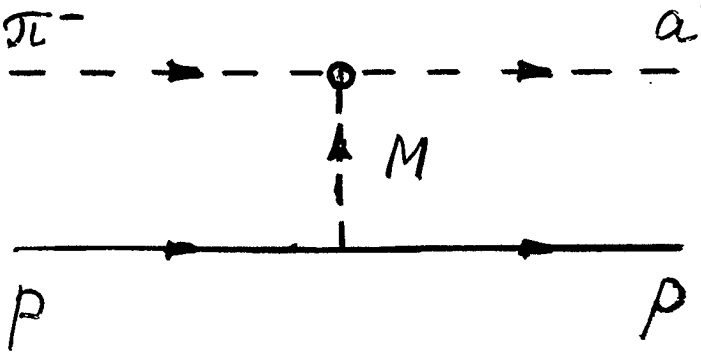

$M = \eta(550)$, $f_1(1285)$, ...? (neutral meson exchange)

$g_{f_1 \pi a_0} \simeq 2.5$

This value is extracted from experimental width of $f_1(1285) \to a_0(980)\pi$ decay

$\Gamma_{f_1 \to a_0 \pi} = (24 \pm 1.2)\ \text{MeV} \cdot 34\%$

and for $\Gamma_{a_0 \to \pi\eta} = 80\ \text{MeV}$ $g_{\eta \pi a_0} \simeq 2.5$

ηNN

$g_{\eta NN} = 6.14$ and cutoff $\Lambda_{\eta NN} = 1.5\ \text{GeV/c}$

$f_1 NN$ (Set A)

$g_{f_1 NN} = 11.2$ and cutoff $\Lambda_{f_1 NN} = 1.5\ \text{GeV/c}$

This parameters are taken from the **Bonn potential model** // R Machleidt et al. Phys Rep 149 N1 (1987)

$f_1 NN$ (Set B)

$g_{f_1 NN} = 14.6$ and cutoff $\Lambda_{f_1 NN} = 2\ \text{GeV/c}$

// M. Kirchbach and D.O. Riska, Nucl Phys A 594, 419 (1995)

Reaction $\pi N \longrightarrow N a_0$

the Effective Lagrangian Approach

The $S-$ and $u-$channel contribution with intermediate nucleon.

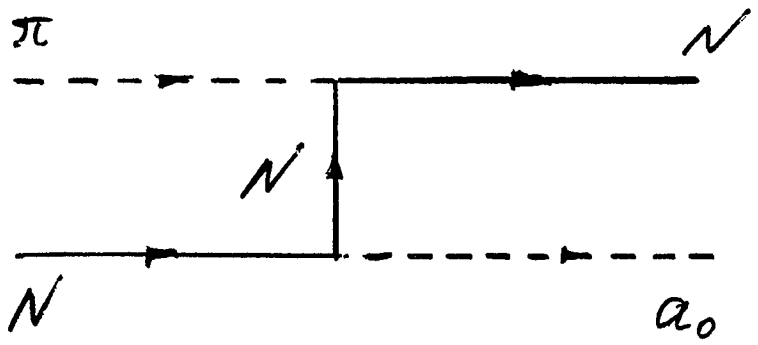

$u-$channel

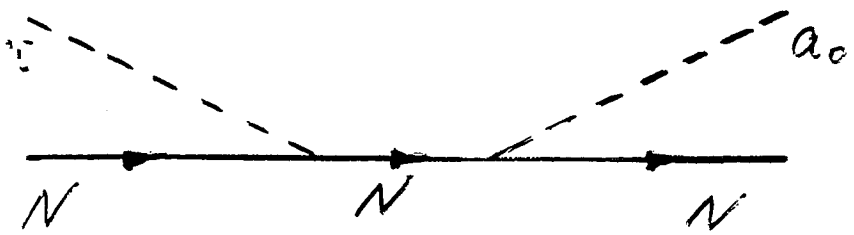

$S-$channel

$f_{\pi NN} \simeq 1$, $g_{a_0 NN} \simeq 3.68$

are taken from the **Bonn potential model**

The form factor for virtual nucleon

$$F_N(q^2) = \frac{\Lambda_N^4}{\Lambda_N^4 + (q^2 - m_N^2)^2}$$

with $\Lambda_N = 1.2$ GeV/c

The experimental forward differential cross section of the reaction $\pi^- p \to n a_0^0$

at $p_{lab} = 2{,}4$ GeV/c

Cheshire
Phys Rev Lett 28
p 520 (1972).

$$\left.\frac{d\sigma}{dt}(\pi^- p \to n a_0^0)\right|_{t=0} = 0{,}49 \text{ mb/GeV}^2$$

What **t-channel** meson exchange mechanism is dominant in this region ?

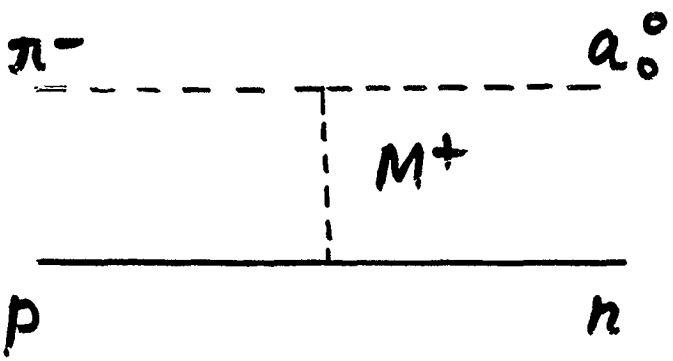

$M^+ = ?$

$\rho_2(2^{--})$ - exchange

$b_1(1^{+-})$ - exchange

Achasov N.N. & Shestakov G.N.
Phys Rev D 56 (1997) 212-220

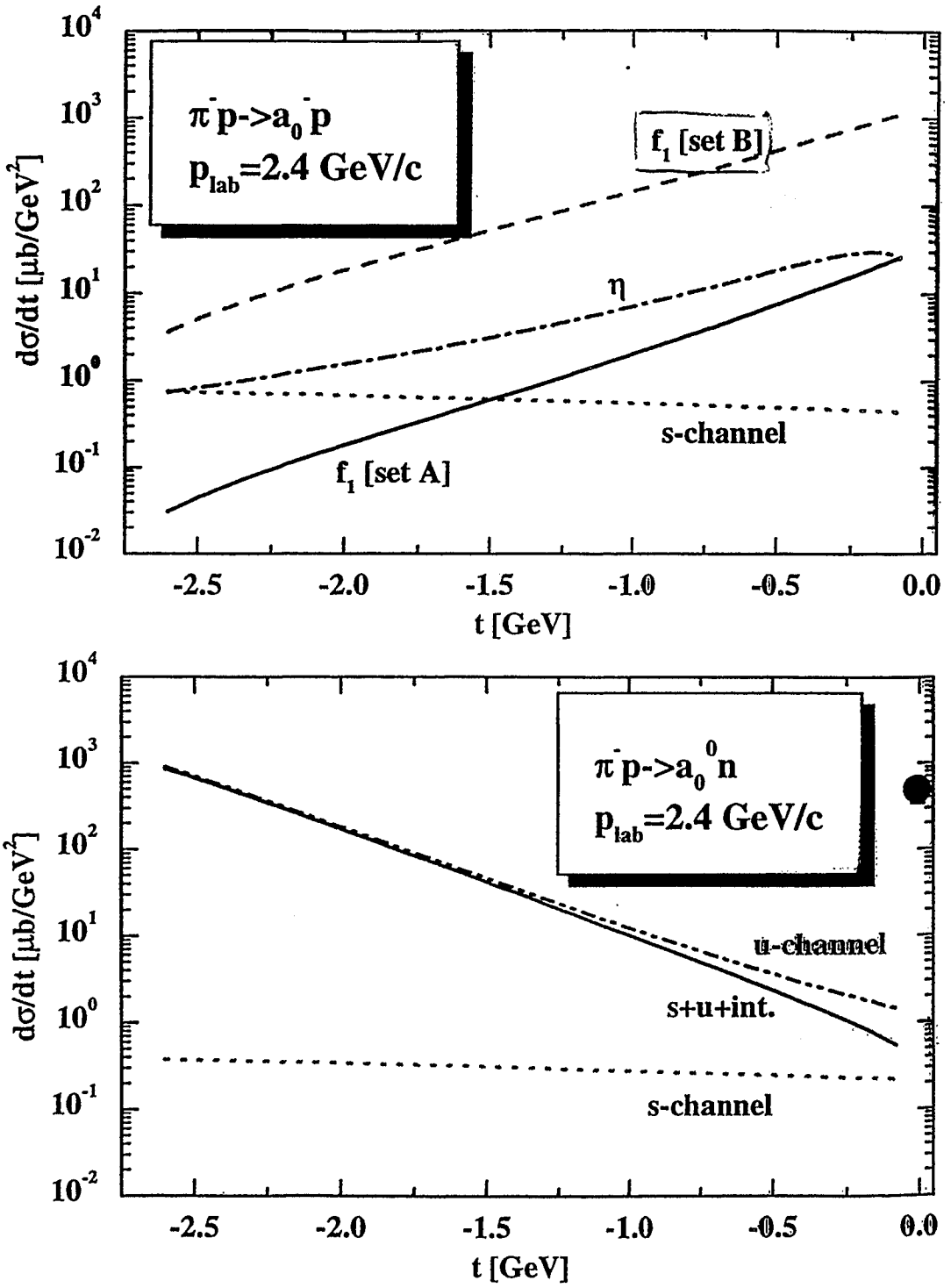
$\pi^- p \to a_0^- p$
p_{lab}=2.4 GeV/c
f_1 [set B]
η
s-channel
f_1 [set A]
dσ/dt [μb/GeV^2]
t [GeV]
$\pi^- p \to a_0^0 n$
p_{lab}=2.4 GeV/c
u-channel
s+u+int.
s-channel
dσ/dt [μb/GeV^2]
t [GeV]

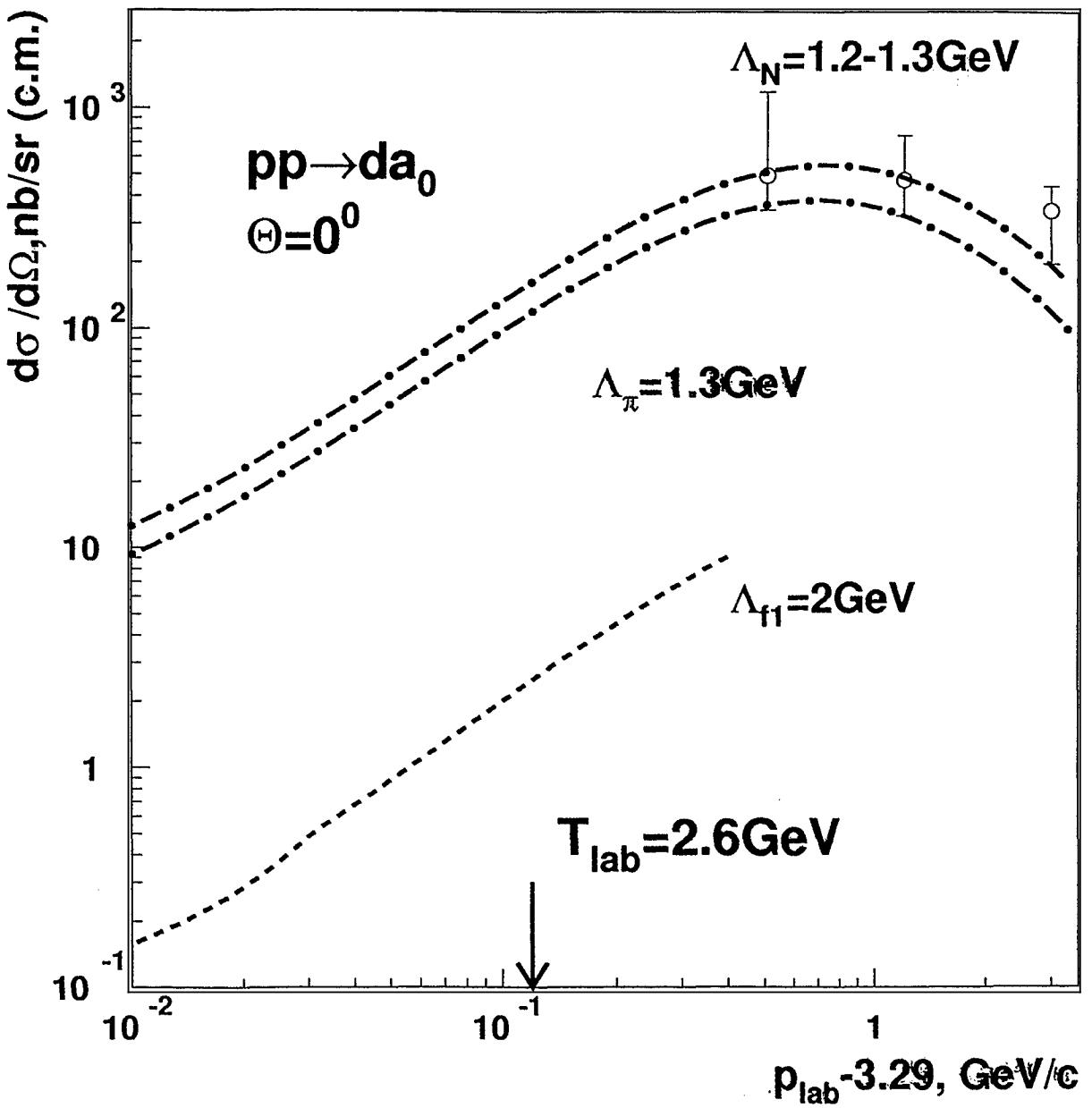

— · — · — is result of calculations with u-channel mechanism for $\pi N \to a^0 N$

set B

- - - - - - - from t-channel contribution with combined $\pi - f_1(1285)$ exchange

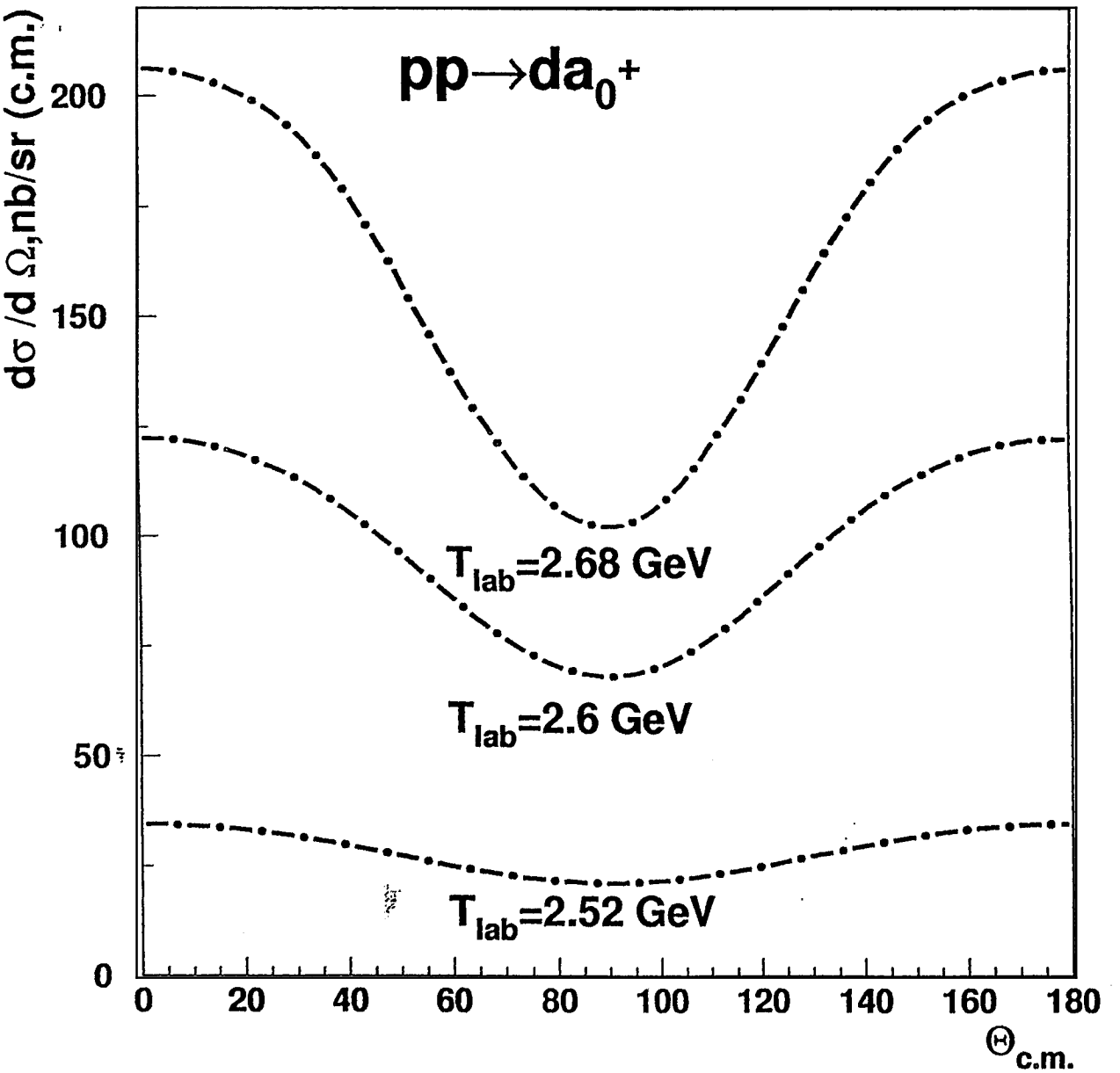
pp→da0+
dσ /d Ω,nb/sr (c.m.)
200
150
100
50
0
Tlab=2.68 GeV
Tlab=2.6 GeV
Tlab=2.52 GeV
0
20
40
60
80
100
120
140
160
180
Θc.m.

Conclusions

1) We analyzed possible mechanisms of the $\pi N \to a_0 N$ transitions.

2) The results are used to calculate the differential and total cross sections of the reaction $pp \to d a_0^+$ near the threshold within the framework of TSM

3) The cross section of the a_0^+ production in the reaction $pp \to d a_0^+$ near the threshold is found to be sufficiently large for experimental observation at COSY-Jülich

$$\frac{d\sigma}{d\Omega_{cm}}_{pp \to d a_0^+} \simeq 100 \text{ nb/sr}$$

at $T_{eab} = 2.6$ GeV

Description of the a_0/f_0 Mesons with the Jülich Model

J. Haidenbauer

Institut für Kernphysik
Forschungzentrum Jülich
52425 Jülich
Germany

Introduction

Recently we have developed meson–exchange models for $\pi\pi$ and $\pi\eta$ scattering and we have used them for investigating the nature of the meson resonances $f_0(980)$ and $a_0(980)$ [1]. These models are based on an effective meson Lagrangian utilising the symmetries of the QCD–Lagrangian as guideline. The resulting potential for meson-meson scattering contains t-channel vector-meson exchanges (ρ, K^*, ω, ϕ) as well as s-channel pole diagrams (ρ, $\epsilon(1400)$, $f_2(1270)$) and is iterated in a three-dimensional scattering equation of Blankenbecler-Sugar type [1].

$\pi\pi$ scattering and the nature of the $f_0(980)$ resonance

The Jülich group has developed a coupled-channel model of $\pi\pi$ and $K\bar{K}$ scattering within the conventional meson-exchange framework. This model is able to produce very good agreement with experimental data on $\pi\pi \to \pi\pi$ in all relevant partial waves and over a wide range of energy. In particular we are able to describe the structure appearing around 1.0 GeV in the isoscalar $\pi\pi$ S-wave which is assigned to the f_0 meson. In our model this resonance-like behaviour is generated dynamically by the strong attraction arising from ρ, ω and ϕ exchange in the $K\overline{K}$ channel and we therefore do *not* need a genuine scalar resonance with mass around 1.0 GeV. On the other hand, it is definitely necessary to include a heavy scalar particle, namely the ϵ with mass around 1.4 GeV, to describe the experimental data beyond 1.0 GeV.

Analysing the pole structure of the $JI = 00$ $\pi\pi$ scattering amplitude we find three poles of physical relevance in the complex plane. Looking at smaller energies, we find a very broad pole at the complex energy $(\mathrm{Re}E, \mathrm{Im}E) = (387, \pm 305)$ MeV. This pole is the origin of the large $\pi\pi$ S-wave phase shifts below 1.0 GeV; we denote it $\sigma(400)$. It should be mentioned, however, that this pole does *not* correspond to a real σ meson but is just a manifestation of the strong attraction between the two pions. Looking at higher energies, we find the poles generated by the ϵ s-channel diagram necessary to describe data above 1.0 GeV. This pole defines the parameters of a genuine scalar particle which effectively includes the singlet and the octet member of the scalar nonet. We denote it by $f_0(1400)$ although it is more likely an effective parameterisation of two scalar resonances, such as $f_0(1400)$ and $f_0(1590)$. Both poles, $\sigma(400)$ and $f_0(1400)$, form a background to the $f_0(980)$.

In the most interesting energy region around $K\overline{K}$ threshold we find a single pole (on sheet II) at $(1015, \pm 15)$ MeV which clearly has to be assigned to the f_0 meson and to the corresponding structure in $\pi\pi$ data. In the zero $\pi\pi/K\overline{K}$ coupling limit the pole moves back to the real axis below $K\overline{K}$ threshold [$(985, 0)$ MeV] which clearly demonstrates the bound state nature of the f_0 within our model. From the pole position we obtain $m_{f_0} = 1015$ MeV, $\Gamma_{f_0} = 30$ MeV which is a rather high value for the f_0 mass compared to the value given by the Particle Data Group and turns out to be a consequence of the bound state structure within our model.

$\pi\eta$ scattering and the nature of the $a_0(980)$ resonance

Next we turn our attention to the $\pi\eta$ channel and the structure of the a_0. For details of the model the reader is again referred to Ref. [1] but it should be mentioned that the entire $\pi\eta$ scattering amplitude is obtained with the addition of only one new parameter compared to the $\pi\pi$ case. Since we want to extend the concepts applied to the $\pi\pi$ interaction *consistently* to the $\pi\eta$ system the $K\overline{K}$ interaction required for a $\pi\eta/K\overline{K}$

coupled-channel approach is taken to be exactly the same as for the $\pi\pi$ case (projected now onto isospin $I = 1$). However, the important ρ exchange between two kaons becomes repulsive for isospin I=1 destroying the $K\overline{K}$ bound state we found for I=0.

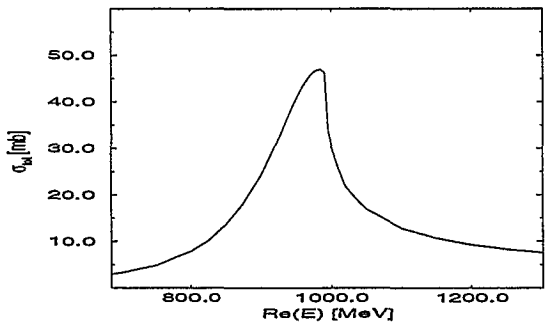

Figure 1: The $\pi\eta$ cross section for our full model.

Figure 1 demonstrates that we nevertheless obtain a resonance-like structure close to $K\overline{K}$ threshold when we calculate the $\pi\eta$ cross section within our model. The resonance parameters naively derived from the cross section by Breit-Wigner fitting are in reasonable agreement with experimental data ($m_{a_0} \simeq$990 MeV; $\Gamma_{a_0} \simeq$110 MeV). Moreover, we find a single pole corresponding to this structure at (990, $\pm$101) MeV (on Sheet II). Since this pole is still present when the direct $K\overline{K}$ interaction is turned off (though at a different position) the only remaining conclusion concerning the origin of this pole and therefore about the nature of the a_0 must be that of a dynamically generated coupled-channel effect.

In summary, we evaluated realistic meson-exchange models for $\pi\pi$ and $\pi\eta$ scattering which are in good agreement with the available experimental data sets. We obtain a consistent understanding of the scalar mesons $f_0(980)$ *and* $a_0(980)$ within the same framework and found the interesting result that their underlying structure is quite different.

[1] G. Janssen et al., Phys. Rev. D **52**, 2690 (1995).

Description of the $a_0/f_0(980)$ mesons with the Jülich model

G. Janßen
O. Krehl

Outline

(I) The Jülich model for meson-meson scattering

- Motivation
- Meson-exchange model for $\pi\pi$- and $\pi\eta$ scattering
- Structure of the $f_0(980)$ and $a_0(980)$ resonances
- $f_0(980)$ and $a_0(980)$ mixing

(II) The model of the Valencia group

(III) Conclusions

$a_0(980)$ and $f_0(980)$ are seen as resonance structures in $\pi\eta$ and $\pi\pi$ mass spectra near the $K\bar{K}$ threshold.

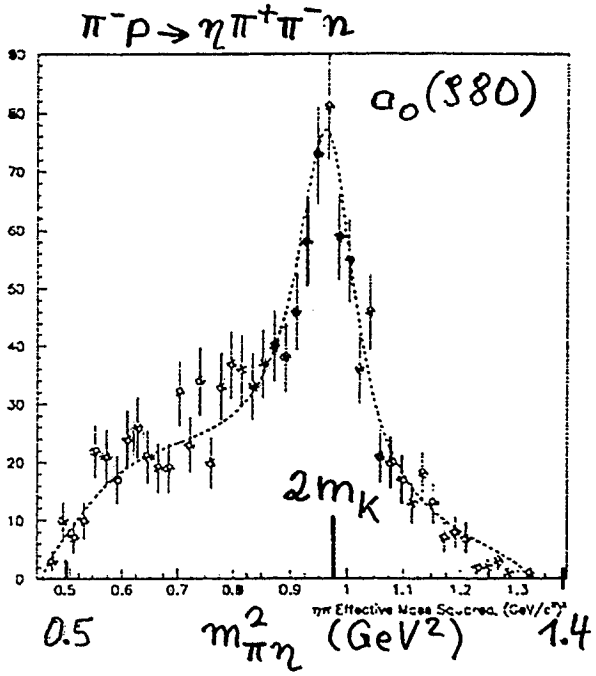

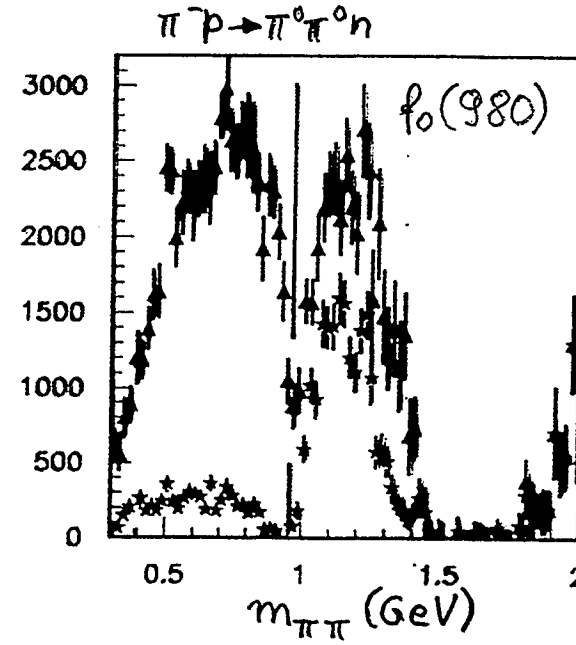

$a_0(980)$

$I^G(J^{PC}) = 1^-(0^{++})$

$m_{a_0} = (983{,}5 \pm 0{,}9)$ MeV

$\Gamma_{a_0} = (50 - 100)$ MeV

$f_0(980)$

$I^G(J^{PC}) = 0^+(0^{++})$

$m_{f_0} = (980 \pm 10)$ MeV

$\Gamma_{f_0} = (40 - 100)$ MeV

decay modes

$\pi\eta$	dominant	$\pi\pi$	$(78{,}1 \pm 2{,}4)\,\%$
$K\bar{K}$	seen	$K\bar{K}$	$(21{,}9 \pm 2{,}4)\,\%$

Where are the scalar mesons?

pseudoscalar (0^-)

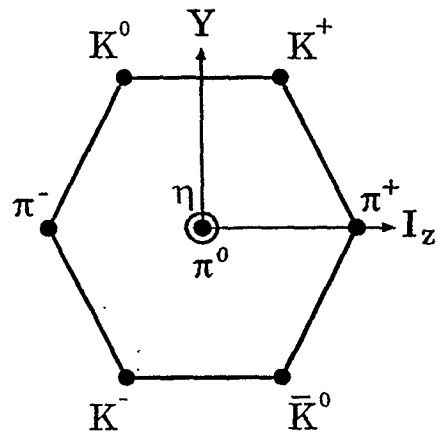

vector (1^-)

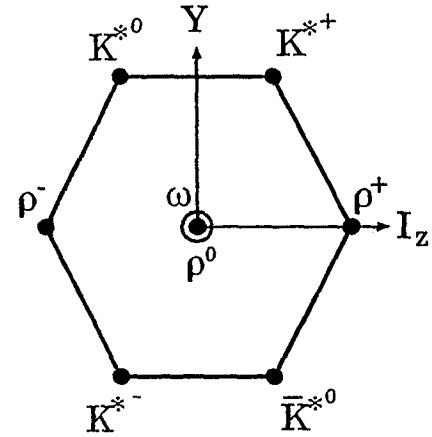

scalar (0^+)

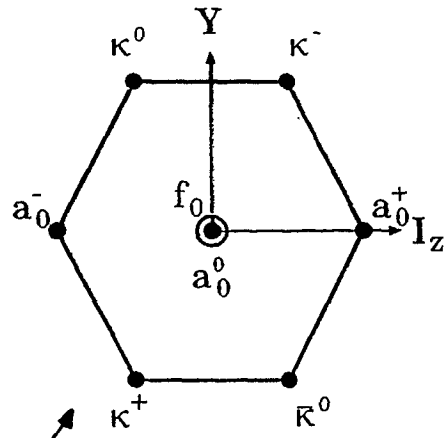

$a_0(980)$

$f_0(980)$

$\kappa(1430)$

$a_0(1450)$?

$f_0(1370)$?

$f_0(1500)$?

?

glueball

$q\bar{q}$ state

$q^2\bar{q}^2$ state

$K\bar{K}$ molecule

Meson-exchange model for $\pi\pi$ and $\pi\eta$ scattering

$\mathcal{L}_{PPV} = g_V \phi_P \partial_\mu \phi_P \phi_V^\mu$

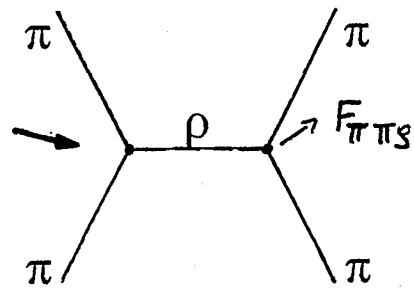

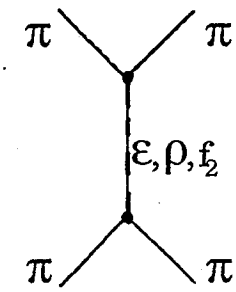

$\pi\pi$

$g_{\pi\pi g} = 6{,}04$

(from experiment)

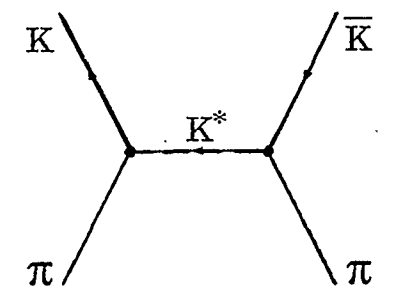

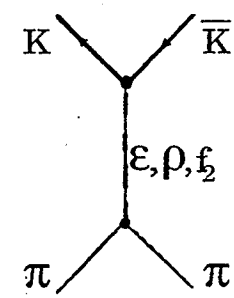

$\pi\pi \leftrightarrow K\bar{K}$

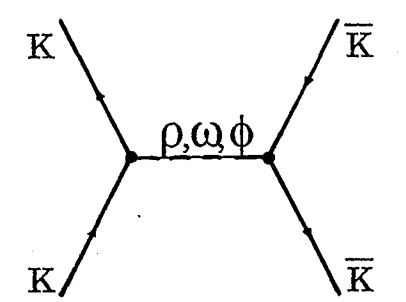

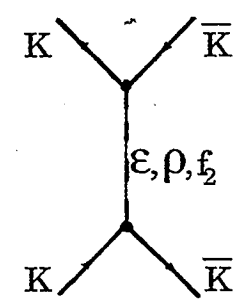

$K\bar{K}$

SU(3)

$g_{\pi KK^*}$, g_{KKg}, ..., $g_{\eta KK^*}$

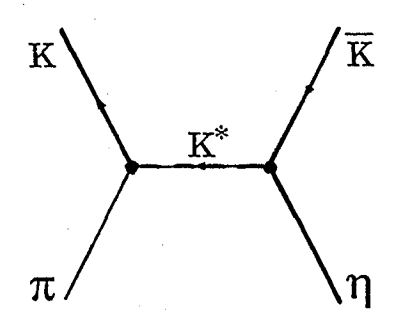

$\pi\eta \leftrightarrow K\bar{K}$

$g_{\pi\pi f_2}$ from data

$\epsilon \sim f_0(1300\text{-}1500)$

$$F_{\pi\pi g}(q^2) = \left(\frac{2\Lambda_{\pi\pi g}^2 - m_g^2}{2\Lambda_{\pi\pi g}^2 + \vec{q}^{\,2}}\right)^2, \text{ etc.}$$

$\Lambda_{\pi\pi g}, \ldots$ free parameters of the model

Lagrangians and vertex parameters

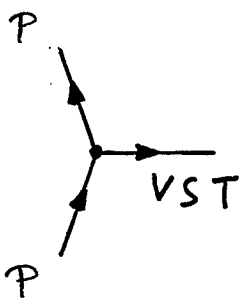

$$\mathcal{L}_{PPV} = g_V \phi_P \partial_\mu \phi_P \phi_V^\mu$$

$$\mathcal{L}_{PPS} = \frac{g_S}{m_P} \partial_\mu \phi_P \partial^\mu \phi_P \phi_S$$

$$\mathcal{L}_{PPT} = \frac{g_T}{m_P} \partial_\mu \phi_P \partial_\nu \phi_P \phi_T^{\mu\nu}$$

TABLE I. Vertex parameters for t channel exchanges. Relations between coupling constants are obtained using SU(3) and ideal mixing between the octet and singlet.

Vertex	g	Λ [MeV]
$\pi\pi\rho$	6.04	1355
πKK^*	$g_{\pi KK^*} = g_{\pi\overline{KK}^*} = -\frac{1}{2} g_{\pi\pi\rho}$	1900
$KK\rho$	$g_{KK\rho} = g_{\overline{KK}\rho} = \frac{1}{2} g_{\pi\pi\rho}$	1850
$KK\omega$	$g_{KK\omega} = -g_{\overline{KK}\omega} = \frac{1}{2} g_{\pi\pi\rho}$	2800
$KK\phi$	$g_{KK\phi} = -g_{\overline{KK}\phi} = \frac{1}{\sqrt{2}} g_{\pi\pi\rho}$	2800
ηKK^*	$g_{\eta KK^*} = -g_{\eta\overline{KK}^*} = -\frac{\sqrt{3}}{2} g_{\pi\pi\rho}$	3290

TABLE II. Vertex parameters for s-channel exchanges. The exchanged meson is identified with a superscript (0) since it is a bare meson. The $\epsilon^{(0)}$ contributes to the description of the $f_0(980)$. None of the other parameters contribute to f_0 or a_0.

Vertex	g	Λ [MeV]
$\pi\pi\epsilon^{(0)}$	0.286	925
$KK\epsilon^{(0)}$	-0.286^a	1200
$\pi\pi\rho^{(0)}$	5.32	1647
$KK\rho^{(0)}$	$\frac{1}{2} g_{\pi\pi\rho^{(0)}}$	830
$\pi\pi f_2^{(0)}$	1.23	995
$KKf_2^{(0)}$	$\frac{2}{3} g_{\pi\pi f_2^{(0)}}$	937

[a]Since the singlet-octet mixing angle for the scalar nonet is not known, $g_{KK\epsilon^{(0)}}$ is a free parameter.

Coupled-channel model for $\pi\pi$- and $K\bar{K}$ scattering

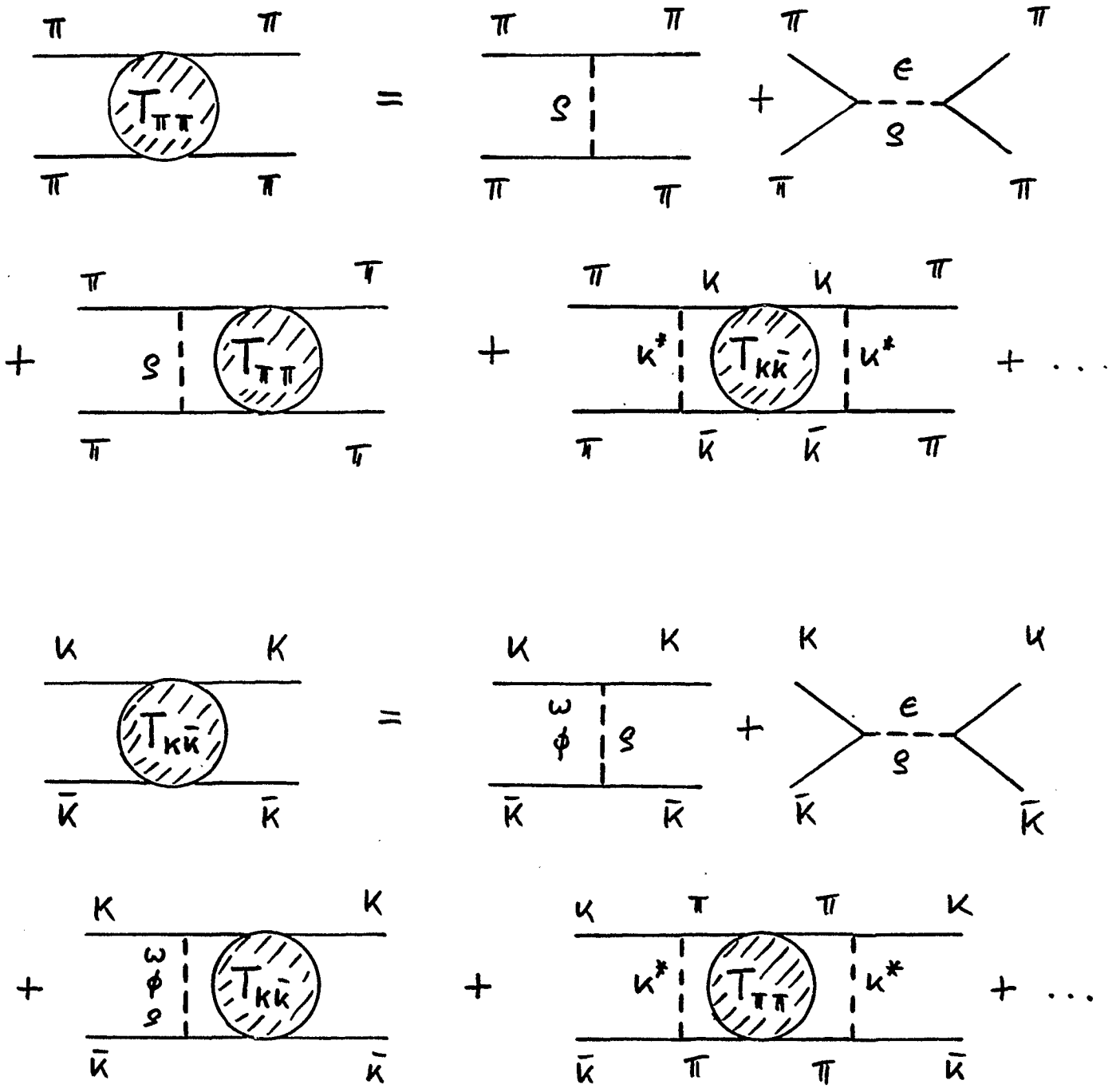

$K\bar{K}$: for $I=0$ all contributions attractive

$\Rightarrow$ <u>bound state (molecule)</u>

$\pi\pi$-scattering

in $I=2$ only t-channel exchange

------ t-channel & $K\bar{K}$ coupling

——— & scalar meson ~ 1400 MeV

δ_{JI}

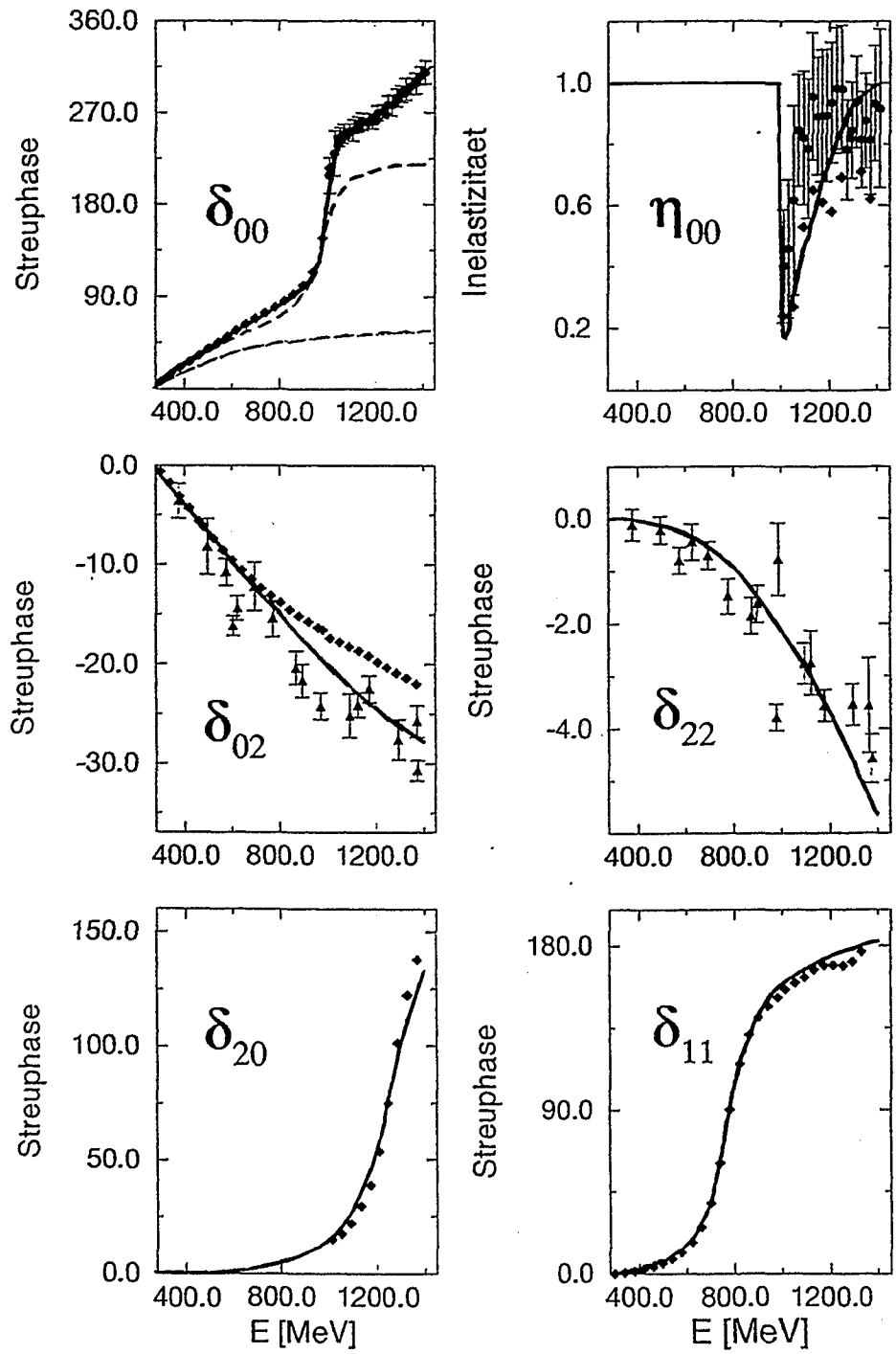

$\pi\pi \to K\bar{K}$ production

- reasonable agreement with the most recent analy...
- large uncertainties in experimental data

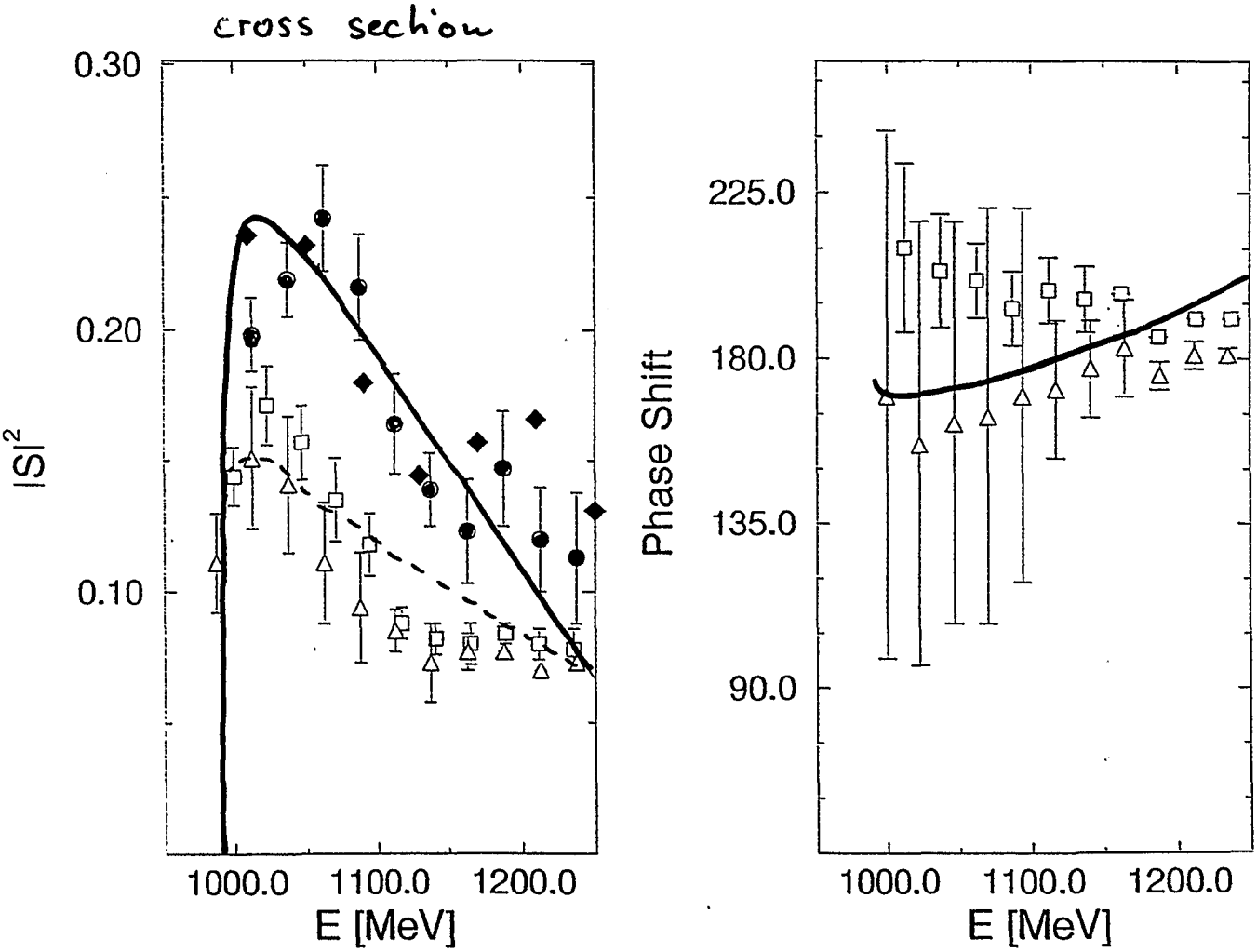

◆ : result from elastic $\pi\pi$ scattering

Decay data $J/\psi \to \phi\pi\pi / \phi K\bar{K}$

- quality of $K\bar{K}$-model comparable with those of alternative models

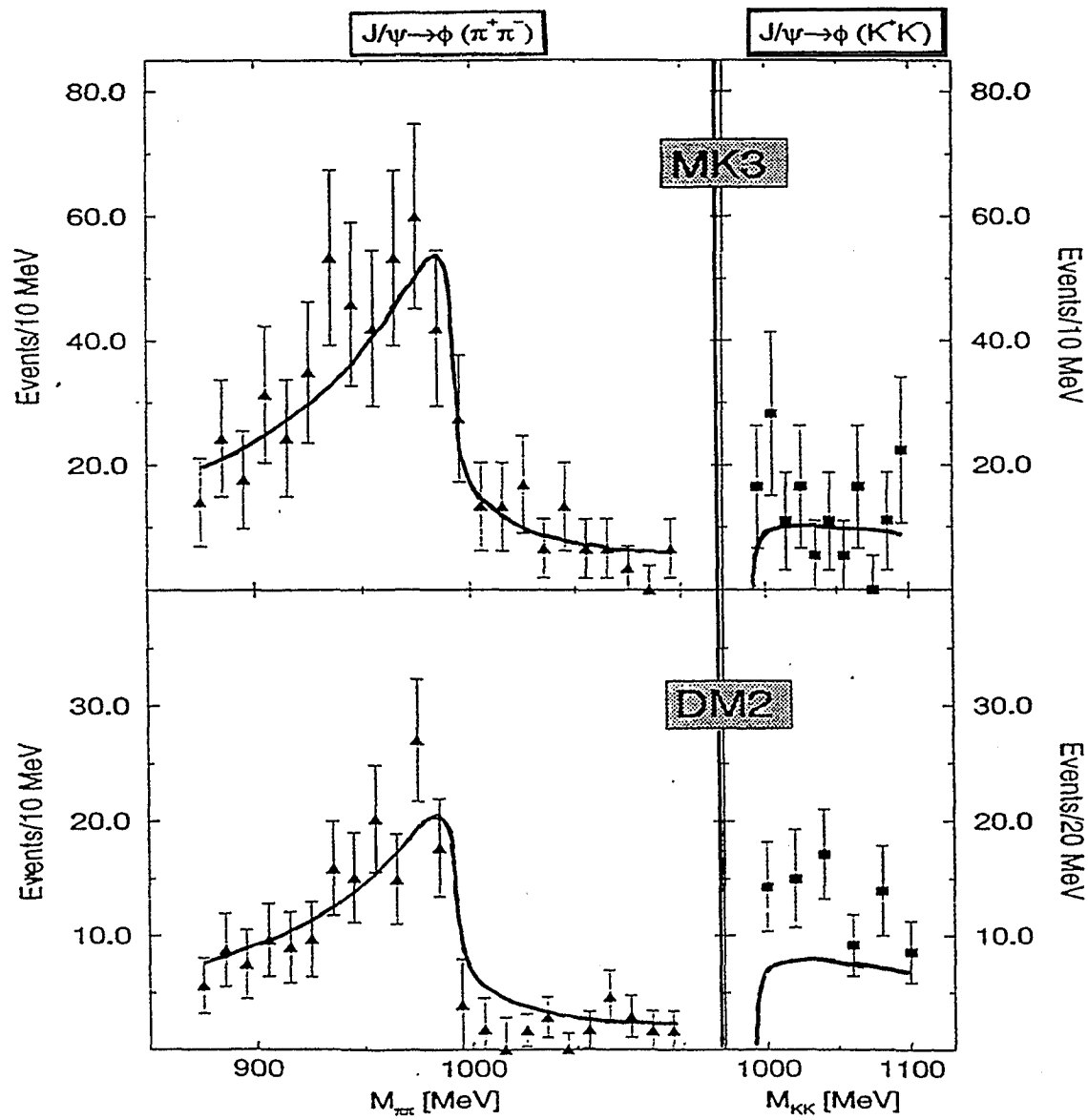

Sheet structure

$$E = \sqrt{k_0^2 + m_1^2} + \sqrt{k_0^2 + m_2^2}$$

$$k_0 = \frac{\sqrt{(E^2 - (m_1+m_2)^2)\,(E^2 - (m_1-m_2)^2)}}{2E}$$

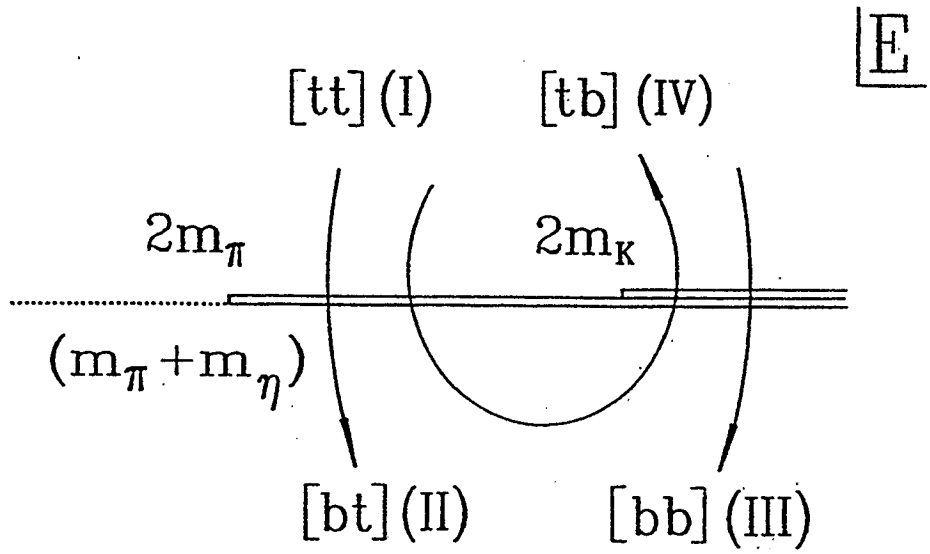

Sheet	konventionelle Bezeichnung	Charakterisierung
$[tt]$	(I)	Im $k_0^{\pi\pi(\pi\eta)} > 0$, Im $k_0^{K\overline{K}} > 0$
$[bt]$	(II)	Im $k_0^{\pi\pi(\pi\eta)} < 0$, Im $k_0^{K\overline{K}} > 0$
$[tb]$	(IV)	Im $k_0^{\pi\pi(\pi\eta)} > 0$, Im $k_0^{K\overline{K}} < 0$
$[bb]$	(III)	Im $k_0^{\pi\pi(\pi\eta)} < 0$, Im $k_0^{K\overline{K}} < 0$

$f_0(980)$: generated by strong direct $K\bar{K}$ interaction

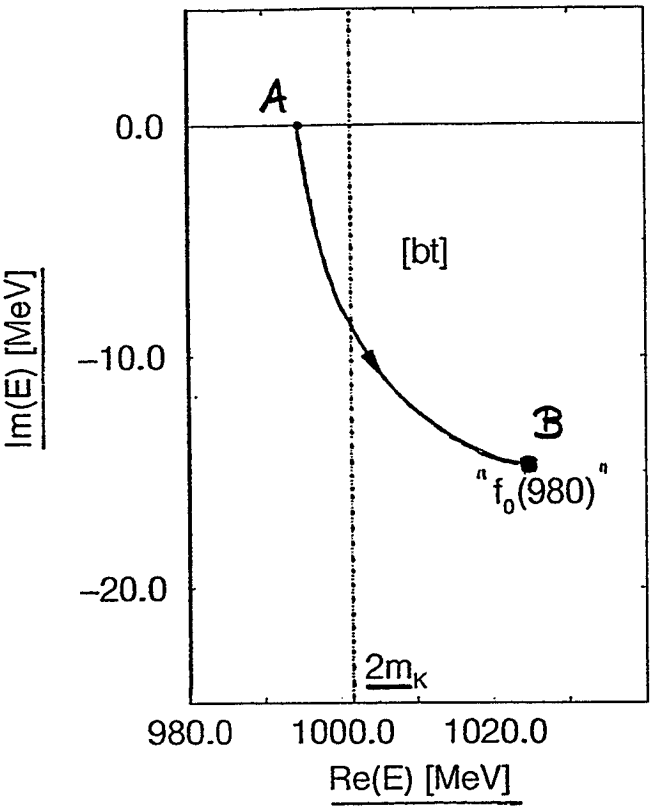

A: no $\pi\pi/K\bar{K}$ coupling B: full model

$\Rightarrow$ pole structure identifies $K\bar{K}$ bound state

$\Rightarrow$ $f_0(980)$ is characterized by

large mass: $m_{f_0} = 1015$ MeV

small width: $\Gamma_{f_0} = 30$ MeV

$\pi\eta$ - scattering

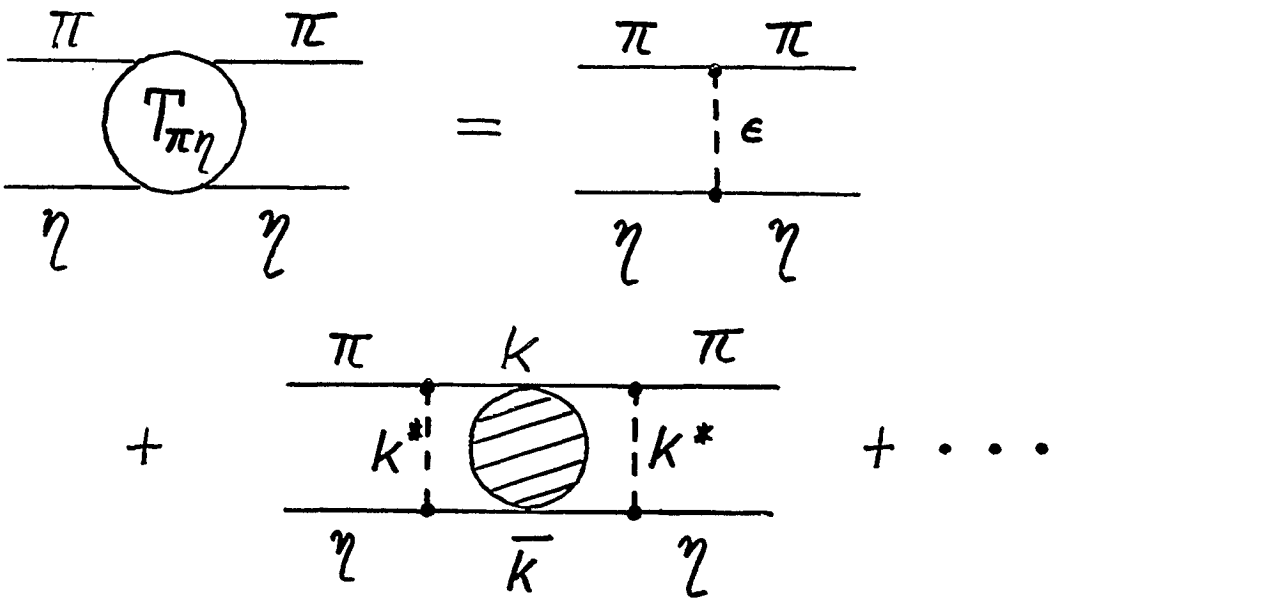

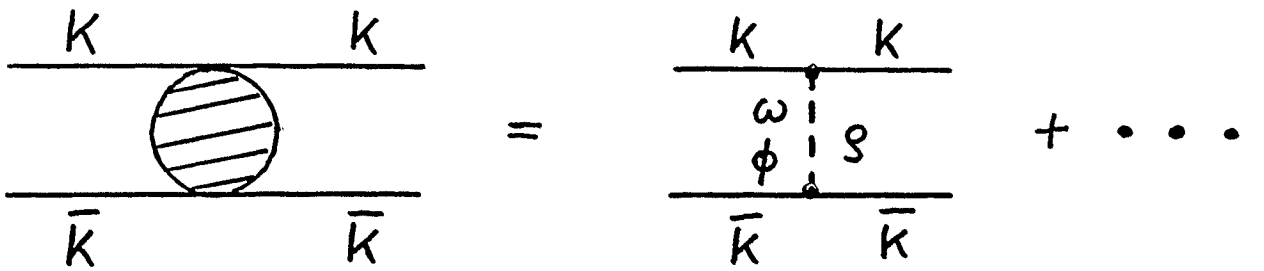

ϱ changes sign and cancels a large fraction of the attraction.

$\Rightarrow$ no bound isovector $K\bar{K}$ molecule

$\pi\eta$ cross section (I=01)	pole positions

full (coupled channel) model

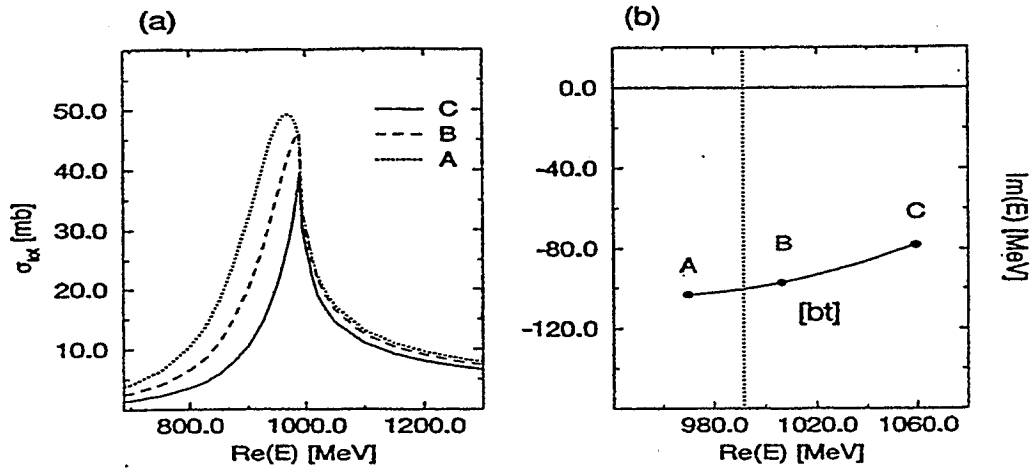

$\Lambda_{\eta KK^*}$: A (3.6 GeV); B (3.1 GeV); C (2.6 GeV)

direct $K\bar{K}$ interaction is omitted

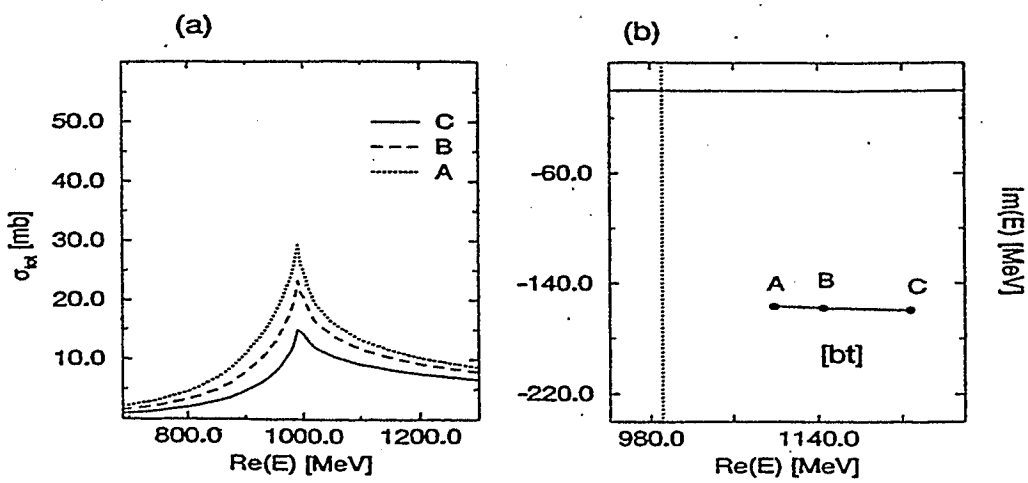

$\Lambda_{\eta KK^*}$: A (5.0 GeV); B (4.0 GeV); C (3.1 GeV)

$\pi\eta$ cross sec'on

$J=0, I=1$

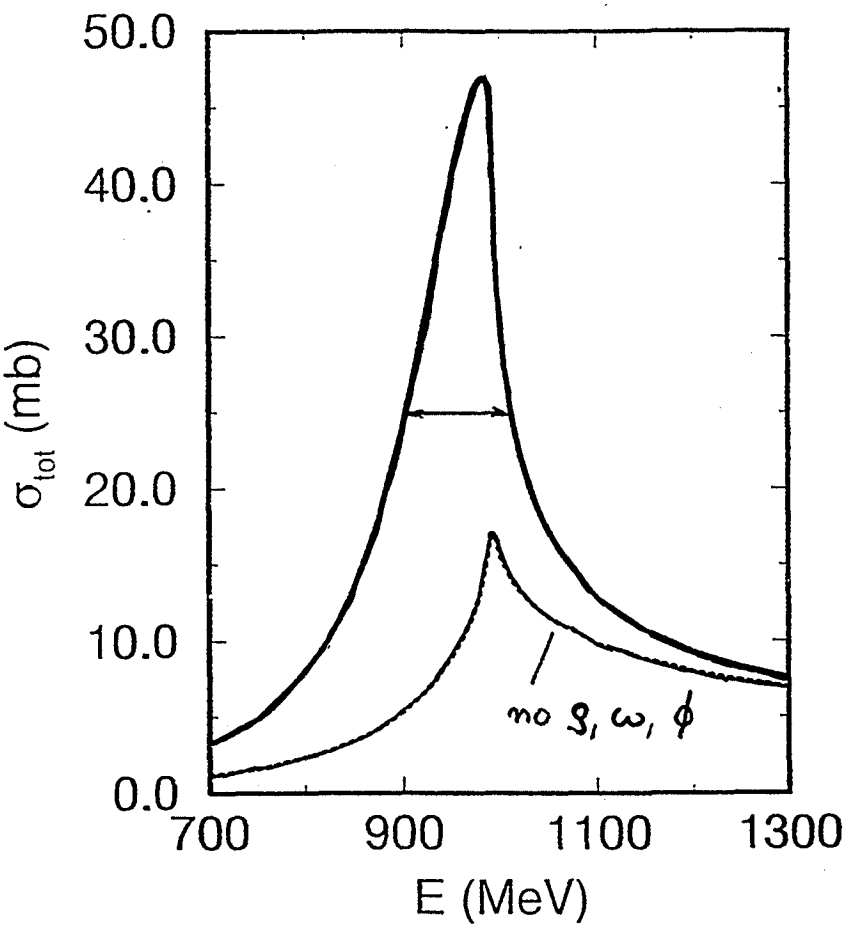

$\Gamma_{a_0} = 110$ MeV

PDG: $\Gamma_{a_0} = (50-100)$ MeV

used to fix $\Lambda_{\eta KK^*}$!

pole structure

$a_0(980)$: [bt] (II) $(991; \pm 101)$ MeV

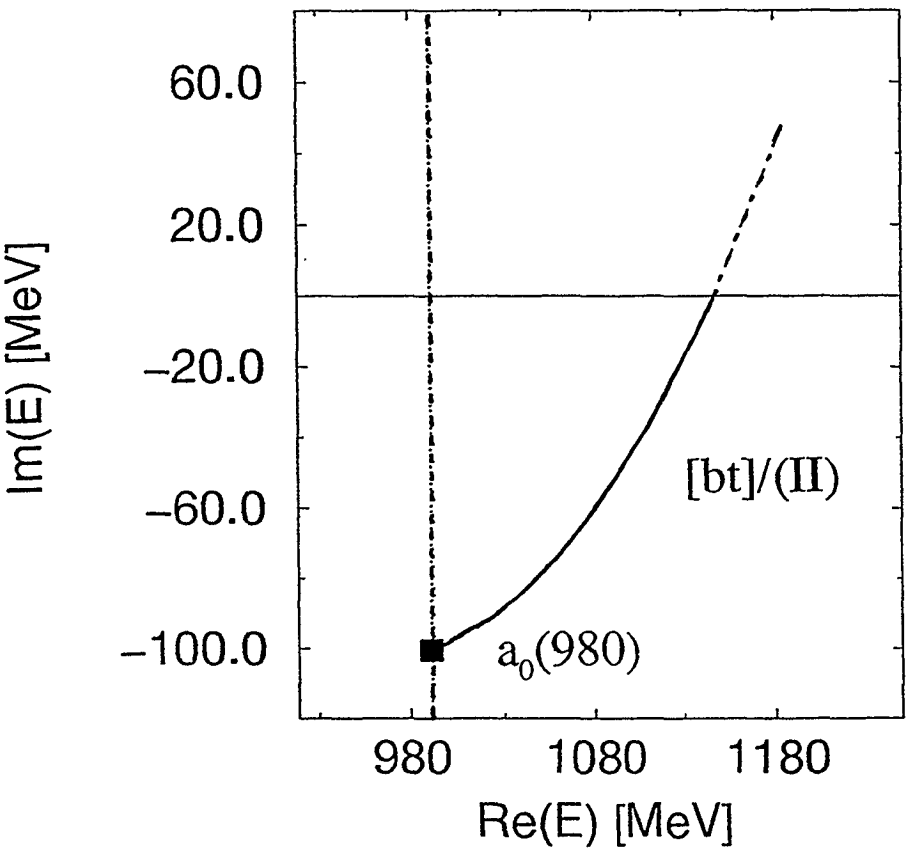

- $a_0(980)$ is a dynamically generated coupled-channel effect $\pi\eta - K\bar{K}$

$m_{a_0} = 991$ MeV

$\Gamma_{a_0} = 202$ MeV

$f_0(980)$ and $a_0(980)$ mixing

$f_0 \rightleftharpoons \pi^0\pi^0$, $\pi^+\pi^-$ $\qquad a_0 \Rightarrow \pi^0\eta$

Isospin and G-parity forbidden

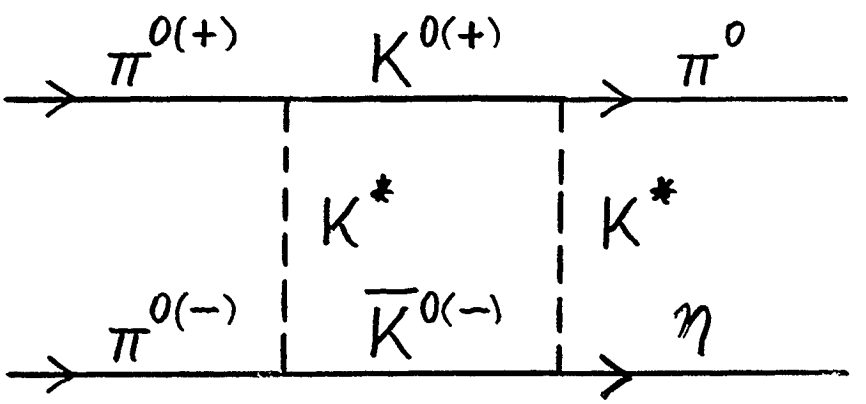

a) G-parity-"mixing" via $K\bar{K}$

b) Isospin-"mixing" due to mass splitting $\pi^{\pm}/\pi^0$ and $K^{\pm}/K^0$

$\Longrightarrow$ "particle basis" instead of "isospin basis"

$\pi\pi \to \pi\eta$

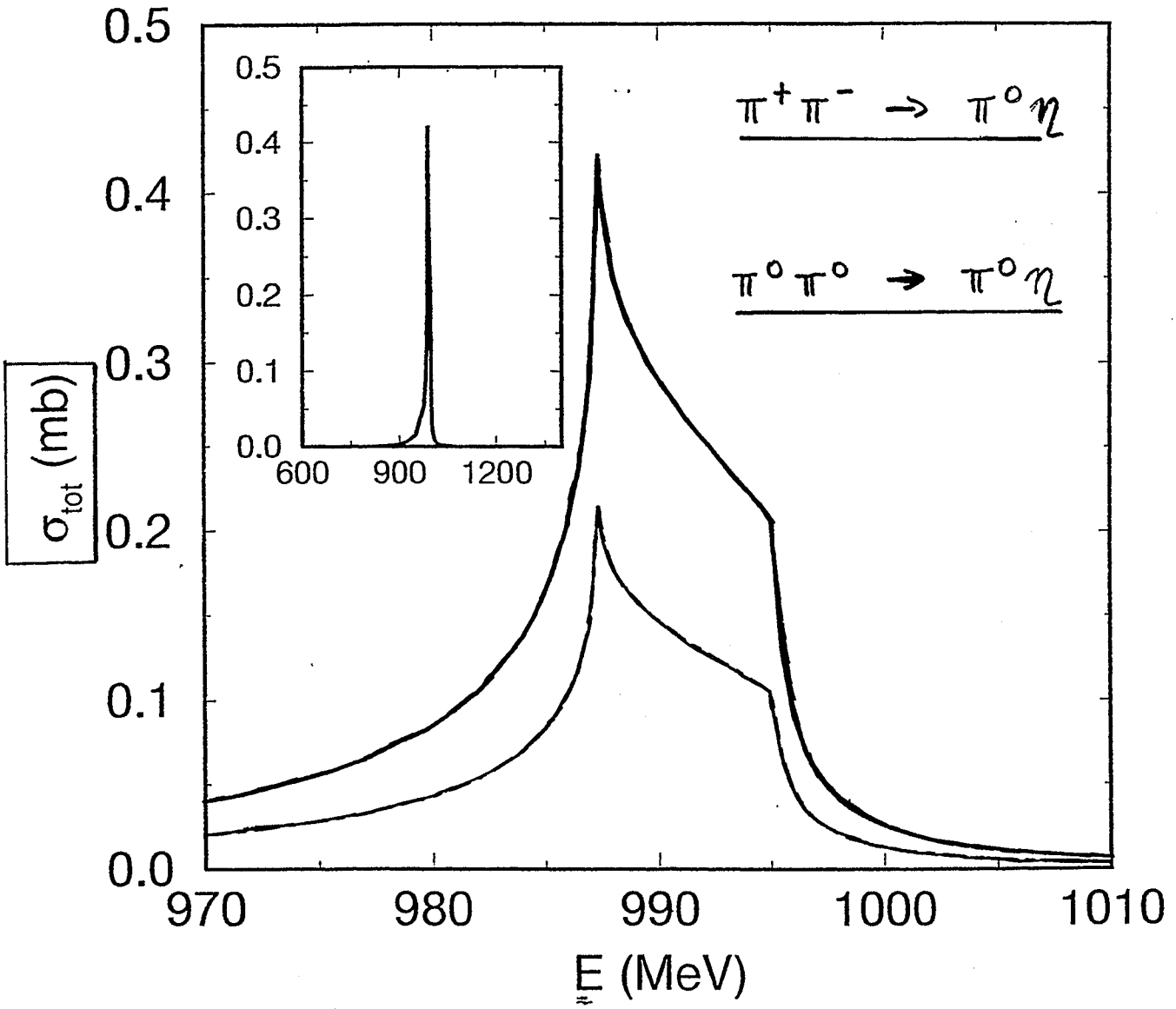

Model of J.A. Oller & E. Oset

(NPA 620, 438 (1997) + NPA 652, 407 (1999))

different philosophy – similar results

- derive meson-meson interaction from lowest order chiral Lagrangian assuming SU(3) flavour symmetry

$$\mathcal{L}_2 = \frac{1}{12f^2}\langle (\partial_\mu \phi\phi - \phi\partial_\mu\phi)^2 + M\phi^4 \rangle$$

f ... pion decay constant

$$\phi = \frac{\vec{\lambda}}{\sqrt{2}}\vec{\phi} = \begin{pmatrix} \frac{1}{\sqrt{2}}\pi^0 + \frac{1}{\sqrt{6}}\eta_8 & \pi^+ & K^+ \\ \pi^- & -\frac{1}{\sqrt{2}}\pi^0 + \frac{1}{\sqrt{6}}\eta_8 & K^0 \\ K^- & \bar{K}^0 & -\frac{2}{\sqrt{6}}\eta_8 \end{pmatrix}$$

$$M = \begin{pmatrix} m_\pi^2 & 0 & 0 \\ 0 & m_\pi^2 & 0 \\ 0 & 0 & 2m_K^2 - m_\pi^2 \end{pmatrix} \qquad \begin{matrix} (m_u = m_d) \\ (\eta := \eta_8) \end{matrix}$$

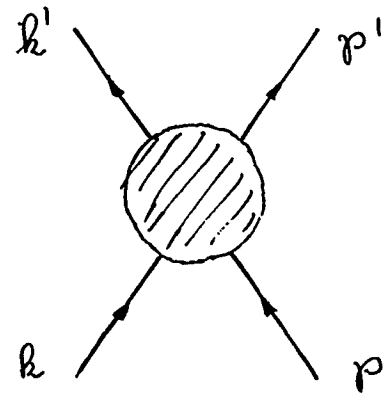

$T=0$,

$$V_{11} = -\langle K\bar{K}|\mathcal{L}_2|K\bar{K}\rangle = -\frac{1}{4f^2}\left(3s + 4m_K^2 - \sum_i p_i^2\right),$$

$$V_{21} = -\langle \pi\pi|\mathcal{L}_2|K\bar{K}\rangle = -\frac{1}{3\sqrt{12}f^2}\left(\frac{9}{2}s + 3m_K^2 + 3m_\pi^2 - \frac{3}{2}\sum_i p_i^2\right),$$

$$V_{22} = -\langle \pi\pi|\mathcal{L}_2|\pi\pi\rangle = -\frac{1}{9f^2}\left(9s + \frac{15m_\pi^2}{2} - 3\sum_i p_i^2\right),$$

$T=1$,

$$V_{11} = -\langle K\bar{K}|\mathcal{L}_2|K\bar{K}\rangle = -\frac{1}{12f^2}\left(3s - \sum_i p_i^2 + 4m_K^2\right),$$

$$V_{21} = -\langle \pi^0\eta|\mathcal{L}_2|K\bar{K}\rangle = \frac{\sqrt{3/2}}{12f^2}\left(6s - 2\sum_i p_i^2 + \frac{4}{3}m_\pi^2 - \frac{4}{3}m_K^2\right),$$

$$V_{22} = -\langle \pi^0\eta|\mathcal{L}_2|\pi^0\eta\rangle = -\frac{1}{3f^2}m_\pi^2,$$

where $p_1 = k$, $p_2 = p$, $p_3 = k'$, $p_4 = p'$ and the sum over momenta squared runs from 1 to 4. For on shell amplitudes $p_i^2 = m_i^2$. $s = (k+p)^2, t = (k-k')^2, u = (k-p')^2$.

$T=0$,

$$|K\bar{K}\rangle = -\frac{1}{\sqrt{2}}|K^+(q)K^-(-q) + K^0(q)\bar{K}^0(-q)\rangle,$$

$$|\pi\pi\rangle = -\frac{1}{\sqrt{6}}|\pi^+(q)\pi^-(-q) + \pi^-(q)\pi^+(-q) + \pi^0(q)\pi^0(-q)\rangle,$$

$T=1$

$$|K\bar{K}\rangle = -\frac{1}{\sqrt{2}}|K^+(q)K^-(-q) - K^0(q)\bar{K}^0(-q)\rangle$$

$$|\pi\eta\rangle = |\pi^0(q)\eta(-q)\rangle,$$

standard χPT can't be used in resonance region

$\Rightarrow$ obtain a potential from lowest order Hamiltonian

$$V_{11} := V_{K\bar{K}} = -\langle K\bar{K} | \mathcal{L}_2 | K\bar{K} \rangle$$

$$V_{22} := V_{\pi\pi} = -\langle \pi\pi | \mathcal{L}_2 | \pi\pi \rangle$$

$$V_{12} := V_{\pi\pi - K\bar{K}} = -\langle \pi\pi | \mathcal{L}_2 | K\bar{K} \rangle$$

$$\vdots$$

and iterate it in a coupled channel LS equation:

$$\begin{pmatrix} t_{11} & t_{12} \\ t_{21} & t_{22} \end{pmatrix} = \begin{pmatrix} V_{11} & V_{12} \\ V_{21} & V_{22} \end{pmatrix} + \begin{pmatrix} V_{11} & V_{12} \\ V_{21} & V_{22} \end{pmatrix} \begin{pmatrix} G_1 & 0 \\ 0 & G_2 \end{pmatrix} \begin{pmatrix} t_{11} & t_{12} \\ t_{21} & t_{22} \end{pmatrix}$$

with $G_i = i\left(q^2 - m_{1i}^2 + i\epsilon\right)^{-1}\left((P-q)^2 - m_{2i}^2 + i\epsilon\right)^{-1}$

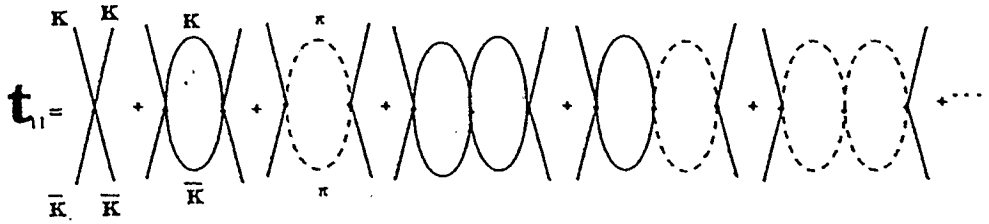

LO $\Rightarrow$ V_{ij} are purely s-waves

put V_{ij} onshell $\Rightarrow$ LS equation reduces to an algebraic equation

introduce a cutoff $\Lambda = q_{max}$ in the momentum

Results for $f_0(980)$

$\pi\pi$ $(IJ = 00)$

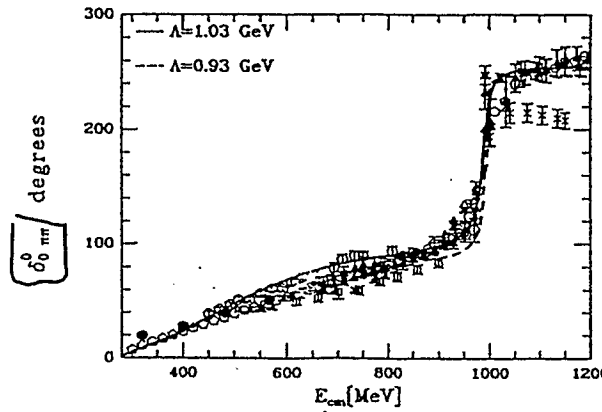

$\pi\pi \to K\bar{K}$ production

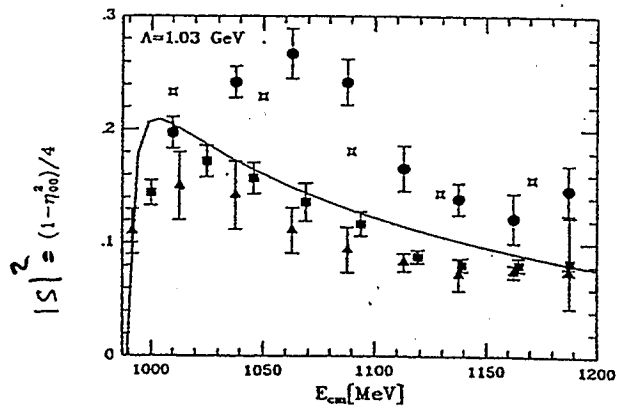

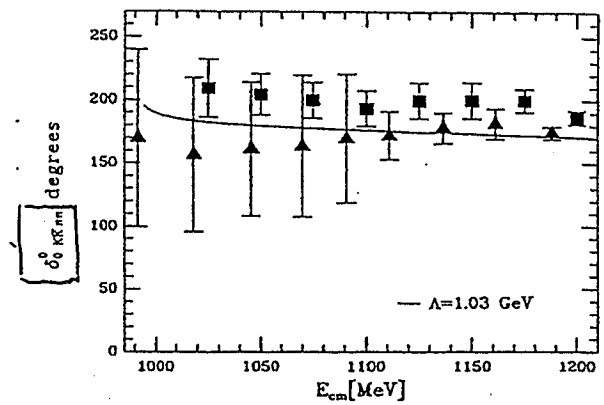

Table 1
f_0 Mass and partial widths ($\Lambda = 1.03$ GeV)

f_0	Our results	Experiment
Mass: Pole position [MeV]	993.5	980 ± 10
Mass: Peak of the t_{21} amplitude [MeV]	982	980 ± 10
Γ_{tot} [MeV]	25	40–100
$\Gamma_{\pi\pi}/(\Gamma_{\pi\pi} + \Gamma_{K\bar{K}})$	0.68	0.67 ± 0.009
		$0.81 \pm^{0.004}_{0.009}$
		0.78 ± 0.003
		(av.) 0.781 ± 0.024

Results for $a_0(980)$

$\pi\eta$ invariant mass distribution for

$K^- p \to \Sigma^+(1385)\,\pi^-\,\eta$

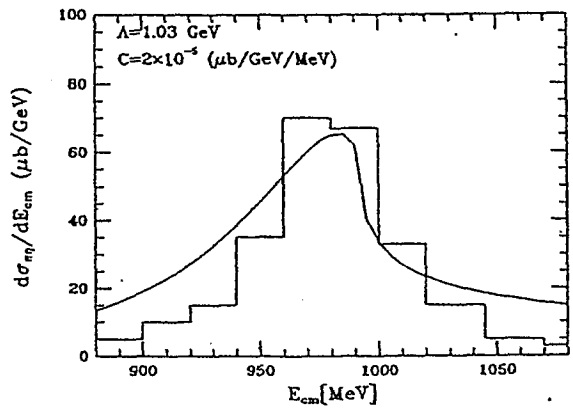

Table 2
a_0 Mass and partial widths ($\Lambda = 1.03$ GeV)

a_0	Our results	Experiment
Mass: Pole position [MeV]	1009.2	983.5 ± 0.9
Mass: Peak of the t_{21} amplitude [MeV]	982	983 ± 0.9
Γ_{tot} [MeV]	112	50–100
$\Gamma_{K\bar{K}}/\Gamma_{\eta\pi}$	0.60	1.16 ± 0.18
		0.7 ± 0.3
		0.25 ± 0.008

Results for $a_0, f_0 \to \gamma\gamma$

Model: $\Gamma_{a_0}^{\gamma\gamma} = 0.78$ keV $\quad \Gamma_{a_0}^{\gamma\gamma}\dfrac{\Gamma_{a_0}^{\eta\pi}}{\Gamma_{a_0}^{\text{tot}}} = 0.49$ keV $\quad \Gamma_{f_0}^{\gamma\gamma} = 0.20$ keV

PDG: $0.24^{+0.08}_{-0.07}$ keV. $\quad 0.39^{+0.10}_{-0.13}$ keV

Conclusions

- Dynamical model for $\pi\pi$ and $\pi\eta$ scattering

  $\Rightarrow$ number of free parameters restricted due to SU(3) symmetry

  $\Rightarrow$ consistent description of resonant and non-resonant channels

- The scalar (isoscalar) meson $f_0(980)$ is a $K\bar{K}$ bound state with relatively high mass but small width

  $m_{f_0} \approx 1015$ MeV $\Gamma_{f_0} \approx 30$ MeV

  $\Rightarrow$ additional scalar objects ~ 1400 MeV (effective description of genuine scalar mesons and glueballs (?))

- The scalar (isovector) meson $a_0(980)$ is a dynamically generated coupled-channel effect in the $\pi\eta$ s-wave channel

  $\Rightarrow$ no $K\bar{K}$ bound state

  $\Rightarrow$ broad in contrast to 'naively' derived results from $\pi\eta$ cross sections

  $m_{a_0} \approx 990$ MeV $\Gamma_{a_0} \approx 200$ MeV

The Perspectives to Study the Lightest Scalar $a_0^-(980)$ in the Reaction $pd \to ppa_0^- p_s$ Close to Threshold

V. Baru, A. Kudryavtsev, V. Tarasov, V. Chernyshev

Institute for Experimental and Theoretical Physics
B. Cheremushkinskaya 25
117259 Moscow
Russia

J. Haidenbauer

Institut für Kernphysik
Forschungzentrum Jülich
52425 Jülich
Germany

The study of the lightest scalar mesons $f_0(980)0^+(0^{++})$ and $a_0(980)1^-(0^{++})$ is one of the most fundamental problem in physics of hadrons. Both these mesons are strongly coupled to the $K\bar{K}$-channel and have practically equal masses. We suggest to study fundamental characteristics of the a_0^--meson by measuring its production cross section in nucleon-nucleon collisions, i.e. in the reaction $pn \to ppa_0^-$. To study this reaction we need to use a deuterium target, i.e. to measure the reaction $pd \to ppa_0^- p_s$ at low momenta of the proton spectator $p_s < 150$ MeV/c. The privilege of this reaction is that all final particles may be identified and measured. To reconstruct the kinematics one needs to measure all final protons in this reaction, i.e. both fast protons and the proton spectator. The decay mode $a_0^- \to K^-K^0$ may be identified by measuring negative kaons and the mode $a_0^- \to \pi^-\eta$ by measuring the decay $\eta \to 2\gamma$. In the case of the reaction $pn \to ppa_0^-$ in the laboratory system close to threshold all final particles are in a narrow cone around the beam direction. The longitudinal momenta of all particles (protons and a_0) are of the order of 1 GeV and the transverse momenta are small. For example for the excess energy $Q = 50$ MeV the maximal proton scattering angle is small, around 10°. The scattering angles for η and π are not so small because of a large energy release in the decay $a_0 \to \pi\eta$.

To estimate the production amplitude for the reaction $pn \to ppa_0^-$ close to threshold we use a simple fusion model with intermediate η- and π-mesons. The $a_0\eta\pi$-coupling is determined by the relation:

$$\Gamma_{\pi\eta} = \frac{g^2_{a_0\pi\eta}}{8\pi} q_{\pi\eta}, \tag{1}$$

where $q_{\pi\eta}$ is the $\eta\pi$-relative momentum. For a bare partial width $\Gamma_{\pi\eta} = 80$ MeV we get $g_{a_0\eta\pi} = 2.5$. We also introduce vertex form factors and apply the antisymmetrisation procedure in respect to the final protons. The expression for the total cross section also includes strong pp FSI effects and the finite width of a_0^-. We also took into account the threshold dependence for the $a_0 \to K\bar{K}$-process. In figure 1a) we present our predictions for the total cross sections of the reaction $pn \to ppa_0^-$ for various intervals of integration over the effective mass of a_0^-: $m_{min} \le \bar{m}_{a_0} \le m_{max}$, where $m_{min} = \bar{m}_{a_0} - C$, $m_{max} = \sqrt{s} - 2m_p - \bar{m}_{a_0}$ and C is a cutoff parameter.

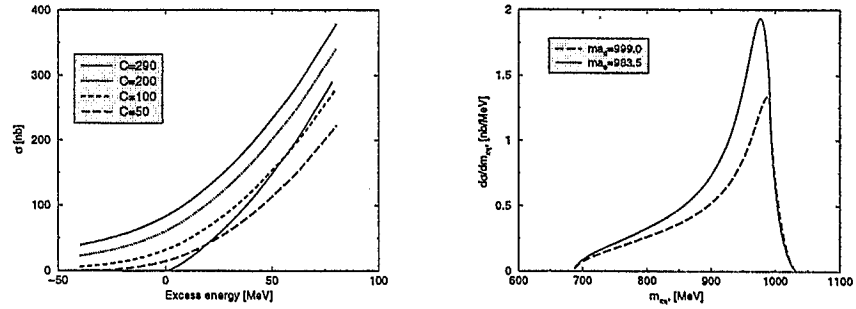

Figure 1: *a) Total cross section of the reaction $pn \to ppa_0^-$ calculated at total width of a_0 equal to 50 MeV and various intervals of integration. b) $\pi\eta$-mass distribution calculated at T_{lab}=2629 MeV, d=0.91*

Distributions for $\frac{d\sigma}{dm_{\pi\eta}}$ are shown in figure 1b) at some fixed value of the ratio

$$d = \frac{g^2_{a_0^- K^- K^0}}{g^2_{a_0^- \pi^- \eta}}, \tag{2}$$

which is taken to be 0.91 according to [1], and typical values of the a_0 mass. As it follows from our preliminary estimates, the differential cross sections are very sensitive to the mass $\bar{m}_{a_0}$ and the width Γ of the a_0-meson. A study of the effective mass distribution gives a possibility to determine these parameters. An analysis of the branchings ratio

$$\frac{Br(a_0 \to K\bar{K})}{Br(a_0 \to \pi\eta)}$$

would allow to extract the ratio d from (2). If the experimental mass resolution for the a_0-meson Δm is about 5 MeV/c^2 one could extract the parameters of the a_0-meson with better accuracy, than it is known for today (see, e.g. [1]). The interaction of a_0 with protons may also be observed if it is not negligibly small (in Gribov's [2] approach it is small). Near the threshold both final protons and the a_0 move slowly and therefore the a_0p-interaction should give some influence on a_0p- and pp-effective mass distributions.

So, the proposed experiment could provide unique information on fundamental characteristics of the a_0-meson and its interaction with protons at low energies.

[1] S.Teige et al. Phys.Rev.D **59, 012001** (1998).
[2] V.N.Gribov , LU-TP-91-7.

V. Baru, V. Chernyshev, A. Kudryavtsev, V. Tarasov (ITEP) and J. Haidenbauer (IKP)

The perspectives of study lightest scalar $a_0^-(980)$ in the reaction $pd \to (ppa_0^-) + p_s$

$pd \to (pp\pi^-) p_s$ → ITEP, B. Abramov et al. 1996 at 2 Gev

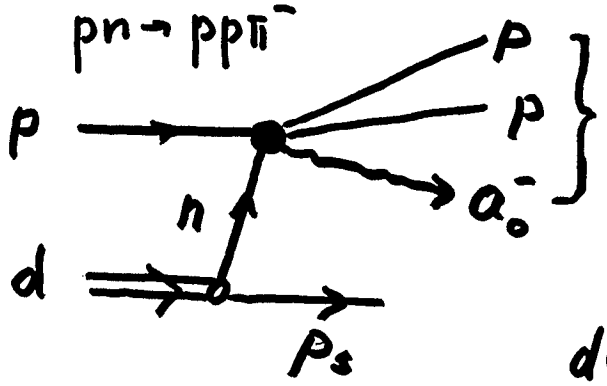

$p_p \sim 0.8 \div 0.9$ Gev/c $\sim p_a$ at $T_p \sim 2600$ Mev

$$\frac{d\sigma}{d\vec{p}_s} = |\psi_d(\vec{p}_s)|^2 \sigma_{pn \to ppa_0}(\sqrt{s'})$$

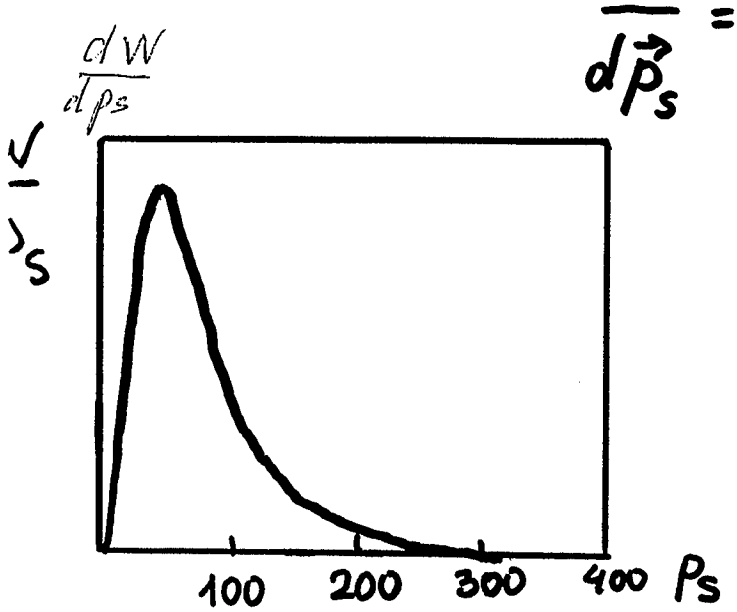

$p_s \leq 150 \div 200$ Mev/c

$p_1, p_2, p_a \sim 300 \div 900$ Mev/c

All particles are charged and may be idlutified.

$\sigma(pn \to pp a_0^-)$?

Simple fusion model:

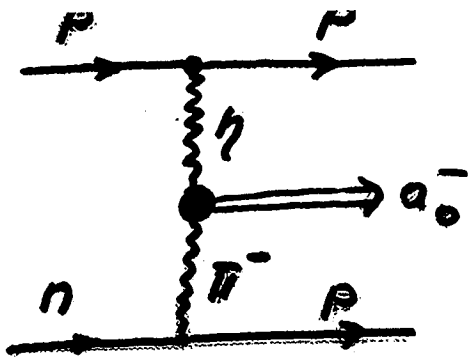

At threshold:

$$\overline{|M|^2} = g^2_{\pi NN}\, g^2_{\eta NN}\, g^2_{a_0\pi\eta}\, \frac{F_\pi^2(q^2)\, F_\eta^2(q_1^2) m_p^2\, \bar{m}^4}{(q^2-m_\pi^2)^2 (q_1^2-m_\eta^2)^2}$$

At threshold $q^2 = q_1^2 = -m_p \bar{m}$.

$\bar{m}$ is nominal a_0 mass.

$F_{pp}(k)$ - FSI factor

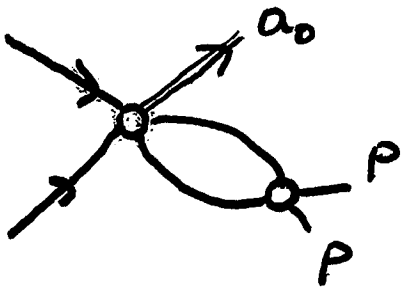

$$\sigma_{pn\to ppa_0} = \frac{\overline{|M|^2}}{I}\, \Phi(\Gamma, Q)$$

$I = 2E_1|\vec{p}_1|$ the flux

$$\Phi(\Gamma, Q) \propto \int dk\, F_{pp}(k) k^2 \int_{m_{min}} \frac{dm\, \Gamma/2\pi \sqrt{m_p(Q+\bar{m}-m-k^2/m_p}}{(m-\bar{m})^2+\frac{\Gamma^2}{4}}$$

$Q = \sqrt{s} - \bar{m}$ is energy excess.

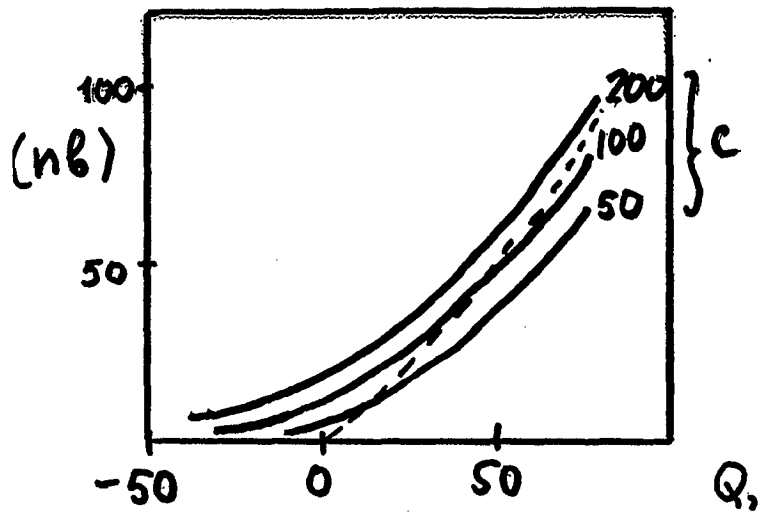

$m_{min} = \bar{m} - C$

$\downarrow$

$m(\pi\eta)$

$a_0 \to \pi\eta \quad Q \approx +290\ MeV$ open

$a_0 \to K\bar{K} \quad Q \approx -10\ MeV$ closed

$$\Gamma_{a_0} = \Gamma_{\pi\eta} + \Gamma_{K\bar{K}}(m)$$

S. Flatte (1976):

$$\Gamma_{K\bar{K}}(m) = \frac{g^2_{a_0 K\bar{K}}}{8\pi} \sqrt{2m_{K\bar{K}}(m - m_{K_0} - m_{K^-})}$$

$$d = \frac{g^2_{a_0 K^- K^0}}{g^2_{a_0 \pi\eta}}$$

$d \sim 1.5$ Gay, 76

$d = 0.91 \pm 0.11$ Teige, 98

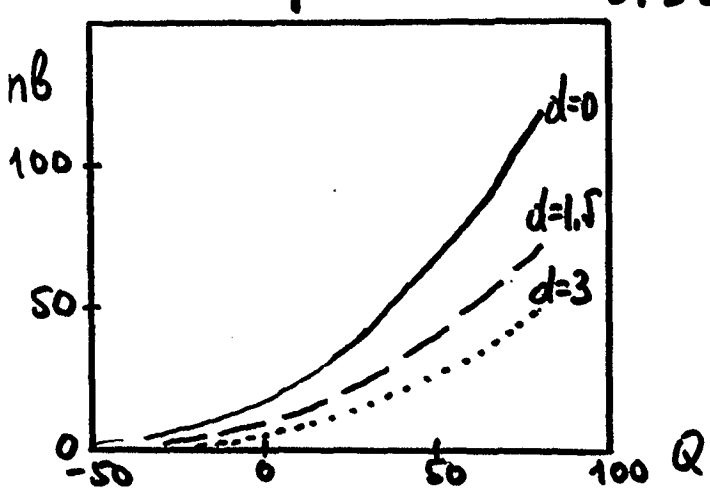

$K\bar{K}$ channel decrease cross-section.

$\Gamma_{vis} < \Gamma_{\pi\eta}$ (Flatte)

$$\Gamma_{\pi\eta} = \Gamma_{bare} = \frac{g^2_{a_0\pi\eta}}{8\pi} q_{\pi\eta}$$

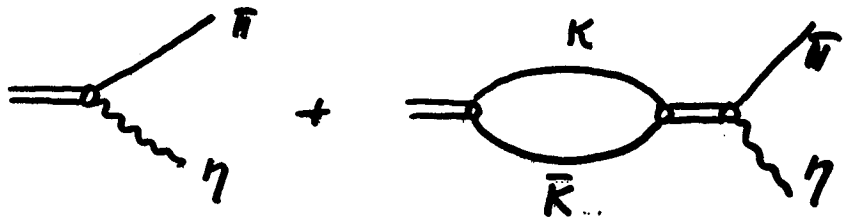

destructive interference

$G(pn \to pp\, a_0^-) \to$ $\bar{m}$, $g_{a_0\pi\eta}$, $g_{a_0 K\bar{K}}$ — 3 parameters

a) $Q > 0$

$$\frac{Br(a_0 \to K^- K^0)}{Br(a_0 \to \pi^- \eta)} = \frac{g^2_{aK\bar{K}}}{g^2_{a\pi\eta}} \frac{\sqrt{2m_{K^-K^0}(m - m_{K^0} - m_{K^-})}}{q_{\pi\eta}}$$

Expected: $d = \frac{g^2_{K\bar{K}}}{g^2_{\pi\eta}} \sim 0.9 \div 1.5$ from existing experiments

b) $\frac{d\sigma}{dm_{\pi\eta}}$ in wide interval of $m_{\pi\eta}$

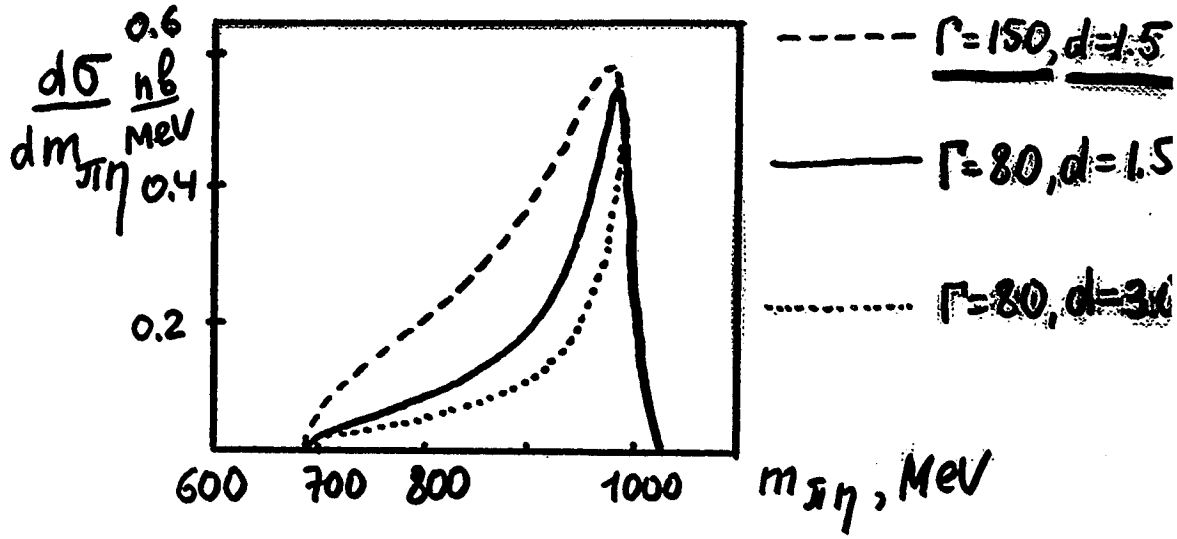

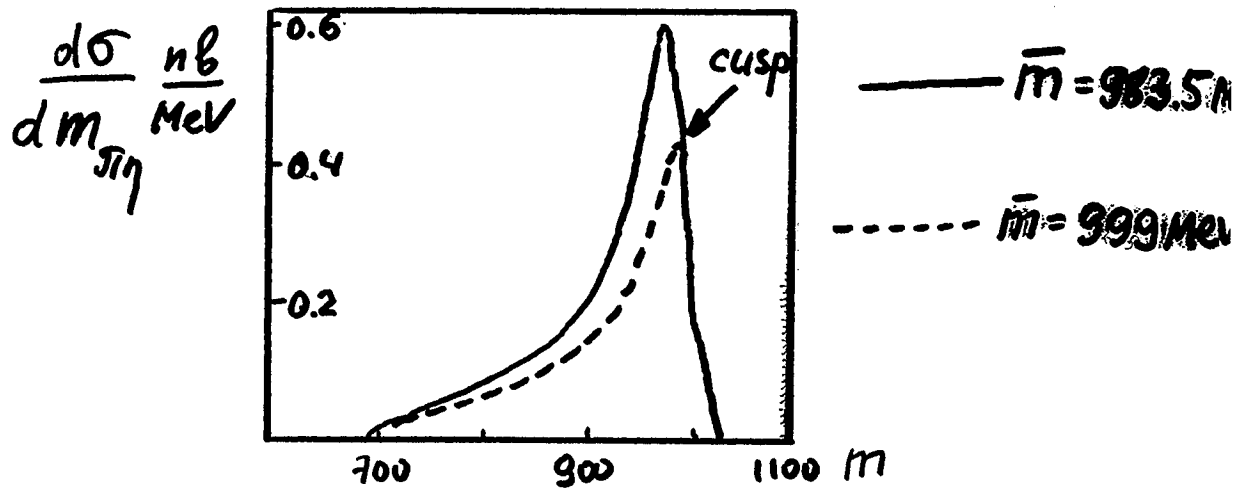

$\frac{d\sigma}{dm_{\pi\eta}}$ is sensitive to both parameters $g^2_{a_0\pi\eta}$ and $\bar{m}$

χ^2-procedure is to be done to extract these parameters.

$\frac{d\sigma}{dm_{K^-K^0}}$ is much less informative, because the absolute normalization is not known with a good accuracy

$\frac{d\sigma}{dm_{K^-K^0}}$ $\frac{nb}{MeV}$

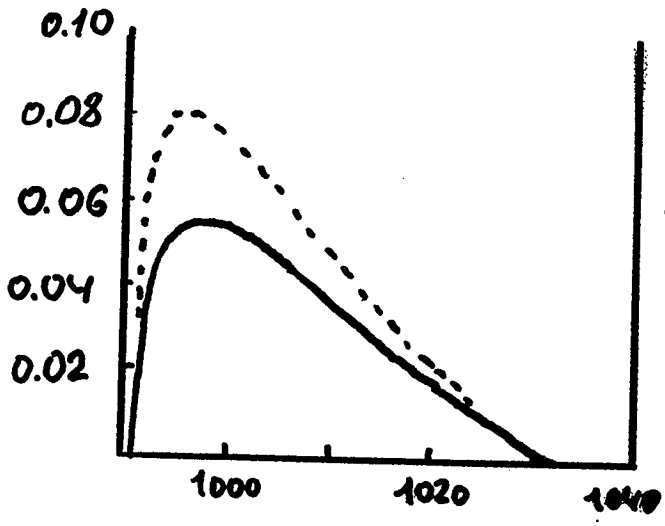

—— $\Gamma=80, d=1.5$

----- $\Gamma=80, d=3.0$

$Q=50$ MeV

c) Binnie's method:

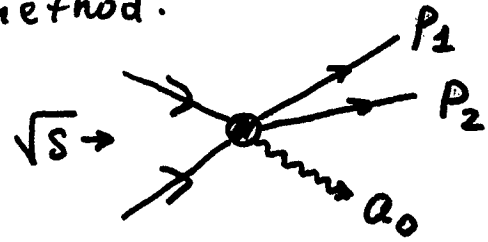

$\vec{p}_1+\vec{p}_2=\vec{P}$

$\vec{p}_1-\vec{p}_2=2\vec{k}$

$$\left.\frac{d^2\sigma}{dP\,dk}\right|_{p^*,k^*\ \text{fixed}} \propto \frac{F_{pp}(k^*)\,k^{*2}p^{*2}}{\left|Q-\frac{p^{*2}}{2\mu}-\frac{k^{*2}}{2m_{pp}}+i\frac{\Gamma}{2}\right|^2}$$

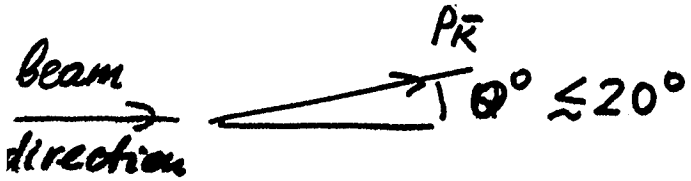

Possibility for Direct Measurements of a_0-f_0 Mixing

V. E. Tarasov, A. E. Kudryavtsev

Institute for Experimental and Theoretical Physics
B. Cheremushkinskaya 25
117259 Moscow
Russia

The nature of the lightest scalars $a_0(980)$ ($I^G J^{PC} = 1^- 0^{++}$) and $f_0(980)$ ($0^+ 0^{++}$), which masses are very close to each other, as well as the possible mixing of these mesons due to isospin breaking (IB) a_0-f_0 transitions is one of the most fundamental problems of hadron physics. We suggest to study this IB effect in the reaction

$$pn \to da_0^0 \tag{1}$$

near threshold. The a_0^0-meson may be identified by the $a_0^0 \to \pi^0\eta$ decay channel. If isospin is conserved a_0^0-mesons from reaction (1) will be produced in P-wave ($L = 1$). Note, that the production of the final da_0-system in S-wave ($L = 0$) is forbidden due to the conservation of isospin (I), parity (P) and total angular momentum (J). However, in the reaction

$$pn \to df_0 \tag{2}$$

the f_0-meson may be produced in S-wave. Thus, a_0^0-mesons could be produced from reaction (2) in S-wave through the IB transition $f_0 \to a_0$. Let us first consider a_0 as a stable particle with nominal mass $\bar{m}_a$. Then the cross-sections of these processes have the following near-threshold energy dependences:

$$\sigma(P - wave) \sim Q^{3/2}, \qquad \sigma(S - wave) \sim Q^{1/2},$$

where $Q = \sqrt{s} - m_d - \bar{m}_a$ is the excess energy ($\sqrt{s}$, m_d – total energy in CM and the deuteron mass, respectively). So the production of a_0^0 in S-wave through IB effect is to be relatively enhanced at low Q. The best way to observe the IB effect is to study "forward-backward" asymmetry $A = (\sigma_+ - \sigma_-)/(\sigma_+ + \sigma_-)$ ($\sigma_\pm \equiv \mathrm{d}\sigma/\mathrm{d}\Omega$ at $z = \cos\theta = \pm 1$) coming from the interference of P- and S-wave amplitudes. Note that in both amplitudes the initial pn-state has the same total spin $S = 1$. So the interference term may contribute to $\mathrm{d}\sigma/\mathrm{d}\Omega$ in the reaction (1) with unpolarised particles. To estimate the asymmetry let us consider the "tree" diagrams and suppose that a_0^0- and f_0-mesons are coupled to nucleons with the same constant, i.e. $g_{NNa} = g_{NNf}$. The diagram of direct f_0 production includes subprocess of the transition $f_0 \to a_0^0$. We estimate this transition amplitude λ_{fa} from a simple dynamical model, in which the process $f_0 \to a_0^0$ takes place due to the $\pi^0\eta$ transition in the decay channels, i.e. through the chain $f_0 \to \pi\pi \to \pi\eta \to a_0^0$. The transition amplitude $\lambda_{\pi\eta}$ is known from the analysis of $\eta \to 3\pi$ decays. We use the value $\lambda_{\pi\eta} = -5000$ MeV^2 [1]. Calculating λ_{fa} in this way we get for the a_0^0-f_0 mixing angle the value $\sin\theta_{af} \simeq 0.006$. Recently, Kerbikov and Tabakin [2] have obtained a much larger mixing $\sin\theta_{af} \simeq 0.14$. Their approach is based on the a_0-f_0 mixing due to $K\bar{K}$ intermediate states with the mass difference between neutral and charged kaons taken into account. We shall vary $\sin\theta_{af}$ within these limits. In our analysis we also must take into account the finite width of the a_0-meson. We use the value $\Gamma_a = 50$ MeV. Thus, the differential cross-section $\mathrm{d}\sigma/\mathrm{d}\Omega$ is to be integrated over a certain region of mass m of a_0 around the nominal value $\bar{m}_a$, i.e. $m_{min} < m < m_{max}$. Considering further $Q < \Gamma_a$, we take $m_{max} = Q + \bar{m}_a$ (the upper phase space limit) and $m_{min} = \bar{m}_a - C \cdot \Gamma_a/2$. Here C is a cut-off parameter.

Results

- In the case of small mixing $\sin\theta_{af} \simeq 0.006$, the asymmetry A for two values $C = 1$ and $C = 2$ is shown to be in the range $Q = -10$ to $+10$ MeV. The result depends on the cut-off parameter C. The asymmetry A decreases slowly from 0.038 (0.025) at $Q = -10$ MeV to 0.02 (0.025) at $Q = 10$ MeV for $C = 1$ ($C = 2$). So we obtain the effect $A \sim 2$ to 3 %, which is small but observable.

- In the case of large mixing $\sin\theta_{af} \simeq 0.14$ we get $A \sim 0.4$ to 0.6 in the region $Q = -10$ to $+10$ MeV. Now we obtain a large effect $A \sim 50$ %.

Conclusion

In the reaction $pn \to da_0^0$ in the near-threshold region one may expect a sizeable "forward-backward" asymmetry of order of 10 to 20 % due to the isospin violating a_0^0-f_0 mixing effect.

[1] S.A.Coon and M.D.Scadron, Phys.Rev.C **51**, 2923 (1995); S.A.Coon *et al.*, Phys.Rev.D **34**, 2784 (1986); Ll.Ametller, C.Ayala and A.Bramon, Phys.Rev.D **30**, 674 (1984); J.A. Niskanen, e-print nucl-th/9809009, 1998.
[2] B.Kerbikov and F.Tabakin, e-print nucl-th/0006017, 2000.

V. Tarasov, A. Kudryavtsev (ITEP)

"A possibility for direct measurements of a_0-f_0 mixing"

0^{++} 0^{++}

$m(a_0) \approx m(f_0) \approx 980$ MeV

$I=1$ $I=0$

Isospin breaking effect $a_0^0 \rightleftarrows f_0$

$pn \to d a_0^0$

a_0^0 may be identified by $a_0 \to \pi^0\eta$ decay channel

$pn \to d a_0^0$	
$I=1$	$I=1$
$S=1$	$S=1$
$L=1,3$	$L=1$
$P=-1$	$P=-1$

a_0 is in P-wave

$pn \to d f_0$	
$I=0$	$I=0$
$S=1$	$S=1$
$L=0,2$	$L=0$
$P=+1$	$P=+1$

f_0 is in S-wave

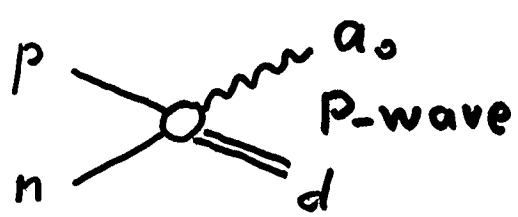

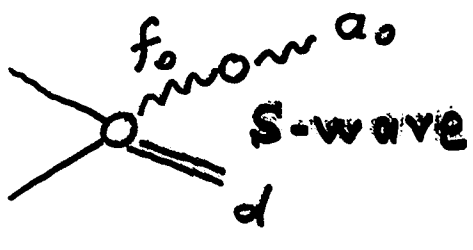

If isospin is conserved, a_0 is produced in P-wave only (not in S-wave !)

$$\left.\begin{aligned}\sigma(P) &\sim Q^{3/2}\\ \sigma(S) &\sim Q^{1/2}\end{aligned}\right\}\ \text{close to threshold}$$

So the production of a_0 in S-wave through isospin breaking effect is to be enhanced at low excess energy Q.

$$Q = \sqrt{s} - m_d - \bar{m}_a$$

The best way to observe this effect is to study „forward-backward" asymmetry

$$A = \frac{\sigma_+ - \sigma_-}{\sigma_+ + \sigma_-}\ ,\quad \sigma_\pm = \frac{d\sigma}{d\Omega}\ \text{at}\ z = \cos\vartheta = \pm 1$$

To estimate this effect let us consider the diagrams

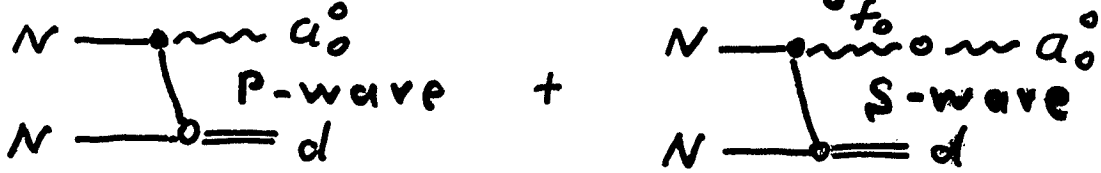

$$\frac{d\sigma}{d\Omega} = N\,|a + bz|^2 \cdot k\ ,\quad A = \frac{2\,\mathrm{Re}(a^* b)}{|a|^2 + |b|^2}$$

$k = \sqrt{2\mu Q}$ ← relative momentum in final da_0 system

$$\mu = \frac{m_d \bar{m}_a}{m_d + \bar{m}_a}$$

f_0-a_0 transition amplitude

Let us estimate this amplitude, using simple dynamical model

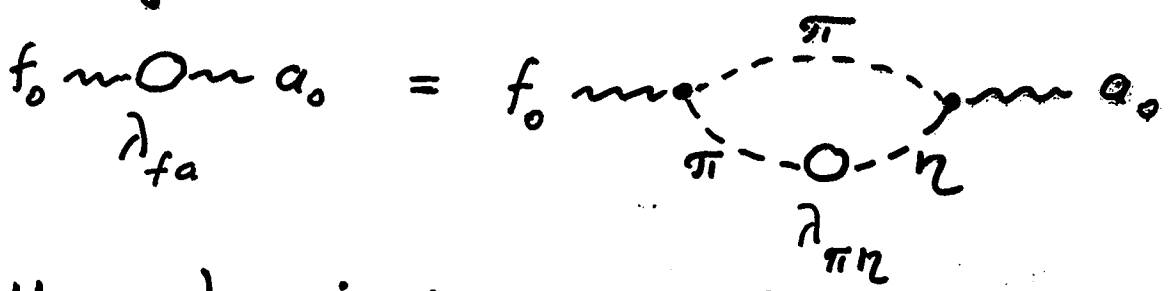

Here $\lambda_{\pi\eta}$ is isospin violating π^0-η transition amplitude

$$\lambda_{\pi\eta} \simeq -5000\ \text{MeV}^2$$

{ see e.g. Nishanen 1998; Coon et.al 1986, 1995; Amettler 1984

From this model for a_0-f_0 mixing angle we get

$$\sin\vartheta_{fa} \simeq 0.006$$

Recently Kerbikov and Tabakin (nucl-th/0006017, 2000) obtained much larger mixing

$$\sin\vartheta_{fa} \simeq 0.14$$

(Their approach is based on the a_0-f_0 mixing due to the $K\bar{K}$ intermediate state with the mass difference of neutral and charged kaons taken into account)

We shall vary mixing angle within these limits

Now we are to take into account the finite width of a_0-meson, $\Gamma_a \simeq 50$ MeV.

Then for the cross-section we get

$$\frac{d\sigma}{d\Omega} = N \cdot \int_{m_{min}}^{m_{max}} |a+bz|^2 \cdot k \cdot \frac{1}{\pi} \frac{\Gamma_a/2}{(m-\bar{m}_a)^2 + \Gamma_a^2/4}\, dm =$$

$$= \tilde{a} + \tilde{b}\cdot z + \tilde{c}\cdot z^2$$

The limits m_{max} and m_{min} depend on experimental limitations

Here we take $m_{min} = \bar{m}_a - C\cdot\frac{\Gamma_a}{2}$

Asymmetry: $A = \tilde{b}/(\tilde{a}+\tilde{c})$

The results

i) The case of small mixing angles ($\sin\vartheta_{fa} \simeq 0.006$)

We get asymmetry A to be of order $(2 \div 3)\%$.

What is not very small effect.

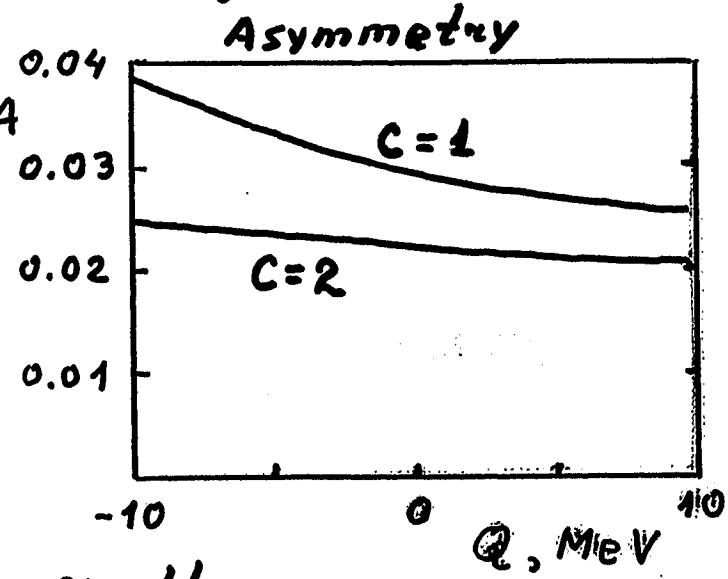

The result depends on the cut-off parameter m_{min}.

ii) The case of large mixing angle ($\sin\theta_{fa} \simeq 0.14$)

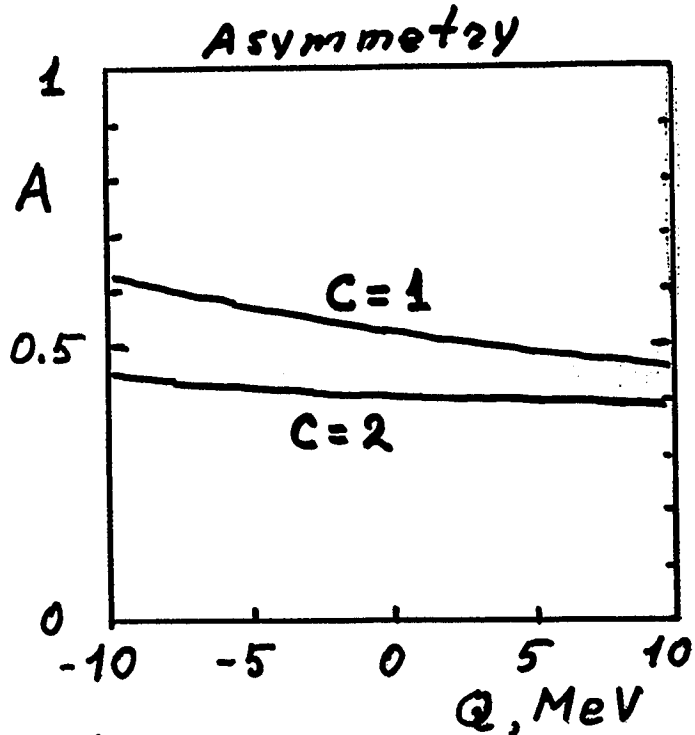

In this case the asymmetry A gets the value of order 50 %

Conclusion

In the reaction $pn \to d a_0$ in the near threshold region one may expect the „forward - backward" asymmetry due to isospin violation effects of order of $10 \div 20$ %.

The reaction $dd \to a_0^0\, {}^4He$

is forbidden, if isospin is conserved.

Isospin breaking mechanism :

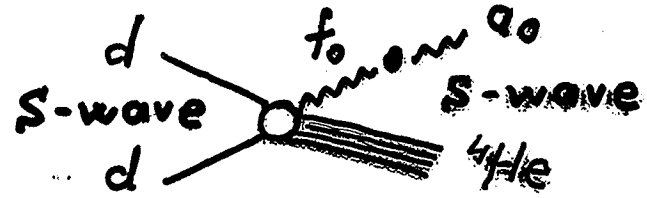

The production of a_0 in this process has some privelegies in comparison to the another isospin violating process $dd \to \pi^0\, {}^4He$.

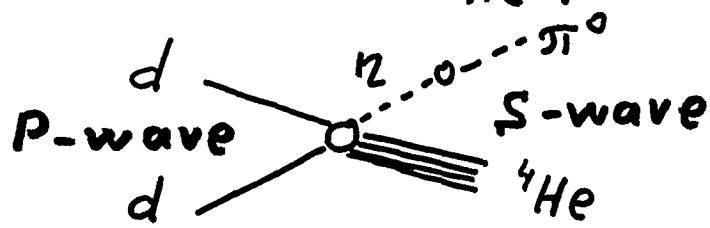

In the case of a_0 production the process may come from initial <u>S-wave</u> dd-state. The reaction $dd \to \pi^0\, {}^4He$ may come from initial <u>P-wave</u>. So the π^0 production is accompanied by strong rearangement of nucleons wave functions, and the reaction amplitude gets some small factor.

Superallowed a_0-f_0 Mixing

B. O. Kerbikov

Institute for Experimental and Theoretical Physics
B. Cheremushkinskaya 25
117259 Moscow
Russia

A model independent description of a_0-f_0 mixing due to kaon loops is presented. The a_0-f_0 propagator is calculated in a close analytic form. As compared to the standard meson mixing (e.g. ρ-ω) the a_0-f_0 mixing is superallowed which means that it is proportional to $\sqrt{\alpha}$ instead of α.

The characteristic invariant mass interval within which mixing is strong is of the order of 10 MeV, i.e. the mass difference between the $K^0\bar{K}^0$ and K^+K^- thresholds. The coupling constants of a_0 and f_0 to their decay channels are taken from recent experimental data of the Novosibirsk group. For more details see Ref. [1].

[1] B. Kerbikov and F. Tabakin, nucl-th/0006017

SUPERALLOWED f_0-a_0 MIXING

Kerbikov and Talakin nucl th/0006017

The correct treatment of f_0-a_0 mixing goes back to Achasov, Devyanin, Shestakov 1979

In K & T the most general expression for the f_0-a_0 formfactor applicable to any reaction is derived and all parameters are fixed from recent Novosibirsk data on $\phi \to \gamma f_0/a_0$

The driving idea: isospin invariance is intrinsically broken due to δ Mev K^+K^- and $K^0\bar{K}^0$ thresholds splitting. The fundamental scale is u-d mass difference but phenomenologically mixing is characterized in terms of $\alpha = 1/137$.

Superallowed mixing $\sim \sqrt{\alpha}$

"normal" ρ-ω mixing $\sim \alpha$

Universal quantity: f_0-a_0 formfactor,
or propagator

$\langle out | f_0\text{-}a_0 | in \rangle$, $|out\rangle = \pi\pi, K\bar{K}, \pi\eta$

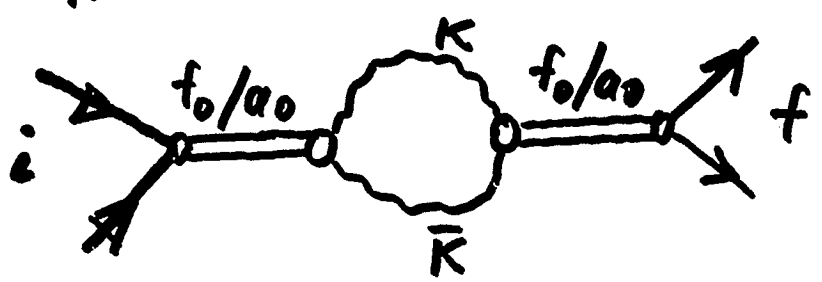

$$T_\alpha = V_{\alpha i} G_{ik} F_k \qquad \alpha = K\bar{K}, \pi\pi, \pi\eta$$
$$i,k = f_0, a_0$$

G_{ik} - the propagator matrix

What suppressed means?

ρ-ω $\qquad H = \begin{pmatrix} m_\omega - i\frac{\Gamma_\omega}{2} & s \\ s & m_\rho - i\frac{\Gamma_\rho}{2} \end{pmatrix}$ $\qquad s \sim \alpha m_\rho$ normal mixing

f_0-a_0 $\qquad s \sim \dfrac{|V_{fK^+K^-} V_{K^+K^-a}|}{m_f} \underbrace{\sqrt{\dfrac{2(m_{K^0} - m_{K^+})}{m_{K^\pm}}}}_{\sim 0.13 \sim \sqrt{\alpha}}$

$V \sim 3\,GeV$

Resonance mixing – generals

# of papers >> 1/α

Stodolsky 1970

Kobzarev, Nikolaev, Okun 1969

Kudryavtsev 1969

Tsentsev 1970

. . . . . .

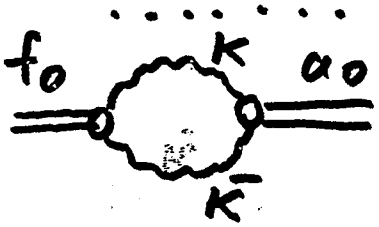

drastically depends on energy (on m_x) close to $K\bar{K}$ threshold

$$\sum_{K\bar{K}} V_{nK\bar{K}} \frac{1}{m_x - E_{K\bar{K}} + i0} V_{K\bar{K}m}$$

while 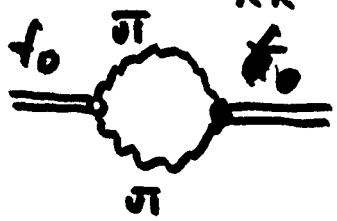

and 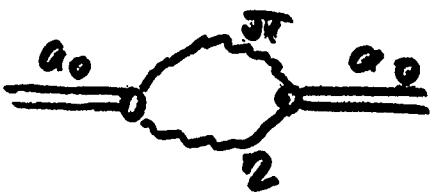

are almost energy independent and may be parametrized as

$$\begin{pmatrix} m_x - E_f + i\frac{\Gamma_f}{2} & \\ & m_x - E_a + i\frac{\Gamma_a}{2} \end{pmatrix}$$

4

The leading contribution from the kaon loop

$$\frac{1}{m_X^3}\int\frac{d^3p}{(2\pi)^3}\frac{1}{m_X-2m_K-\frac{p^2}{m_K}+i0}\simeq\frac{-i}{32\pi m_X}\sqrt{\frac{m_X-2m_K}{m_K}+i0}$$

Then the f_0-a_0 propagator reads:

$$iG^{-1}=\begin{pmatrix} m_X-E_f+i\frac{\Gamma_f}{2} & 0 \\ 0 & m_X-E_a+i\frac{\Gamma_a}{2}\end{pmatrix}+$$

$$+\mathcal{D}\begin{pmatrix}1 & s\\ s^* & |s|^2\end{pmatrix}\sqrt{\frac{m_X-2m_{K^+}}{m_{K^+}}+i0}+i\mathcal{D}\begin{pmatrix}1 & -s\\ -s^* & |s|^2\end{pmatrix}\sqrt{\frac{m_X-2m_{K^0}}{m_{K^0}}+i0}$$

$$\mathcal{D}\equiv\frac{|V_{K^+K^-f}|^2}{32\pi m_X}\,,\qquad \Gamma_{n\kappa\bar\kappa}=\frac{|V_{n\kappa\bar\kappa}|^2}{16\pi m_X}\sqrt{\frac{m_X-2m_\kappa}{m_\kappa}}\,,$$

$$s\equiv\frac{V_{K^+K^-a}}{V_{K^+K^-f}}\,,\qquad V_{K^+K^-f}=V_{K^0\bar K^0 f}\,,\ V_{K^+K^-a}=-V_{K^0\bar K^0 a}\,,$$

$s=1$ in the $q^2\bar q^2$ model (Jaffe)

Parameters of the model – from recent Novosibirsk data on $e^+e^- \to \varphi$

$$\frac{|\Gamma_{f\pi\pi}|^2}{4\pi} = 0.446\,\text{GeV}^2, \quad R = \frac{|\Gamma_{fK\bar{K}}|^2}{|\Gamma_{f\pi\pi}|^2} = 3.77$$

Isospin relations: $|\Gamma_{f\pi^+\pi^-}|^2 = \frac{2}{3}|\Gamma_{f\pi\pi}|^2$

$$|\Gamma_{fK^+K^-}|^2 = \frac{1}{2}|\Gamma_{fK\bar{K}}|^2$$

$\Gamma_f = \Gamma_a = 0.1\,\text{GeV}$

$E_f = 0.947\,\text{GeV}$

$\Gamma_{fK^+K^-} = 3.23\,\text{GeV}$

$\Gamma_{a\pi\eta} = 3.086\,\text{GeV}$

$S = 1$

or $S = |S|e^{i\varphi}$

mixing strongly depends on φ

$$S \equiv \frac{\Gamma_{K^+K^-a}}{\Gamma_{K^+K^-f}}$$

Typical plots

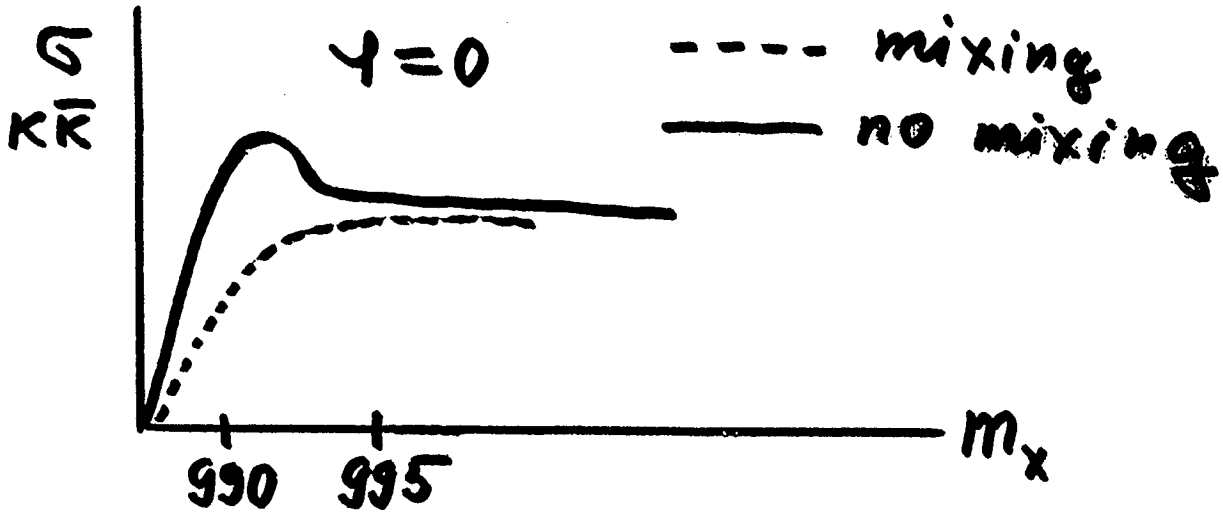

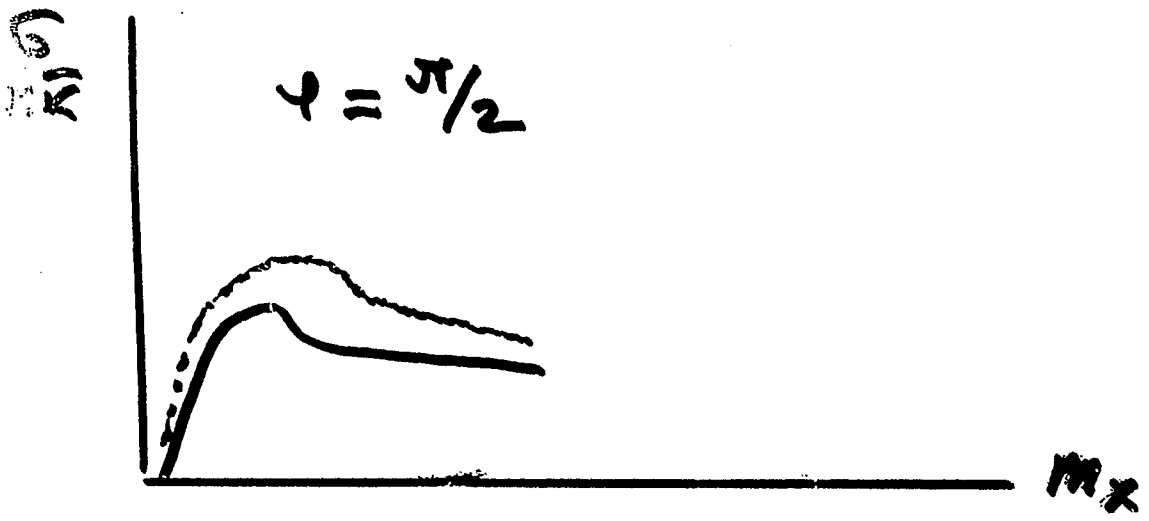

Mixing in pion channel

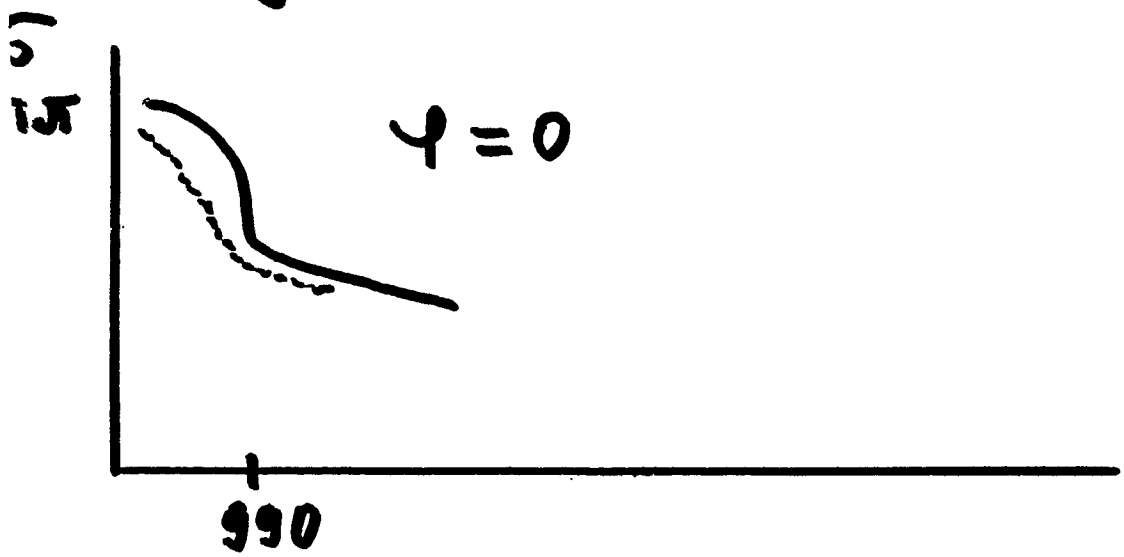

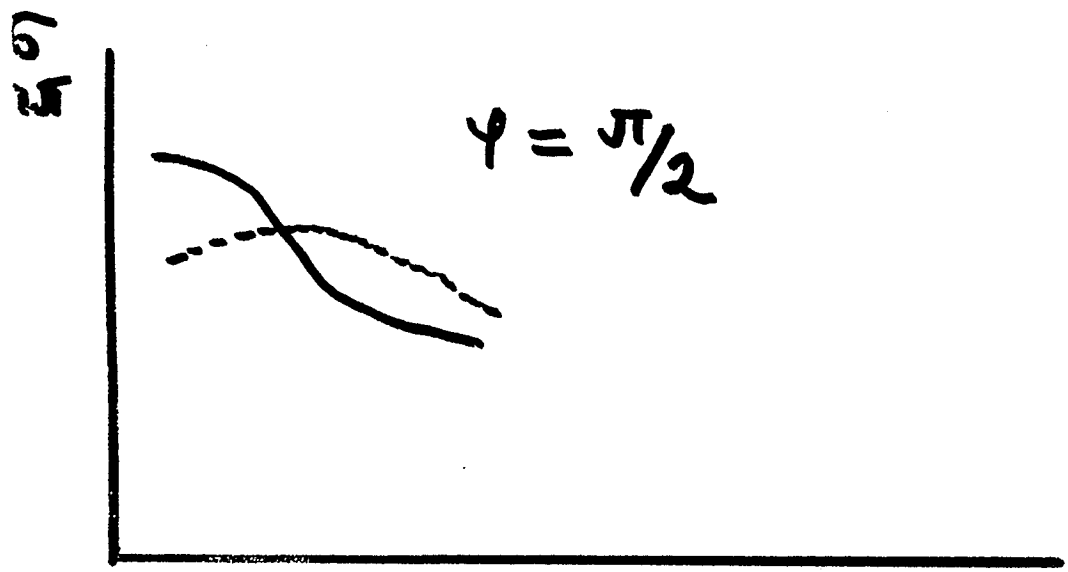

Simulations on a_0^+ Detection at ANKE

V. Kleber

Institut für Kernphysik
Forschungzentrum Jülich
52425 Jülich
Germany

Some new results of simulations on a_0 detection using the ANKE-GEANT simulation package are presented.

- First, the calculation of the count rate estimates is explained (see transparency 2). If they are correct we expect to detect 13 coincident dK^+ and 23 coincident $d\pi^+$ events per hour with ANKE.

- Second, the missing mass distribution stemming from a_0 decays into $\pi^+\eta$ and $K^+\overline{K}^0$, respectively, is demonstrated (see transparency 3). The missing mass distribution of $a_0 \rightarrow K^+\overline{K}^0$ decays is kinematically limited to a small region between 991 and 1022 MeV.

- Further, the geometrical acceptance for dK^+ in dependence of the missing mass of the a^0 is shown (see transparency 4). It is about constant from threshold to 1007 MeV and is decreasing for higher masses.

- One kind of possible background is due to nonresonant $K^+\overline{K}^0$ production. Resonant and nonresonant $K^+\overline{K}^0$ pairs cannot be distinguished by their momentum or missing mass distributions (see transparency 6) since the available phase space in our case is small. Nevertheless we found a method with which we believe to be able to determine at least the ratio of resonant and nonresonant events (see transparencies 7 to 9). We assumed d, K^+ and $\overline{K}^0$ from nonresonant production to be emitted via a S-wave which gives a flat angular distribution of the deuterons while the same distribution shows P-wave behaviour (and a small D-wave contribution) in the case of resonant production [1]. The distribution from experimental data which is the sum of both has to be corrected with the detection efficiency and can be fitted by Legendre polynomials. The ratio of A/B allows then to estimate the ratio of resonant to nonresonant production.

[1] V.Yu.Grishina et al., submitted to EPJ and nucl-th/0007074

Workshop on a_0 Physics with ANKE

July 13/14, 2000

ITEP, Moscow

Simulations on a_0^+ detection at ANKE

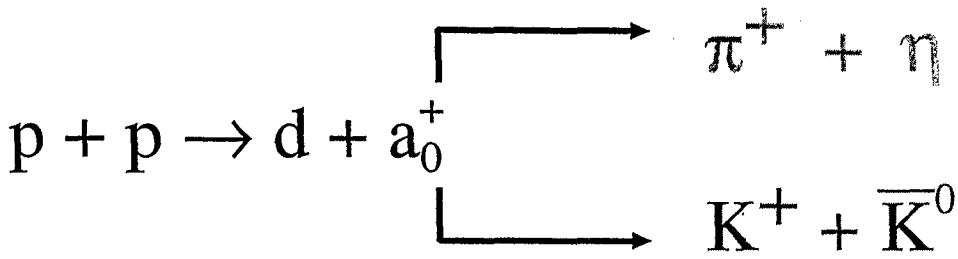

Simulations - Count Rate Estimates

'non-decay' probability:
K^+ : 30 %
π^+ : 90 %

luminosity of cluster jet target:
$L = 3*10^{30}\ cm^{-2}s^{-1}$

total cross section:
$p^+ + p^+ \rightarrow d + a_0^+$: 1.12 μb

$$\dot{n} = L * \varepsilon_{geo} * \varepsilon_{decay} * \varepsilon_{det} * \sigma * \Gamma$$

branching ratio*:
$a_0^+ \rightarrow K^+ + \bar{K}^0$: 12 %
$a_0^+ \rightarrow \pi^+ + \eta$: 88 %

geometrical acceptance:
$K^+ + d$: 11 %
$\pi^+ + d$: 0.3 %

detection efficiency:
$K^+ + d$: (30 * 90) % = 27 %
$\pi^+ + d$: (90 * 90) % = 81 %

$$\dot{n}\,(dK^+) = 13\ h^{-1}$$

$$\dot{n}\,(d\pi^+) = 23\ h^{-1}$$

* A. Abele et al., Phys. Rev. D57 (1998) 3860, with phasespace correction

Simulations - Missing Mass Distribution

$$p + p \rightarrow d + a_0^+ \rightarrow \pi^+ + \eta$$
$$\rightarrow K^+ + \overline{K}^0$$

$$m^2_{miss} = m^2(a_0^+)$$
$$= (T_p + 2*m_p - E_d)^2 - [\vec{p}_p - \vec{p}_d]^2$$

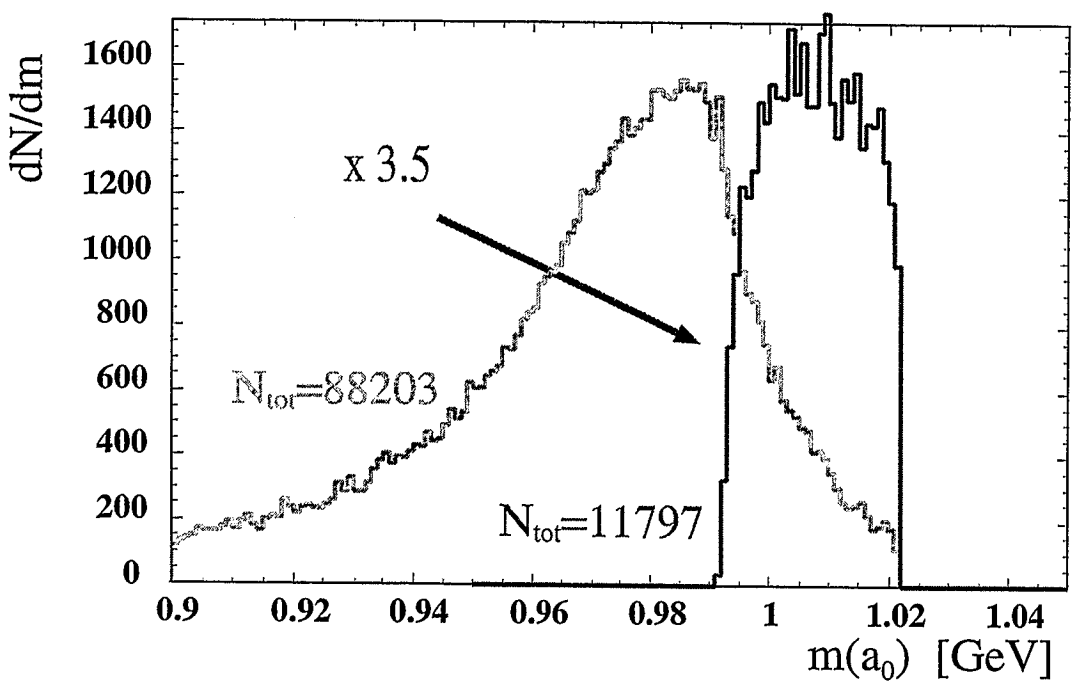

kinematical limits:

upper $m_{a,max} = s_{d,a}^{1/2} - m_d = (2.898 - 1.876)\ \text{GeV} = 1.022\ \text{GeV}$

lower (for Kaons) $m_{a,min} = m_{K^+} + m_{\overline{K}^0} = (0.494 + 0.497)\ \text{GeV} = 0.991\ \text{GeV}$

Simulations - Geometrical Acceptance

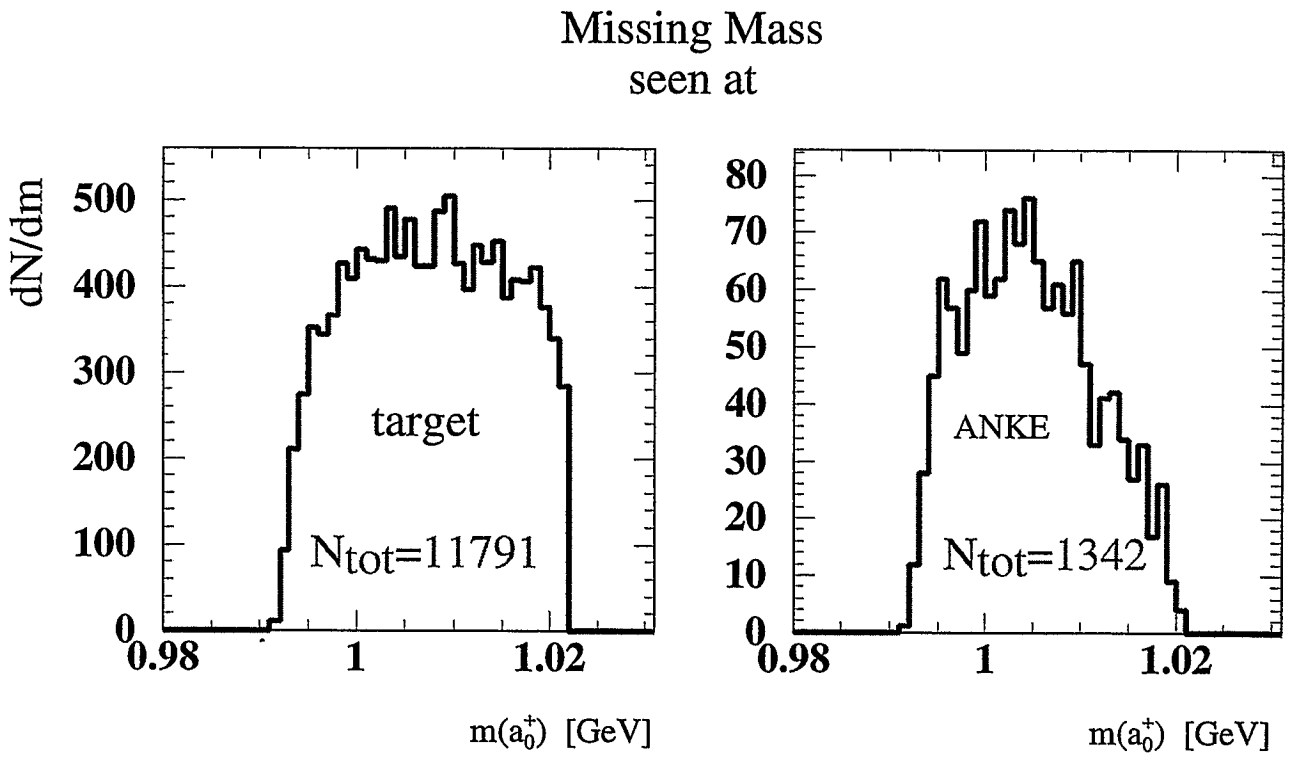

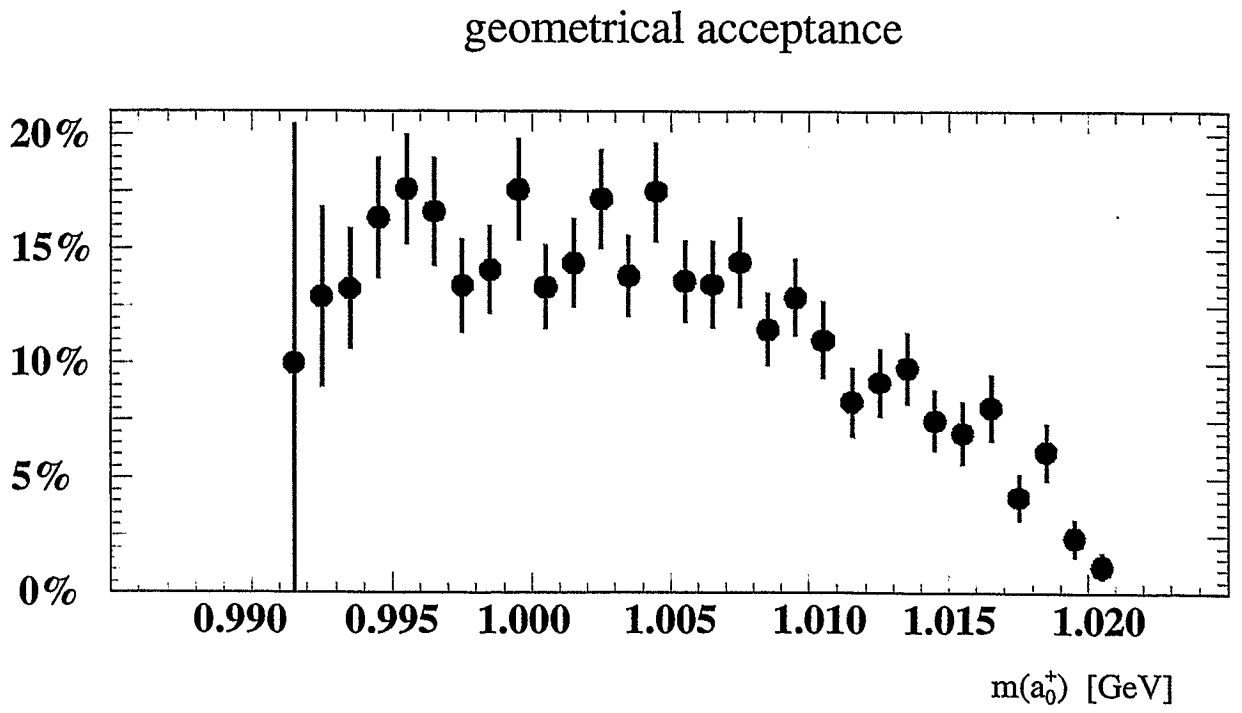

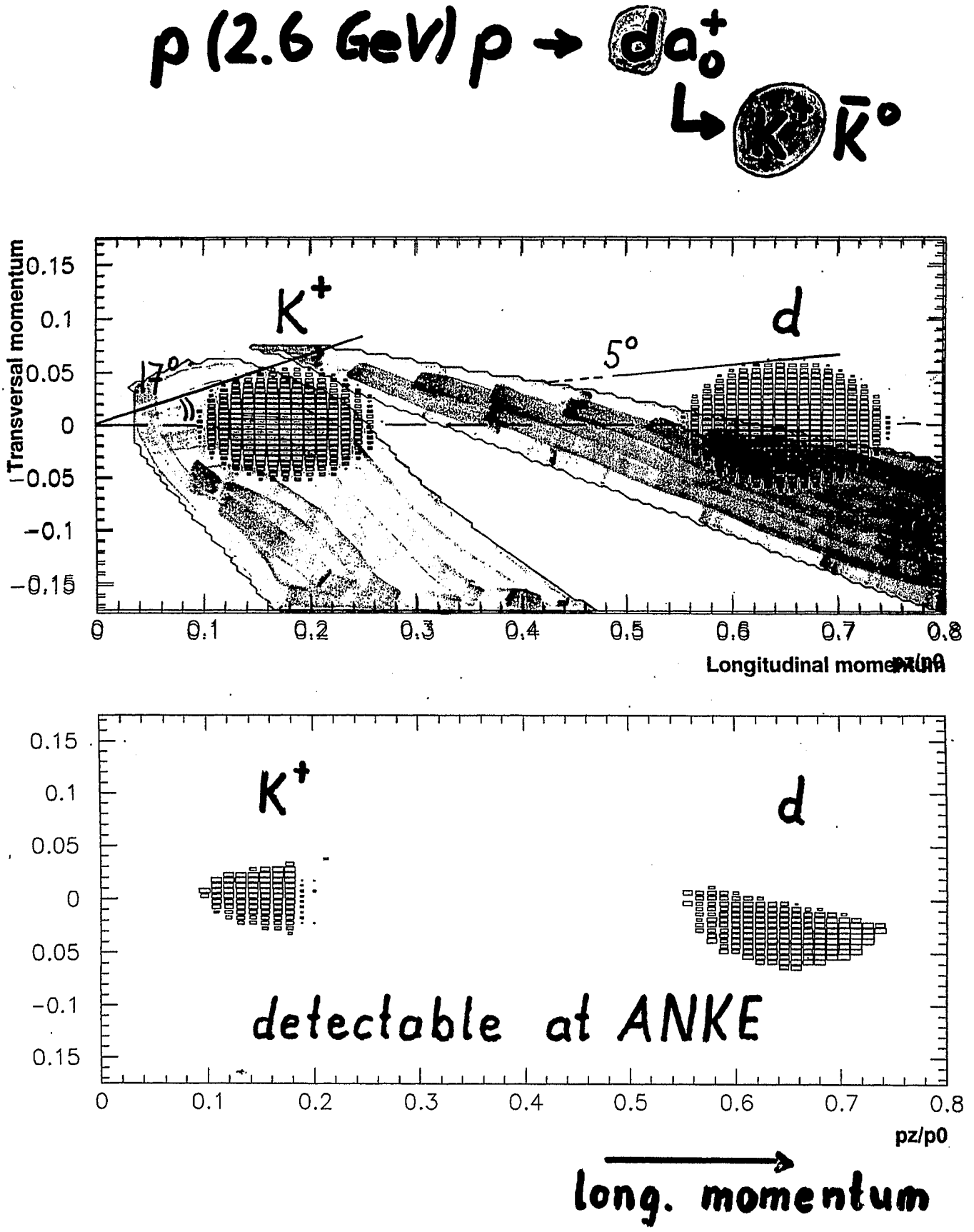
p (2.6 GeV) p → d a0+
↳ K+ K̄0
Transversal momentum
0.15
0.1
0.05
0
−0.05
−0.1
−0.15
K+
d
17°
5°
0
0.1
0.2
0.3
0.4
0.5
0.6
0.7
0.8
Longitudinal momentum pz/p0
K+
d
detectable at ANKE
pz/p0
long. momentum

Simulations - Nonresonant Background

resonant $p + p \rightarrow d + a_0^+ \rightarrow d + K^+ + \bar{K}^0$

nonresonant $p + p \rightarrow d + K^+ + \bar{K}^0$

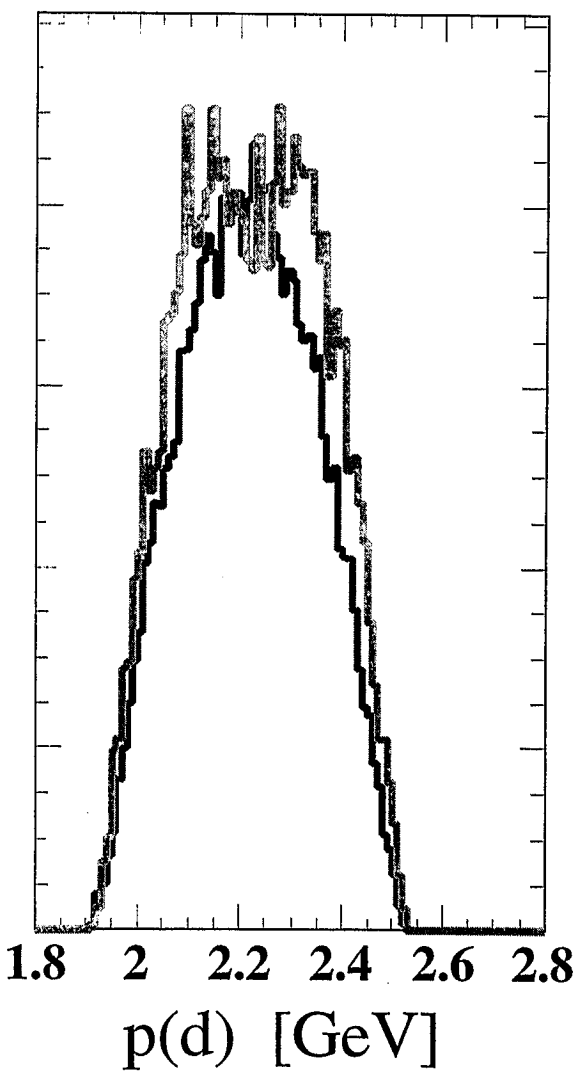

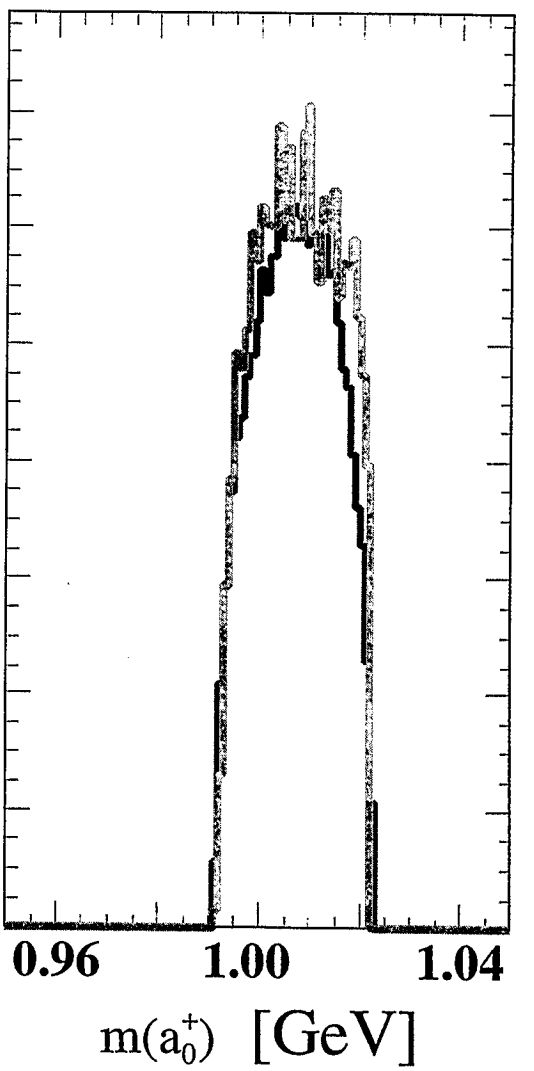

Simulations - Nonresonant Background

resonant

$dN/d\Omega_{cm} = A + B*\cos^2(\vartheta_{cm}) + C*\cos^4(\vartheta_{cm})$

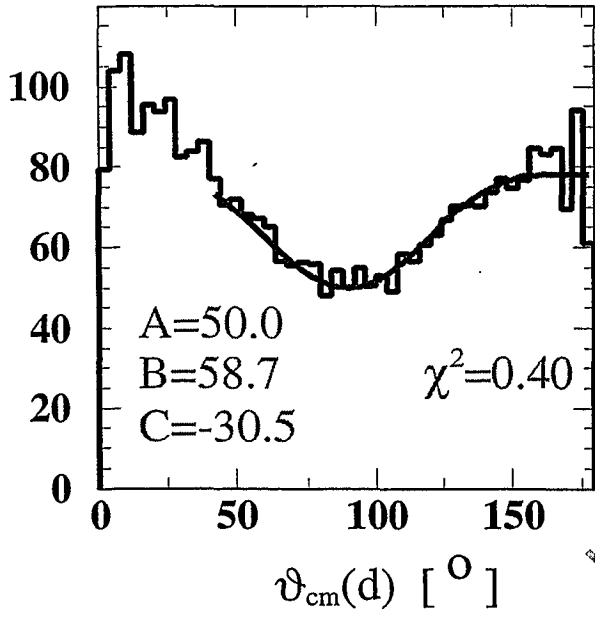

nonresonant

$dN/d\Omega_{cm} = A^*$

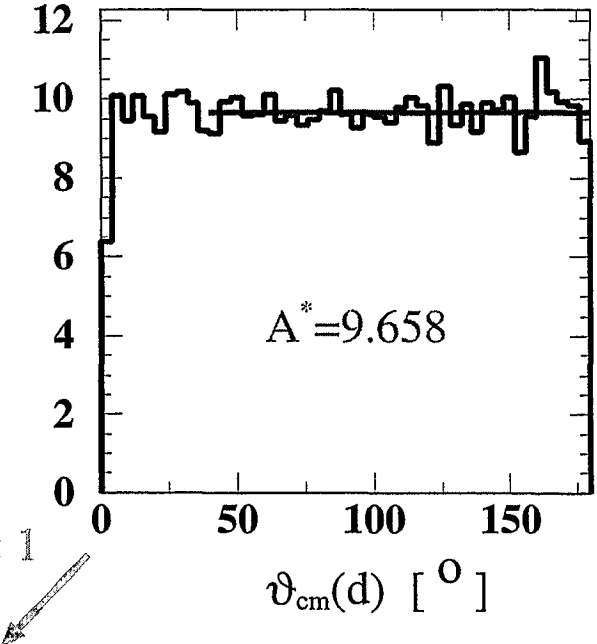

8 : 1

$dN/d\Omega_{cm} = (A + A^*) + B*\cos^2(\vartheta_{cm}) + C*\cos^4(\vartheta_{cm})$

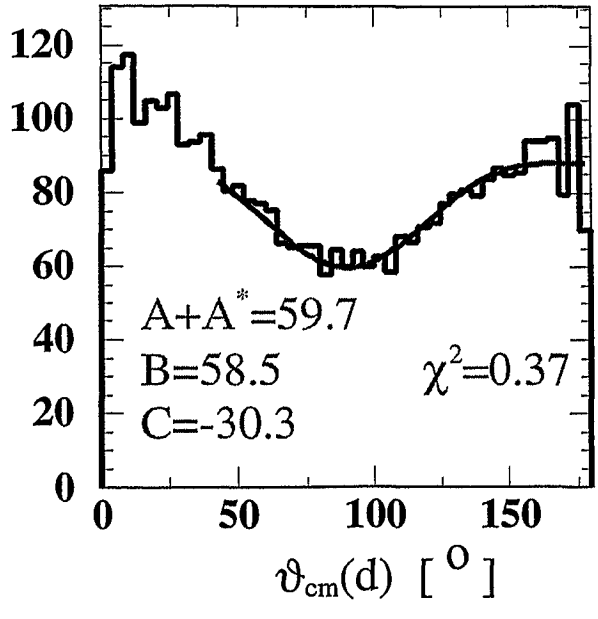

Simulations - Nonresonant Background

resonant channel

$dN/d\Omega_{cm}$ at the target

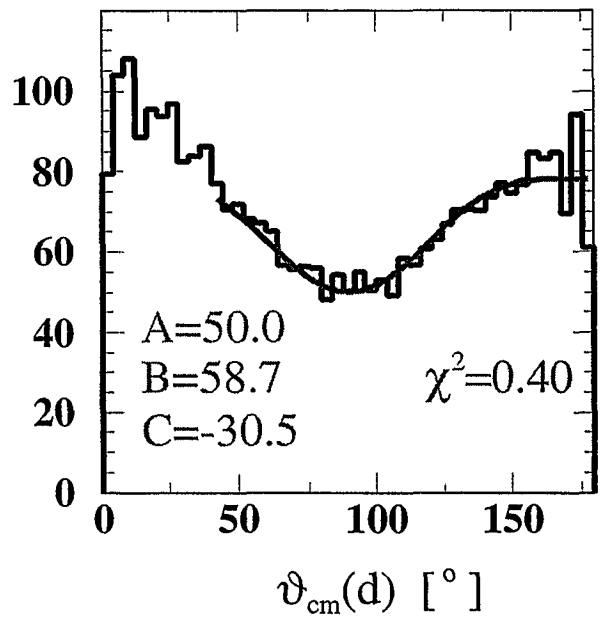

$dN/d\Omega_{cm}$ seen at ANKE

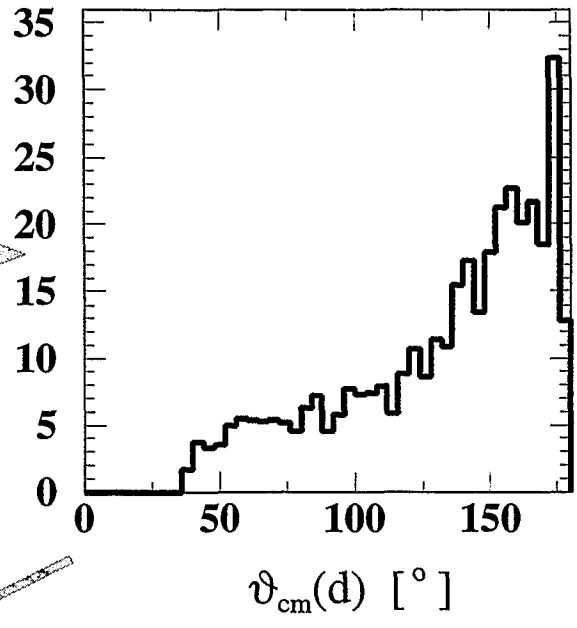

detection efficiency

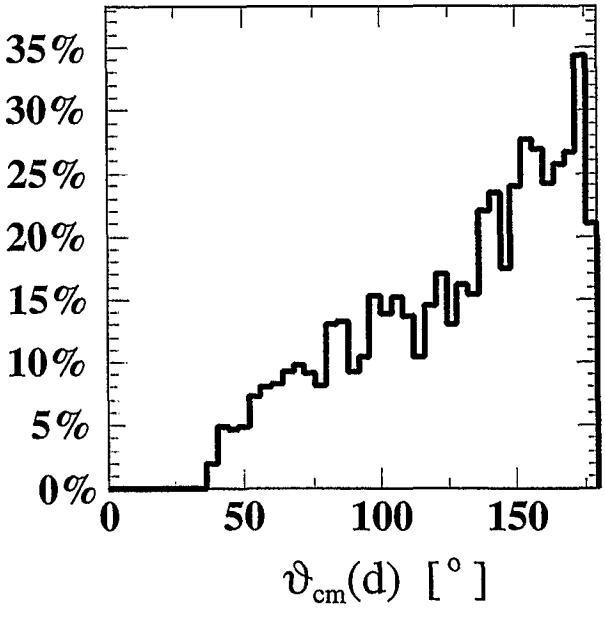

$dN/d\Omega_{cm}$ corrected for efficiency

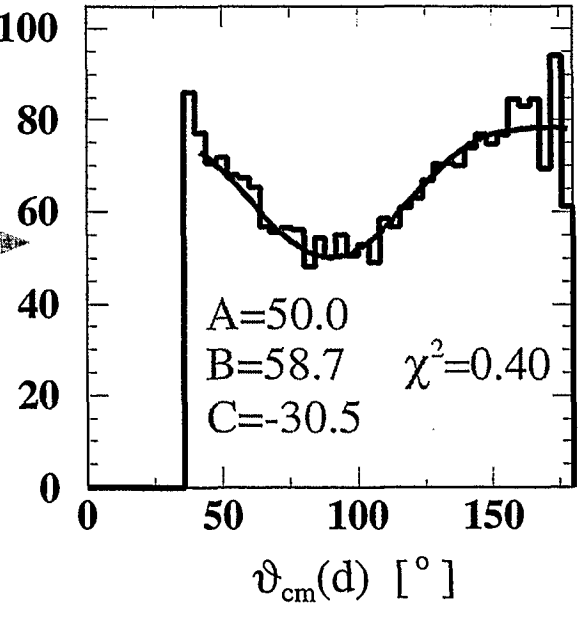

Simulations - Nonresonant Background

resonant + nonresonant

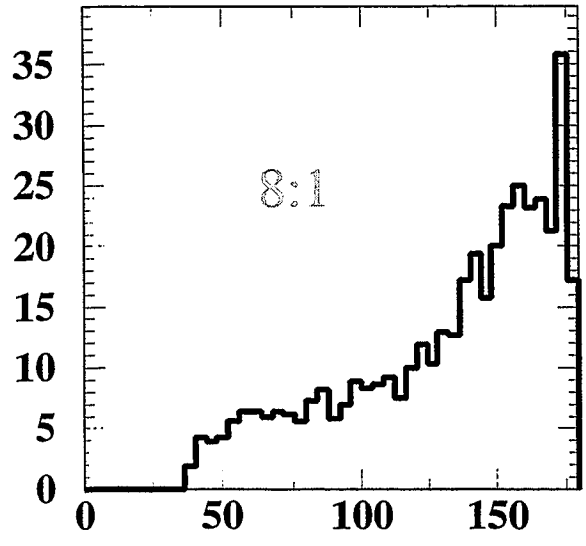

detection efficiency (resonant)

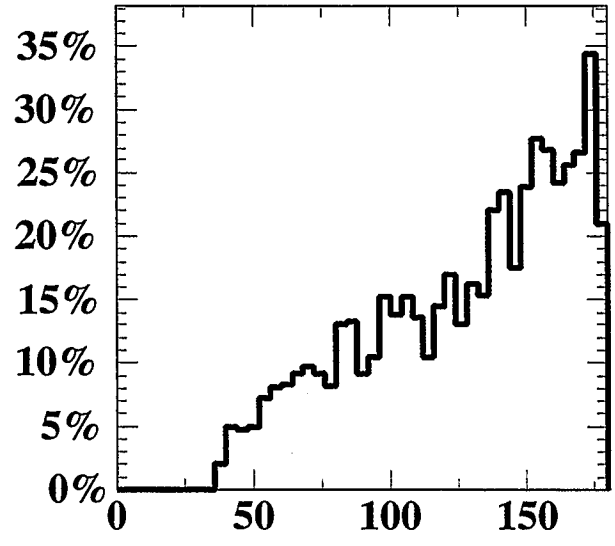

efficiency corrected spectrum

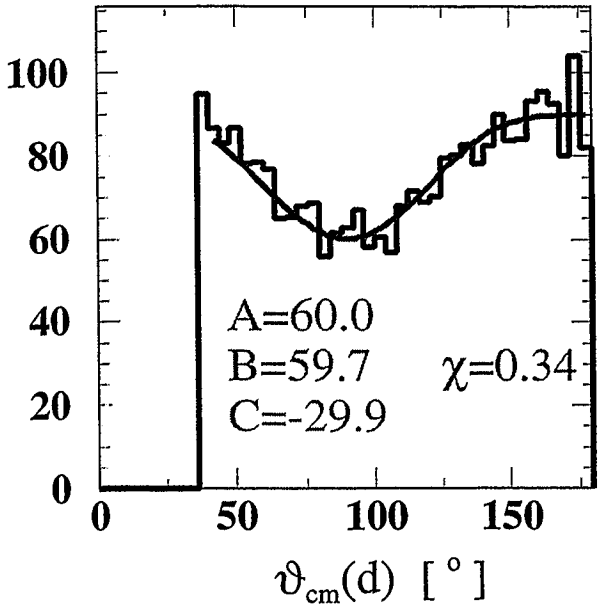

A/B

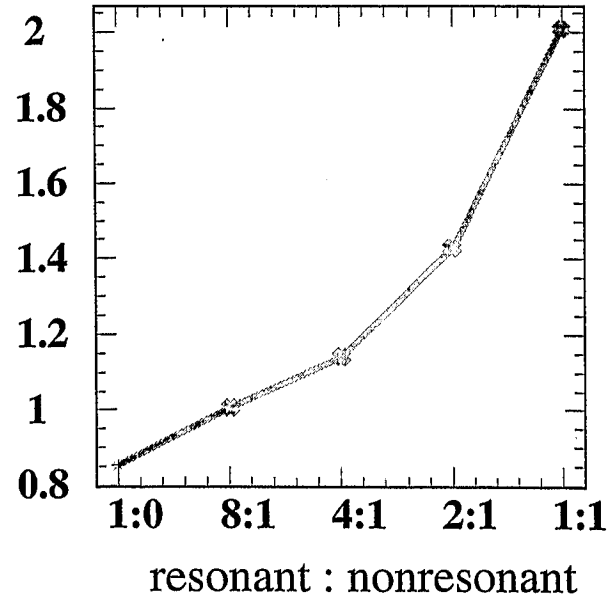

Conclusion and Outlook

conclusion on simulations:

→ 'at the moment completed'

outlook:

→ momentum reconstruction

→ study of missing mass resolution
on experimental data

Status of the Cluster Target

N. Lang

Institut für Kernphysik
Universität Münster
48149 Münster
Germany

Technical overview

Since September 1999 a cluster target, providing cluster beams from hydrogen- and deuterium gas, is available at ANKE for internal experiments.

To produce a cluster beam hydrogen gas at a pressure of about 18 bars is supplied to a laval nozzle which is cooled to a temperature of 20 - 40 K. During expansion the gas cools down and the saturated gas condensates to a cluster beam. This first broad cluster beam is peeled off by a skimmer and a collimator. After this procedure the beam expands with very well defined and sharp dimensions towards the scattering chamber.
To get information about the density of the cluster beams, which depends on the temperature and pressure at the nozzle, systematic investigations have been carried out. In particular, we obtained information on the phase space in which the vapour pressure curve of hydrogen is located (See transparency 5, density distribution). The density of the cluster beams is plotted in the third dimension represented by a colour scale. Selecting a certain pair of parameters, we can immediately make predictions for the density of the target beam. In order to achieve high densities we have to set a stable working point in an area, which represents densities of $\rho \approx 6 \cdot 10^{13}$ atoms/cm^3.
To measure the beam dimensions we use a pair of movable rods, which can be brought into overlap with the cluster beam. As a consequence the pressure in the concerned pumping stages rises. The shape of the pressure curve from this measurement gives direct information about the target dimensions.

If the target runs with deuterium we can use a system for deuterium recuperation, which recovers more than 95 % of the deuterium gas. Most of the used gas is pumped away from the skimmer stage. It can be cleaned from possible oil contamination, compressed and refilled to the gas supply system.

Luminosity Determination

To get information on the luminosity and target density during the beam time 9/99, we performed an analysis of runs 1801,1822,1823 and 1824. By determining the count rate for events from the reaction $pp \rightarrow d\pi^+$ we can calculate the luminosity using known values for the cross section from literature and acceptance. The acceptance is calculated with a GEANT simulation. In a missing mass as well as in a momentum plot, obtained from the sorter software, we can easily identify entries from the reaction $pp \rightarrow d\pi^+$. If we demand an additional coincidence of a deuteron hit in the forward scintillator with an identified pion in the side detection system, we achieve a very good suppression of the background from the three body reaction $pp \rightarrow pn\pi^+$. With first estimations of the detection efficiency and dead time we can calculate the lower limit of the luminosity. It turned out that the resulting lower limit for luminosity was $3.3 \cdot 10^{28}\,\mathrm{cm}^{-2} \cdot \mathrm{s}^{-1}$. It is too low by a factor of ten compared to the expected values.

Outlook

After investigation of realistic dead time and efficiency corrections the values for the luminosity will be recalculated. Also a differential cross section for this recalculation will be used according to V. Koptev's suggestion.

For investigations on a_0 production a very high luminosity ($> 10^{30}\,\mathrm{cm}^{-2} \cdot \mathrm{s}^{-1}$) is required. Therfore, we will put the target into operation at a working point of high density. Furthermore, the beam-target overlap has to be optimised. A new collimator is ready to be installed, which will provide larger beam dimensions.

Status of the Clustertarget

a_0-Workshop

Moscow, July 2000

Norbert Lang

WWU Münster

Scheme of the Clustertarget

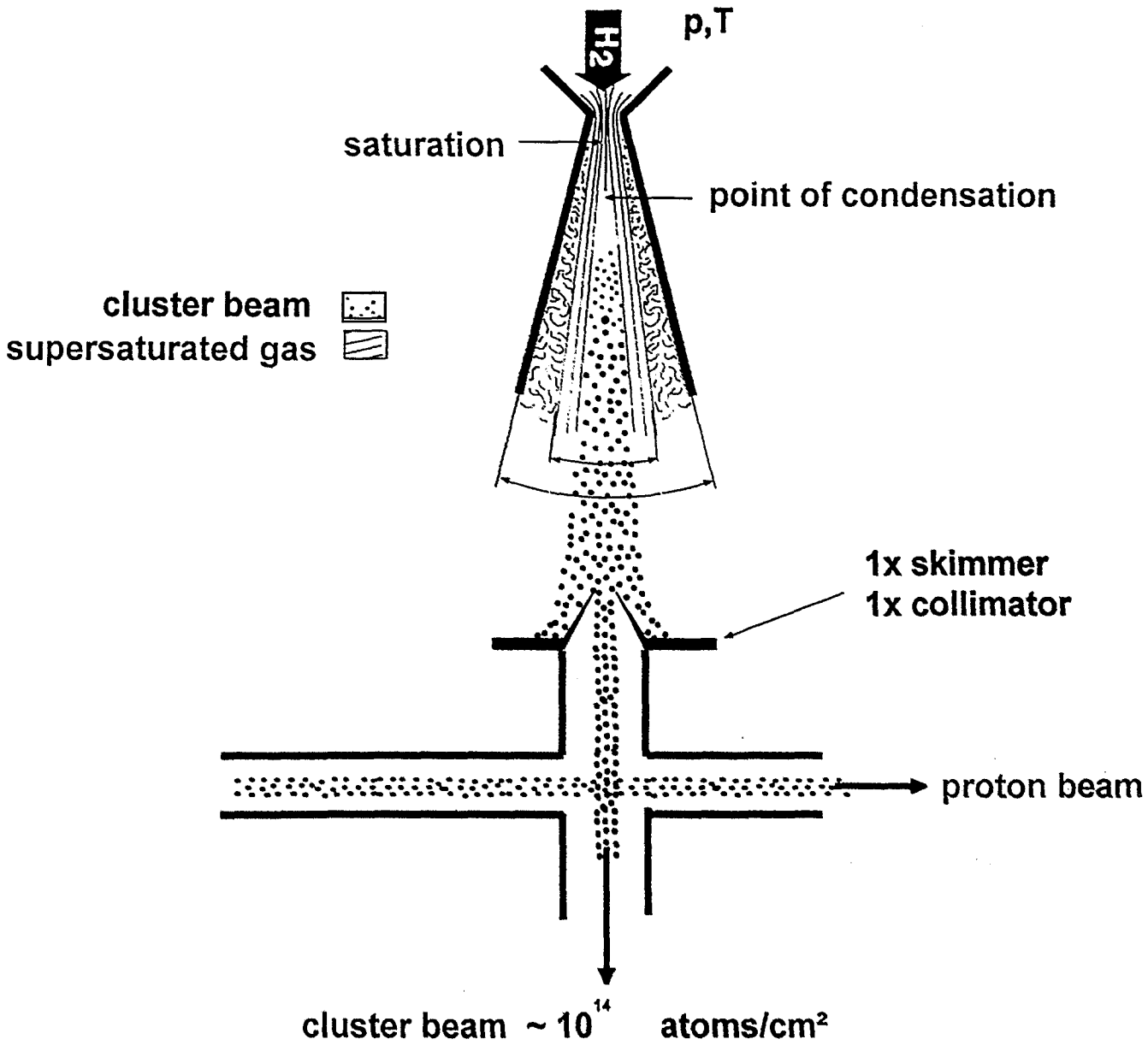

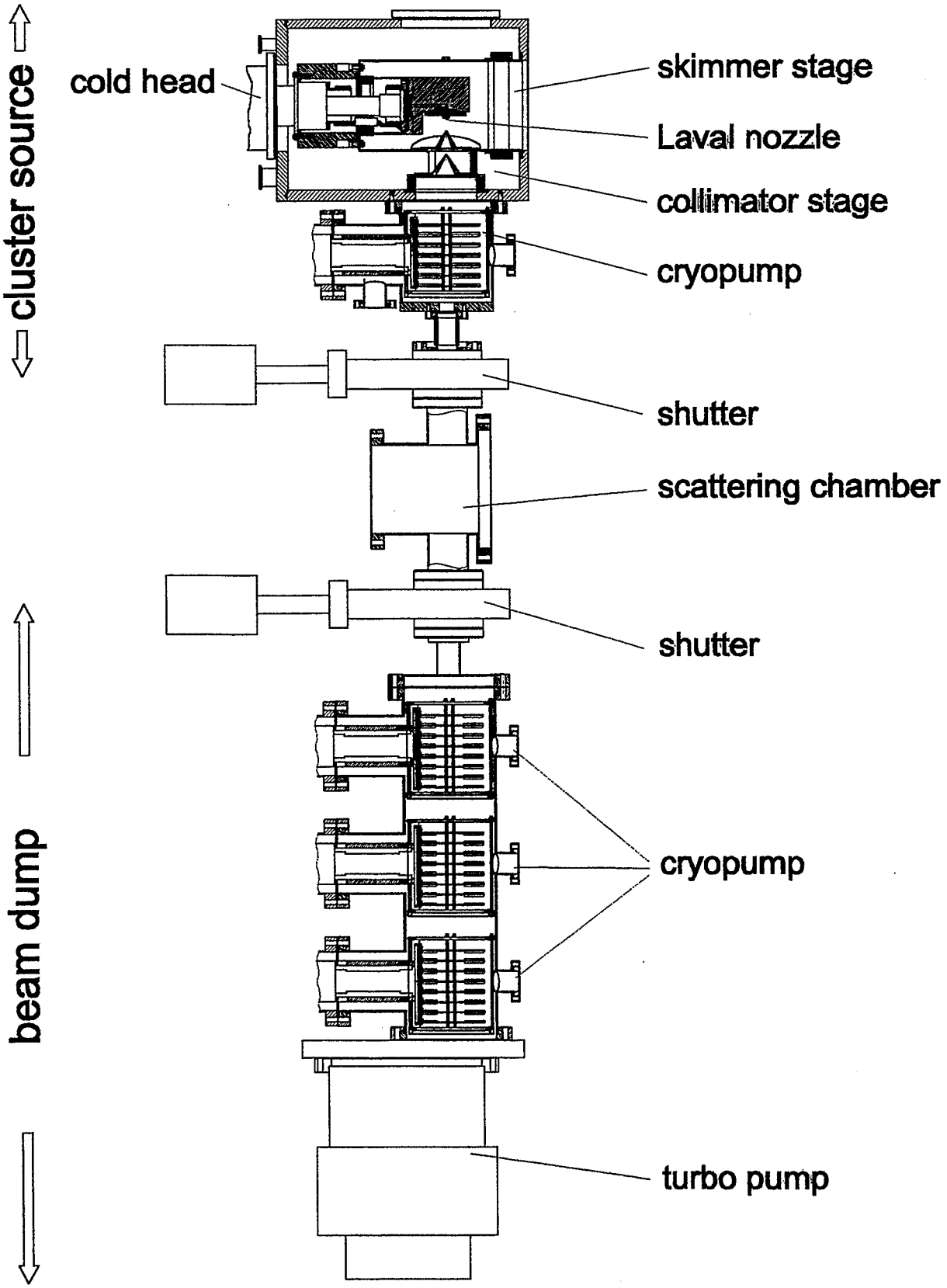
cluster source
beam dump
cold head
skimmer stage
Laval nozzle
collimator stage
cryopump
shutter
scattering chamber
shutter
cryopump
turbo pump

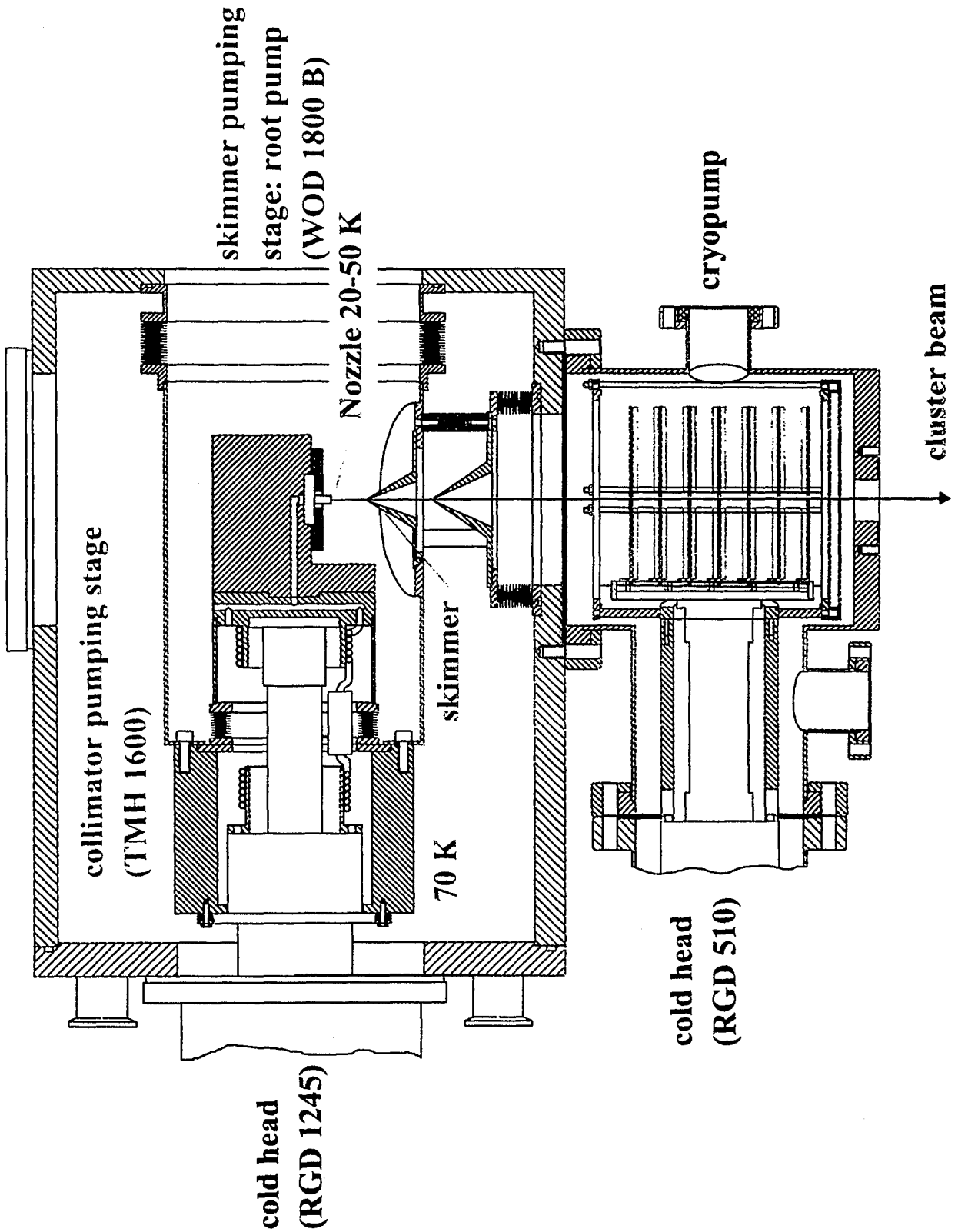
skimmer pumping
stage: root pump
(WOD 1800 B)
Nozzle 20-50 K
cryopump
cluster beam
collimator pumping stage
(TMH 1600)
skimmer
70 K
cold head
(RGD 1245)
cold head
(RGD 510)

density distribution

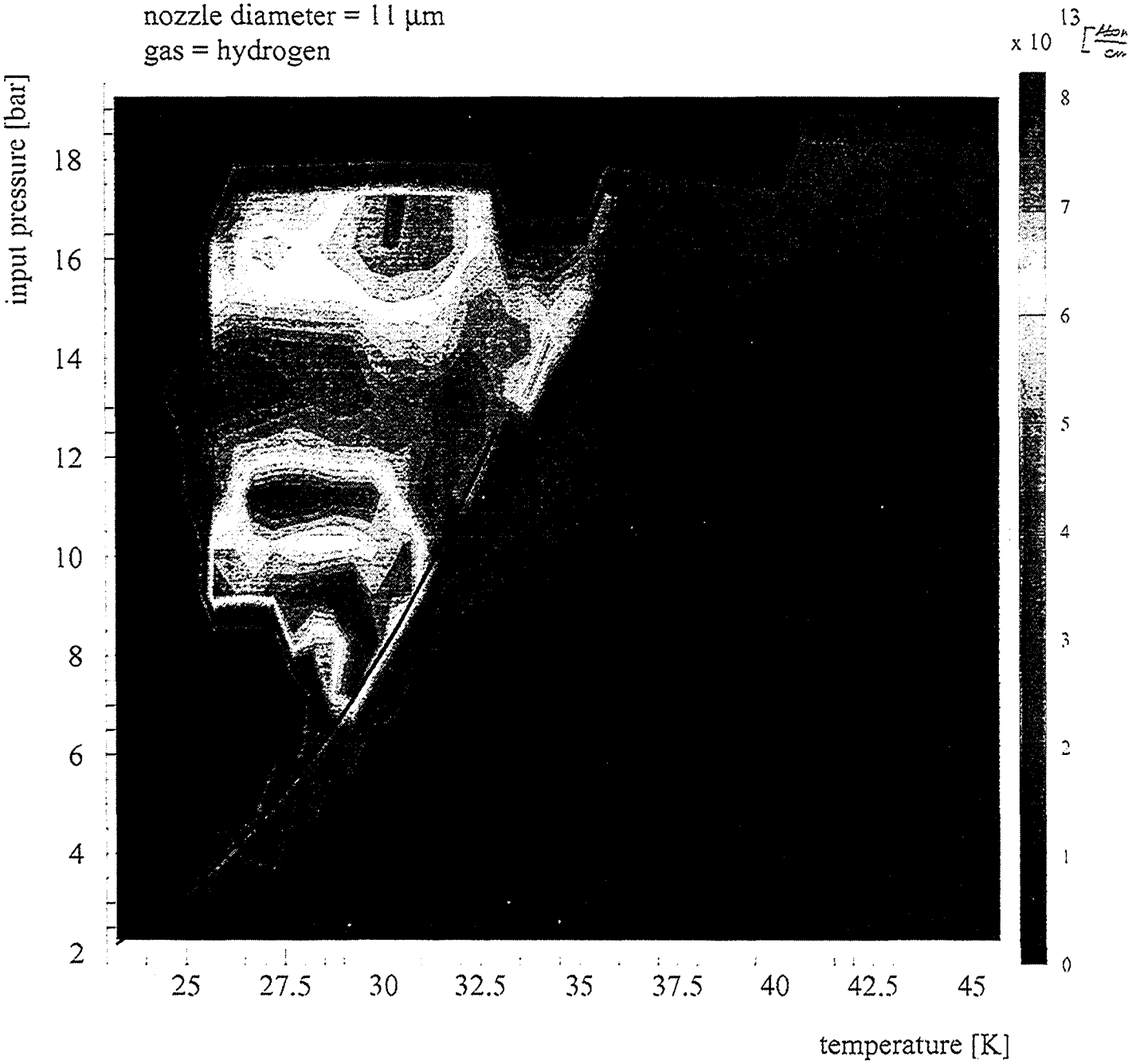

Device for Beam Dimension Measurement

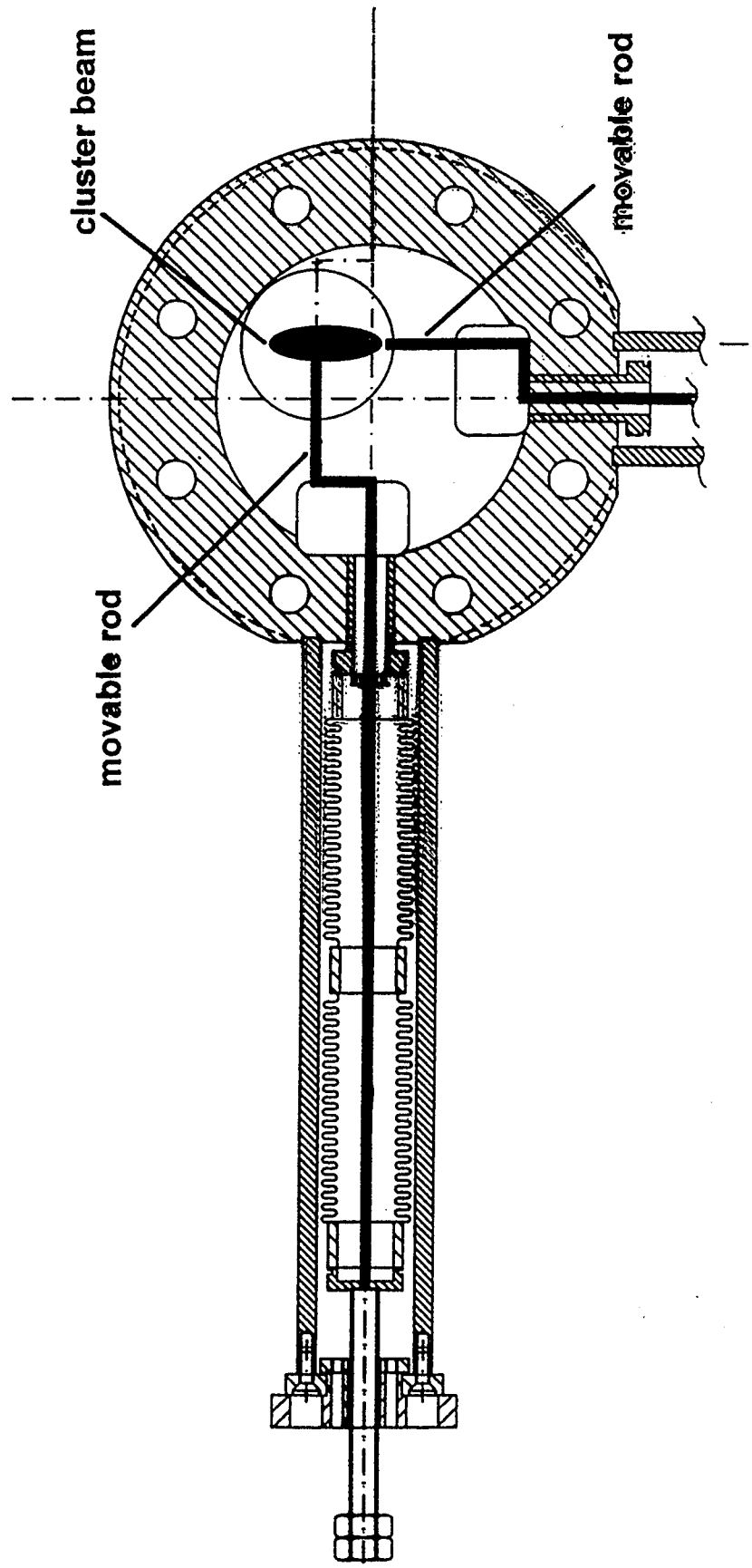

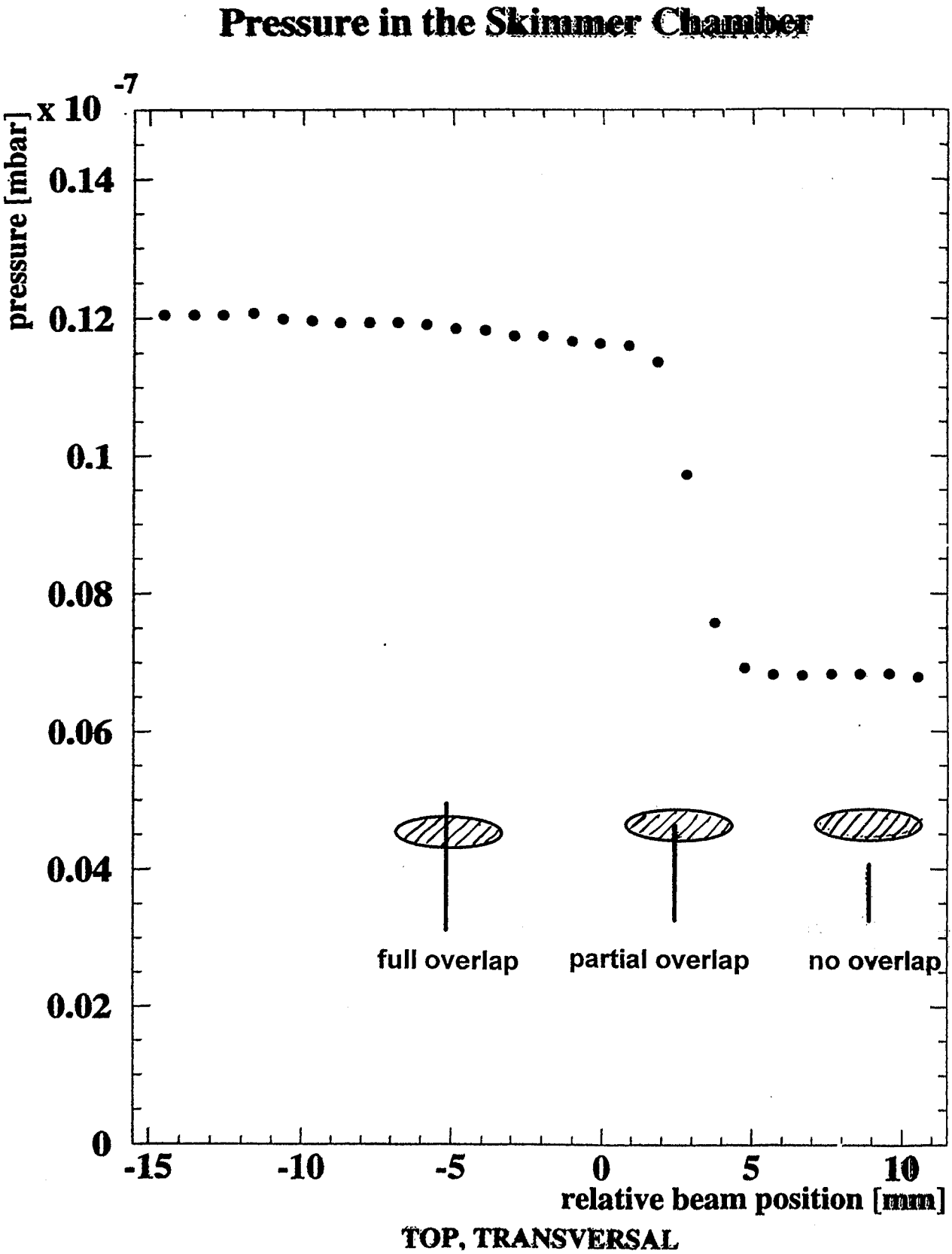
Pressure in the Skimmer Chamber
pressure [mbar]
x 10 -7
0.14
0.12
0.1
0.08
0.06
0.04
0.02
0
-15
-10
-5
0
5
10
relative beam position [mm]
full overlap
partial overlap
no overlap
TOP, TRANSVERSAL

Target Dimensions

- bottom,longitudinal: $\Delta y \approx 11{,}0$ mm
  $\Rightarrow \Delta y \approx 9{,}0$ mm in the scattering chamber
  offset $\approx$ -1,0 mm

- bottom,transversal: $\Delta x \approx 4{,}5$ mm
  offset $\approx 0{,}5$ mm

- top,transversal: $\Delta x \approx 2{,}5$ mm
  offset $\approx 3{,}0$ mm

- top longitudinal: not determined

Deuterium Recuperation System

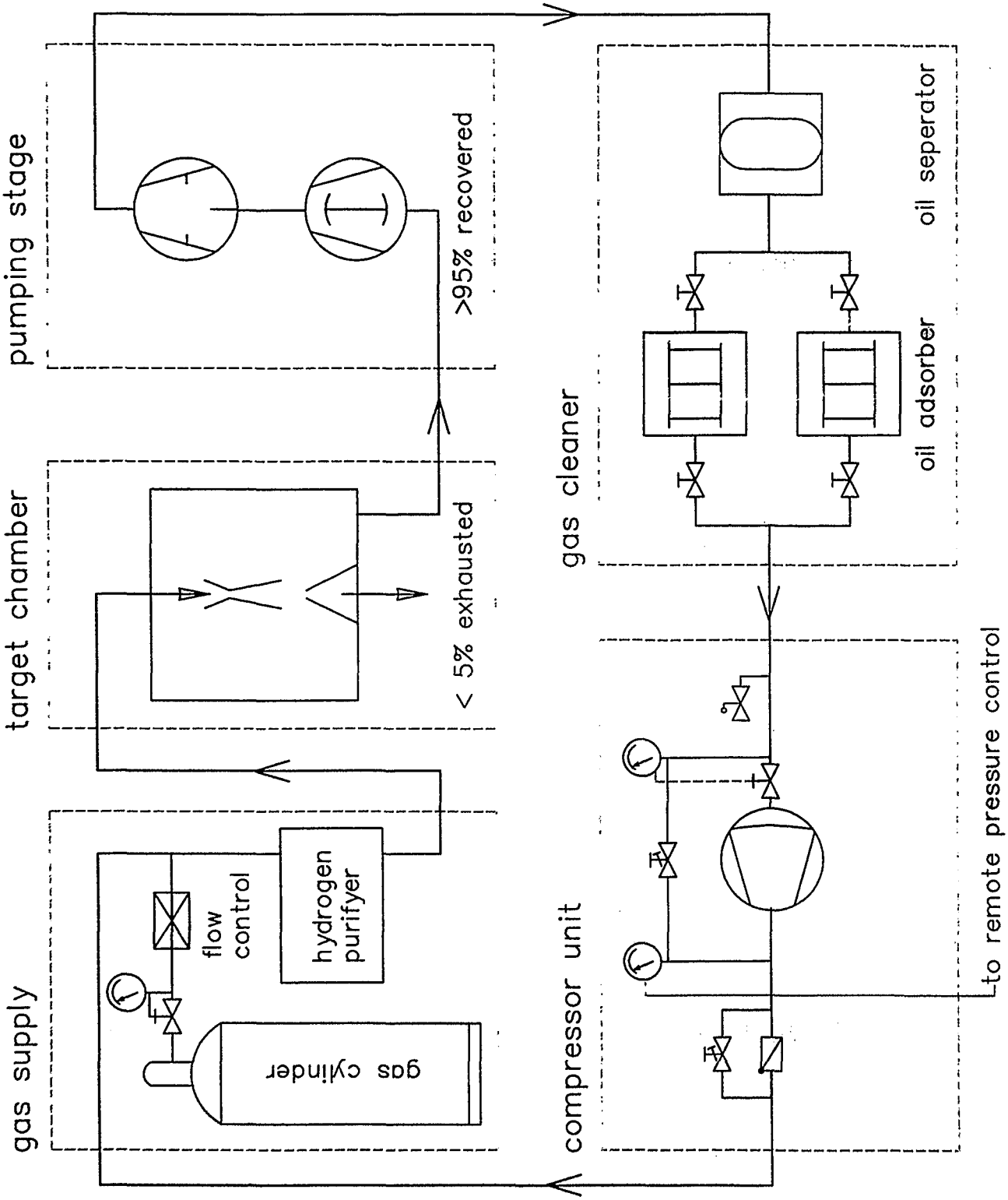

Parameters for Runs 1801,1823,1824

- beam momentum: p=1,0833 GeV/c
- excess energy ($pp \rightarrow d\pi^+$): Q=94,337 MeV
- deflection angle: φ=10,6°
- Field in D2: $B = 0,861$ T

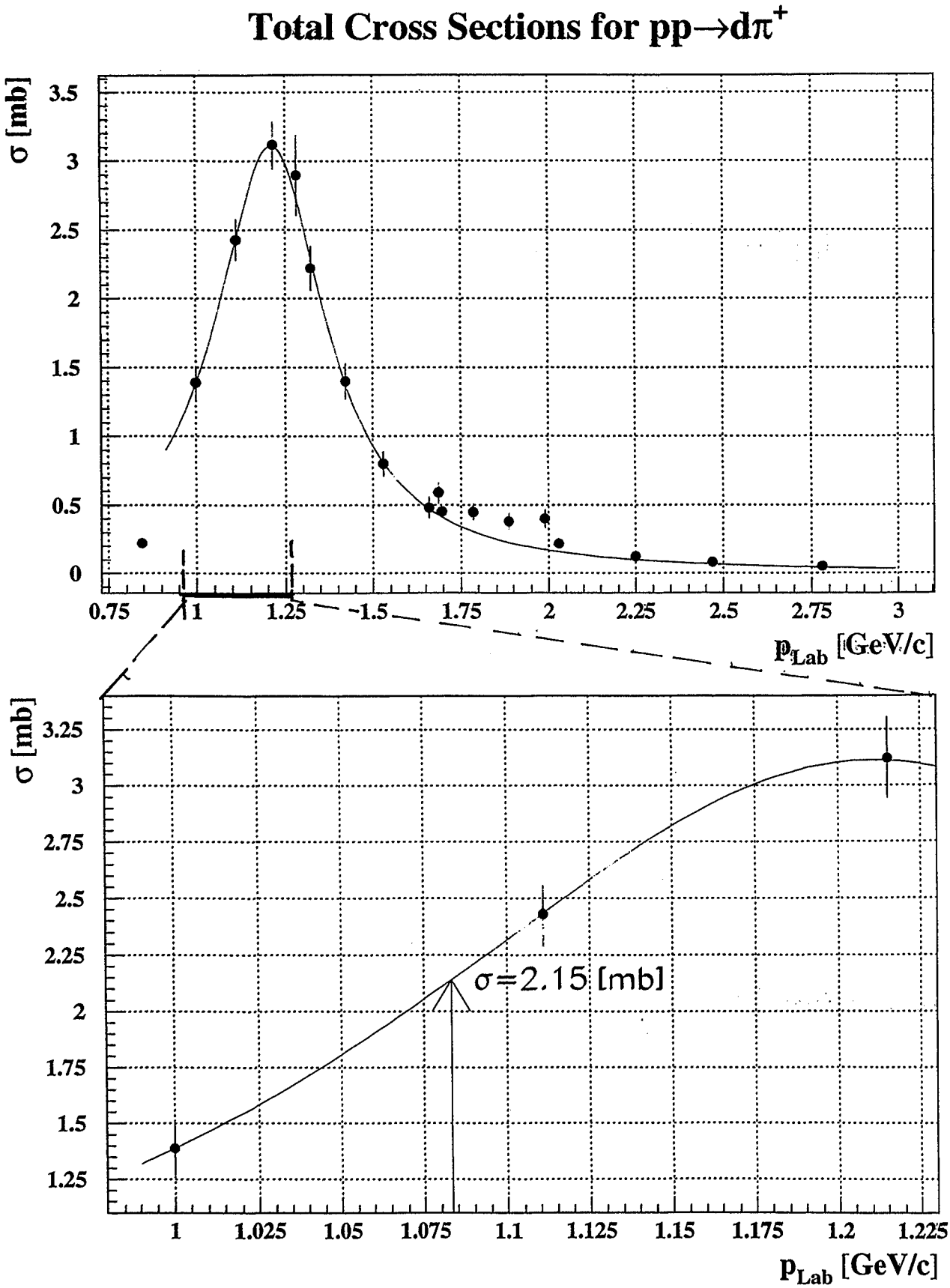
Total Cross Sections for pp→dπ+
σ [mb]
3.5
3
2.5
2
1.5
1
0.5
0
0.75
1
1.25
1.5
1.75
2
2.25
2.5
2.75
3
pLab [GeV/c]
σ [mb]
3.25
3
2.75
2.5
2.25
2
1.75
1.5
1.25
σ=2.15 [mb]
1
1.025
1.05
1.075
1.1
1.125
1.15
1.175
1.2
1.225
pLab [GeV/c]

Trajectories for the Reaction $pp \longrightarrow d\pi^+$

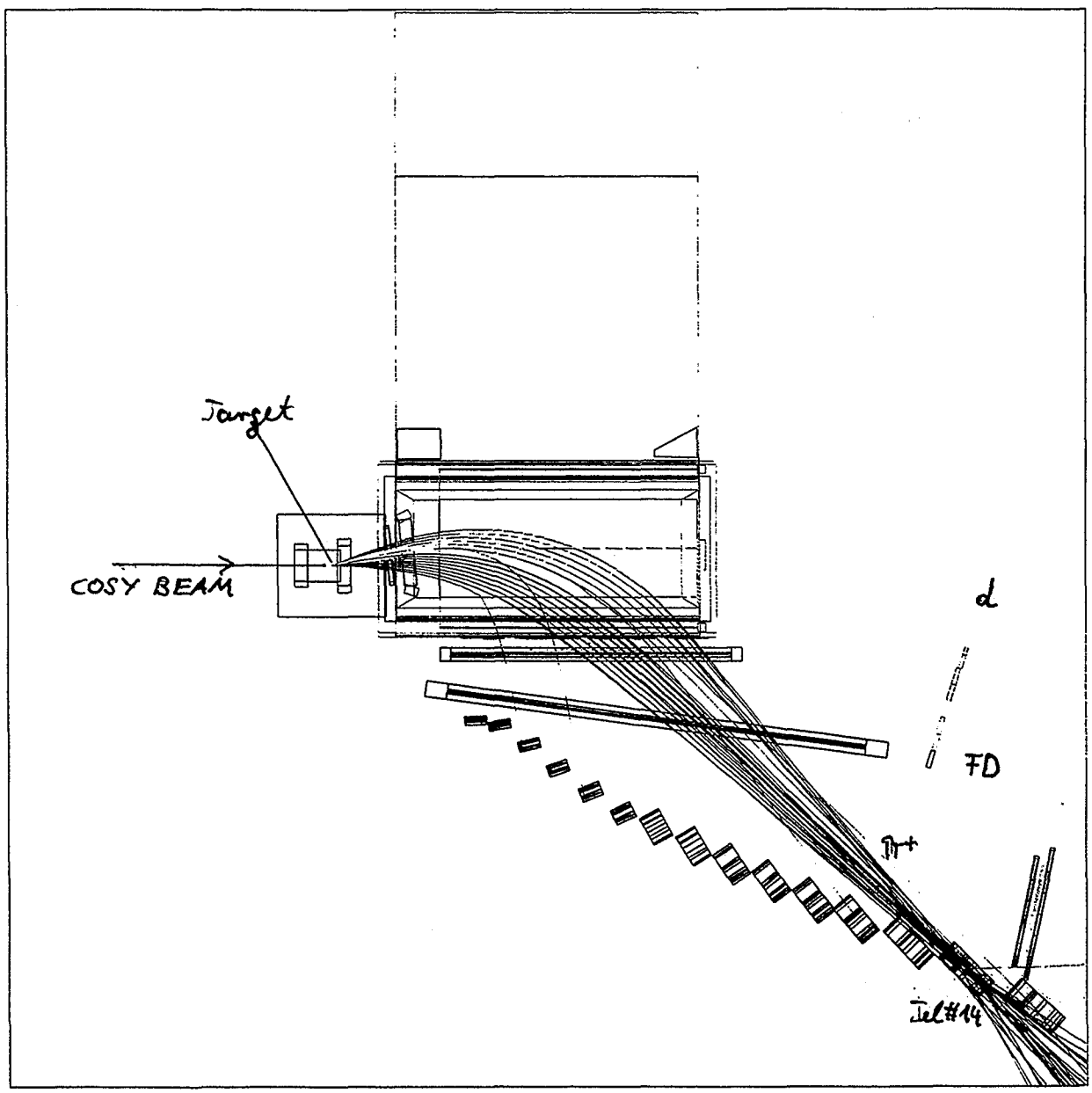

Hit Distribution For Run 1801

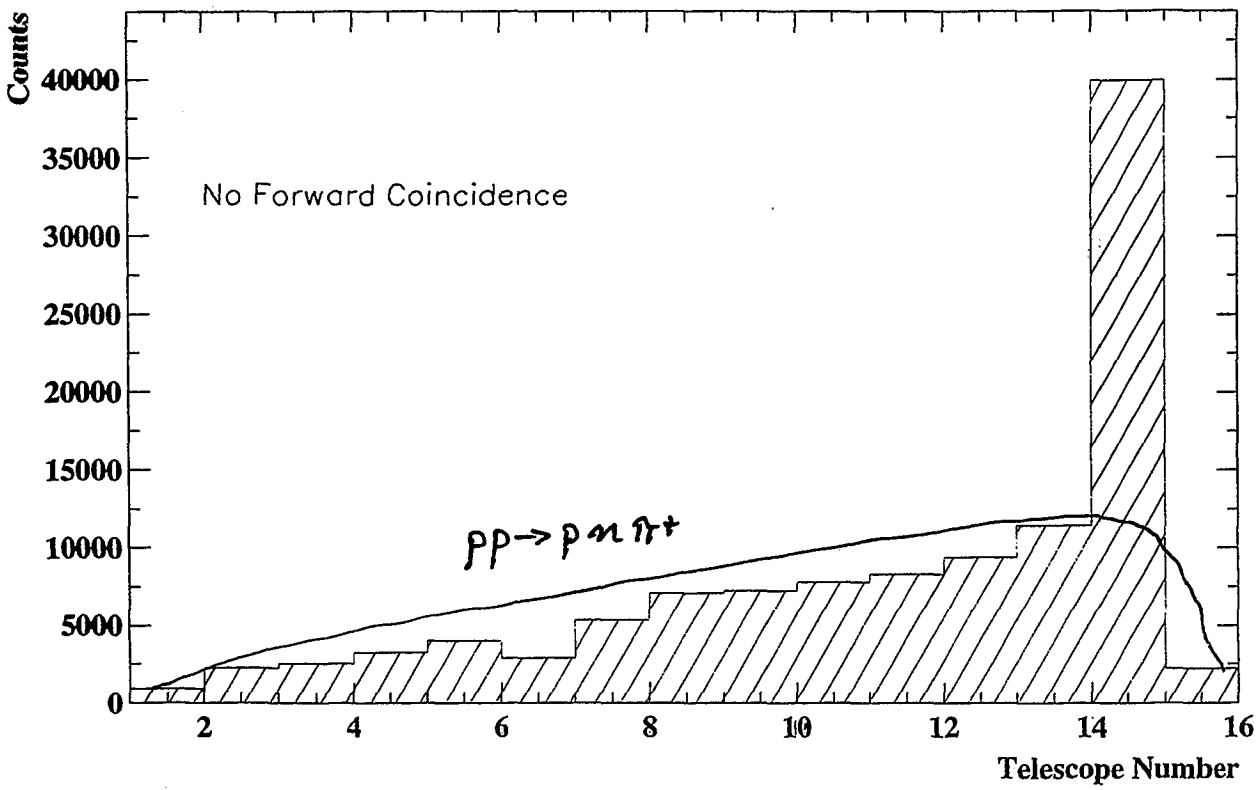

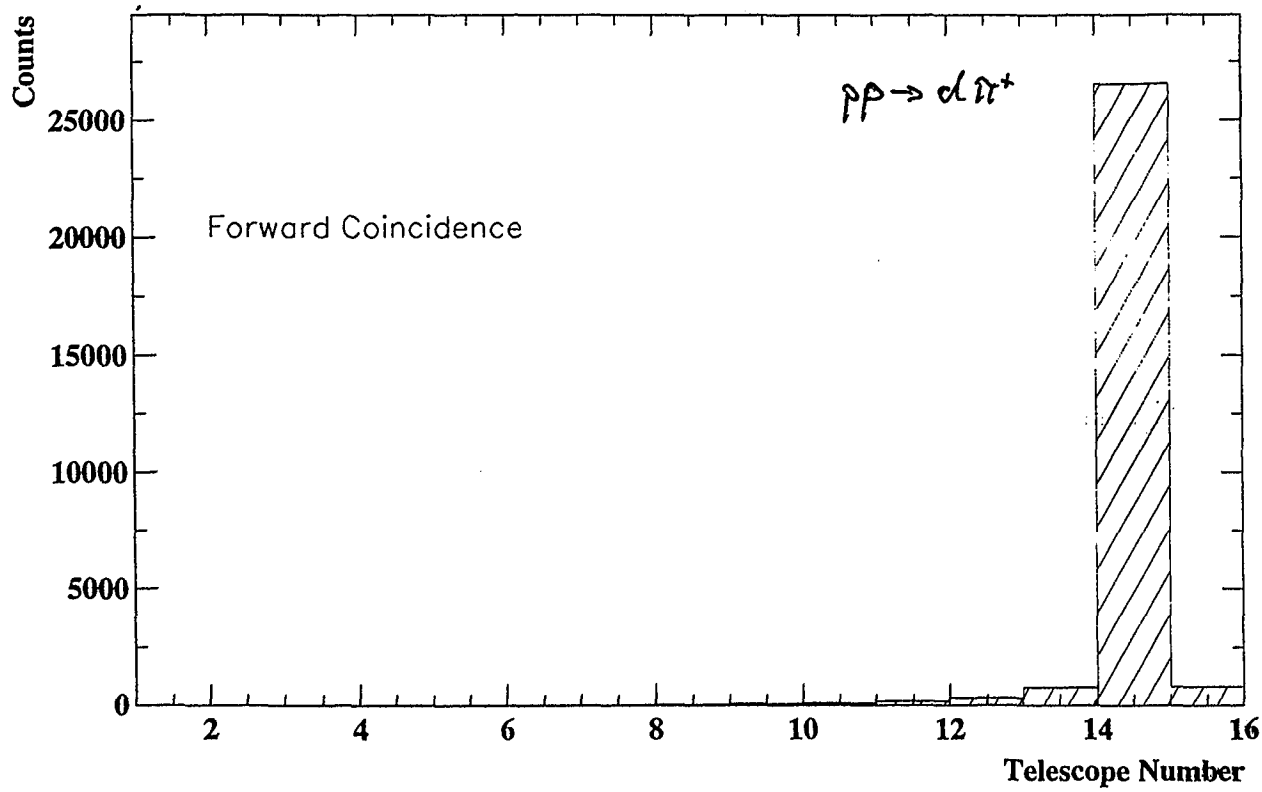

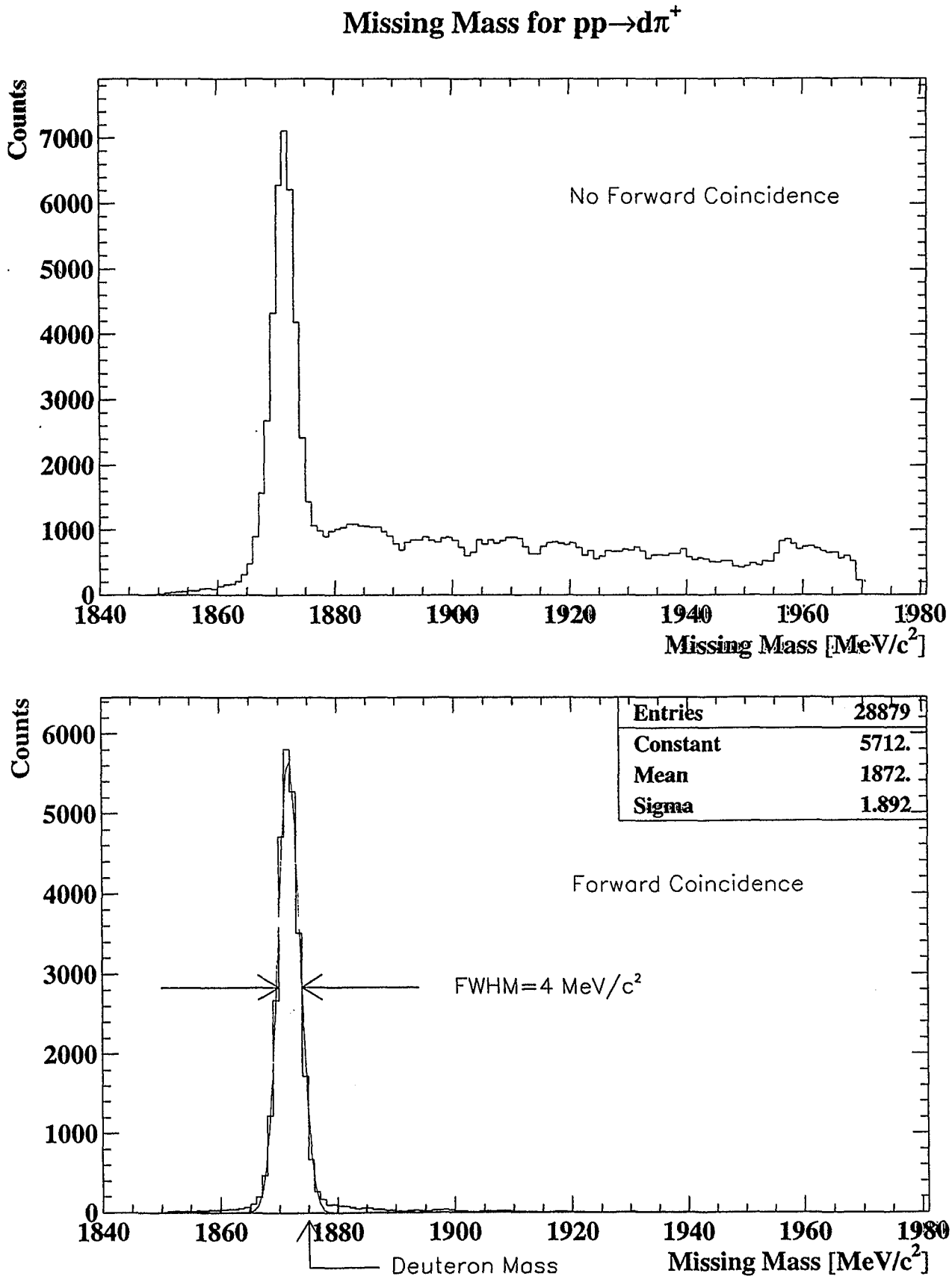
Missing Mass for pp→dπ+
Counts
No Forward Coincidence
Missing Mass [MeV/c2]
Entries 28879
Constant 5712.
Mean 1872.
Sigma 1.892
Forward Coincidence
FWHM=4 MeV/c2
Deuteron Mass
Missing Mass [MeV/c2]

Luminosity Determination for

$$pp \rightarrow d\pi^+$$

$$L = \frac{R}{\epsilon\ \sigma} \cdot \frac{1}{\eta\ \nu}$$

L = luminosity

R = counting rate

η = dead time factor

ν = detection efficiency

ϵ = acceptance

σ = total cross section

Lower Limit for Run 1801

$$
\begin{aligned}
R &= 1,057 \pm 1\% \quad [s^{-1}] \\
\eta &= 1 \text{ (yet undetermined)} \\
\nu &= 100\% \text{ (assumed)} \\
\epsilon &= (1.56 \pm 0.02)\% \\
\sigma &= 2,125 \pm 0.02 \quad [mb]
\end{aligned}
$$

$$
\Longrightarrow L = 3,3 \cdot 10^{28} [\frac{1}{cm^2 \cdot s}]
$$

Lower Limit for the Target Density

$$\rho = \frac{L}{f \cdot N_{COSY}}$$

ρ = target density
f = COSY frequency
N_{COSY} = number of protons in COSY

$f_{1801} = 1,2344$ MHz
$N_{COSY} = 7 \cdot 10^9$
$L = 3,3 \cdot 10^{28}$

if beam-target overlap = 100 %

$$\Rightarrow \rho_{1801} = 3,8 \cdot 10^{12} [\frac{atoms}{cm^2}]$$

in contradiction with target data

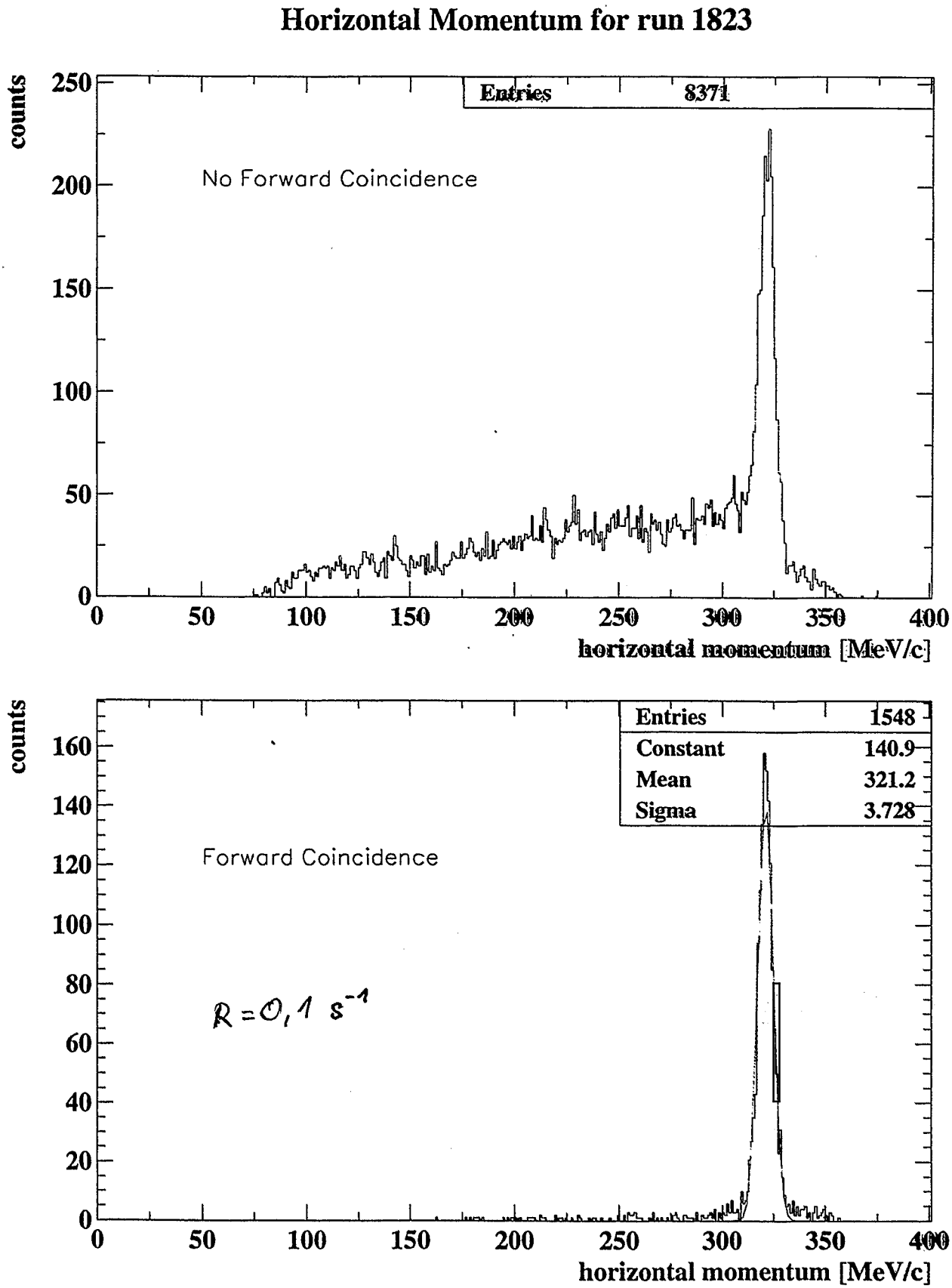
Horizontal Momentum for run 1823
counts
Entries 8371
No Forward Coincidence
horizontal momentum [MeV/c]
Entries 1548
Constant 140.9
Mean 321.2
Sigma 3.728
Forward Coincidence
R = 0,1 s⁻¹
counts
horizontal momentum [MeV/c]

DISCUSSION

reasons for low luminosity values

- beam target overlap too low, drifting COSY beam ?
- wrong acceptance from GEANT data ?
- wrong estimations for efficiency and dead-time ?

BUT ...

- excellent missing mass resolution
- stable target
- efficient background suppression

Status of the Forward Detector

V. Komarov

Joint Institute for Nuclear Research
141980 Dubna
Russia

The detector consists of three main parts:

- A two-layer hodoscope of scintillation counters (FH): 8 (and 9) counters in the layer;
- A set of MWPCs (three XY-strip packages)
- A Ĉerenkov counter hodoscope: one layer from 8 counters both in the upper and the lower half of the layer.

Amplitude calibration

The FH operates at ANKE for some time already and had been calibrated for the particle energy losses in the individual counters during the last beam-time (April/May 2000). The data at 0.5 GeV with and without D2 magnetic field, and at 2.0 GeV without the field have been used. Peaks caused by elastically scattered protons and the pp→dπ^+ deuterons are well seen in the amplitude spectra of the counter signals (figures 1,2). Existence of the peaks in the definite counters is in a good agreement with kinematics of the processes and the FH acceptance. The amplitude spectra have been "equalised", summed for the upper and lower PMTs, corrected after that for the rest vertical coordinate dependence. The corresponding energy depositions in the scintillators have been calculated by GEANT/Monte Carlo simulation. An example of the obtained dependences: QDC channel-deposited energy is shown in figure 3. Parameters of the approximating nonlinear curves are obtained and stored in a class-type code describing the calibration procedure. The code is available for data handling of each experiment using the FH. A similar procedure is recommended to develop for any other energy loss measuring scintillation counters at ANKE.

Luminosity measurement

If it is of a practical interest to learn to what accuracy the luminosity can be determined using only the data coming the FH alone. In this case the luminosity can be found rather immediately without the use of other detectors, therefore simplifying the procedure and avoiding additional uncertainties. Besides, the efficiency of the 1.5 cm - 2.0 cm thick scintillation counter is very close to 100%, and the small corrections can be neglected with a high accuracy. The only significant correction is caused by the dead-time of the data acquisition system but not the counters efficiency itself.

A simple formula for the luminosity calculation (figure 4) can be used for each counter individually to check consistency of the values obtained and therefore to get an estimate of the systematic error levels. Indeed, the individual counters cut off rather different parts of the angular-momentum acceptance of the setup (figure 5 illustrates that), and the differential cross section of the calibration processes also change significantly in the angular intervals covered by different counters (see figure 6, where hatching denotes the angular ranges accepted by FH). The cross sections calculated by the SAIDE code show high accuracy and reliability (Table 7 in figure 7). Figures 8,9 demonstrate the angular acceptance factors calculated by the GEANT/Monte Carlo simulation. The corresponding angles are shown at kinematical locuses in figure 10. Tables 2 - 8 show the experimental numbers obtained in several runs. In figure 13 the event distribution for one counter pair is shown at the plane deposited energy in the 1st layer versus the same in the second layer. The distribution shows that the most clean separation of the process is achieved for the low-momentum branch of the $pp \to d\pi^+$ process. Therefore, the luminosity values are shown in figure 12 right for these deuterons. It is seen that the values obtained in

any run the counters 2,3,4,5 are compatible with an accuracy of several percents. The average luminosity in the D2-off runs is systematically higher than in the D2-on ones in accordance with the known intensity of the COSY beam. The L values obtained for the high-momentum branch deuterons are consistent with the low-momentum results.

The $pp \rightarrow pp$ data systematically overestimate (at factor 2 - 4) the luminosity if all events in the proton peaks are assumed to be elastically scattered. It evidently indicates contamination by inelastically processes and nontarget background. Therefore, a clean separation of the pp-elastic events definitely requires the additional momentum analysis of the data.

Forward MWPCs at ANKE

Two packages of the FD MWPCs are mounted at ANKE at present. The third one, constructed and assembled in Dubna is ready now for delivering to Jülich in beginning of September. The first and second MWPCs for the first time operated with the electronics at ANKE in the April/May 2000 run. Their gas supply system at ANKE was not yet tuned at that time, so an efficiency close to 100% has only been achieved for the second package. The first one had a low efficiency of about 60%. One believes that the efficiency can only be improved by an accurate tuning of the gas supply.

Figures 14,15 demonstrate the opportunity for a permanent check of the chamber-efficiency properties during tuning of the chambers and data taking. The efficiency distribution over the sensitive surface of the chamber is obtained using the information from the both chamber packages and the FH counters during one of the runs.

Forward Čerenkov Detectors

Tests of the Čerenkov hodoscope have been started during the last beam time. It requires some obvious procedures to be done: choice of proper HV values, careful equalisation of the PMT amplifications, measurement of the detection efficiency for particle of different velocities and the dependence of the amplitude on the inclination angle. Therefore, only very preliminary results can be reported now. Nevertheless, these results reported by G. Macharashvili show strong differences of the amplitudes caused by protons of 2 GeV and 0.5 GeV energy. That is promising for the p/d separation in the momentum range near 2 GeV/c.

Status of the Forward Detector

1. Forward Hodoscope of the scintillation counters.
   - Amplitude calibration
   - Luminosity determination

2. Forward Multiwire Proportional Chambers

3. Forward Hodoscope of the Cherenkov counters

:0/05/26 18.22

Run 2715 Apr 00. Forward Hodoscope calibrated Amplitudes. 1 Layer

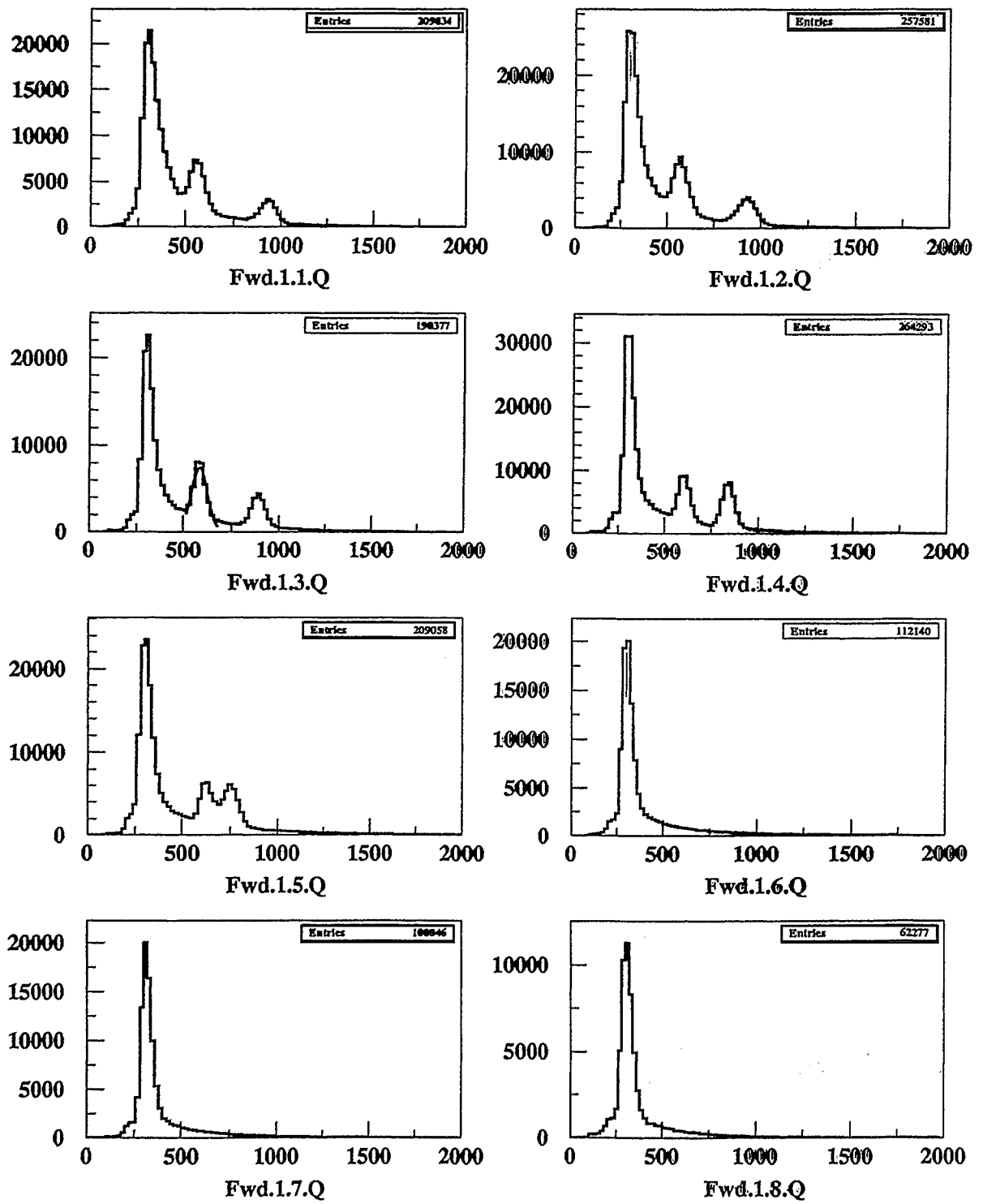

Fig.1

Apr 2000. Run 2683. Beam 500 MeV. D2-On. Target H-Cluster

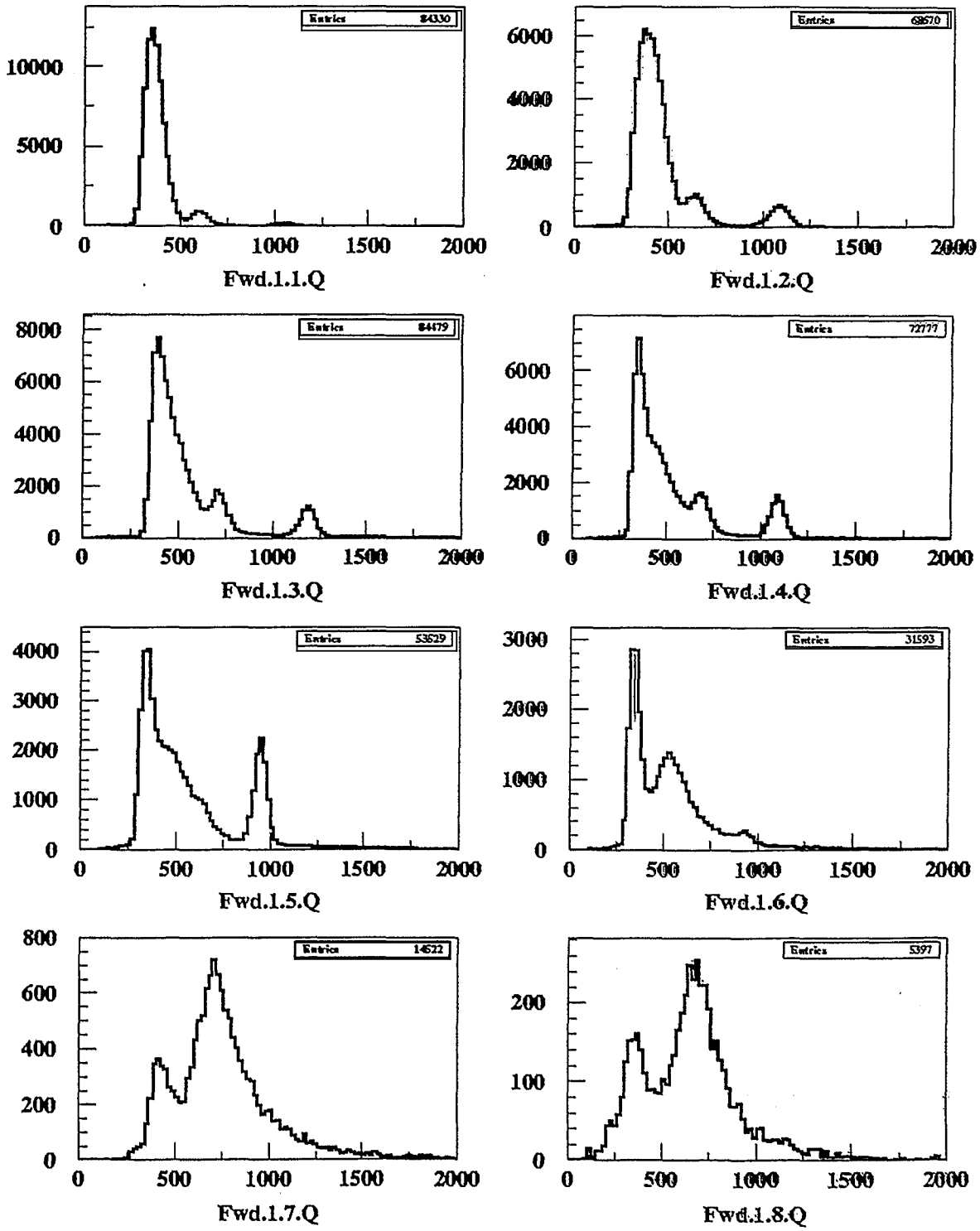

Fig. 2

Calibration Function For Forw Scintillation Counters

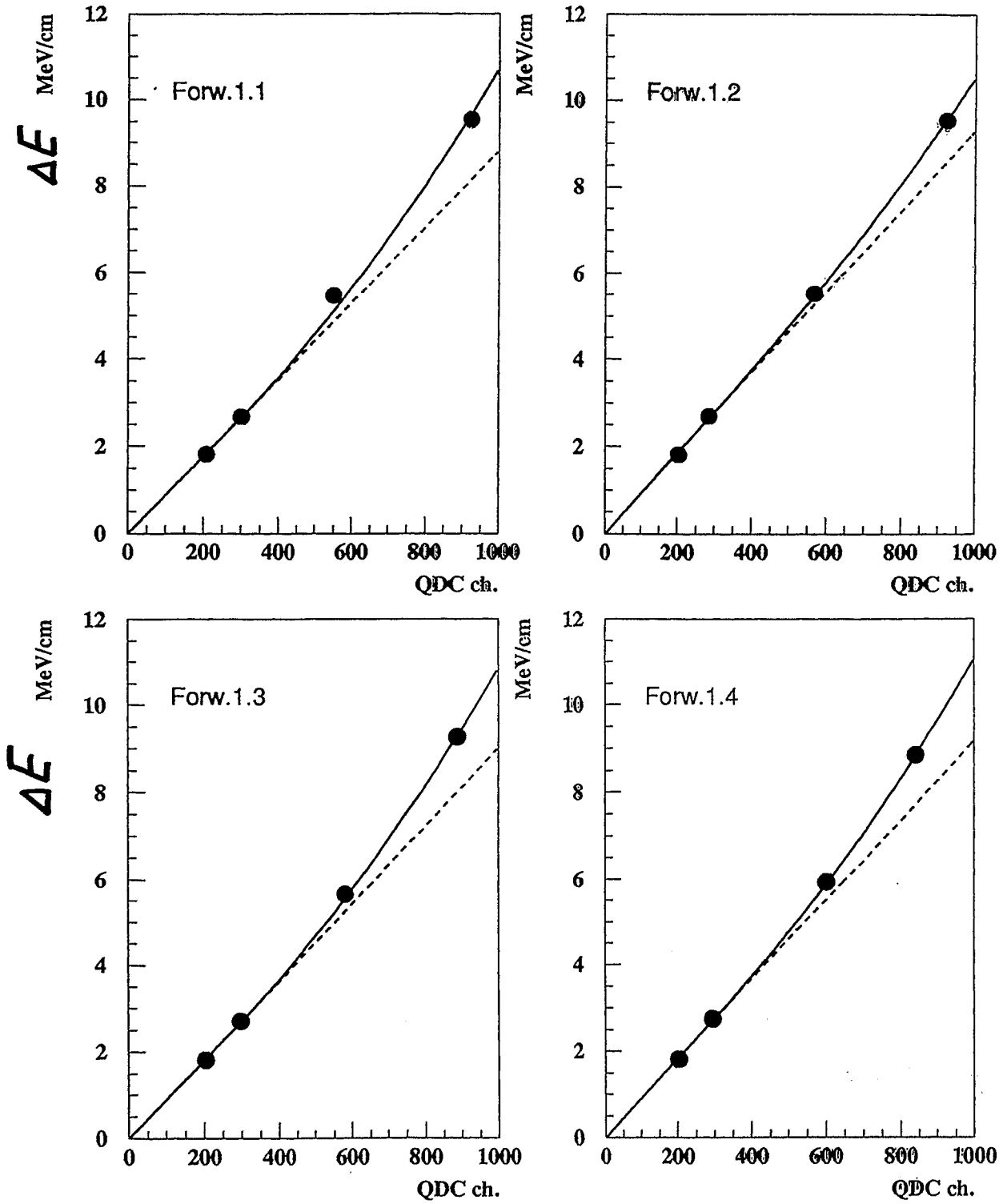

Fig. 3.

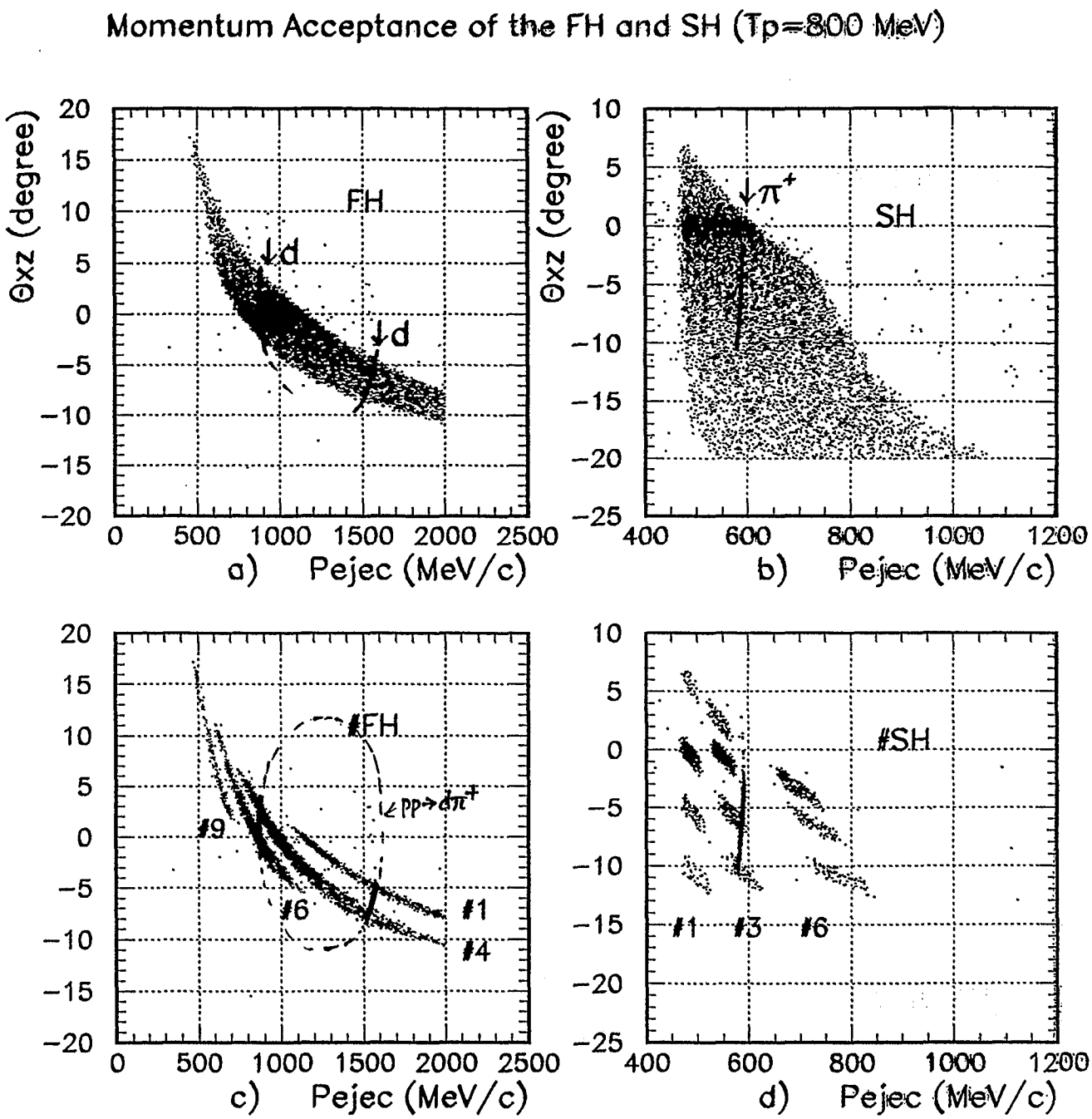
Momentum Acceptance of the FH and SH (Tp=800 MeV)
Θxz (degree)
FH
↓d
↓d
a) Pejec (MeV/c)
↓π+
SH
b) Pejec (MeV/c)
#FH
∠pp→dπ+
#9
#6
#1
#4
c) Pejec (MeV/c)
#SH
#1
#3
#6
d) Pejec (MeV/c)

Fig.5

Luminosity measurement with FH counters

$$L=(R/\varepsilon)\left[\int_{\Delta\Omega}\frac{d\sigma}{d\Omega}^{calib} d\Omega\right]^{-1}\simeq R/\varepsilon\left[2\pi\sum_i \frac{d\sigma}{d\Omega_i}^{calib}\Delta\Omega_i\frac{N_{det}^i}{N_0^i}\right]^{-1}$$

R – counting rate

ε – efficiency of registration (DAS dead-time)

$\frac{d\sigma}{d\Omega}^{calib}$ – dif. cross sect. of a calibration process

$\frac{N_{det}^i}{N_0^i}$ – angular acceptance factor

Calibration processes available: $pp\to d\pi^+$

$pp\to pp$

L can be found for the each counter of the Hodoscope to check compatibnce of the luminosity values obtained by use of different processes and counters.

Fig. 4.

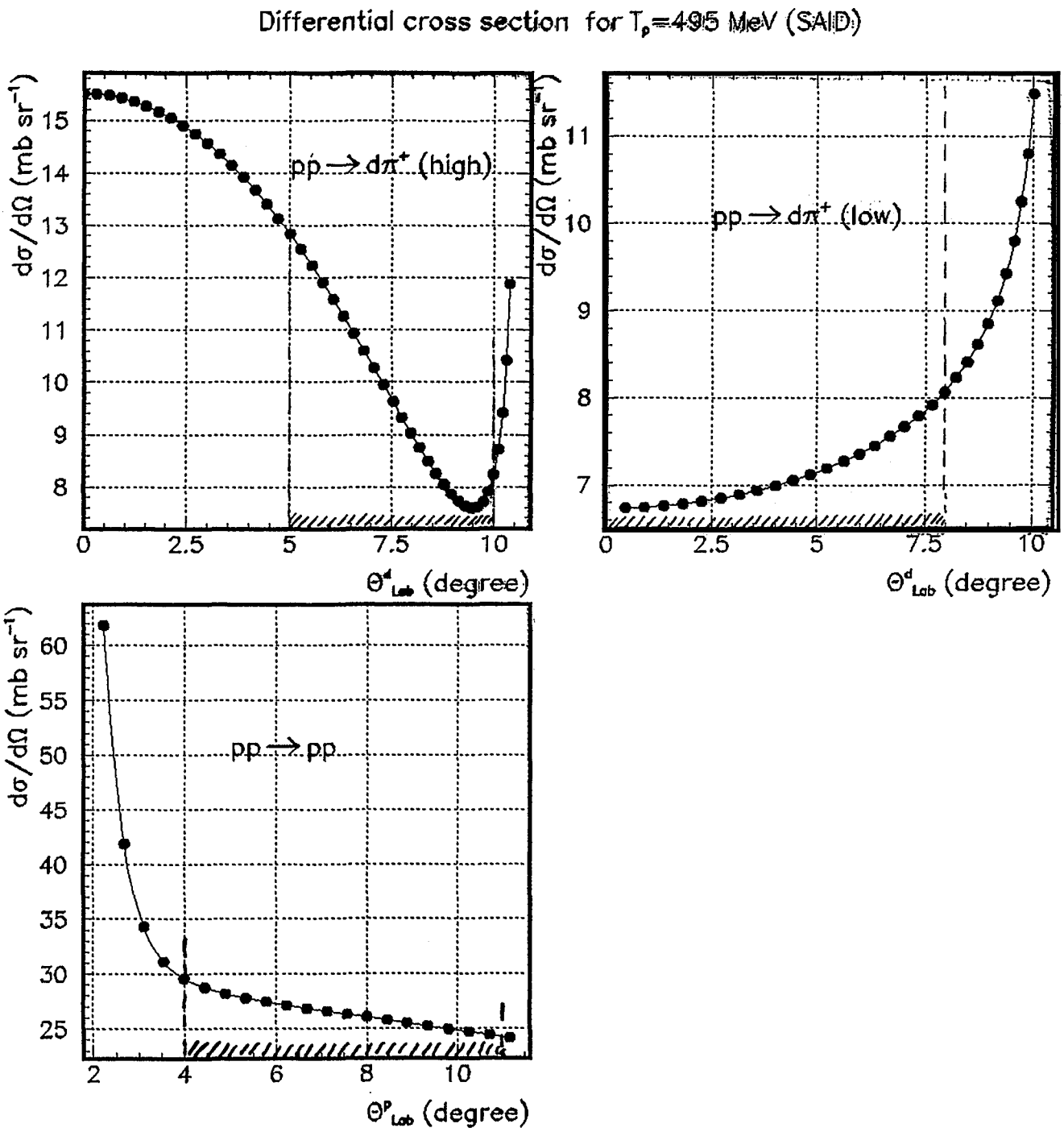
Differential cross section for T_p=495 MeV (SAID)
pp → dπ+ (high)
pp → dπ+ (low)
pp → pp
dσ/dΩ (mb sr⁻¹)
Θ^d_{Lab} (degree)
Θ^p_{Lab} (degree)

Fig. 6.

Table.5 Experimental Count Rate for $pp \rightarrow pp$ (D2 on)

Run	# FH1	$N_i^d \pm \Delta N$ (Exp.)	Δt (s)	R_i (s^{-1})	$\bar{R}_i$ (s^{-1}) (corr.)
2683	1	$79,532 \pm 00$	8,357	9.52	52.93
	2	$54,500 \pm 00$	8,357	6.52	36.25
	3	$63,720 \pm 00$	8,357	7.62	42.37
2684	1	$72,581 \pm 00$	9,107	7.97	41.56
	2	$54,800 \pm 00$	9,107	6.02	31.39
	3	$63,490 \pm 00$	9,107	6.97	36.35
2685	1	$56,010 \pm 00$	6,757	8.29	42.55
	2	$39,940 \pm 00$	6,757	5.91	30.34
	3	$44,840 \pm 00$	6,757	6.64	34.08

Table.6 Experimental Count Rate for $pp \rightarrow pp$ (D2 off)

Run	# FH1	$N_i^d \pm \Delta N$ (Exp.)	Δt (s)	R_i (s^{-1})	R_i (s^{-1}) (corr.)
2715	1	$461,300 \pm 00$	15,936	28.95	35.14
	2	$562,100 \pm 00$	15,936	35.30	42.85
	3	$623,576 \pm 00$	15,936	39.13	47.50
2721	1	$539,600 \pm 00$	24,986	21.60	23.48
	2	$663,330 \pm 00$	24,986	26.55	28.86
	3	$727,093 \pm 00$	24,986	29.10	31.63
2722	1	$235,400 \pm 00$	10,754	21.89	23.77
	2	$285,500 \pm 00$	10,754	26.55	28.83
	3	$317,243 \pm 00$	10,754	29.50	32.04

Table.7 Differential cross section.

process	E_π (MeV)	$\theta_\pi^{c.m.}$	$d\sigma/d\Omega$ ($\frac{mb}{sr}$) /SAID/	$d\sigma/d\Omega$ ($\frac{mb}{sr}$) /Exp./
$\pi^+ d \rightarrow pp$	110	168.3	3.649 /SP96/	$3.746 \pm 0.006(0.2\%)$
	110	168.3	3.538 /C500/	Phys.Rev C27,
	110	168.3	3.594 /average/	(1983), p.1685
$\pi^+ d \rightarrow pp$	95	168.3	3.317 /SP96/	$3.063 \pm 0.038(1.2\%)$
	95	168.3	3.225 /C500/	Phys.Rev C27,
	95	168.3	3.271 /average/	(1983), p.1685
process	E_p (MeV)	$\theta_\pi^{c.m.}$	$d\sigma/d\Omega$ ($\frac{mb}{sr}$) /SAID/	$d\sigma/d\Omega$ ($\frac{mb}{sr}$) /Exp./
$pp \rightarrow d\pi^+$	516	18.43	0.3875 /SP96/	$0.3812 \pm 0.0053(1.4\%)$
	516	18.43	0.3770 /C500/	Nucl.Phys A402,
	516	18.43	0.3823 /average/	(1983), p.429

Fig.7

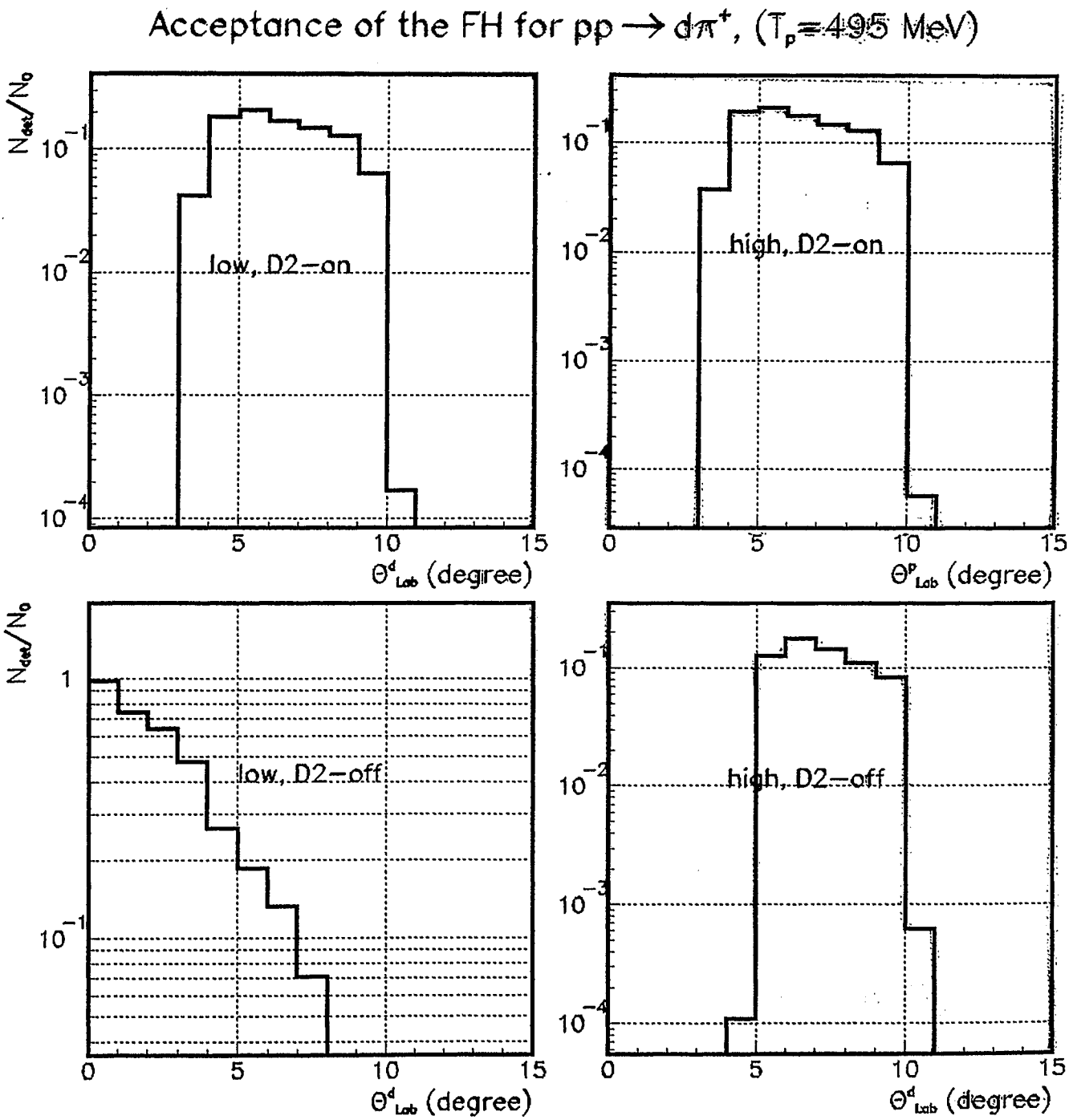
Acceptance of the FH for pp → dπ+, (Tp=495 MeV)
Ndet/N0
low, D2−on
high, D2−on
low, D2−off
high, D2−off
Θd Lab (degree)
Θp Lab (degree)

Fig. 8

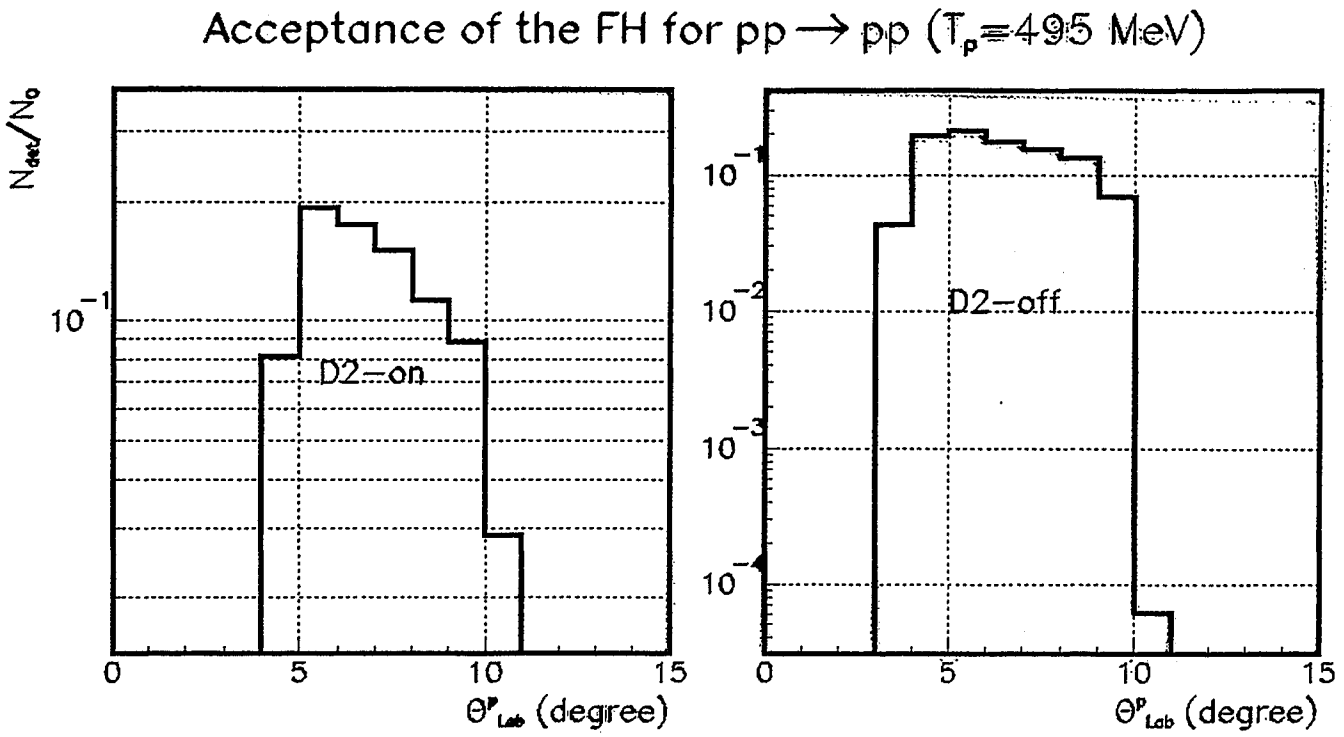
Acceptance of the FH for pp → pp (T_p=495 MeV)
N_det/N_0
10^-1
D2=on
0
5
10
15
θ^p_Lab (degree)
10^-1
10^-2
10^-3
10^-4
D2=off
0
5
10
15
θ^p_Lab (degree)

Fig.9

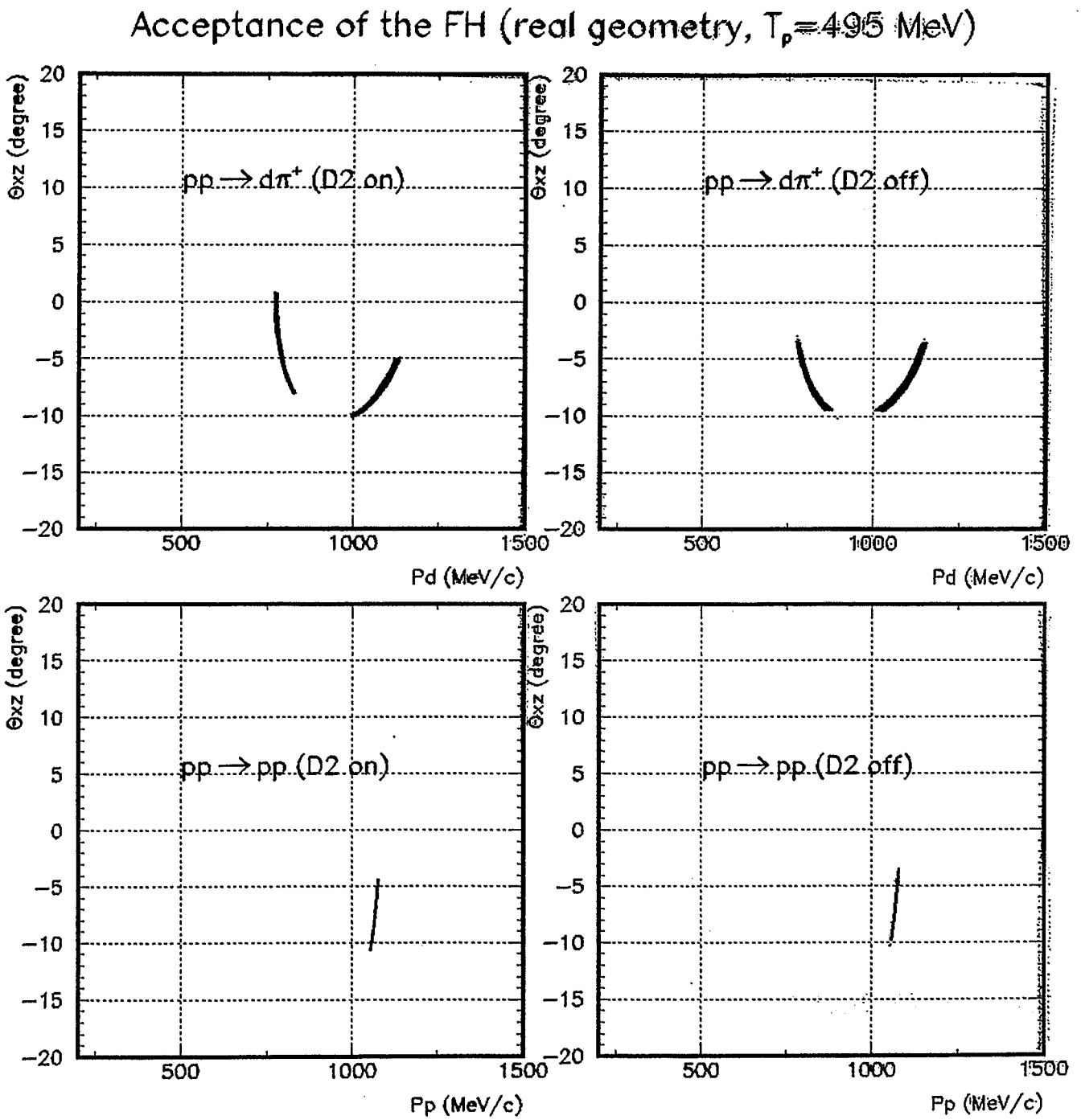
Acceptance of the FH (real geometry, T_p=495 MeV)
pp → dπ+ (D2 on)
pp → dπ+ (D2 off)
pp → pp (D2 on)
pp → pp (D2 off)
θxz (degree)
Pd (MeV/c)
Pp (MeV/c)

Fig.10.

Table.2 FD Trigger in / Trigger out (Tp=495 MeV, H_2 target)

Run	$D2$	$I(10^9)$	Trig in	Trig out	True ev.	$f_{dt} = \frac{T_{in}}{T_{out}}$	$\frac{T_{out}}{True_{ev}}$
2683	on	13.0	2,367,453	1,937,480	425,490	1.222	4.55
2684	on	15.0	2,009,643	1,716,702	385,880	1.171	4.45
2685	on	12.0	1,531,009	1,306,074	298,450	1.172	4.38
2715	off	26.0	6,410,710	5,816,457	5,714,400	1.102	1.02
2721	off	26.0	7,727,195	7,178,936	7,095,700	1.076	1.01
2722	off	26.0	3,330,598	3,097,969	3,062,000	1.075	1.01

Table.3 Experimental Count Rate for $pp \rightarrow d\pi^+$ (D2 on, low)

Run	# FH1	$N_i^q \pm \Delta N$ (Exp.)	Δt (s)	R_i (s^{-1})	R_i (s^{-1}) (corr.)
2683	1	1102 ± 47	8,357	0.132	0.734
	2	4137 ± 79	8,357	0.495	2.752
	3	5579 ± 90	8,357	0.668	3.714
	4	6492 ± 97	8,357	0.777	4.320
	5	8547 ± 115	8,357	1.023	5.688
2684	1	958 ± 42	9,107	0.105	0.548
	2	3671 ± 72	9,107	0.403	2.102
	3	4838 ± 84	9,107	0.531	2.769
	4	5378 ± 87	9,107	0.591	3.082
	5	7616 ± 132	9,107	0.836	4.360
2685	1	514 ± 38	6,757	0.076	0.390
	2	2447 ± 63	6,757	0.362	1.858
	3	3415 ± 74	6,757	0.505	2.592
	4	4274 ± 73	6,757	0.632	3.244
	5	5276 ± 83	6,757	0.781	4.010

Table.4 Experimental Count Rate for $pp \rightarrow d\pi^+$ (D2 off, low)

Run	# FH1	$N_i^q \pm \Delta N$ (Exp.)	Δt (s)	R_i (s^{-1})	R_i (s^{-1}) (corr.)
2715	1	$47,061 \pm 393$	15,936	2.95	3.58
	2	$71,072 \pm 464$	15,936	4.46	5.42
	3	$100,790 \pm 521$	15,936	6.32	7.67
	4	$111,314 \pm 524$	15,936	6.98	8.47
2721	1	$74,967 \pm 415$	24,986	3.00	3.26
	2	$112,902 \pm 522$	24,986	4.52	4.91
	3	$159,890 \pm 599$	24,986	6.40	6.96
	4	$178,339 \pm 626$	24,986	7.14	7.76
2722	1	$32,660 \pm 274$	10,754	3.04	3.30
	2	$47,545 \pm 349$	10,754	4.42	4.80
	3	$67,191 \pm 394$	10,754	6.25	6.79
	4	$76,355 \pm 411$	10,754	7.10	7.71

Fig.11.

Table.8 Detected cross sections ($\sigma_{det} \cdot 10^{-3}$ (mb)) for deuterons and protons.

process	# FH1	low (D2 on)	high (D2 on)	low (D2 off)	high (D2 off)
$pp \rightarrow d\pi^+$	1	6.43	16.64	10.93	21.28
	2	17.04	22.60	18.03	30.25
	3	24.09	24.48	25.26	37.72
	4	26.20	19.18	27.58	29.36
	5	37.58	-	-	-

process	# FH1	D2 on	D2 off
$pp \rightarrow pp$	1	44.94	48.76
	2	63.07	68.15
	3	88.05	87.99
	4	86.65	88.03
	5	12.68	32.66

Table.9 Luminosity (L $\cdot 10^{29}$ ($\frac{1}{cm^2 \cdot s}$))

process	#	Run2715 D2 off	Run2721 D2 off	Run2722 D2 off	Run2683 D2 on	Run2684 D2 on	Run2685 D2 on
$pp \rightarrow d\pi^+$	1	3.27	2.98	3.02	1.14	0.85	0.61
(low)	2	3.01	2.72	2.66	1.61	1.23	1.09
	3	3.03	2.75	2.69	1.54	1.15	1.08
	4	3.07	2.81	2.79	1.65	1.18	1.23
	5	-	-	-	1.51	1.16	1.07
$pp \rightarrow pp$	1	7.21	4.82	4.88	11.8	9.25	9.47
	2	6.29	4.23	4.23	5.74	4.98	4.81
	3	5.40	3.59	3.64	4.81	4.13	3.87

Fig. 12

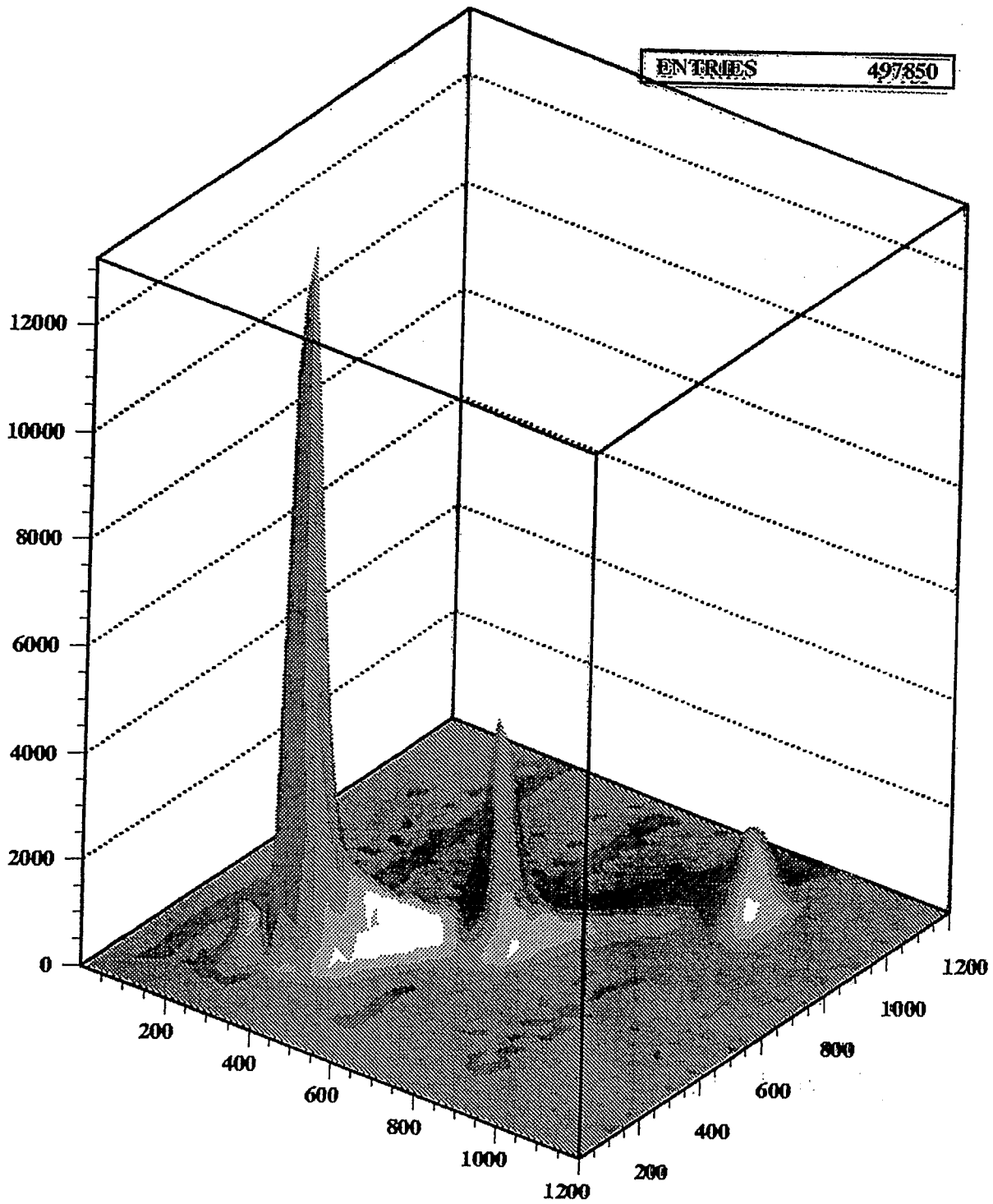
ENTRIES 497850
12000
10000
8000
6000
4000
2000
0
200
400
600
800
1000
1200
200
400
600
800
1000
1200
e1 vs e2 for 3-3

Fig. 13.

2000/07/10 11.03

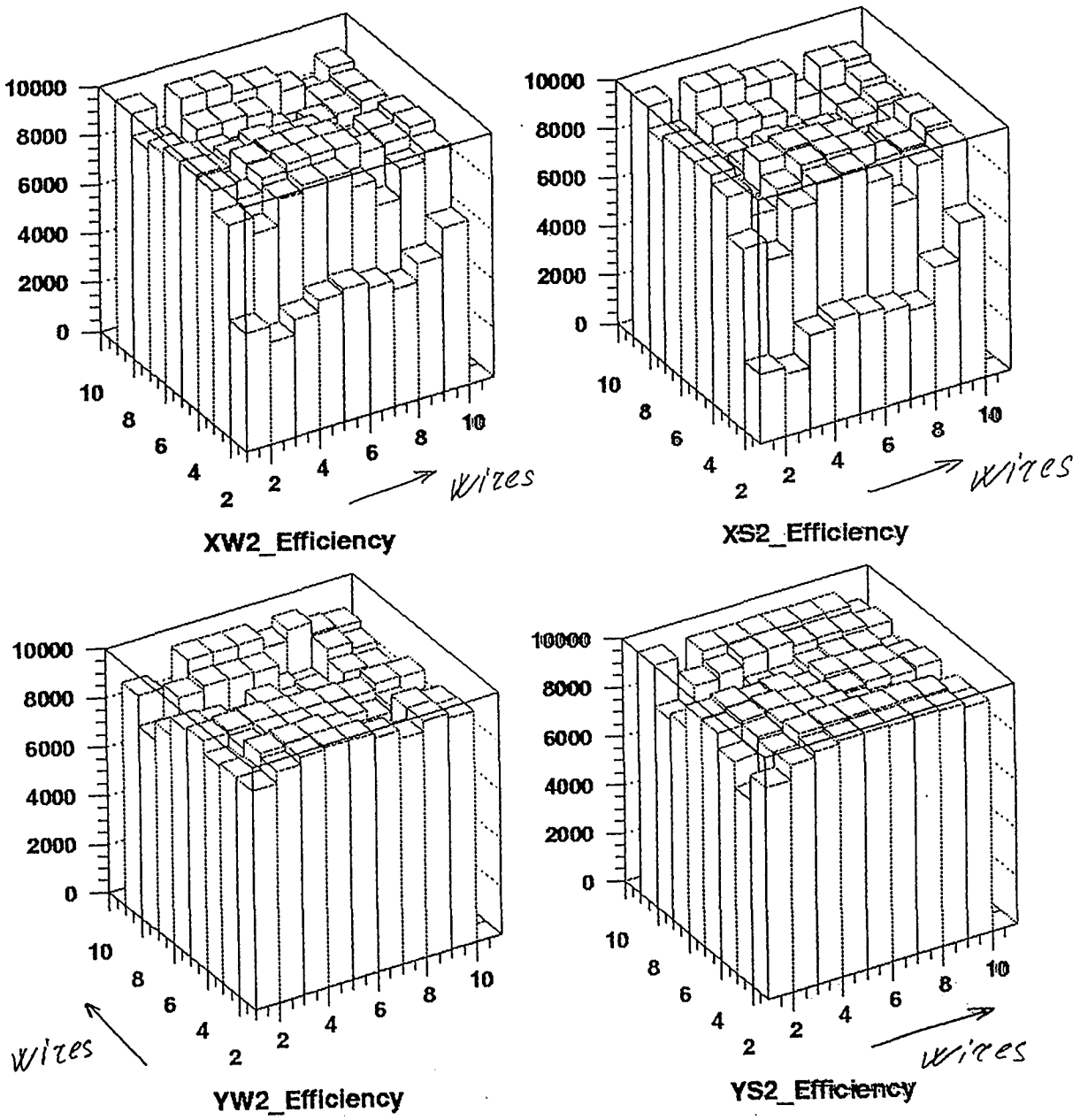

Fig.14.

2000/07/10 11.02

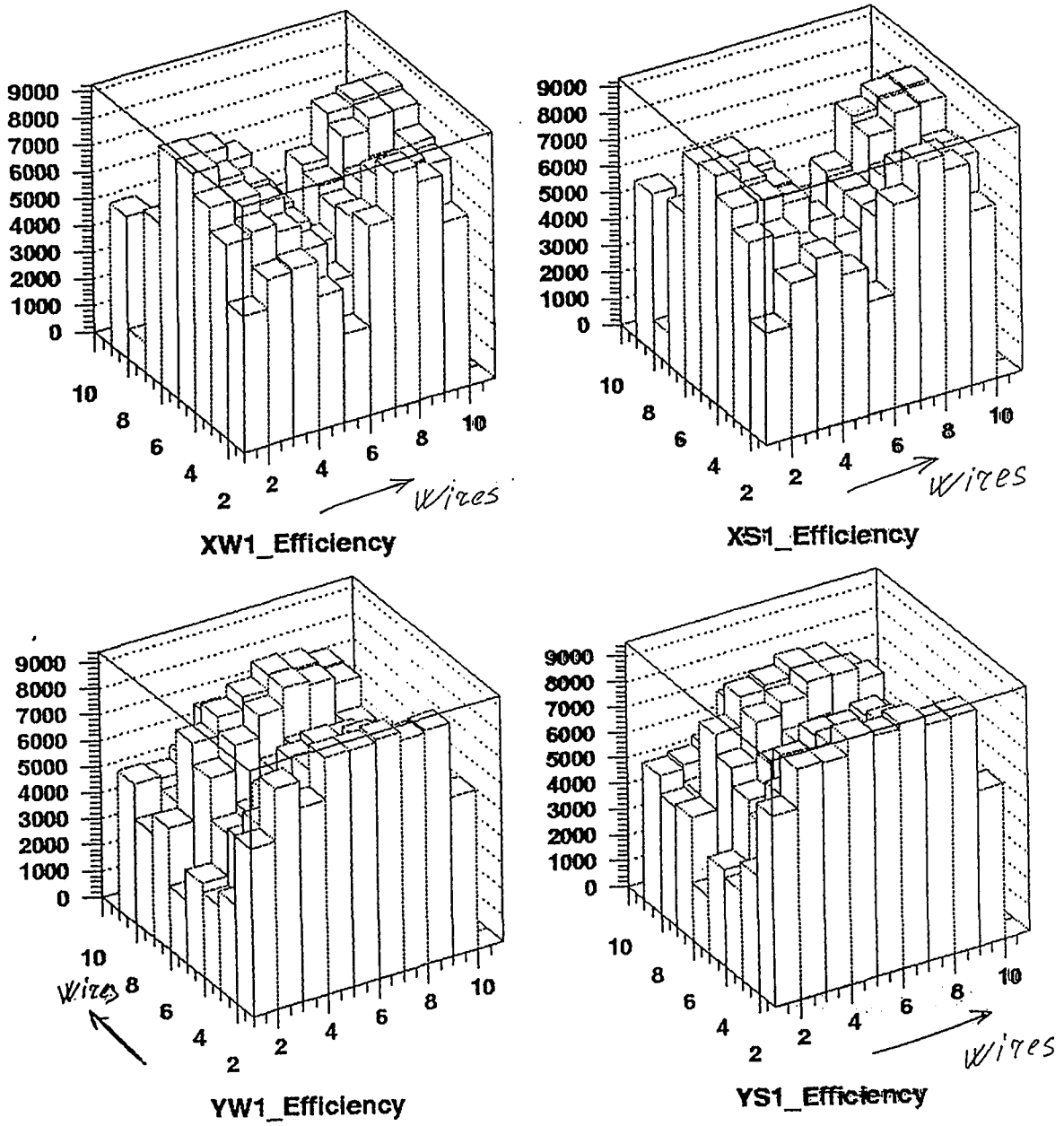

Fig.15.

The Čerenkov Detectors in Forward Direction

C. Leim

Institut für Kernphysik
Forschungzentrum Jülich
52425 Jülich
Germany

The Čerenkov detectors which are part of the detection system in forward direction (i.e. for fast particles) were installed behind the scintillators to separate between deuterons and protons. They were developed in Dubna and Tbilisi, and test data have been accumulated and partially analysed. My task was and will be to perform simulations to estimate the detector behaviour.

Detector Layout

One module consists of two cubes of lucite (n=1.491) which are not connected, each with a photomultiplier attached to one end (see transparency 2). In total there are 8 of such pairs. An important feature is that the detectors can be inclined under some angle θ.

Basic Principles

The Čerenkov effect is well known: If a particle in a medium travels faster than the speed of light in that medium, light is emitted on a cone with an opening angle solely depending on the velocity of the particle and the index of refraction of the material: $\cos\vartheta_{\check{C}} = \frac{1}{\beta n}$. The angle of total reflection (TR) at the backside of the material is determined by the index of refraction alone: $\sin\vartheta_R = \frac{1}{n}$. If a fast particle with $\vartheta_{\check{C}} > \vartheta_R$ enters the detector perpendicular to the surface, the Čerenkov light will be reflected at the backside and after several reflections reach the PM, whereas light from a slow particle ($\vartheta_{\check{C}} < \vartheta_R$) will the leave the detector. Thus, the best case would be: all light from the fast particle reaches the PM, all light from the slow one does not. If $\vartheta_{\check{C}}$ is close to or smaller than ϑ_R, the detectors can be inclined to optimise the separation. If we do so, the Čerenkov-cone is shifted relative to the TR cone, so more photons will be reflected and therefore detected. In principle, this can be used to attenuate light from slower and intensify light from faster particles (lower right corner on transparency 3), if one tunes the angle so that one side of the TR-cone (in an 2D-picture, see transparency 4) lies in between the Čerenkov-cones: $\vartheta_{\check{C}_{slow}} < \vartheta_R < \vartheta_{\check{C}_{fast}}$.

Experimental Setup

The momenta of the deuterons will be 1.9 to 2.3 GeV/c. Transparency 5 shows the Čerenkov-angles of p and d depending on the momentum and the (constant) angle for TR. In the relevant region, light from the deuterons is not reflected, while the Čerenkov-angle of the protons is close to the threshold: for p > 1.95 GeV/c, photons will be reflected. Because of this, effects like vertical smearing (causing different entry angles for the particle) and the broader momentum distribution of the protons (including momenta < 1.95 GeV/c) could have a big effect on whether we get a signal from the proton or not. Thus, the detector must be inclined to shift the angle of the proton-Čerenkov-light to a region where it will be reflected completely. Note that the vertical spread is not huge, only around 3 to 4 degrees, as can be seen in transparency 6. It is even slightly reduced by focusing field effects at the exit of D2.

Questions

Several questions arise: Is a separation between p and d possible, given that the Čerenkov-angle for the protons is close to threshold? Or do even both particles contribute? Those questions could be partially answered by simulations, which have not yielded results by the time of the workshop.

1^{st} Simulation Method (Dubna)

One program for simulations was provided by G. Macharashvili. It is independent of the shape of the counter, and therefore does not respond to different distributions of incoming particles on the surface or the behaviour of photons inside the detector. It calculates the number of photons reaching the PM by using the *Active Arc fraction*, which is a two-dimensional treatment, and applies some random functions to that number. A tracking of the particles from target to counter in order to get realistic distributions has not been implemented yet. Disturbing effects (like photon losses) are dealt with by a global factor.

Active Arc Fraction

For particles with $\vartheta_R > \vartheta_{\check{C}}$, the Čerenkov-light leaves the detector. At the backside, the circle from the Čerenkov-cone is inside the circle from the TR cone (figure in lower left corner on transparency 7). If the detector is inclined, the Čerenkov-cone gets shifted and becomes an ellipse at the backside (lower right corner). The part of the Čerenkov-cone-ellipse, which moves out of the TR-circle, is reflected at the backside. This fraction can be calculated: An approximation was published and used for some test data at ITEP. It works well for large differences between $\vartheta_{\check{C}}$ and ϑ_R, as shown on transparency 9. For small differences (our case!, see transparency 9), the approximation differs much from the exact formula calculated by M. Hennebach in his diploma thesis about Čerenkov-counters for Kaon identification. To improve the Dubna-simulation, the exact formula could be implemented.

2^{nd} Simulation Method (Jülich)

This program was written and used by M. Hennebach and R. Koch and tracks particles from target to detector, thus giving realistic distributions for particles entering the Čerenkov counters. It even tracks photons inside the detector: they are placed randomly on the Čerenkov-cone. So this simulation is fully 3D, and effects like influence of an uneven surface or photon losses can be treated independently. The main advantage is, that this program was already used and tested, and the geometry of the forward-Čerenkov-counters is implemented.

Work To Be Done

The 2^{nd} simulation (most likely) will be completed to a) reproduce the data from the April '00-beam time and b) answer the questions mentioned above, plus to determine the detector efficiency.

THE CERENKOV DETECTORS IN FORWARD DIRECTION

for separation between deuterons and protons

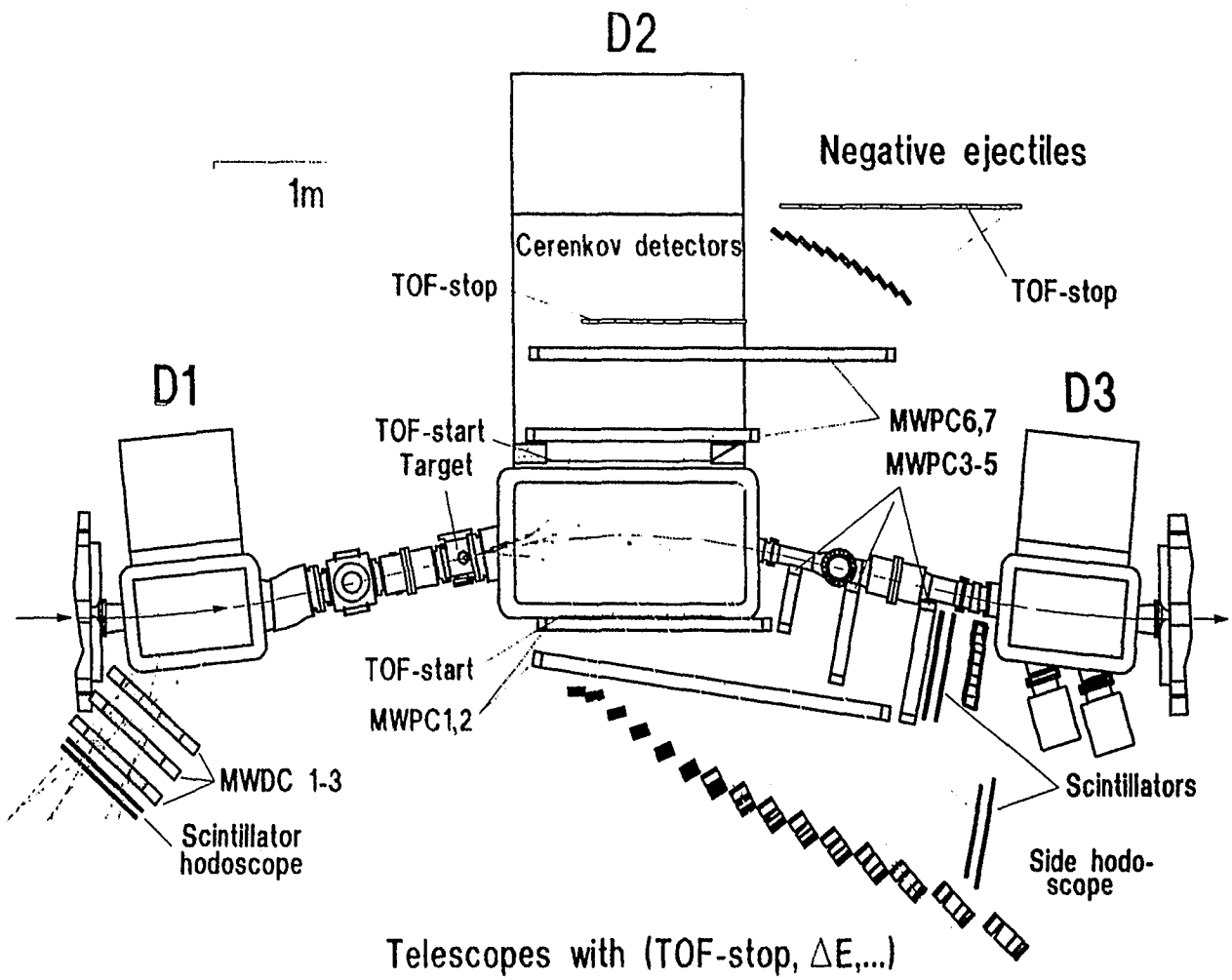

THE LAYOUT OF THE DETECTORS:
as developed in DUBNA/TBILISI

Total number of detectors: 8×2

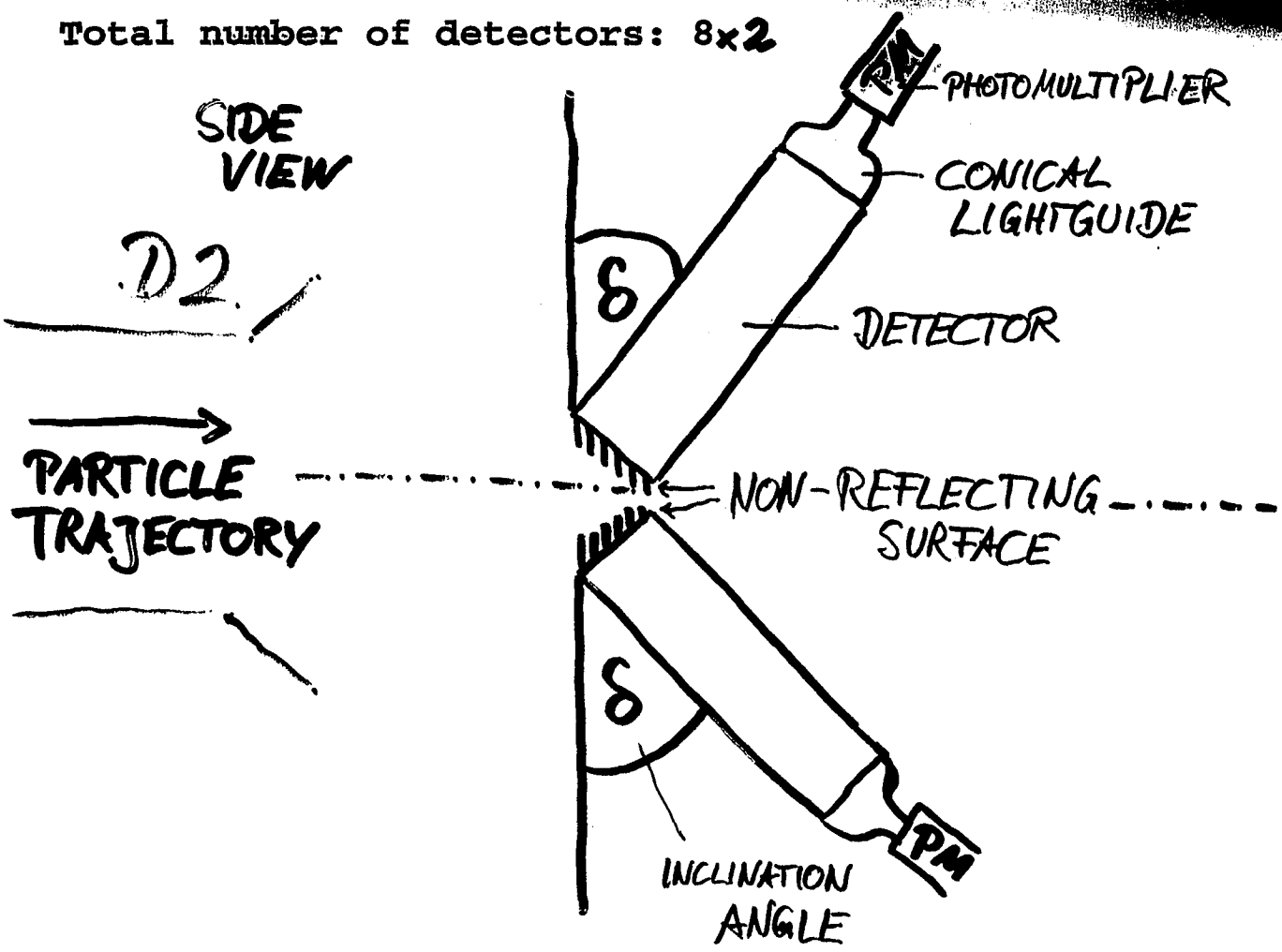

Dimensions:

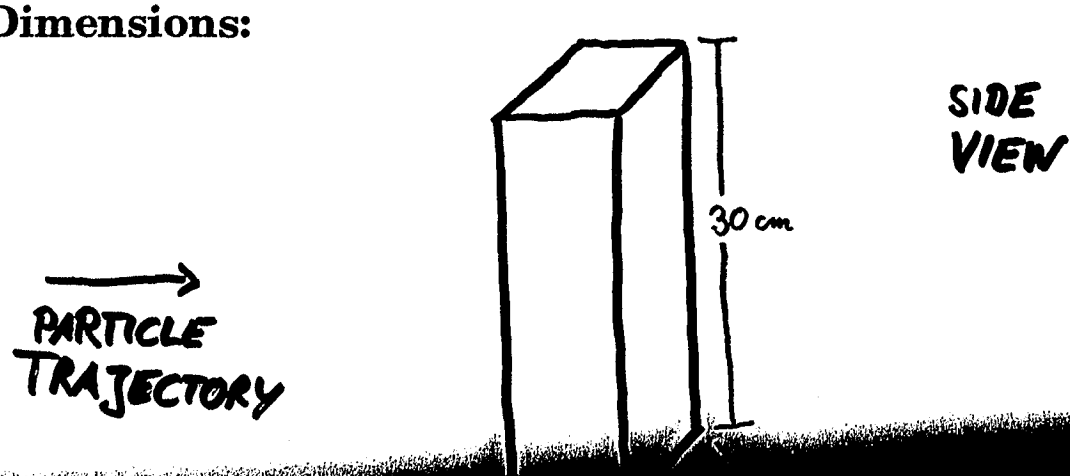

HOW THE DETECTORS WORK:

$$\cos\vartheta_C = 1/\beta n \qquad \sin\vartheta_R = 1/n$$

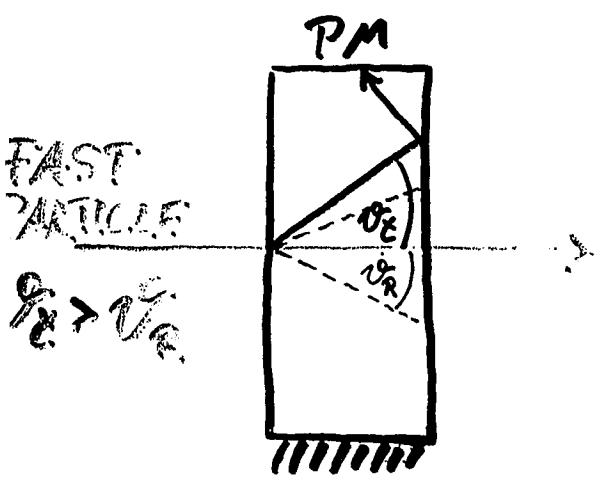

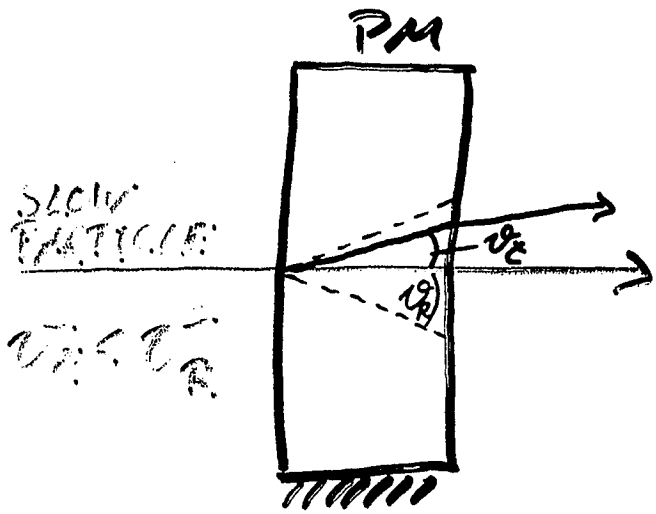

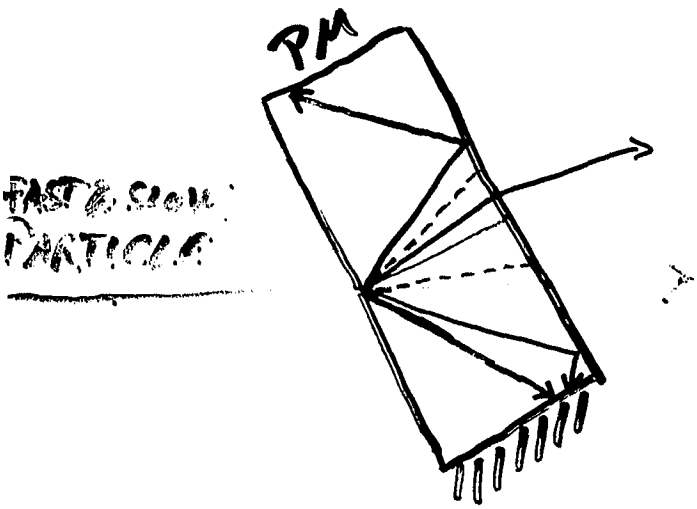

Č-LIGHT OF SLOWER PARTICLE IS SUPPRESSED

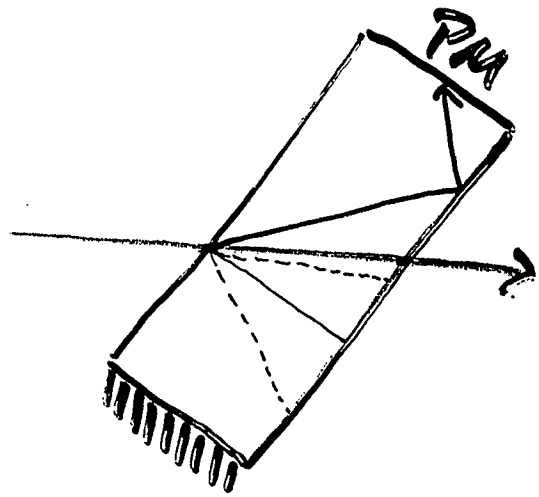

Č-LIGHT OF ~~FAST~~ PARTICLE IS REFLECTED EVEN FOR $\vartheta_C < \vartheta_R$

$pp \to d a_0^+$

$\hookrightarrow K^+ \bar{K}^0$

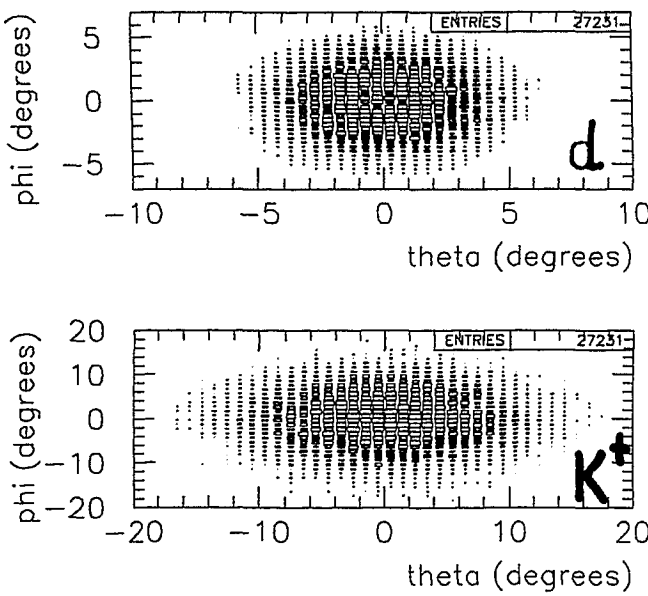

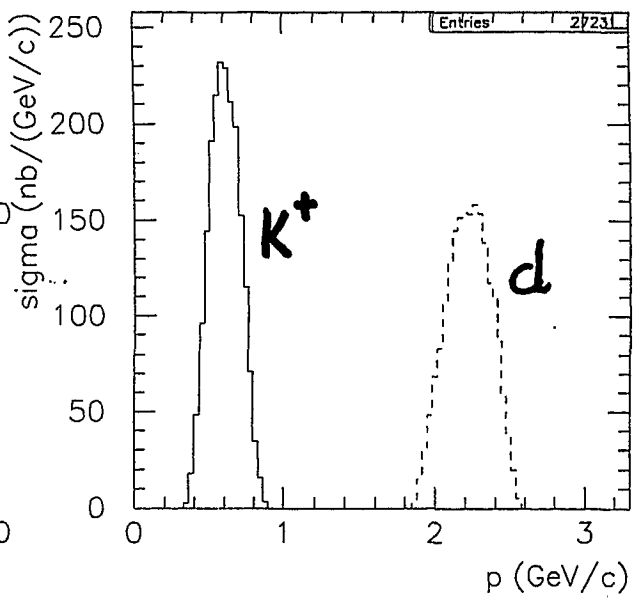

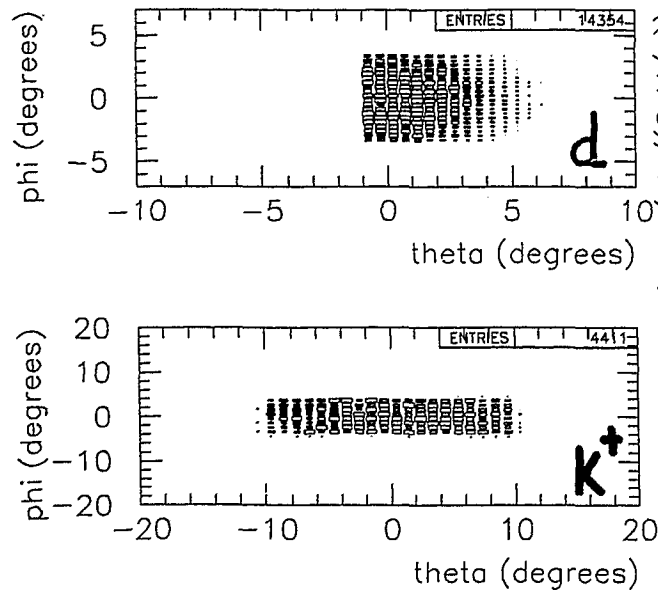

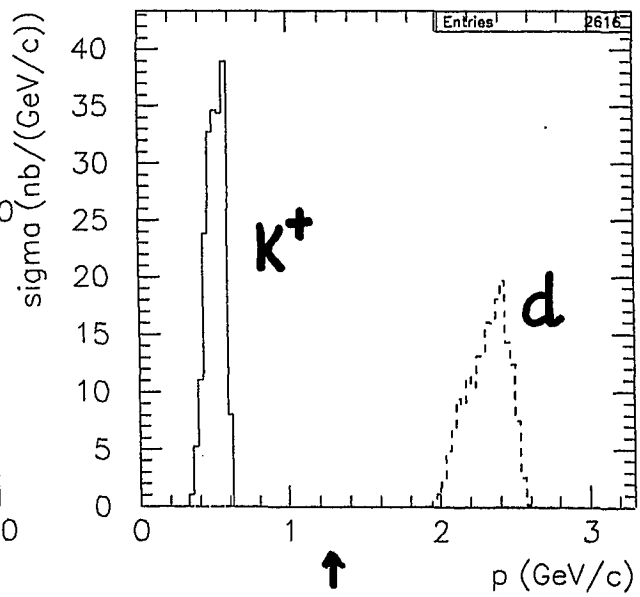

MOMENTUM ACCEPTANCE AT ANKE

$P_d \approx 1{,}9 \ldots 2{,}3$ GeV/c

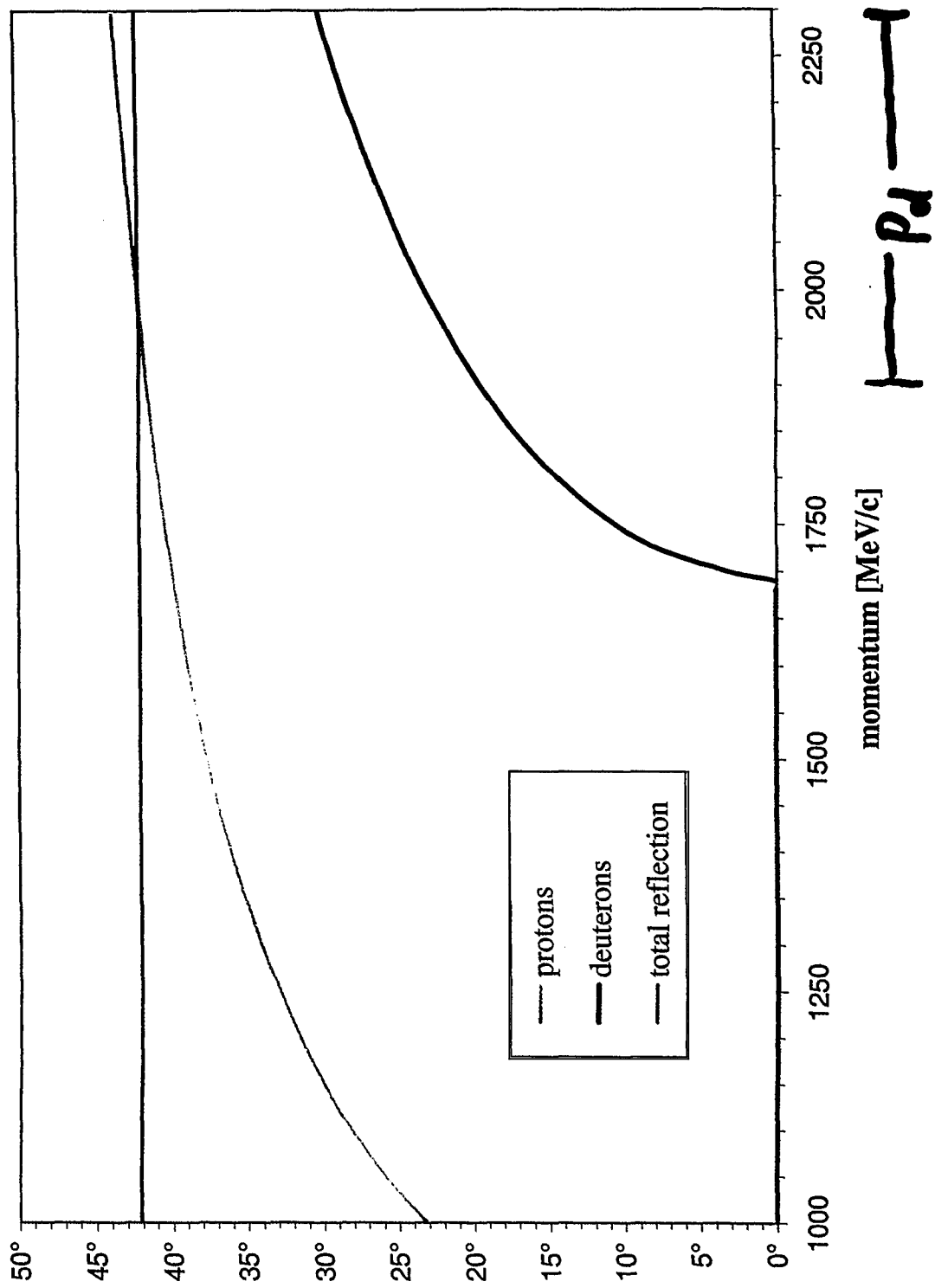
cerenkov angles of protons and deuterons
50°
45°
40°
35°
30°
25°
20°
15°
10°
5°
0°
1000
1250
1500
1750
2000
2250
momentum [MeV/c]
protons
deuterons
total reflection
p_d

QUESTIONS:

- Is d/p-separation possible for realistic particle distributions?

- Which inclination angle is optimal?

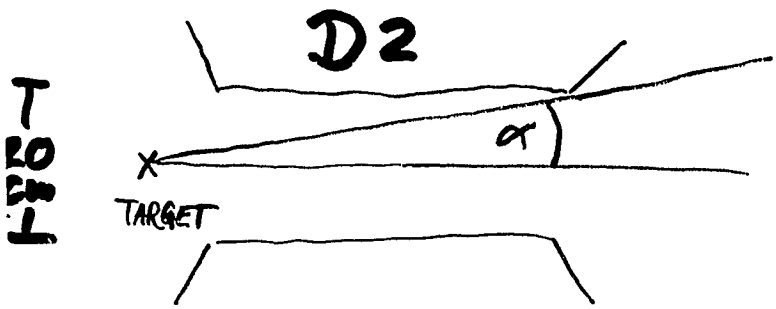

vertical spread in FD: 3°..4°

1. SIMULATION (DUBNA):

- independent of detector shape!

– calculates number of reflected photons by using the 'Active Arc fraction', i.e. 2-dimensional
- simulates PM-response

- no tracking of particles implemented yet

Active Arc fraction:

FOR $\vartheta_R > \vartheta_C$ $\Rightarrow$ INCLINE DETECTOR

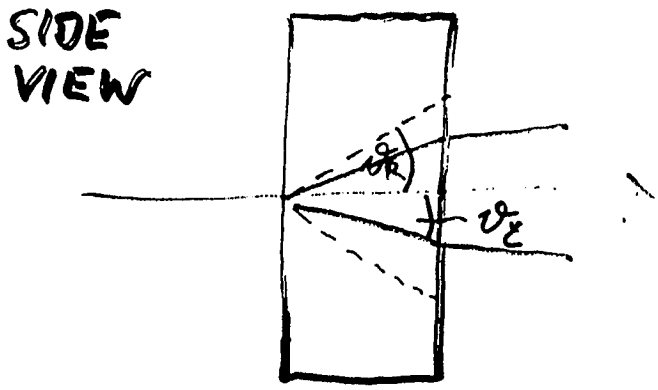

BACKSIDE OF DETECTOR

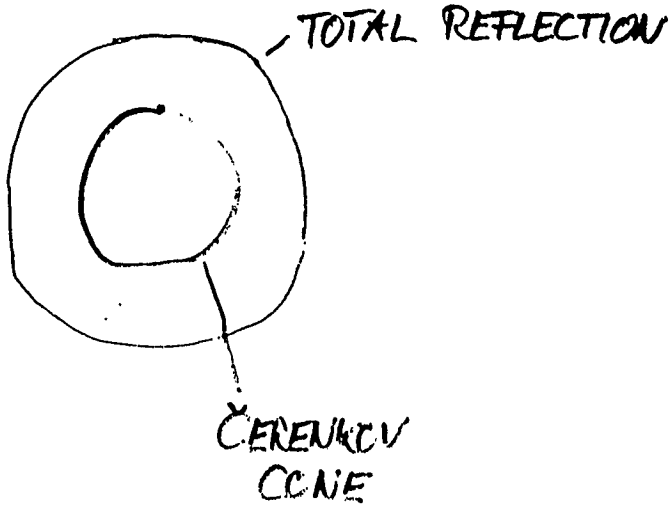

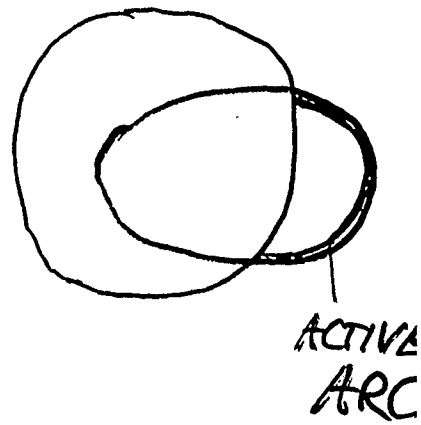

NOT INCLINED

INCLINED

Effect of inclined particle trajectories

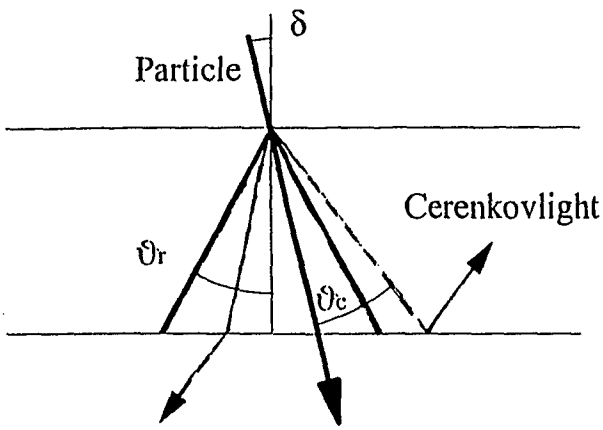

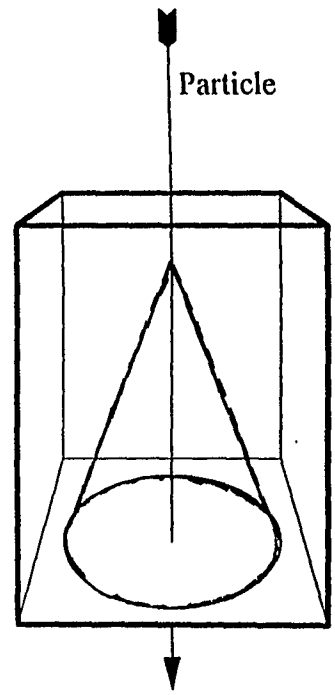

Approximation by Kacharava, Macharashvili, Nioradze et al:

(NIM A 376 (1996))

$$\Delta\phi = 2\arccos\left(\frac{\tan(\vartheta_R + \delta)}{\tan\vartheta_C}\right)$$

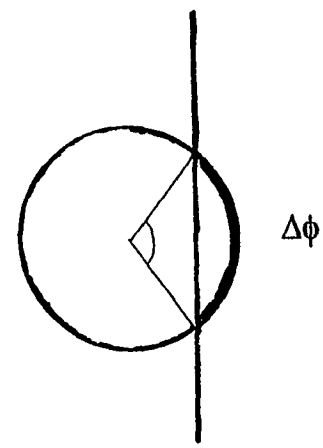

Detailed formula:

$$\Delta\phi = 2\arccos\left(\frac{\sin 2\delta}{2\tan\vartheta_c \cdot \sin^2\delta} \pm \sqrt{\frac{\sin^2 2\delta}{4\cdot\tan^2\vartheta_c\cdot\sin^4\delta} + \frac{1}{\tan^2\vartheta_c} + \frac{\tan^2\vartheta_c - \tan^2\vartheta_R}{\sin^2\delta\cdot\tan^2\vartheta_c(1+\tan^2\vartheta_R)}}\right)$$

(calculated by M.HENNEBACH)

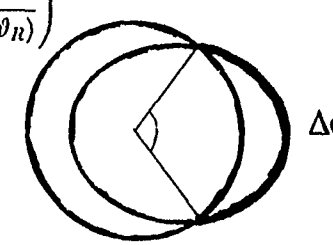

- **Approximation works well for large differences between ϑ_C and ϑ_R:**

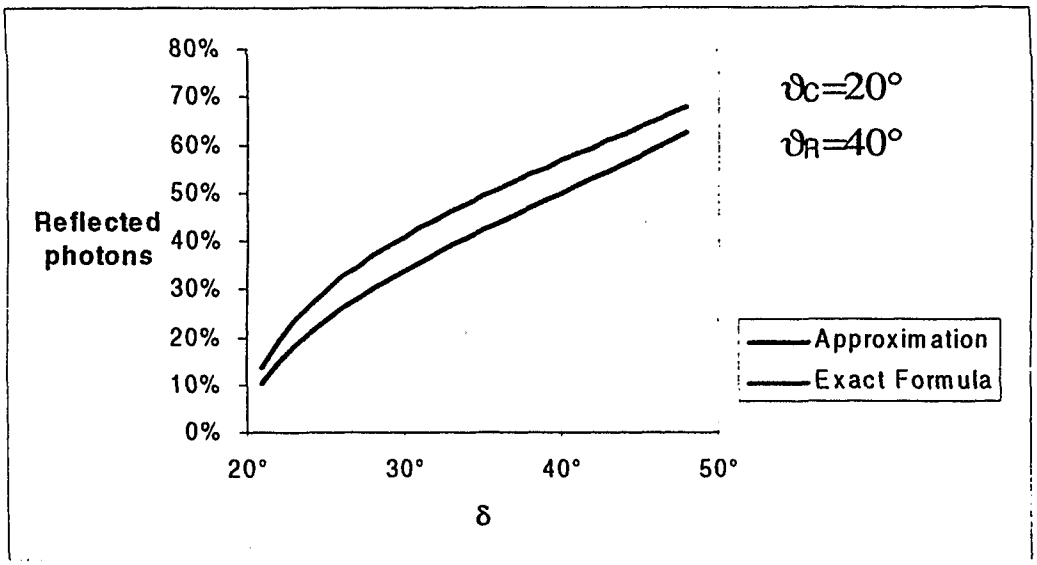

- **For a small difference in angle, the approximation is not as good**

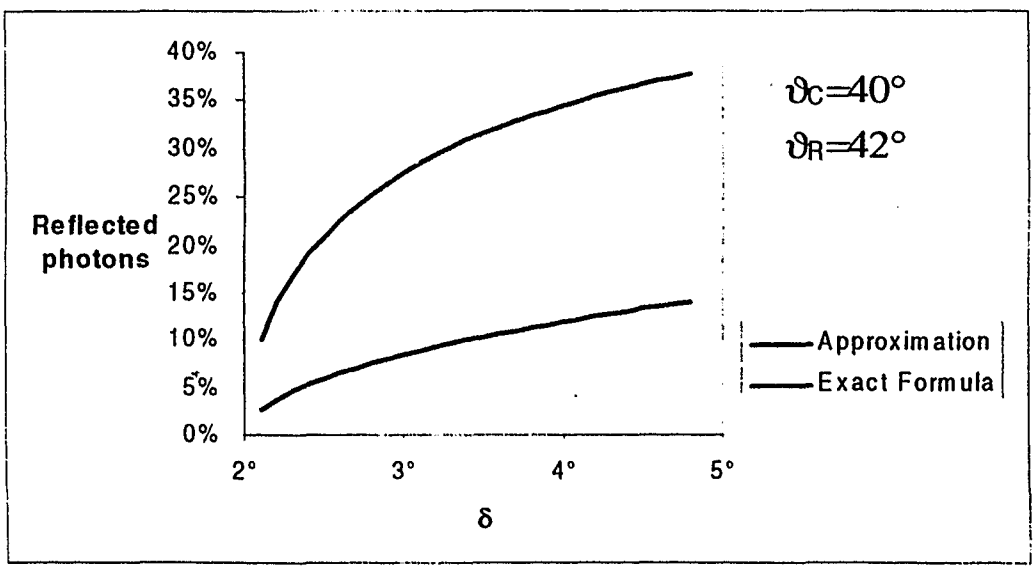

2. Simulation (Jülich):

as used by M. Hennebach/R. Koch for spherical cerenkov counters on negative side

- tracks particles to detector
- tracks photons in detector
  i.e. fully 3-dimensional

- simulates PM response by 25% detection efficiency
- other effects can be adjusted (change of reflection angle, photon-loss)

- already written & used, new geometry implemented

WORK TO BE DONE:

- reproduce detector behaviour from last beamtime (April '00)
- simulate detector response to deuterons / protons
  at beam energy 2,6 GeV
  → can p & d be separated?
  → optimal inclination angle?
  → EFFICIENCY ?

Analysis of Čerenkov Counter Data for Runs from April 2000

G. Macharashvili

Joint Institute for Nuclear Research
141980 Dubna
Russia

Measurement Conditions

For analysis we used two runs: 2739 at $T_p = 2000$ MeV beam and 2721 at $T_p = 500$ MeV beam both with H_2-Cluster target and D2 switched off. The elastically scattered protons as well as deuterons from pp $\rightarrow$ dπ simplify the definition of the momentum for the forward detected particles. Useful events contain only tracks hitting the Čerenkov modules 1 to 5 because the accepted solid angle is restricted by the D2 vacuum window.

All Čerenkov modules are identical with the radiator dimensions 5×8×30 cm^3. The inclination angles were the following (same for each upper/lower pair): $-2°, 0°, 4°, 8°, 12°$ and 15°.

The average momenta and the most probable (mp) deposited energies for these events are the following:

T_p MeV	Particle	p GeV/c	β	ΔE_{mp} MeV/cm
500	p	1.07	0.752	2.7
	d_f	1.14	0.6	5.6
	d_b	0.8	0.53	9.0
2000	p	2.71	0.930	1.8

Event Selection Criteria

In each event the straight-line tracks were reconstructed using MWPC-1,2 data. The MWPC efficiencies and uniformity was not studied. The tracks originating from the target were selected by the 'Vertical and Horizontal Selection':

- 'Horizontal' selection algorithm:
  The projected line equation is the following: $x = \dot{x}\, z + x_0$; $\dot{x} = \frac{\partial x}{\partial z}$.
  These two parameters $\dot{x}$ and x_0 are linearly dependent (in case D2 is off). So:
  if $|\dot{x} - a\, x_0 - b| < \varepsilon$ the projected track is accepted. Here $\dot{x}$ and x_0 are the reconstructed slope and bias of the track, a, b - predefined constants and ε is defined by spatial resolution.

- The same selection algorithm was applied in the vertical direction independent on the D2 operation conditions.

- Is is checked if the track hit both planes of the forward scintillation hodoscopes (counters i and j corresponding). Also the index k of the hit Čerenkov counter (for upper or lower module) was defined. Only events with a distance > 2 cm from the middle plane were accepted. To avoid edge effects (i.e. inefficiency of particle identification near the radiator edge) we excluded also tracks which were closer than 1 cm to the edge of the radiator.

- The different kinds of particles are selected by their deposited energy:
  2.71 GeV/c protons at $1.6 < \Delta E_p < 3$ MeV/cm,
  1.07 GeV/c protons at $2.4 < \Delta E_p < 3.5$ MeV/cm,
  all deuterons at $4.8 < \Delta E_d < 12.0$ MeV/cm
  Nevertheless as it can be seen from the figures that some background particles remain at a beam energy of 500 MeV.

After the event selection the pulse height from the module has been plotted. If the QDC-pulse height is $Q_k > 2$ channels we assumed that the particle was detected by a Ĉerenkov module. However, this is not correct, because at 500 MeV the QDC pedestals (60 channels) were subtracted by hardware from all Ĉerenkov signals.

Results and Discussion

For the Ĉerenkov counters protons with momenta of 1.07 GeV/c are equivalent to deuterons with momenta of 2.1 GeV/c. Consequently, they both produce the same amount of Ĉerenkov light. So we can consider the detection efficiency of protons at a beam energy of 500 MeV to be the same as the deuteron detection efficiency at a momentum of 2.1 GeV/c.

In the upper pictures on the first transparency of the k-th Ĉerenkov module detection efficiencies and amplitude spectra are presented in each page. The upper two pictures correspond to particle detection efficiencies at a beam energy of 500 MeV depending on ΔE. The particles were considered as detected if the Ĉerenkov signal was > 2 QDC channels. The left picture contains two histograms of hit and detected particles in absolute scale. The right one is the detected/hit relation bin by bin. This we interpret as 'detection efficiency'. At the detection efficiency (right picture) we can see a clear peak (sometimes with a efficiency of almost 100 %) at minimal values of ΔE. These particles we consider as inclusive pions which always have a large β (at p $>$ 200 MeV/c). The Landau peak for π^+ as it is seen from the picture is in the range $1.5 < \Delta E < 2.2$ MeV/cm. The constant efficiency of about 20 % independent on ΔE corresponds to slow particles (protons and deuterons). The fact that the efficiency is independent on ΔE (or even increasing slightly for deuterons) indicates that the low intensity scintillation occurs in Ĉerenkov radiator material.

The next two pictures on the first transparency correspond to the same quantities but for the beam energy of 2 GeV. In the efficiency peak (right picture) for protons (2.7 GeV/c) and probably π^+ appears whereas the efficiency of 20 % for slow particles remain.

In the lower left picture on the first transparency the particle detection efficiencies are presented both for fast and slow particles depending on the threshold amplitude value. The lower right picture presents the signal spectra for fast and slow particles.

The next step was to select the desired particle type by ΔE cuts. Pions and protons, respectivly, at a beam energy of 2 GeV were selected by the condition: $1.2 < \Delta E < 1.5$ MeV/cm and $1.5 < \Delta E < 2.5$ MeV/cm, respectivly, deuterons were selected by: $\Delta E >$ 3.2 MeV/cm at a beam energy of 500 MeV. On the second transparency the signal spectra and detection efficiencies are presented for these 3 selected particle types, pions, protons and deuterons, respectively. The proton detection efficiencies are somewhat higher than for unselected events and detection efficiencies for deuterons are lower (after the removal of pions). For Ĉerenkov counters with positive inclination angles (no. 3-5) proton detection efficiencies are around 95 % (except of 3-Low probably caused by low HV). The typical counter (5-Low) shows that the pion signal is slightly larger than the proton signal. So the detection efficiency for pions is somewhat wider than for protons reaching 97 % at a cut level of 2 channels. On the other hand the deuteron detection efficiency at the same cut level is equal to 14 %.

Conclusions

Since deuterons at a beam energy of 500 MeV are seen as well as protons it it probable that the scintillation occurs in the radiator material. It should be noted that the Ĉerenkov radiation threshold is equal to $\beta = 0.67$ for radiator material. So deuterons as well as protons with momenta of 1.07 GeV/c should not produce Ĉerenkov light at all. Nevertheless, a small number of photoelectrons appear at the photomultiplier cathode yielding a detection efficiency of about 20 %. The slow particle detection efficiency does not depend on the deposited energy.

Another reason for the 20 % efficiency of 'deuteron detection' could be due to the accidental coincidence. However, despite of the large sizes of the radiator the efficiency is too large to be caused by accidental coincidences.

It is essential for the p/d separation that the difference between the proton and deuteron signals is very large. Therefore, the use of a low discrimination level allows a low efficiency of the deuteron detection (about 14 %) at practically the same high efficiency for proton detection. For example, for the spectrum of Ĉerenkov counter 5-low in the lower right picture on transparency 2 the cut level of 25 QDC channels results in about 1 % efficiency for deuterons whereas the proton detection efficiency remains at a level of 92 %. Thus, we can expect a fairly good performance of the counters for the p/d-separation. Further study of the matter is necessary. Monte Carlo simulations and beam tests have to be done. We propose the following list of tasks for the September beam time:

- Proper HV selection for each module.
- The pedestal subtraction should be removed.
- Different inclination angles should be tested for each module (2 or 3 positions). The change of the inclination angle for all modules takes around 1/2 h.
- It is necessary to have the tracking information (MWPC-1,2) written on tape. It will allow to achieve a β dependence of the detection efficiency when D2 is on.
- It is necessary to have an on-line sorter with track reconstruction to get the detection efficiency at run-time.
- At the beam time the single counting rates of the Ĉerenkov modules have to be measured by scalers. It is necessary to estimate the accidental coincidence level.

Apr 2000. D2-Off. Beam 500/2000 MeV. Target H-Cluster. Cerenkov Module

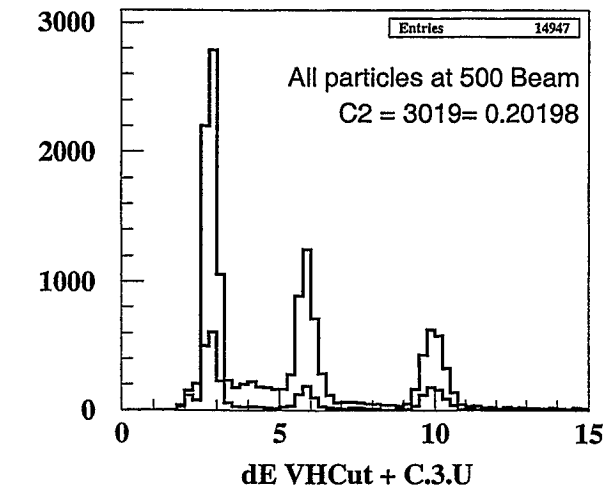

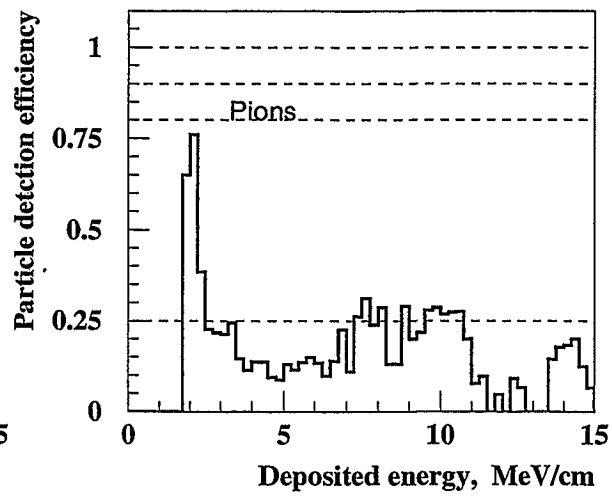

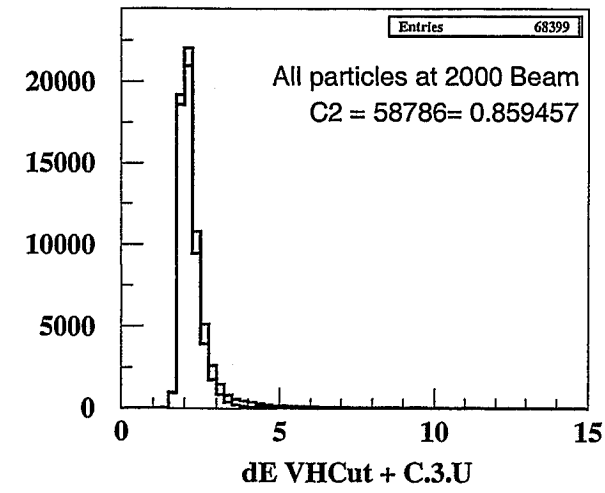

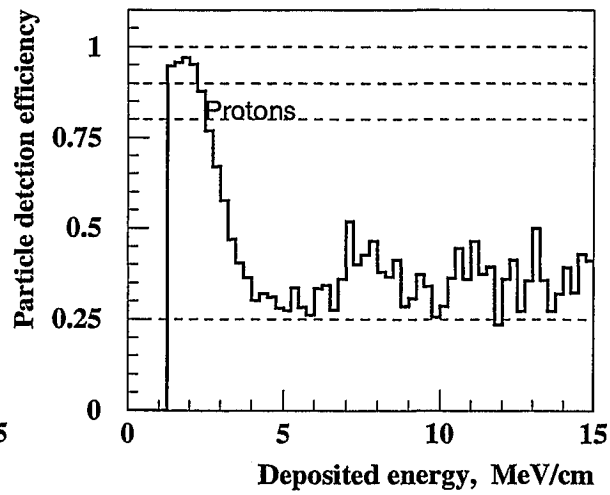

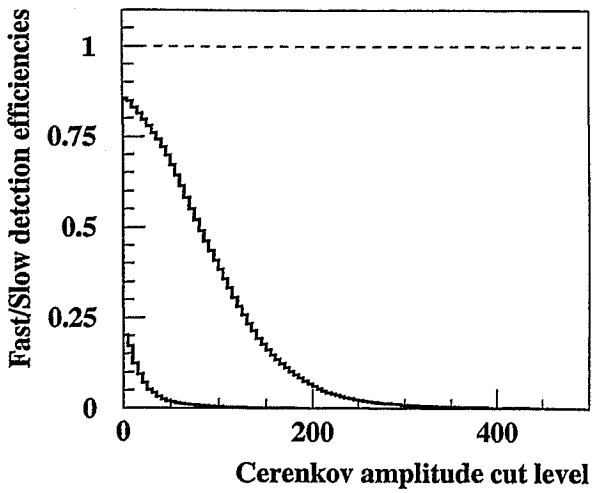

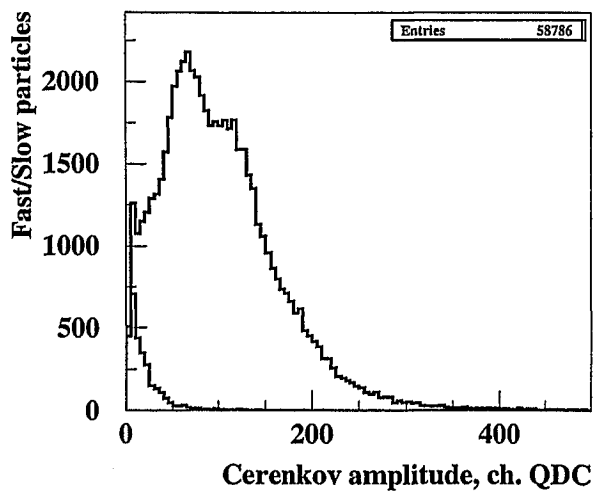

Apr 2000. D2-Off. Beam 500/2000 MeV. Target H-Cluster. Cerenkov Module

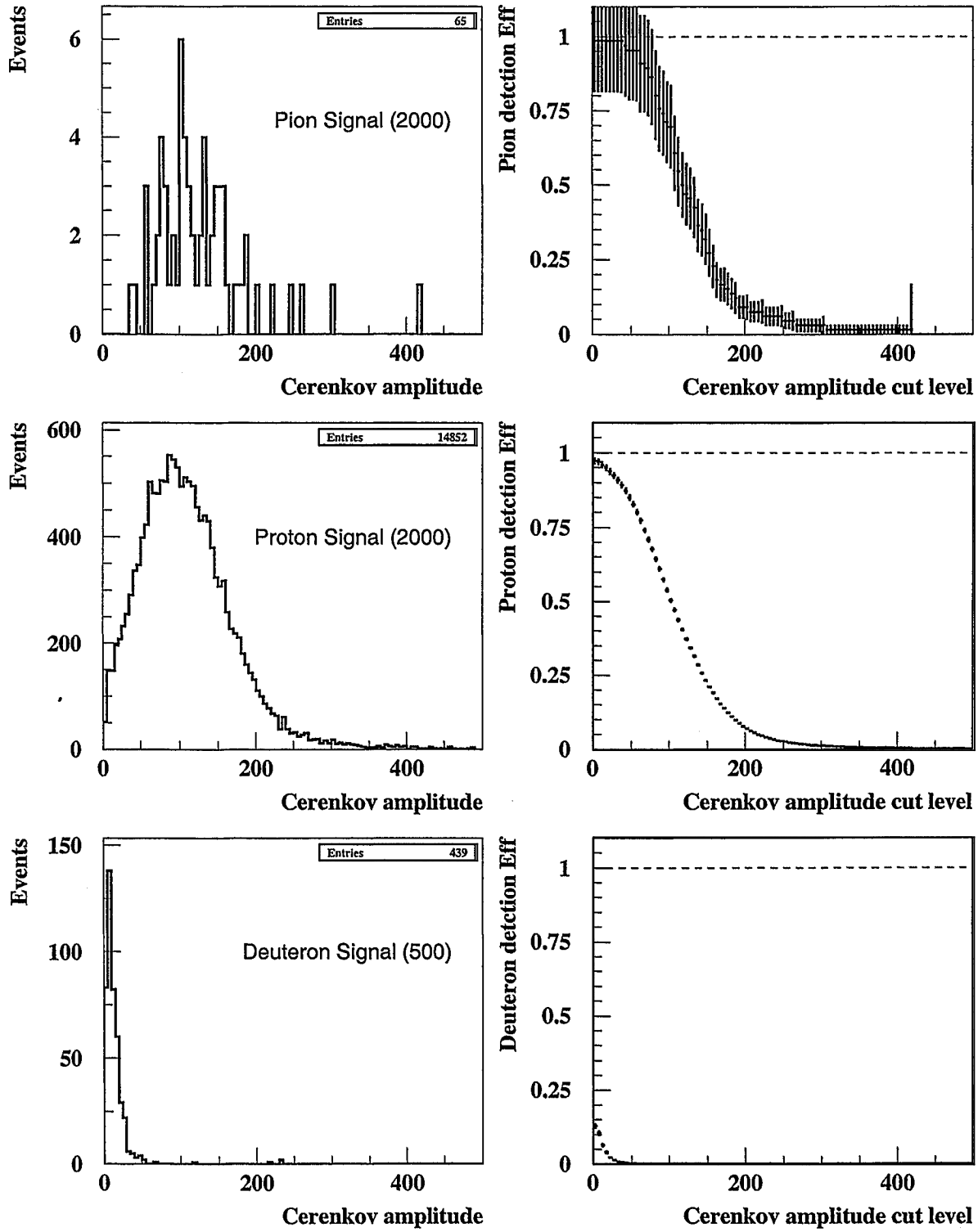

Data-Analysis Software

H. Junghans

Institut für Kernphysik
Forschungzentrum Jülich
52425 Jülich
Germany

The a_0^+ mesons to be investigated with the spectrometer ANKE are produced in the reaction pp→da_0^+. The envisaged decay channels of the a_0^+ meson, K^+K^0 and $\pi^+\eta$, are identified by a coincidence measurement between the deuteron and π^+ or K^+, respectively. Simulations show that these deuterons always hit the forward detector while the pions mainly reach the side wall detector. Kaons are nearly equally distributed over the side wall detector and the telescopes of the side detector. In previous measurements on inclusive K^+-production the kaons could successfully be identified in the telescopes [1]. Sophisticated studies are needed to clarify if kaons can also be identified in the side wall detector.
The analysis software contains the following components:

1. decoding of data with the use of the XD-library [2],
2. (a) analysis of events with C^{++}-based user code,
   (b) values for calibration constants and for analysis cuts,
3. storing of analysed events in spectra using the XD-library,
4. visualisation of spectra with PAW^{++} [3].

Since components 1, 3 and 4 can be adopted from other experiments only step 2 must be prepared. The scintillation detectors provide the user with information ab energy loss of a particle in the detector and the time of flight between the detecto multi-wire proportional chambers supply the user with the information on the trajectories. The user code for the analysis of events will be global in the sen all the steps for the analysis of the detector information are included. When t is analysed only the values for calibration and physical cuts must be adapted. the individual analysis of the three different detector systems a general coincidence logic between these systems will be developed.
Essential for the analysis is the momentum reconstruction of the ejectiles from the track information of the wire chambers. The momentum reconstruction is used to calculate the invariant missing mass of the deuteron and of the pion or kaon. On the one hand with the invariant missing mass the shape of the mass distribution of the a_0^+ can be determined. On the other hand the missing mass provides the suppression of different background reactions:

- pp→dρ^+ where the ρ^+ decays into $\pi^+\pi^0$.
- pp→pπ^+X if the proton is misidentified as deuteron.

For both cases a good missing mass resolution is required. First simulations by the Dubna group show that for the forward detector a resolution of 5 – 15 MeV/c^2 in the interesting mass region (940 – 1020 MeV/c^2) can be achieved. This value should allow to distinguish between different theoretical models on the a_0^+ mass distribution. Furthermore this accuracy provides a sufficient suppression of background reactions due to misidentified protons. The results of the analysis of the sideward chambers by I. Zychor show that at B = 0.8 T in D2 the momentum resolution cannot be better than 3.5 – 4% due to the chamber resolution and small angle scattering. However, this resolution should significantly reduce the background from the ρ^+ decay.

[1] S. Barsov et al., Nucl. Phys., **A 675**, 230 (2000)
[2] P. Zolnierczuk, *Data Analysis Software for GEM Experiments*, Univ. of Krakau (1996)
[3] PAW, *An Introductory Tutorial*, Application Software Group, CERN, Geneva (1994)

Workshop on "a_0 Physics with ANKE"
July 13/14, 2000
ITEP Moscow

Data-analysis software

H. Junghans
IKP, FZ Jülich

14. July 2000

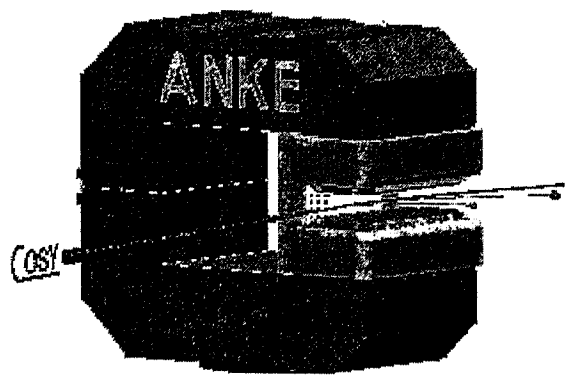

General Considerations

- Decoding of data with the use of XD-library
- Analysis of events with C^{++}-based user code
- Values for calibration of detectors and for cuts located in the "parameter-file"
- Storing of analyzed events in spectra using XD-library
- Display of spectra with PAW^{++}

Results of GEANT simulations:

T_{beam} = 2.6 GeV

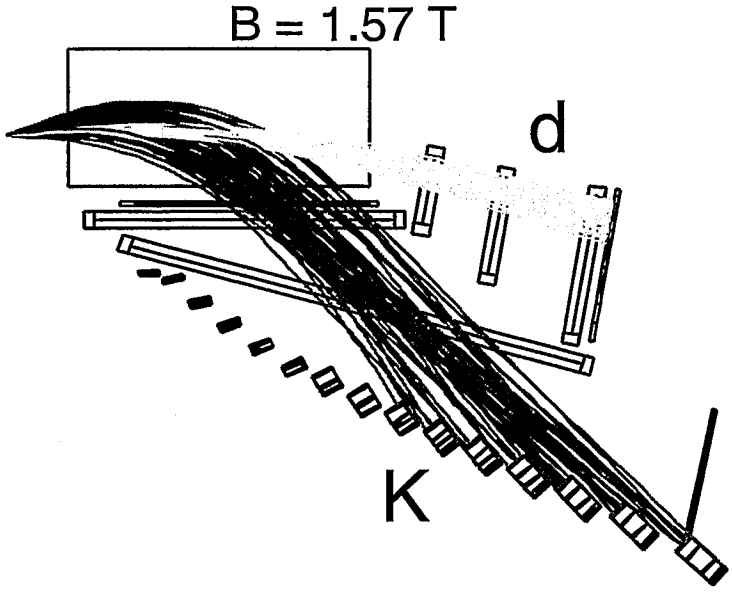

$pp \rightarrow da_0^+$

$\hookrightarrow \bar{K}^+K^0$

$\varepsilon = 12.0\ \%$

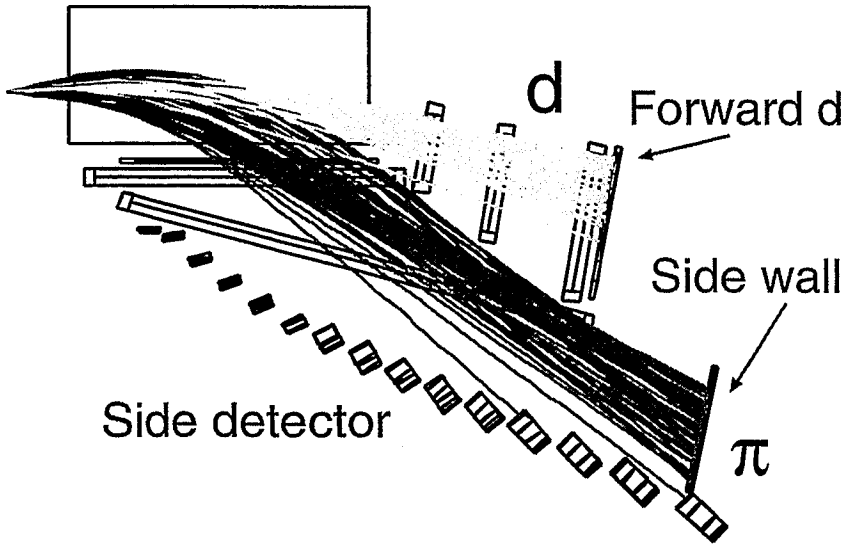

$pp \rightarrow da_0^+$

$\hookrightarrow \pi^+\eta$

$\varepsilon = 0.3\ \%$

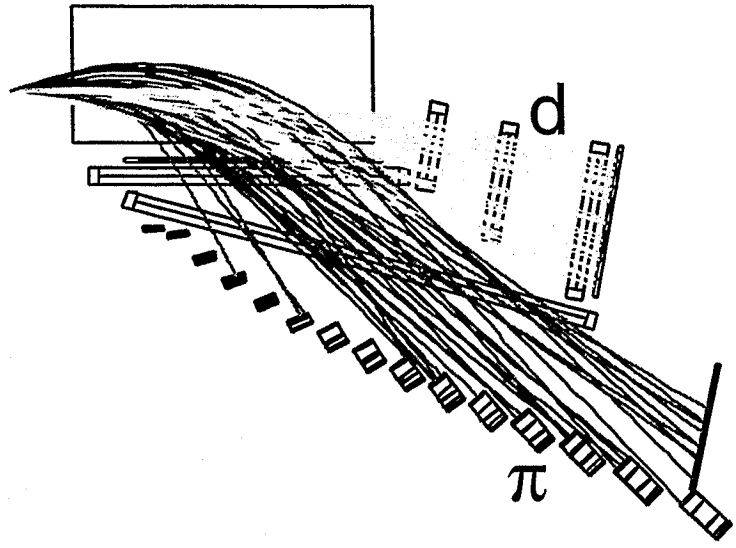

$pp \rightarrow d\rho^+$

$\hookrightarrow \pi^+\pi^0$

$\varepsilon = 0.03\ \%$

User part must contain:

- Analysis of side detector (K^+)
- Analysis of side wall (π^+)
- Analysis of forward detector (d)
- Coincidence logic between the different detectors

17.03.00 junghans

The Spectrometer ANKE

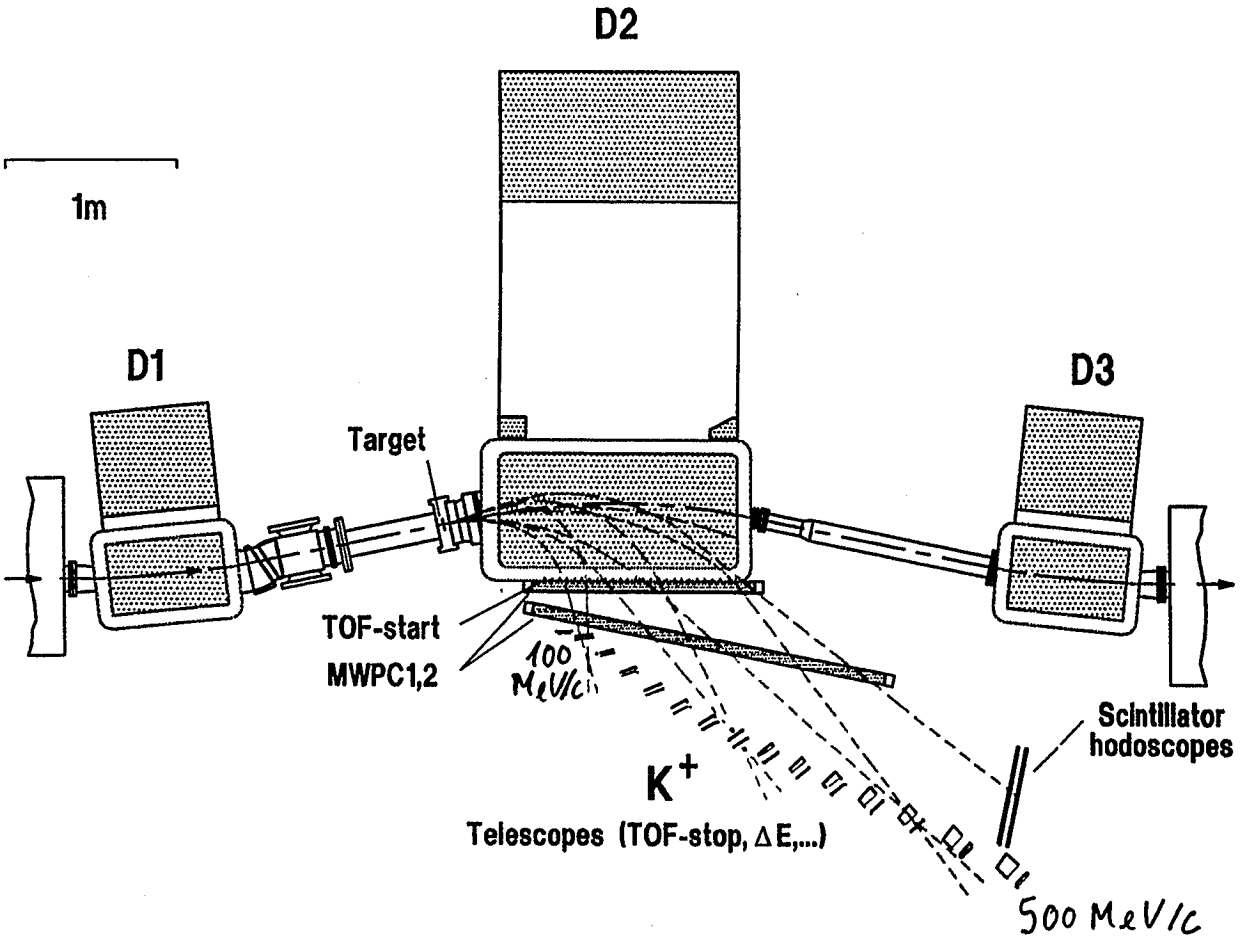

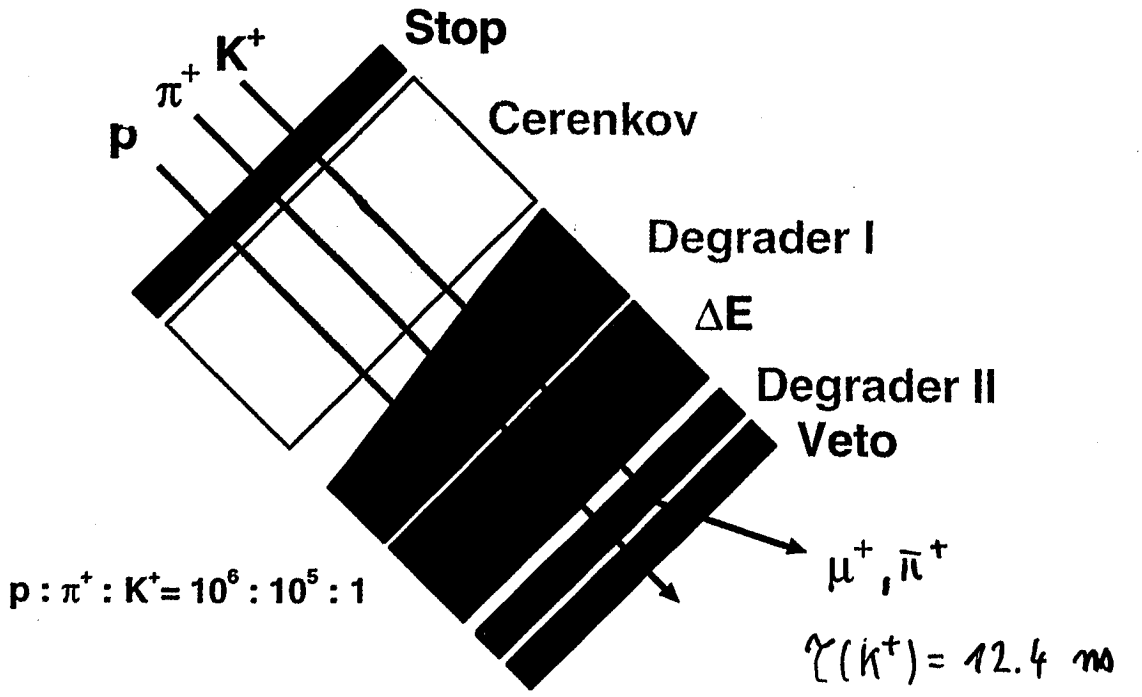

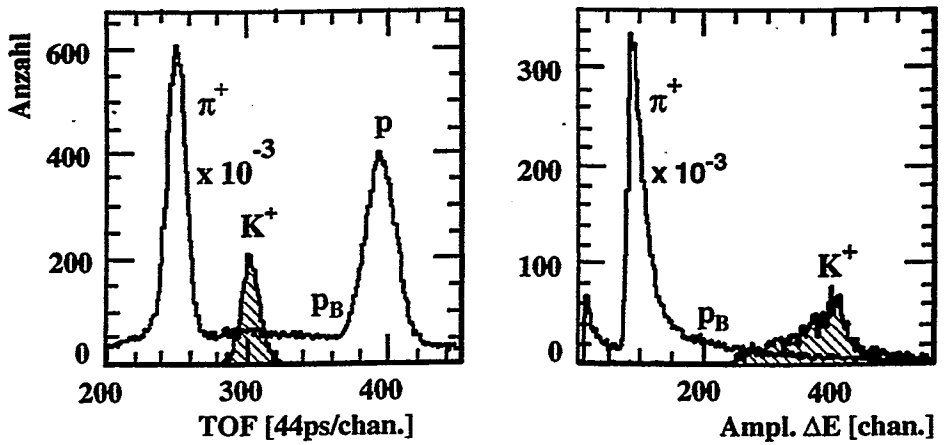

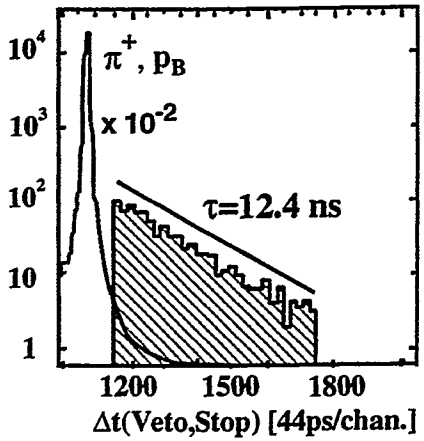

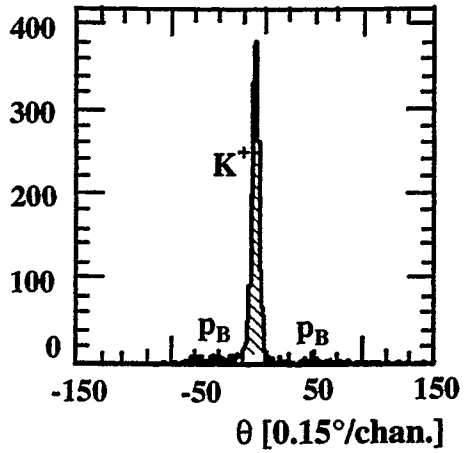

Tp=2.3 GeV

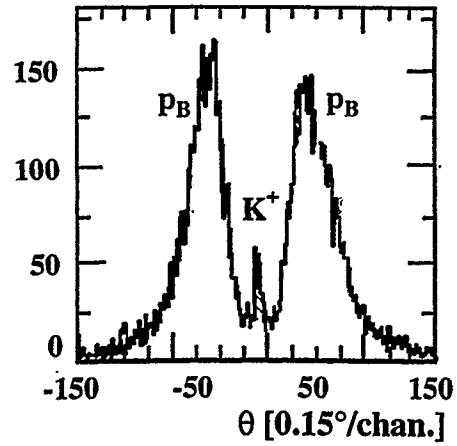

Tp=1.0 GeV

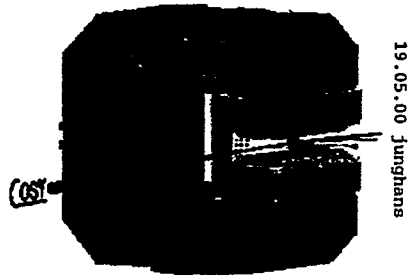

Used criteria:

- **focal plane**
- **10% momentum bite in each telescope**
- **1.5 ns TOF gate, resolution 0.6 ns**
- **energy loss in start and stop counter**
- **range (ΔE counter)**
- **stopped K^+ -> decay (veto counter)**
- **track reconstruction (MWPC)**

H.Junghans, CIPANP 2000

Momentum and Missing Mass Reconstruction

- background reduction
- a^0 mass determination

Momentum reconstruction in each event for two particles:

- K^+, π^+ with side MWPCs
- d with forward MWPCs

$\pm 5, \pm 20$

π^+, d - coin
no angle cuts

reconstructed SORTER

Izabella Zychor

2000/07/04 16.15

run 110 stop 8 coeff from ALL starts and mom for ALL starts

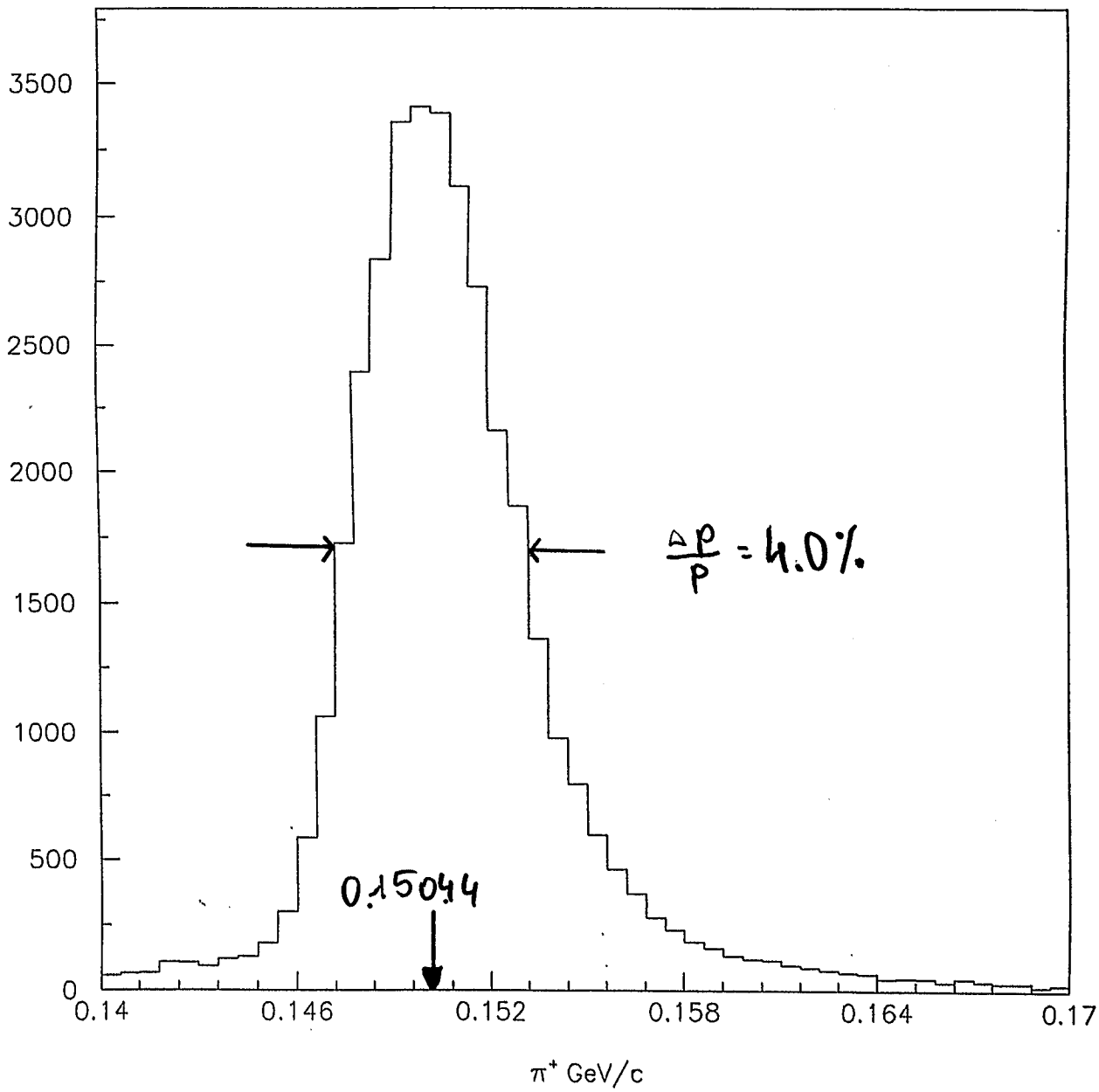

Izabella Zychor

2000/07/11 14.53

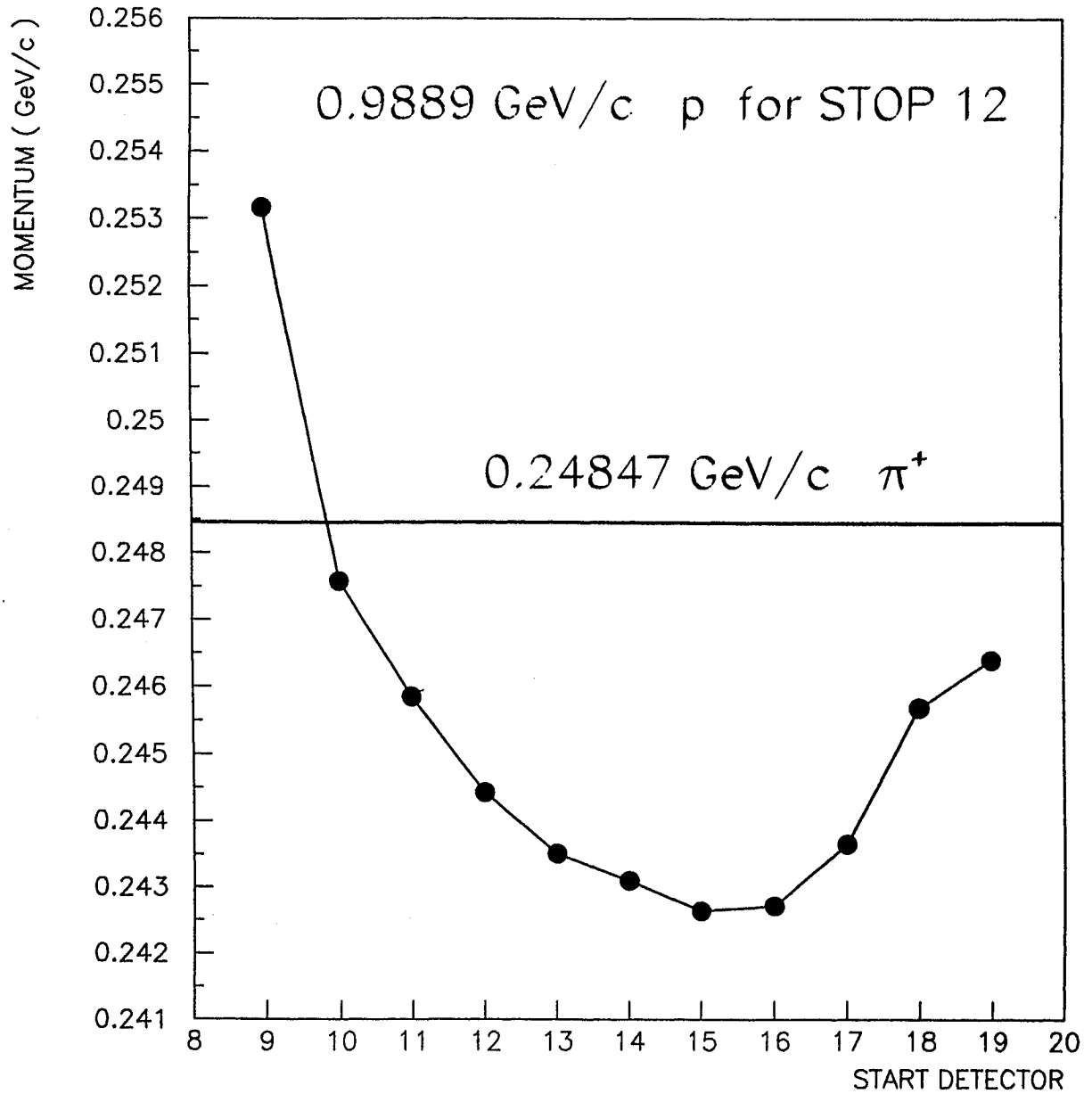

S. Lymov

Missing Mass Resolution for Forward Detector

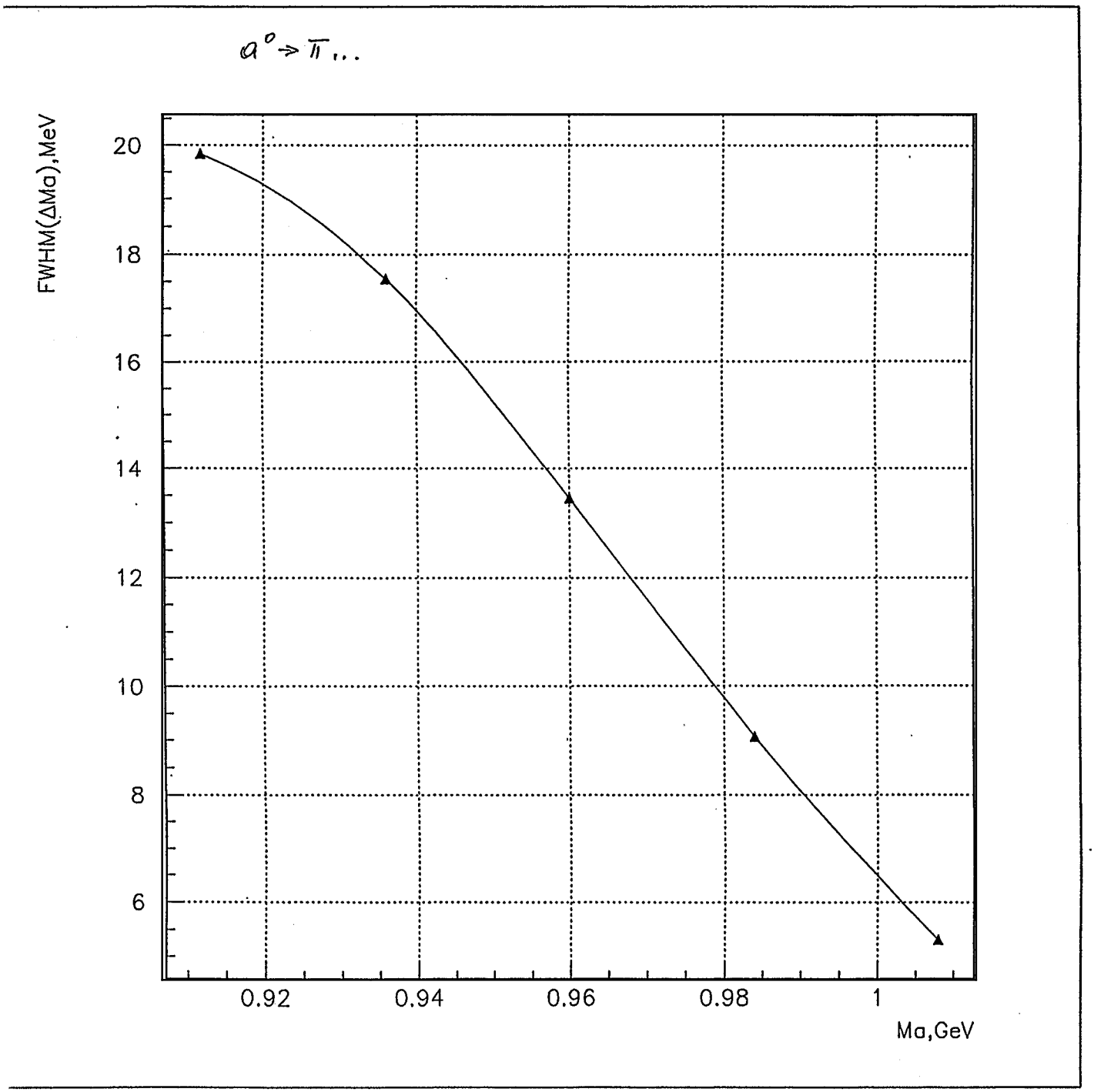

500 μm Al window

$\sigma_{MWPC} = 1.05$ mm, MWPC 1+2

Target size $6 \times 6 \times 15$ mm^3

16.05.00 markus

Reconstructed mass distribution

(missing mass of the deuteron)

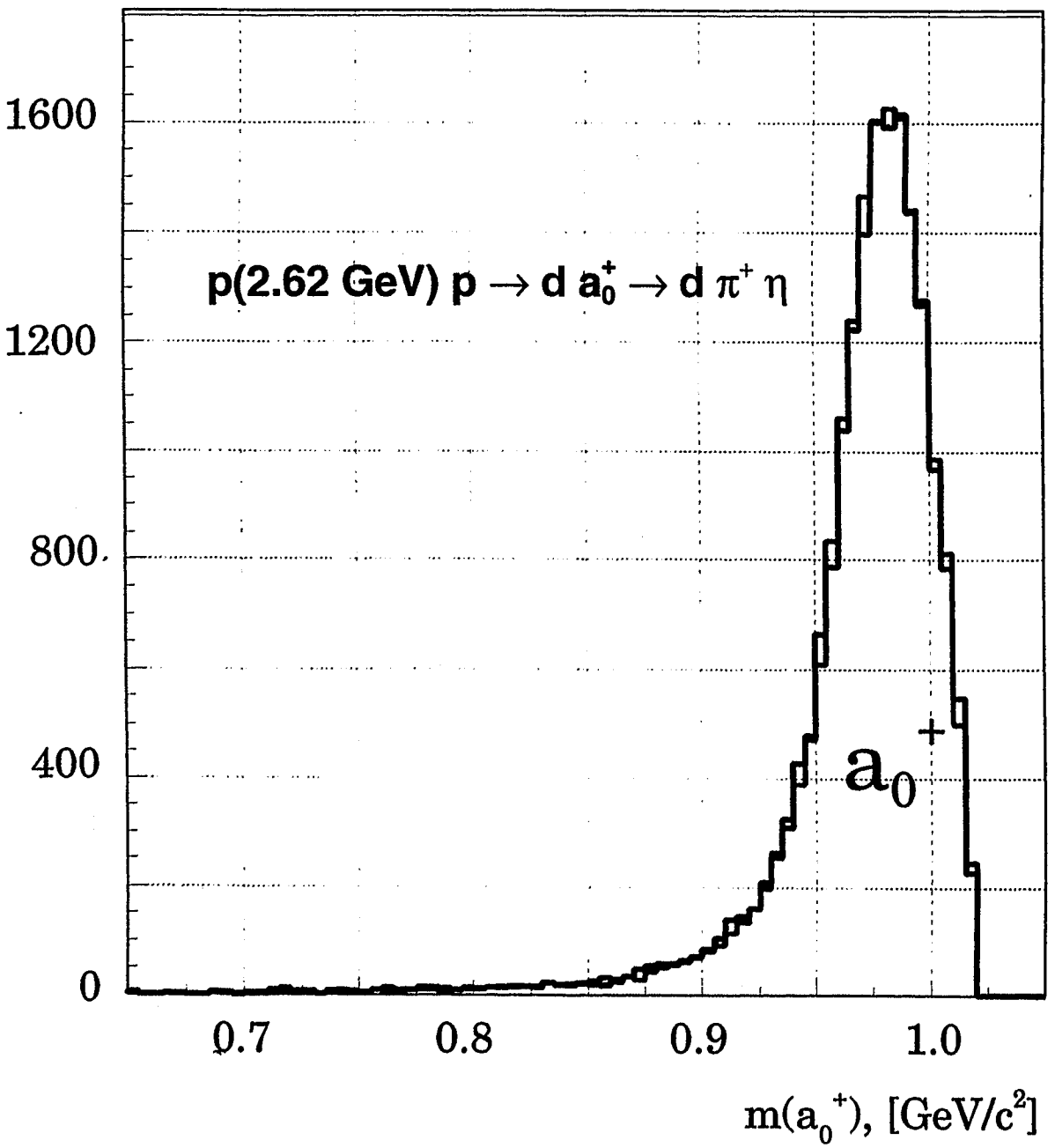

M.Büscher, 4/00

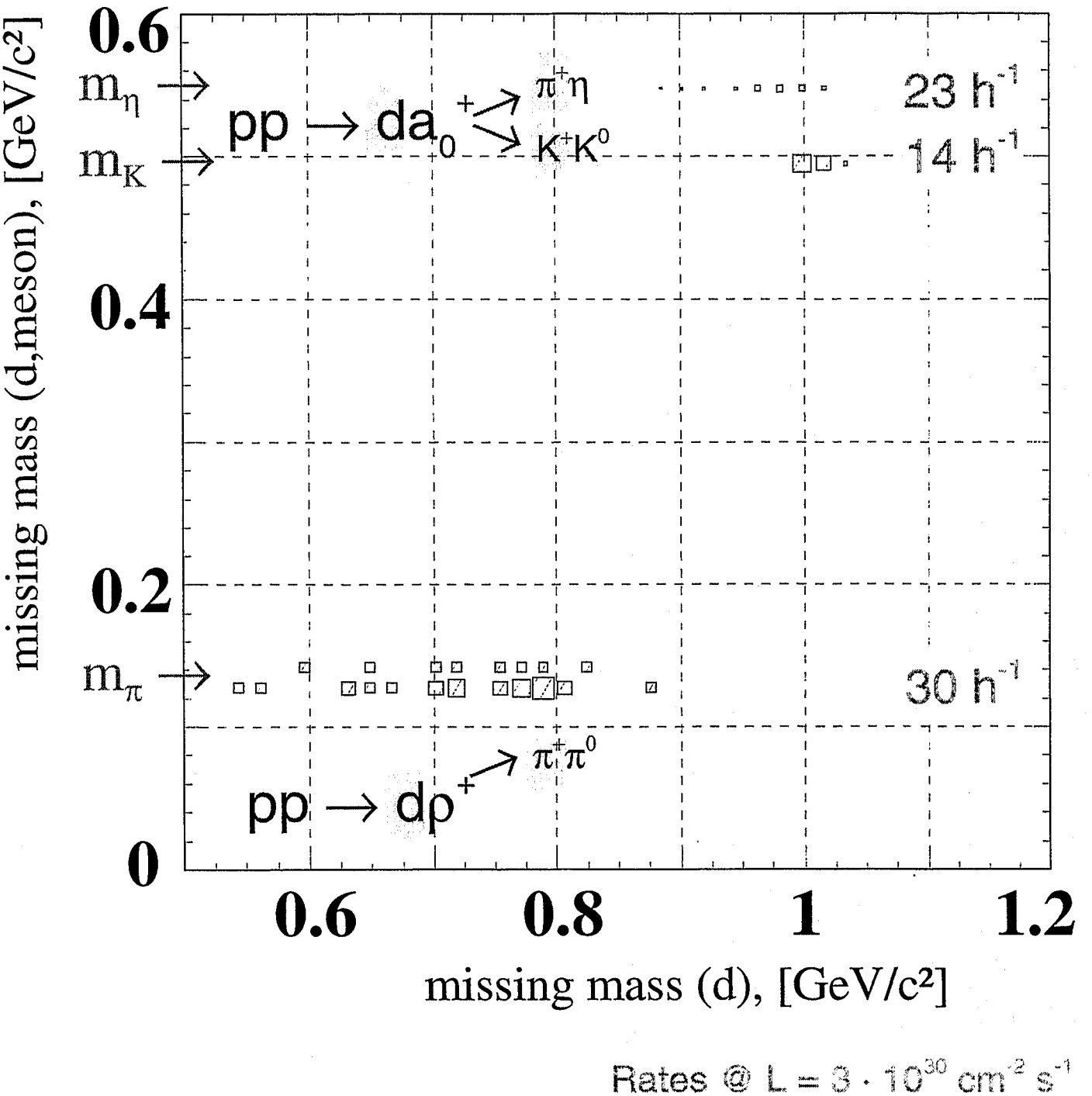

Rates @ $L = 3 \cdot 10^{30}$ cm^{-2} s^{-1}

M Bäscher, IKP

26.04.00 markus

Background suppression II

(missing mass)

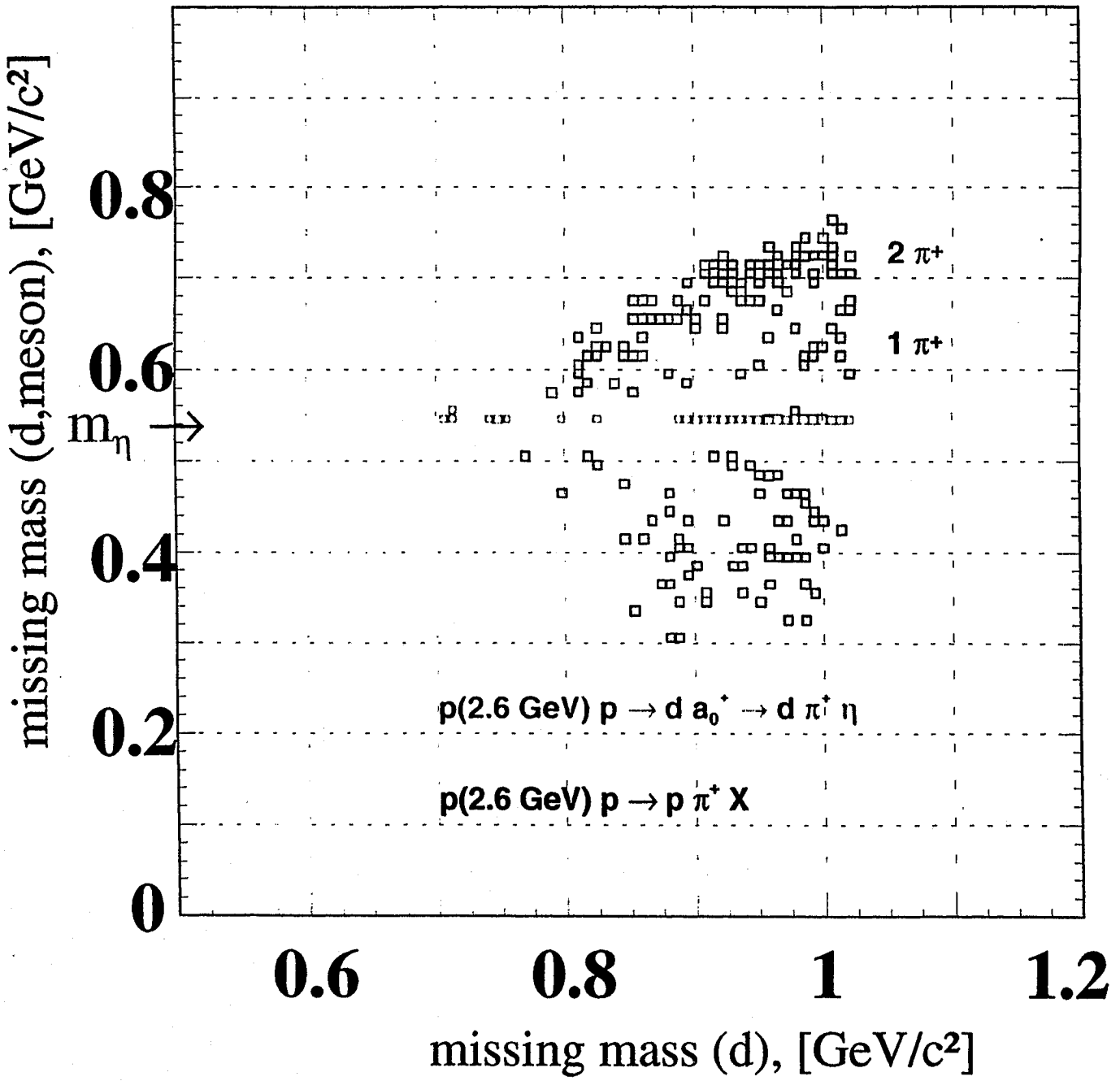

M.Büscher, 4/00

Summary

- Software for analyzing side detector, side wall and forward detector is developed and runs successfully (K^+, $d\pi^+$, NN FSI)

Near Future

- Definition of a common structure (classes) in the analysis of the different detectors
- Developing of a general coincidence logic between the different detectors
- Test of the performance of Cerenkov counters
- Fine tuning of degraders for 1.6 T mode

Luminosity Monitoring with the Spectator Setup at ANKE

I. Lehmann

Institut für Kernphysik
Forschungzentrum Jülich
52425 Jülich
Germany

For any cross section measurement luminosity determination is needed. A way to determine the luminosity directly, is to choose a reaction with a well known cross section and measure the production rate parasitically during the experiment. Because of its well known cross section over the whole COSY-energy range pp-elastic scattering is perfectly suited for this purpose. At ANKE this can be done with the so called Spectator Setup.

The Spectator Setup is a telescope-like structure of three silicon detectors situated inside the target chamber of ANKE. (See the first two transparencies of the talk.) It is designed to realise measurements on an effective neutron target by measuring low energetic (T_p = 1.5 – 30 MeV) spectator protons on a deuterium target. The coverage of slight forward angles ($\leq 80°$) together with the particle identification allows parasitic measurements of elastically scattered protons on a H_2-target (and deuterons on a D_2-target). In this angular regime the rate of protons on a hydrogen target (respectively the rate of deuterons on a deuterium target) allows the determination of the luminosity, since cross sections for other reactions are negligible.

Experimentally the accuracy of our energy measurement and the distinction of deuterons and protons has been proved to be fully satisfactory (see transparency 3). Due to limitations by the target chamber only part of the target is covered with the current setup. The recorded luminosity of: $L = f_{\text{target}}^{-1} \cdot 0.67(5) \cdot 10^{29} \frac{1}{\text{cm}^2\text{s}}$ is therefore strongly dependent on the fraction f_{target} of the target, which is seen by elastic scattering in the chosen energy range.

This fraction can be estimated assuming a step function in beam-target overlap along the beam axis, with the target dimensions given by gas-pressure measurements (see the talk by N. Lang). On a deuterium target the beam-target overlap can also be scanned along the beam axis, by the selection of protons emitted under a fixed angle from the target. On transparency 4 the selection of this protons with a fixed cross section in a well understood acceptance range of the telescope is shown as well as the experimentally obtained spatial distribution in the 300 μm thick detector. If we use this to determine the seen fraction of the target we get the following luminosity[1]:

$$\mathbf{L = 2.4(5) \cdot 10^{29} \frac{1}{cm^2 s}}$$

We can conclude, that it is possible to determine the luminosity with the Spectator Setup within 20%. Our errors are determined by the uncertainties in beam-target overlap and will immediately decrease as soon as the target will be shifted upstream in the beam (f_{target} larger). Therefore it is planned to shift the target a few millimetres for the beam time in September 2000. Furthermore a new target chamber is planned to be installed in the beginning of 2001, where the target is shifted by 5 cm, which will allow to determine the luminosity within a few per cent for both the H_2- and the D_2-target[2].

[1] April 2000, D_2-cluster target with 10^{10} protons at $T_p = 2$ GeV in the COSY ring.

[2] For the D_2-target pp-quasi-free-elastic scattering can be used with a coincidence in forward, because pd-elastic-cross sections are not known within less than 7%.

Luminosity Monitoring with the Spectator Setup at ANKE

INTI LEHMANN
for the
ANKE COLLABORATION

July 2000

Institute for Nuclear Physics
Forschungszentrum Jülich

pp-Elastic Scattering at ANKE

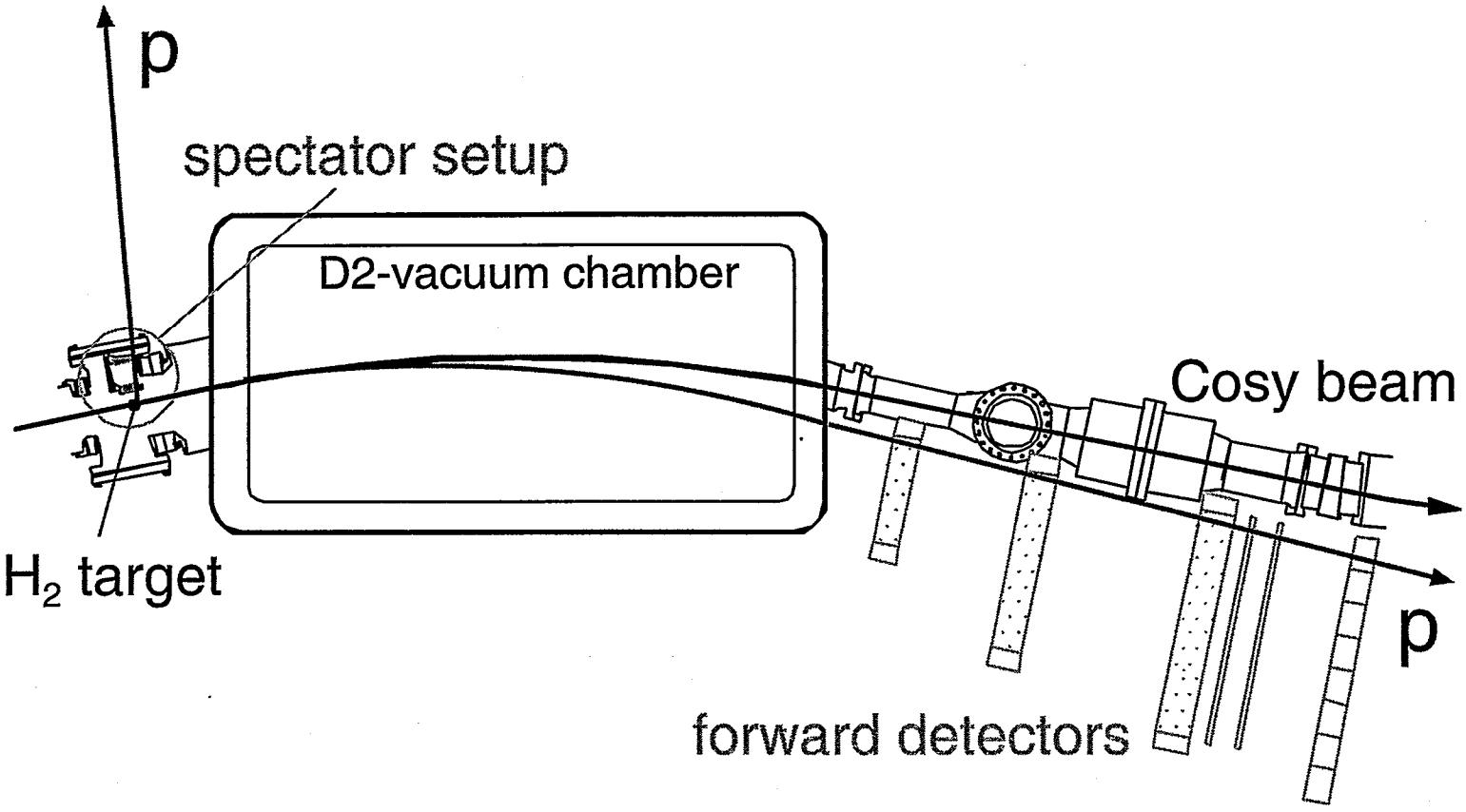

- missing mass of the proton in the forward detector
- energy and angle of the proton the spectator detector (small background)

Spectator Setup

telescope from 3 silicon detectors; $T_p = 1.5 - 30$ MeV

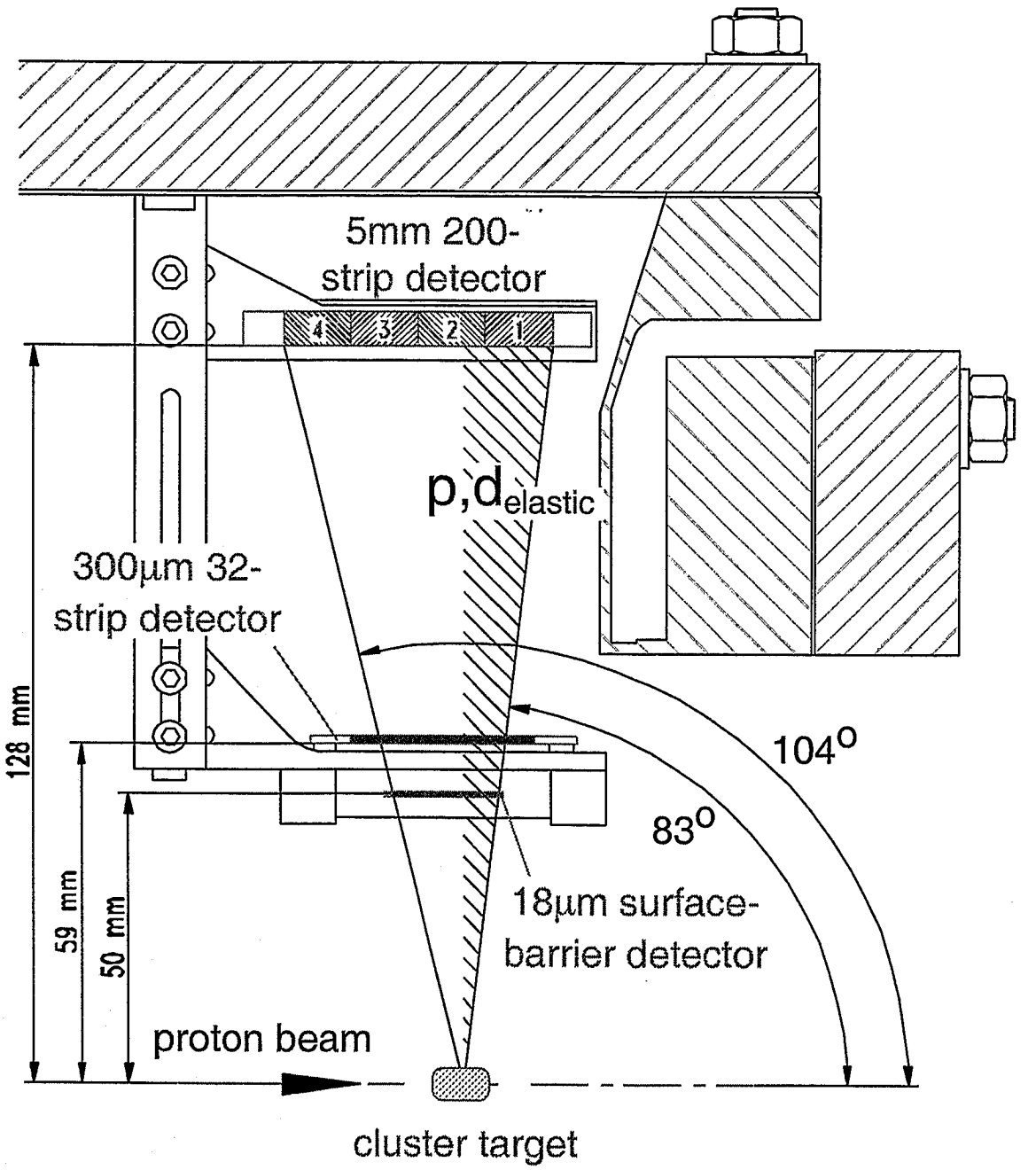

- tagging of spectator protons (D_2-target)
- luminosity monitoring under forward angles

Selection of Elastically Scattered d,p

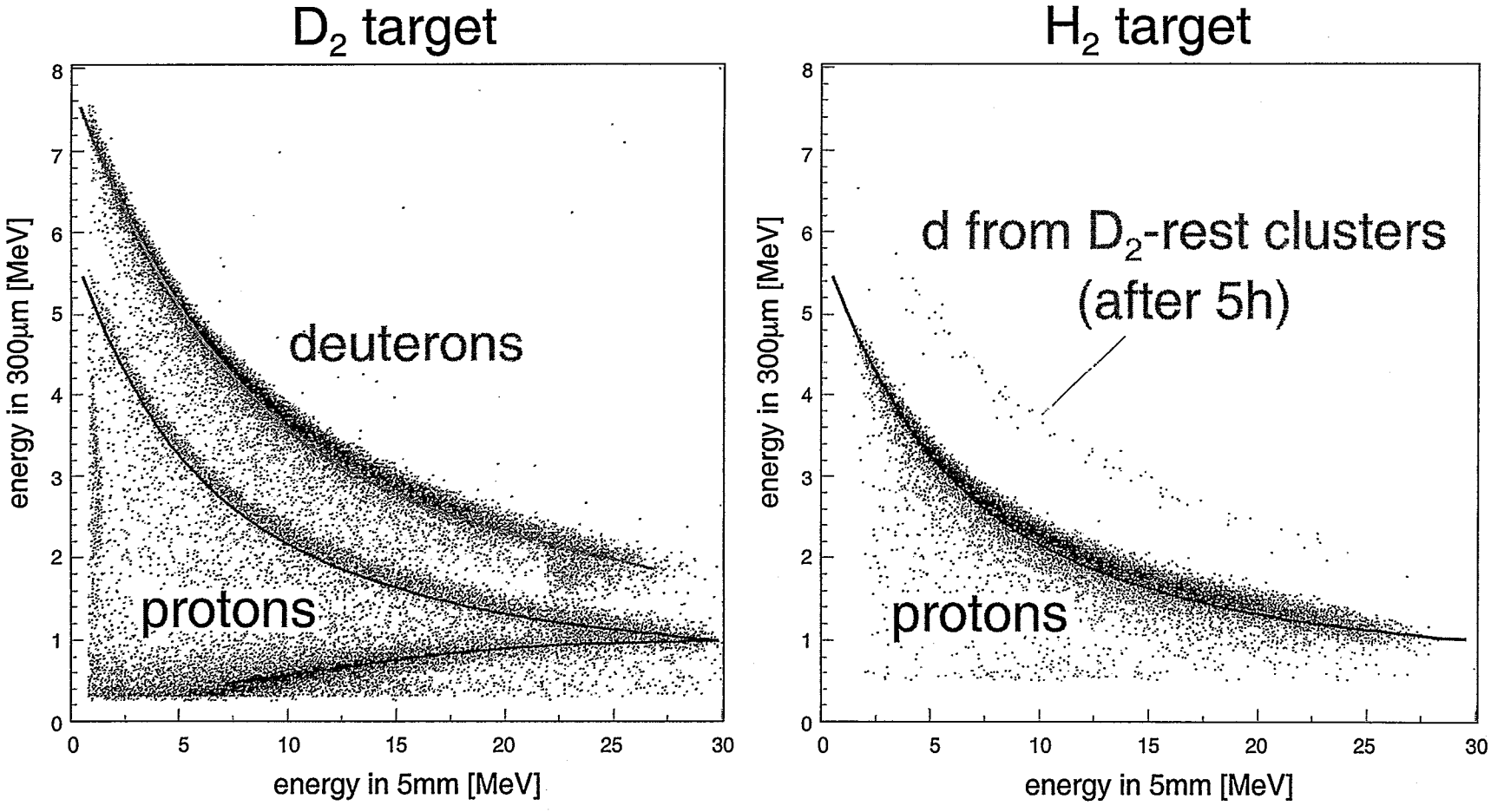

$$\Rightarrow \quad \mathbf{L = f_{target}^{-1} \cdot 0.67(5) \cdot 10^{29} \frac{1}{cm^2 s}} \qquad (D_2\text{-target})$$

f_{target}: fraction of the target seen by elastic scattering

Target Dimensions

Selection of protons on a D_2-target under a fixed angle

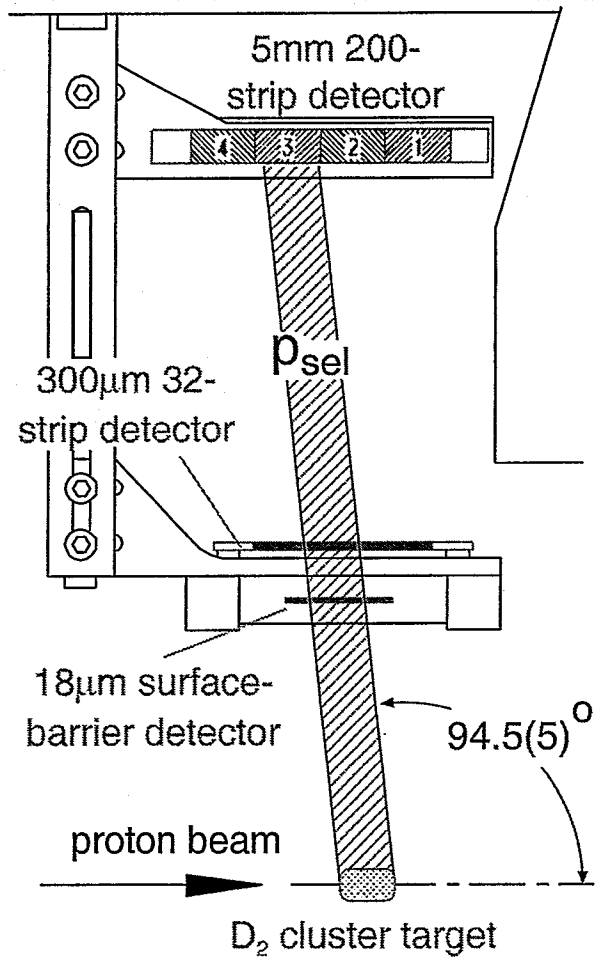

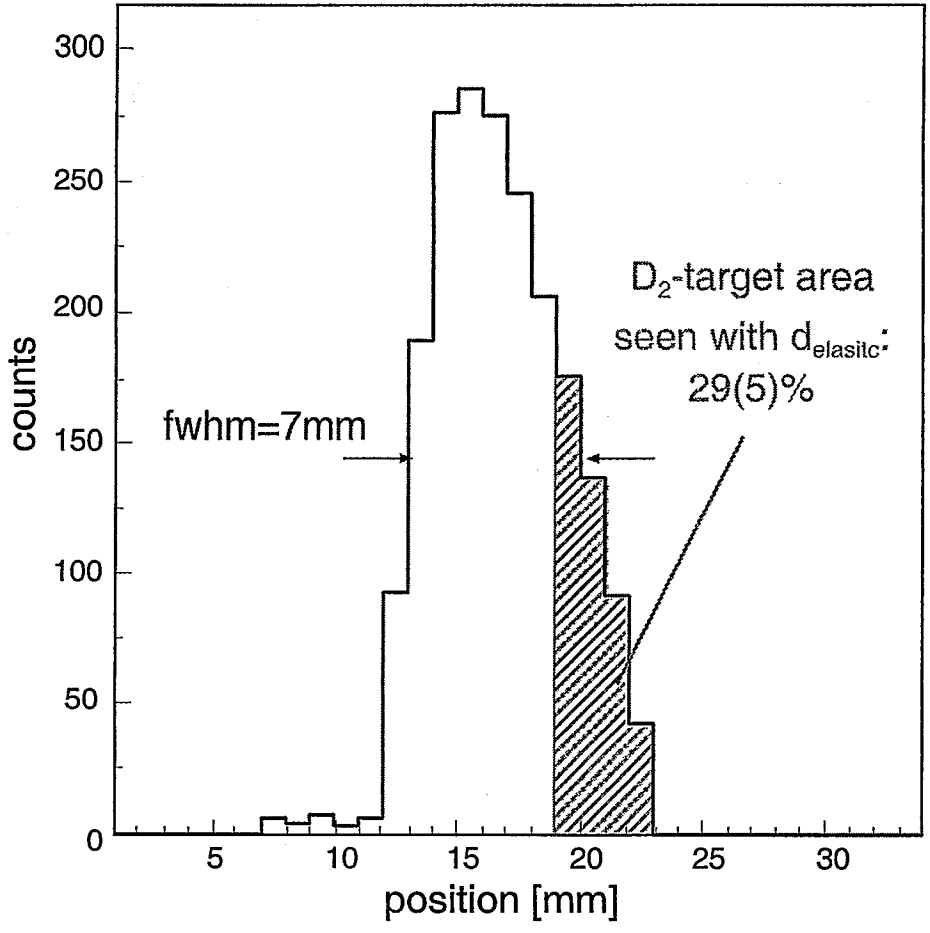

$$\Rightarrow L = \mathbf{2.4(5)\cdot 10^{29}} \frac{1}{\mathbf{cm^2 s}}$$ (10^{10} protons at T_p=2 GeV in COSY)

Conclusions

current setup:

- absolute Luminosity within 20%

future improvements:

- September 2000:
  few mm target shift
  $\Rightarrow$ more of the target seen: $\rightarrow$ $\Delta L \approx 10\%$

- beginning of 2001:
  5 cm target shift (new chamber)
  $\Rightarrow$ the hole target seen: $\rightarrow$ $\Delta L =$ few %

Future Activities at ITEP, Status of the Pellet Target

V. Chernyshev

Institute for Experimental and Theoretical Physics
B. Cheremushkinskaya 25
117259 Moscow
Russia

The infrastructure at ITEP for the data analysis of future a_0/f_0 meson experiments is in a preparation. It is planned to start data analysis of the first a_0 measurements with the cluster target in the beginning of 2001. Simultaneously the ITEP group developed topics for the possible future ANKE physics proposals (see reports of A. Kudryavtsev, V. Tarasov and B. Kerbikov). Now the pellet target activity is continued in both scientific centres, ITEP and FZJ. The first target test was performed at ITEP during November 1999 and February 2000. The successful generation of hydrogen droplets opened the possibility for the following work stage at the IKP of FZJ. In March 2000 the target equipment has been transfered from ITEP to FZJ and the preparation for the final stage of target tests has been started. In parallel to the ANKE-target preparation the development of a second-generation solid gas target set-up has already been started at ITEP. New experiments to study stable conditions of cryogenic liquid drops generation is in progress at MPEI (Moscow). A possibility to develop the target with polarised atoms inside the pellets is studied theoretically. It it planned in the nearest future to start to study this problem experimentally at the ITEP and MPEI facilities.

Future activities at ITEP/Status of the pellet target.

a_0^+ program

a) Preparation for a_0^+ measurements at COSY

- Data analysis procedure development
- Equipment and software for data analysis at ITEP preparation

B) Participation in a_0^+ measurements with cluster target.

- Background analysis
- a_0^+ event selection

Planned physics program

ω/ϕ - production in pn - collisions
(measurements and data analysis)

New topics:

a_0 - production studies
a_0/f_0 mixing measurements

Current status of pellet target

Tests at ITEP

November 1999 - February 2000

Results: liquid H_2 jet and droplet was obtained.

From March 2000 the pellet target is assembling <u>at TKP</u>

Vacuum system assembled and tested

$P \sim 10^{-7}$ mBar

H_2 supply system assembled

He supply is partly assembled

Control is in a progress

Dumping ....

Diagnostic ...

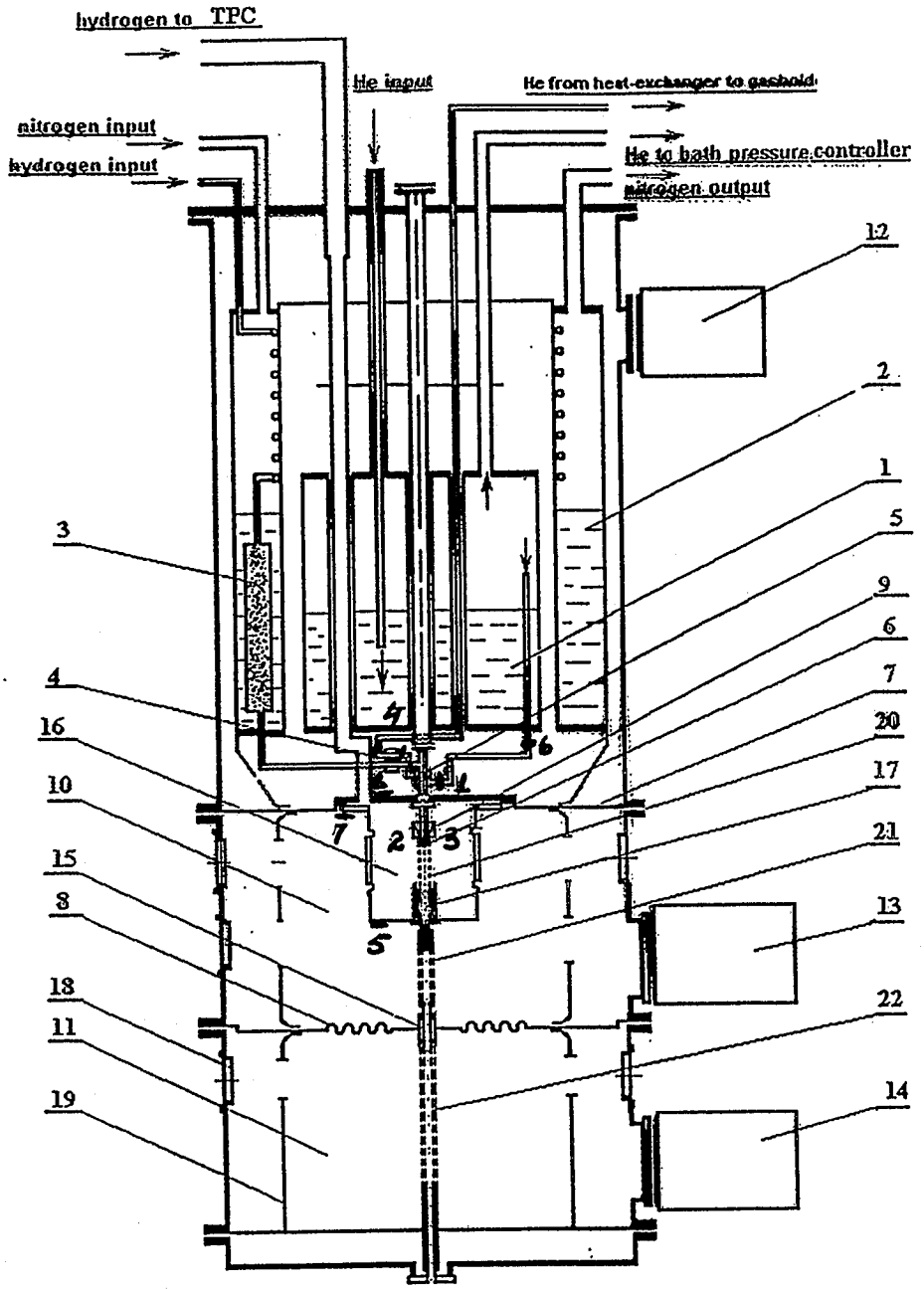
hydrogen to TPC
He input
He from heat-exchanger to gasholder
nitrogen input
hydrogen input
He to bath pressure controller
nitrogen output
12
2
1
5
9
6
7
20
17
21
13
22
14
3
4
16
10
15
8
18
11
19

Fig. 2

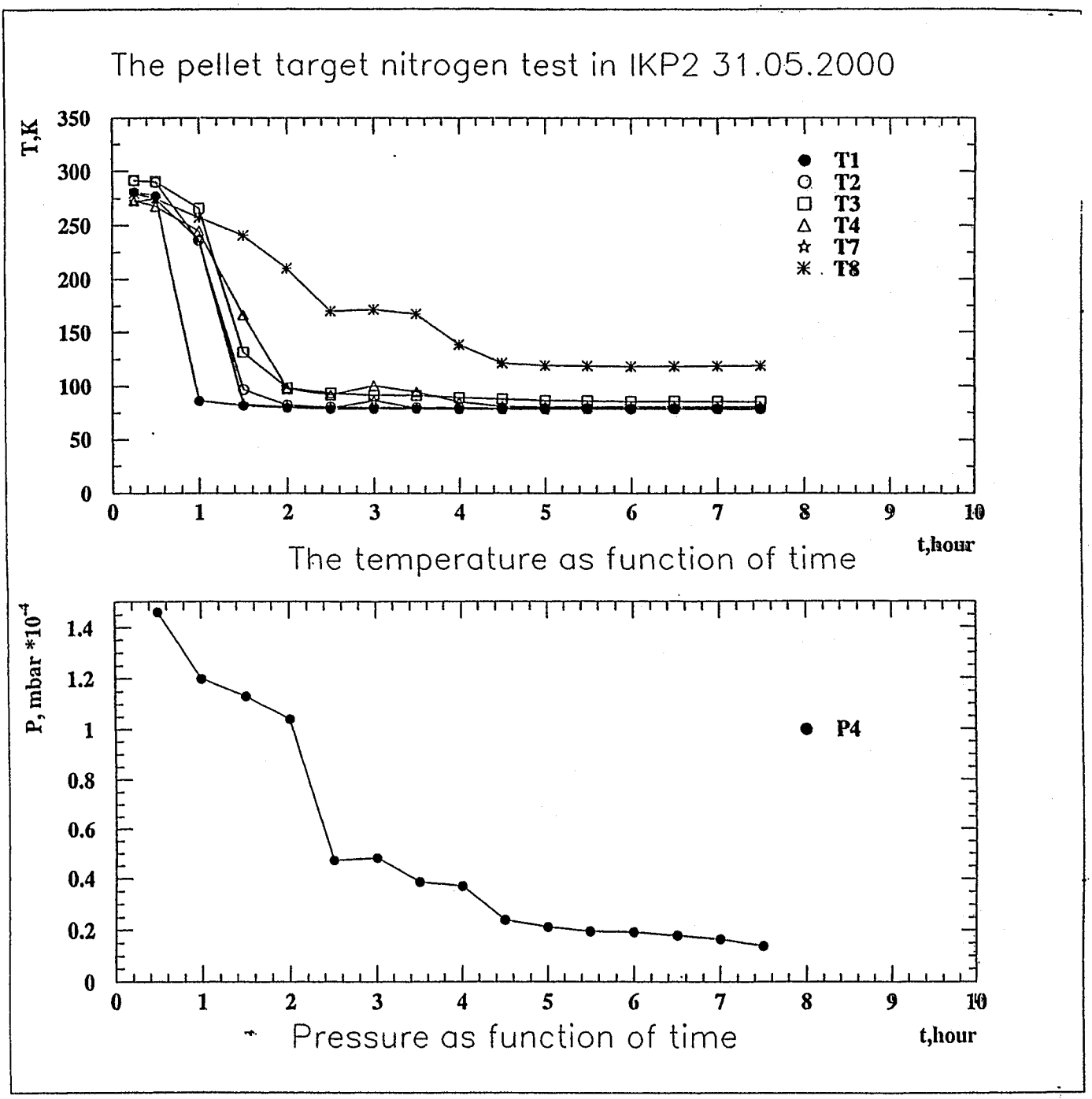
The pellet target nitrogen test in IKP2 31.05.2000
T,K
350
300
250
200
150
100
50
0
0
1
2
3
4
5
6
7
8
9
10
t,hour
T1
T2
T3
T4
T7
T8
The temperature as function of time
P, mbar *10⁻⁴
1.4
1.2
1
0.8
0.6
0.4
0.2
0
P4
Pressure as function of time
t,hour

The pellet target test in ITEP from 11.01 to 13.01

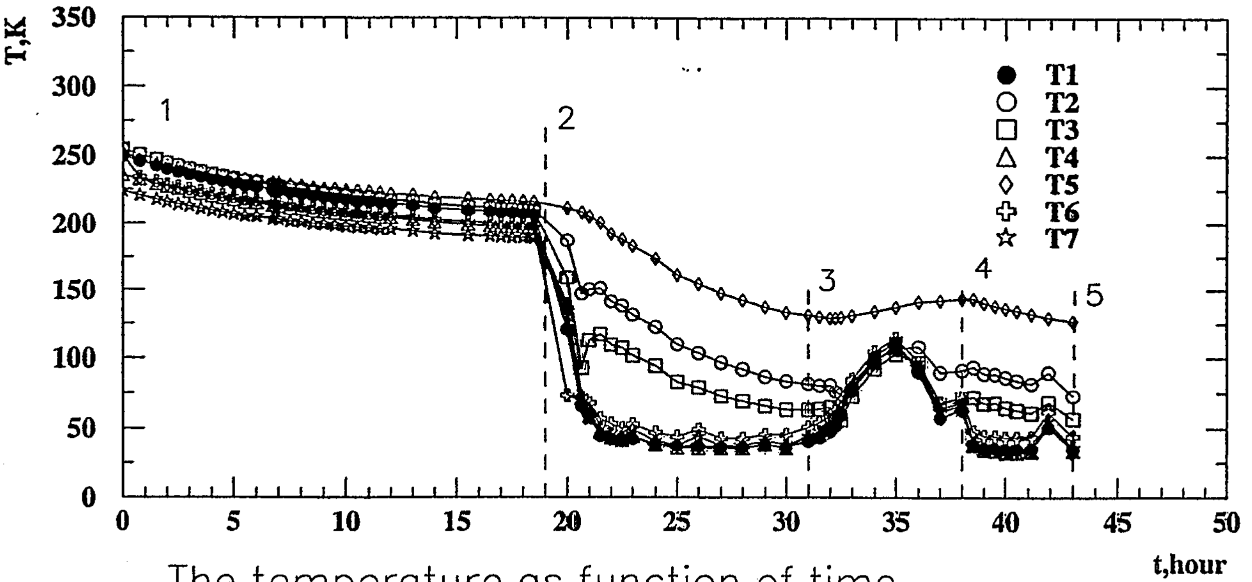

The temperature as function of time

1 – Start LN cooling
2 – Start LHe cooling
3 – Stop LHe cooling
3–4 – LN cooling
4 – Start LHe cooling
5 – Stop LHe cooling

новый экспер. смешанной
упр. [illegible] мишени – ценное

T,K

The pellet target test in ITEP from 18.02 to 20.02

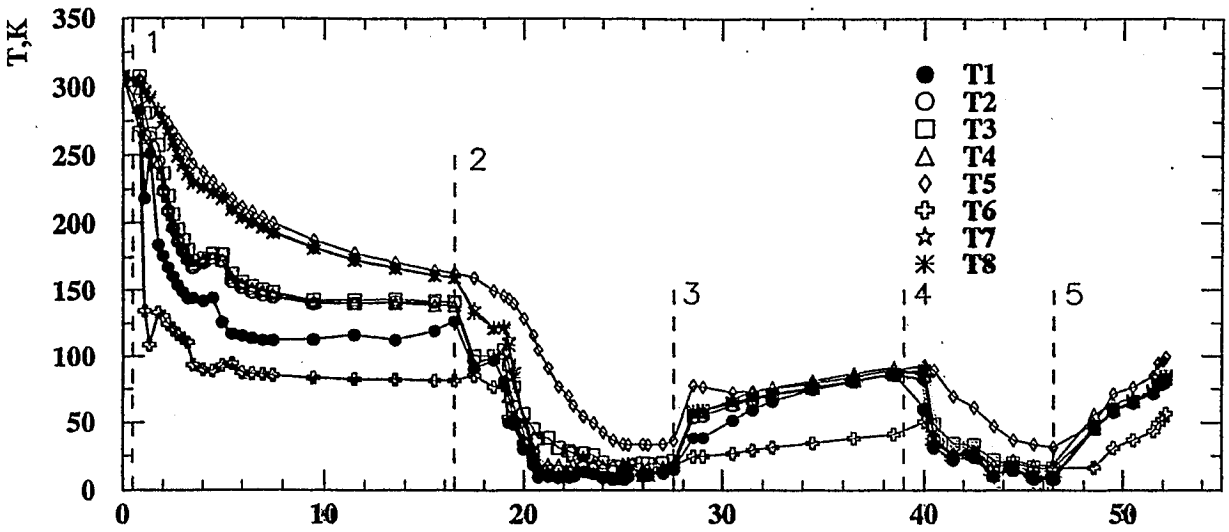

The temperature as function of time

1 – Start LN cooling
2 – Start LHe cooling
3 – Stop LHe cooling
3–4 – LN cooling
4 – Start LHe cooling
5 – Stop LHe cooling

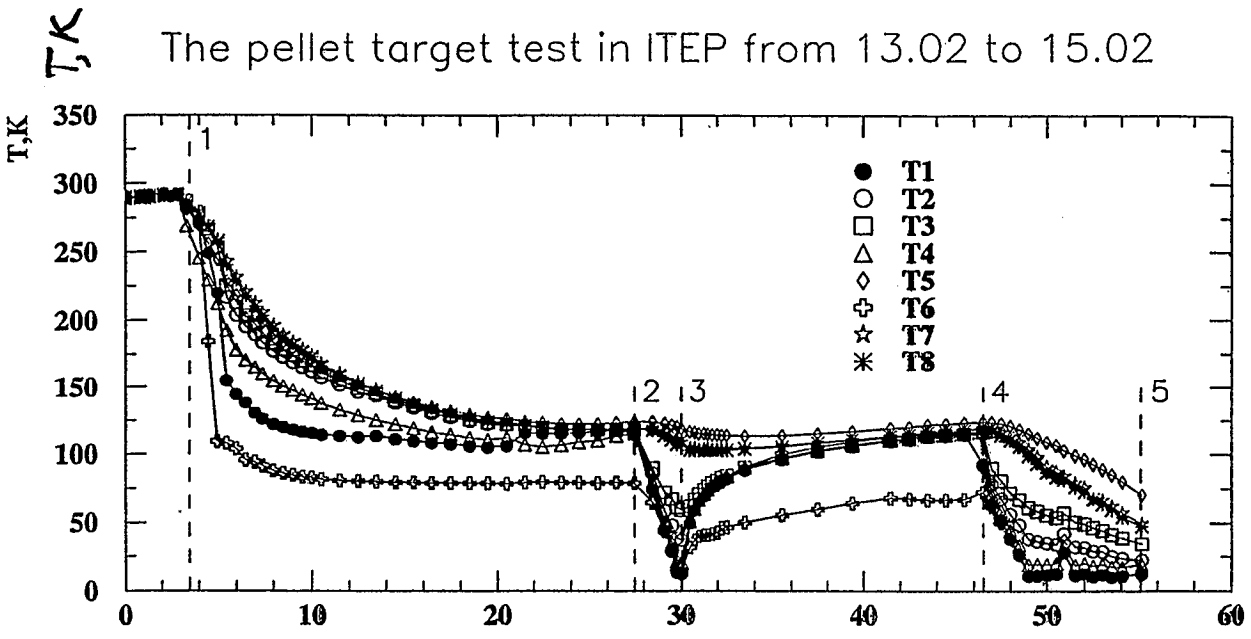

The temperature as function of time

1 – Start LN cooling
2 – Start LHe cooling
3 – Stop LHe cooling
3–4 – LN cooling
4 – Start LHe cooling
5 – Stop LHe cooling

The vacuum pellet target tests in IKP 25.06.2000 – 27.06.2000

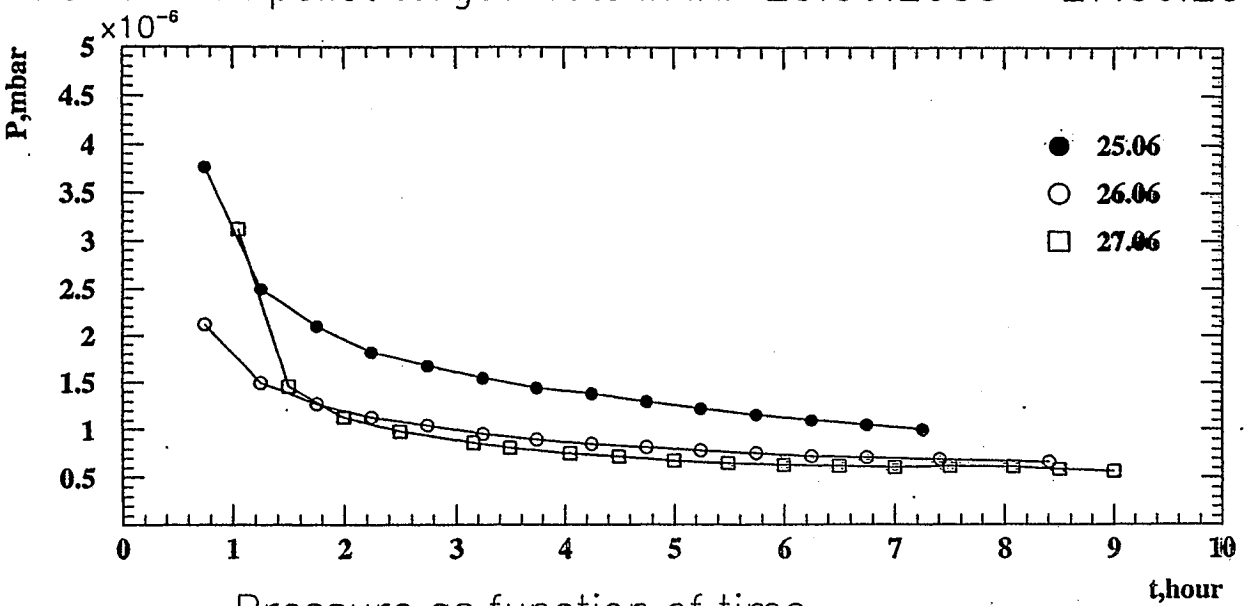

Pressure as function of time
Detector N3

Target preparation for the operation at COSY includes:

- Target control and diagnostic assembling
- Target operation regimes tests.

Methodical studies (at ITEP)

- Nuclei pellet target development.
- Next generation of H_2 (D_2) pellet target development.
- Strip solid H_2 target development
- Polarized solid H_2 target (pellet type) development

Nearest plans:

Nov 2001 H_2 droplet (pellet) generation

Feb 2001 Dumping assembling

Apr-June 2001 PC control and diagnostic tests.

Future Activities at ANKE

H. Ströher

Institut für Kernphysik
Forschungzentrum Jülich
52425 Jülich
Germany

ANKE (Apparatus for Studies of Nucleon and Kaon Ejectiles) is an internal experiment in the straight section of COSY-Jülich next to the electron cooler.

Present Status

Currently ANKE comprises:

- The magnetic spectrometer (3 dipole magnets D1, D2, and D3).
- The target (strip target or cluster jet target).
- The positively charged particle detection system with the following components:
  scintillation start counters,
  multi-wire proportional counters,
  telescopes: stop scintillators, energy loss scintillators,
  passive degraders and Čerenkov-detectors.
- The forward-, side-, and backward hodoscope.
  The setup has been described in an internal report [1], and a recent NIM-paper [2]. Up to now, the facility has been used for experiments on 'subthreshold K^+-production' on nuclear strip targets (K momentum spectra, cross sections and A-dependence) in order to investigate the production mechanism (1-step or 2-step process).

Immediate Future

For the immediate future, ω-production and d-breakup on the deuteron cluster target as well as the a_0^+-experiment in pp-interactions are planned.

Near Future

In the near future, the detection system for negatively charged particles (TOF scintillators, MWPCs for tracking and Čerenkov-detectors for π/K-discrimination) will be implemented into ANKE. Possible experiments are then 'subthreshold K^--production' on nuclei in order to study asserted kaon mass modifications, and Φ-production with the cluster target. In addition preparatory studies with the COSY beam to use a storage cell in conjunction with the polarised gas target (ABS) are foreseen.

Intermediate Future

The intermediate future will see the completion of the pellet target (for maximum luminosity measurements, for example for the a_0^+-experiment) and of the ABS plus the storage cell (for studies with polarised target nuclei). On the detector side, vertex and spectator detectors will come into operation, enabling studies on an 'effective neutron target'. Further options are the deuteron beam of COSY, which should be available by then, and the use of a polarised ^{3}He gas target.

Long Term Future

Long term perspectives are centred around the new injector together with a new ion source, which will enable high precision double polarisation experiments. In order to be able to detect photon final states, a compact electromagnetic calorimeter for use with ANKE is also foreseen.

Taken all this together, it is fair to state that a rich and very interesting physics program will be possible to study with ANKE; one of these fascinating issues is the scalar meson sector, in particular $a_0^{+,0,-}$.

[1] *Physics with ANKE*, August 1999, available via www:
http://ikpd15.ikp.kfa-juelich.de:8085/doc/Anke.html
[2] S. Barsov et al., *ANKE, a New Facility for Medium Energy Hadron Physics at COSY-Jülich*, June 2000, submitted to NIM A, available via www:
http://ikpd15.ikp.kfa-juelich.de:8085/doc/Anke.html

H. Ströher

Institut für Kernphysik
Forschungszentrum Jülich
Jülich, Germany

Future Activities at ANKE

Overview

Present Status
Near Future
Intermediate Future
Long Term Perspectives

Present Status

- Magnetic spectrometer (D1,D2,D3)
- Target (Strip, Cluster)
- Detector systems for positively charged particles

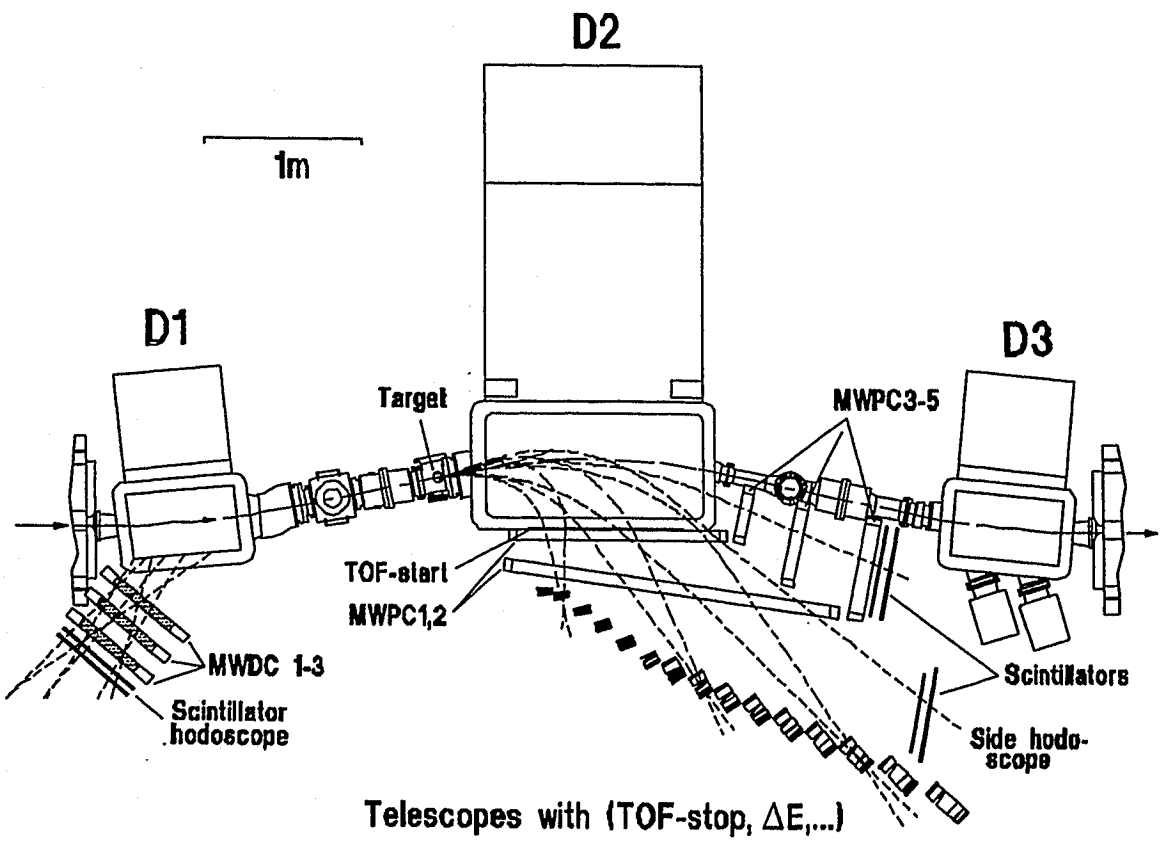

→ "Subthreshold" K^+ production (pA)
→ Deuteron breakup (pd)
→ Meson production (pp, pd)

Notes, Ref's: a) Physics with ANKE, Internal Report 1999

Near Future

- **Detector systems for negatively charged particles**

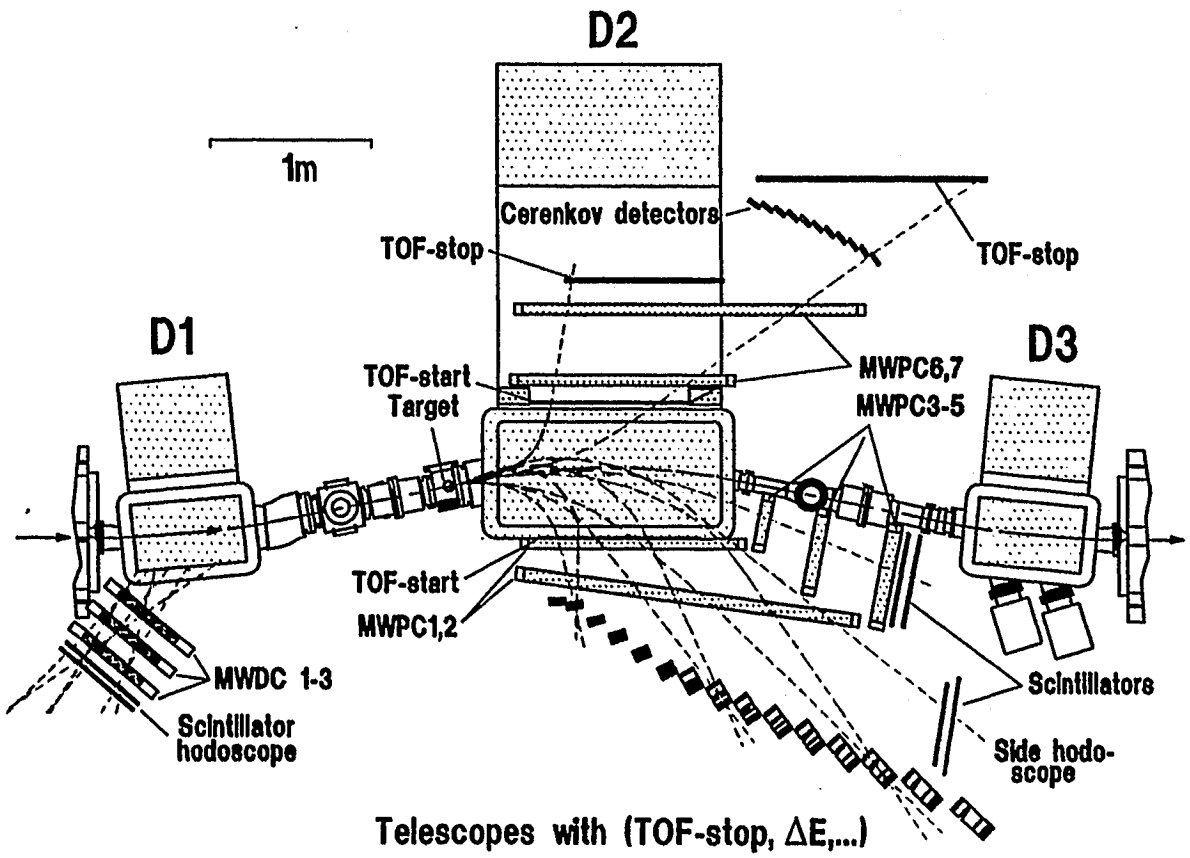

Telescopes with (TOF-stop, ΔE,...)

→ "Subthreshold" K^- production (pA)
→ ϕ production (pp, pd)

operational in 2001 !

Notes, Ref's: a) Physics with ANKE, Internal Report 1999

Intermediate Future

- Targets:
  - a) Pellet
  - b) ABS + storage cell
- Detectors:
  - a) Spectator
  - b) Vertex
- New Target chamber

→ "max. luminosity" measurements (a_o ,...)
→ measurements on effective "neutron-target"
→ double polarization experiments

Notes, Ref's: a) Physics with ANKE, Internal Report 1999

Intermediate Future

- Deuteron beam
- Polarized ^{3}He target
-

Notes, Ref's: a)

Long Term Future

- **Detectors: a) Electromagnetic calorimeter**

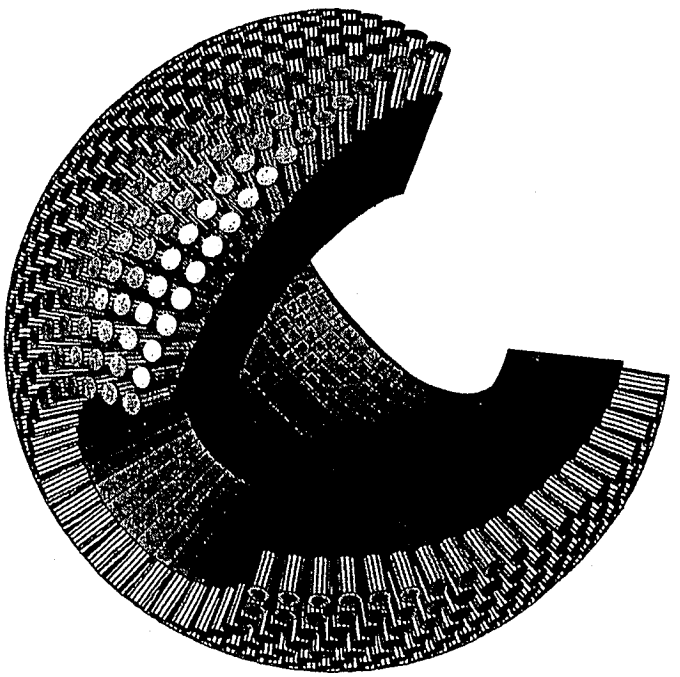

→ **d d →** $\alpha\ \pi^\circ$ **(CSB)**
→ ω**N – resonances**
→ ω **properties in pA collisions**
→ a_o° **and** f_o **(980)**

...

Notes, Ref´s: a) COSY-Proposal #83 ("A Photon Detector for COSY")
Spokesperson: V. Hejny (FZJ)

Long Term Future

- **COSY:**

  a) New injector (LINAC) !
  b) New polarized source !

- **Experiments:**

  a) New internal detector ("Toroid ") ???

Notes, Ref´s:

a) COSY Internal Report ("A New Injector for COSY")
K. Bongart et al. (May 2000)
b) COSY LoI #84 ("Toroid Spectrometer Project")
F. Rathmann et al.

List of responsibilities

- **Coordination** — *FZJ*
  M.Büscher

- **Theory**
  Background estimates: $pp \rightarrow 3\pi X$, $pp \rightarrow dK^+K^0$ (non-res.) — *L.Kondratyuk, Ye. Golubeva*
  New ideas for next beam-time request (fall 2001) — *L.Kondratyuk, N.N.*

- **Accelerator tuning** — *FZJ*

- **Cluster target** — *Univ. Münster*
  Size of cluster beam (width 6 mm →9 mm?) — *V.Komarov*
  Shift target position few mm in -z direction — *A.Khoukaz, N.Lang*
  Pressure monitoring (write data to tape) — *M.Hartmann, N.Lang*

- **Side detectors** — *FZJ, PNPI*
  Degrader tuning — *M.Büscher, H.Junghans, V.Koptev*

- **Forward detectors** — *JINR*
  Installation of 3rd MWPC — *V.Komarov, B.Zalikhanov*

- **Cerenkov counters** — *JINR, HEPITU, FZJ*
  Analysis of existing data (April 2000) — *G.Macharashvili*
  Simulations — *C.Leim*
  Cerenkov counters behind side wall — *V.Komarov, M.Nioradze*
  HV tuning (until 9/2000)

- **Data acquisition** — *FZJ*
  M.Hartmann

- **Data analysis**
  Optimization of momentum reconstruction (side detectors) — *V.Kleber, M.Nekipelov*
  Optimization of momentum reconstruction (forward detectors) — *JINR*
  On-line luminosity monitoring — *N.Lang, JINR*

- **Simulations** — *FZJ*
  M.Büscher, V.Kleber